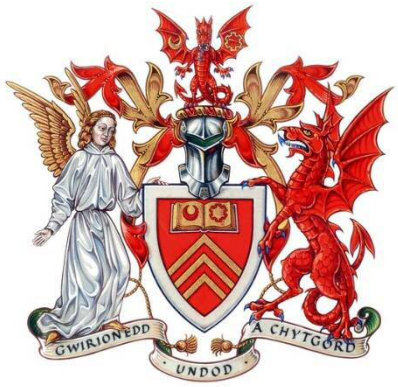

Regulation of Cellular Immunity by Human Cytomegalovirus

A thesis submitted in candidature for the degree of

Doctor of Philosophy (PhD)

by

Mihil Patel

June 2018

Human Cytomegalovirus Research Group
Division of Infection and Immunity
School of Medicine,
Cardiff University,
CF14 4XN, UK

Cydnabyddiaethau/Acknowledgements

I would like to thank my supervisor Dr Eddie Wang allowing me to train under his supervision. Ed's constant support, enthusiasm and patience, in the face of my apparent stubbornness, was invaluable to my development as a scientist.

I'd like to extend this to the other members of the lab including Professor Gavin Wilkinson, Dr Richard Stanton, Dr Peter Tomasec, Dr Ceri Fielding and Mrs Dawn Roberts. Their assistance, resources and valuable insights, were essential for this work.

I am thankful to the Medical Research Council for funding this work. I would like to acknowledge our collaborators Professor Andrew Davison in Glasgow for sequencing of viruses and transcriptome data, and Dr Michael Weekes in Cambridge for providing proteomic data. Another mention must go to Dr Simone Forbes for her input with the T-cell work.

The company I've had during my time in Cardiff has been fantastic. To know that I could come in to work every day and be surrounded by such friendly people made the Ph.D. all the more enjoyable. Outside of work I was very lucky to have amazing housemates, many of whom I've formed lifelong friendships with. I also want to thank my family and close friends for their continued support. The list of all those who have helped would be too long, but I must mention by name Dr James Matthews, who always had time for me.

Summary

The success of HCMV as a lifelong pathogen is attributed at least in part to the broad range of encoded immune evasion molecules that inhibit the host cellular immune response. Indeed, HCMV has become a paradigm for immune evasion, the study of which has revealed a number of basic immunological processes.

To screen for novel immune evasion genes, HCMV-specific CD8+ T-cell lines were grown from seropositive donors and used against a series of block deletion viruses, each missing a region of genes non-essential for replication *in vitro*. UL13-UL20 was flagged as important for inhibition of CD8+ T-cells. Further screening with individual gene knockout HCMVs showed that the published NK-cell inhibitor UL16 could inhibit CD8+ T-cells, but also revealed UL19 as a previously unrecognised strong immune evasin, inhibiting 3 separate CD8+ T-cell lines. UL19 had no effect on HLA-I downregulation indicating that it may affect other pathways involved with T-cell activation.

Proteomic data showed that surface TNFR2 was increased by HCMV infection. This is important as this would influence the response to TNF, a major inflammatory cytokine and soluble effector molecule released by T and NK cells. Screening using different HCMV strains and knockout viruses identified UL148 and UL148D as responsible for the increase in surface TNFR2 but prevented the release of soluble TNFR2, indicating that UL148 and UL148D were influencing the ability of TNFR2 to be retained at the cell surface. Infection with HCMV Merlin profoundly downregulated surface ADAM17, the metalloproteinase responsible for cleaving TNFR2 from the cell surface. Deleting UL148 and UL148D recovered ADAM17 expression, blocking the function of which returned surface and soluble TNFR2 levels to those observed with Merlin. This was also true of TNFR1. HCMV infected cell lysates showed that UL148 and UL148D interfered with the maturation of ADAM17. Thus, UL148 and UL148D allow upregulation of TNFR2 and maintain TNFR1 expression during and HCMV infection by impairing surface ADAM17 expression through impairment of ADAM17 maturation.

Given that ADAM17 is involved with the cleaving of multiple cytokines, cytokine receptors, adhesion molecules and immune cell receptors, this work identifies a novel mechanism through which HCMV can alter the surface and soluble proteome by preventing the shedding of inflammatory/immune receptors and mediators. More detailed studies will be required to define the global impact of this on the immune system.

Contents

List of Figures

List of Tables

Symbols/Acronyms/Abbreviations

°C	Degrees centigrade
Δ	Gene deletion
µg	microgram
µl	microlitre
µM	micromolar
aa	Amino acid
ADAM	A disintegrin and metalloproteinase
AF	Alexaflour
AIDS	Acquired immunodeficiency syndrome
ANOVA	Analysis of variance
APC	Allophycocyanin
APC	Antigen presenting cell
ATCC	American Type Culture Collection
BAC	Bacterial artificial chromosome
BD	Becton Dickinson
BLAST	Basic local alignment search tool
BP	Base pair
BSA	Bovine serum albumin
CAR	Coxsackie adenovirus receptor
CCL	C-C motif chemokine ligand
CD	Cluster of differentiation
CID	Cytomegalic inclusion disease
cm	centimetre
ConA	Concanavalin A
CPE	Cytopathic effect
CTRL	Control

CXCL	Chemokine ligand
DC	Dendritic cell
ddH_2O	Double distilled water
DMEM	Dulbecco's Modified Eagle Medium
DMSO	Dimethyl sulphoxide
DNA	Deoxyribonucleic acid
DNAM1	DNAX Accessory Molecule-1
dNTP	deoxyribonucleotide triphosphate
DTT	Dithiothreitol
EDTA	Ethylenediaminetetraacetic acid
ef660	Eflour660
EGFR	Endothelial growth factor receptor
ELISA	Enzyme linked immunosorbent assay
ER	Endoplasmic reticulum
FACS	Fluorescence-activated cell sorting
FITC	Fluorescein
FMO	Fluorescence minus one
FSC	Forward scatter
g	Gram
g	Gravity
GFP	Green fluorescent protein
GFRA2	GDNF family receptor alpha-2
GM-CSF	Granulocyte-macrophage colony-stimulating factor
h	Hour
HAART	Highly active antiretroviral therapy
HCMV	Human cytomegalovirus
HDAC	Histone deacetylase

HF-CAR	Human TERT immortalised HFFF+CAR
HF-TERT	Human TERT immortalised HFFF
HFFF	Human foetal foreskin fibroblasts
HIV	Human immunodeficiency virus
HLA	Human leukocyte antigen
hpi	hours post infection
HRP	Horseradish peroxidase
HSCT	Hematopoietic stem cell transplant
ICS	Intracellular staining
IE	Immediate early
IFN	Interferon
IKK	IκBα kinase
IL	Interleukin
IPTG	Isopropyl β-D-1-thiogalactopyranoside
IRL	Inverted repeat long
IRS	Inverted repeat short
iu	international units
IκBα	NF-κB inhibitor α
L	Litre
LB	Lysogeny broth/Luria-Bertani medium
LDS	Lithium dodecyl sulphate
LFA	Lymphocyte function-associated antigen
LIR	Leukocyte immunoglobulin-like receptor
M	Molar
mAb	monoclonal antibody
MEGF10	Multiple EGF Like Domains 10
MEM	Minimum essential medium

mg	Milligram
MHC	Major histocompatibility complex
MIC	MHC class I chain-related protein
MIEP	Major immediate early protein
min	Minute
miRNA	Micro-RNA
ml	Millilitre
mm	Millimetre
MOI	Multiplicity of infection
MOPS	3-(N-morpholino)propanesulfonic acid
MRC	Medical research council
mRNA	Messenger RNA
ND10	Nuclear domain 10
NF-κB	nuclear factor kappa-light-chain-enhancer of activated B cells
ng	Nanogram
NIEP	Non-infectious enveloped particles
NK cell	Natural killer cell
NKG2D	Natural killer group 2 D
NRG1	Neuregulin 1
ORF	Open reading frame
PAMP	Pathogen associated molecular patterns
PBMC	Peripheral blood mononuclear cells
PBS	Phosphate buffered saline
PBST	Phosphate buffered saline with Tween
PCR	Polymerase chain reaction
PDGFR	Platelet derived growth factor receptor
PE	phycoerythrin

PE-cy7	phycoerythrin-cyanine 7
PerCP-Cy5.5	Peridinin-Chlorophyll-protein-cyanine 5.5
PFA	Paraformaldehyde
PFU	Plaque forming unit
pp	Phosphoprotein
PVDF	Polyvinylidene fluoride
QTV	Quantitative temporal viromics
RAd	Recombinant adenovirus
RANTES	Regulates on activation, normal T-cell expressed and secreted
RHBDF	Rhomboid family member
RL	Repeat long
RNA	Ribonucleic acid
RPM	Rotations per minute
RPMI	Roswell Park Memorial Institute
SA	Streptavidin
SDS-PAGE	Sodium dodecyl sulphate polyacrylamide gel electrophoresis
SEM	Standard error of the mean
SSC	Side Scatter
T25/75/150	25//75/150cm^2 flask
TAE	Tris Acetate-EDTA
TAP	Transporter of antigenic peptide
T-cell	T lymphocyte
TCR	T-cell receptor
TERT	Telomerase reverse transcriptase

TNF	Tumour necrosis factor
TNFR	TNF receptor
TNFRSF	Tumour necrosis factor receptor superfamily
TRAIL	TNF related apoptosis inducing ligand
TRIS	Tris(hydroxymethyl)aminomethane
T-test	Students T-test
UL	Unique long
ULBP	UL16 binding protein
US	Unique short
UV	Ultraviolet
V	Volts
v/v	Volume/volume
X-gal	5-Bromo-4-Chloro-3-Indolyl β-D-Galactopyranoside

1 Introduction

1.1 The discovery of the Human Cytomegalovirus

The first report of human cytomegalovirus (HCMV) infected cells was by Hugo Ribbert in 1881. He observed large cells in sections of kidney from a stillborn with syphilis (Ribbert, 1904). By 1932 there had been 25 reported cases of a congenital infection characterised by petechiae, hepatosplenomegaly, and intracerebral calcification (Ho, 2008). At the time, the disease was referred to as generalised cytomegalic inclusion disease (CID). The first isolation of HCMV was in 1955 by Margaret Smith from the kidney of a one-month old baby dying of CID. The virus was extracted from the adrenal gland and used to infect uterine tissue. The cytopathic changes “consisted of small, round or oval foci in which the cells were enlarged, rounded or oval, and somewhat refractile in contrast to the normal fibroblasts” (Smith, 1956). Strain Ad.169 (AD169) was isolated from the adenoid tissue of another patient by Wallace Rowe (Rowe et al., 1956), which produced the same cytopathic effect that Thomas Weller (Craig et al., 1957) would later observe. The three scientists exchanged their infective agents and concluded they were dealing with the same virus, which was called cytomegalovirus (Weller, 1970).

1.2 HCMV virus structure

Electron cryomicroscopy revealed that HCMV virions are between 200-230nm in diameter, with a capsid shell composed of hexons, pentons and triplexes (Chen et al., 1999). From inside out, the virion consists of a double stranded DNA genome, capsid, tegument and envelope. The HCMV structure is characteristic of Herpesviridae. HCMV capsids are assembled from 162 capsomeres and 320 heterodimeric protein complexes. These are arranged in an icosahedral lattice (20 faced). Three types of virus particles can be recovered from HCMV culture medium. Virions, which are infectious, dense bodies and non-infectious enveloped particles (NIEPs) (Irmiere and Gibson, 1983). Dense bodies are composed of tegument material, but lack the capsid and genome (Ahlqvist and Mocarski, 2011). NIEPs are equivalent to mature HCMV virions but lack viral DNA.

1.3 HCMV genome

HCMV has the 38th largest genome of any virus discovered to date, but the largest of any virus that infects humans (strain Merlin NC_006373.2). The HCMV genome is

comprised of double stranded DNA. The genome is comprised of a unique long (U_L) region and a unique short (U_S) region, which are flanked by inverted repeats and can be represented as: ab-U_L-b'a'c'-U_S-ca where ab/b'a' and ca/c'a' indicate inverted repeats (Stanton et al., 2010).

Our appreciation of the genetic content of HCMV was transformed by the complete sequencing of strain AD169 (Chee et al., 1990). The study showed that the virus contained at least 9 gene families and 208 designated open reading frames (ORFs). A later comparison was performed between AD169, Towne, Toledo and five clinical isolates and showed that high passage lab strains such as AD169 and Towne had suffered major deletions in the U_L/*b*' region with at least 19 genes missing from AD169 compared to Toledo (Cha et al., 1996). Further sequencing showed that AD169 contained multiple mutations outside of the U_L/*b*' region with AD169-ATCC containing at least 31 mutations outside of U_L/*b'* (Bradley et al., 2009). Clinical HCMV strains have at least 169 genes and a genome of 235kb but only a quarter of HCMV genes are required for replication *in vitro*, with the remainder of genes having other functions (Dunn et al., 2003b). Genes can be separated into gene families based on homology, though genes within the same family may not be adjacent to one another, such as UL14 and UL141 (Figure 1.1,(Davison et al., 2003b).

HCMV strain Merlin was isolated from a congenitally infected infant in Cardiff and was sequenced following 3 passages in human fibroblast cells (Tomasec et al., 2000, Dolan et al., 2004). This showed that UL128 was truncated by a single nucleotide, which led to an in-frame termination codon. Sequencing of multiple clinical and laboratory passaged strains revealed that certain genes exhibit a degree of inter-strain variability. These include genes in the RL11 family, along with important immune evasion functions such as UL18, UL40, UL142 and UL146, which likely reflect past and ongoing host-virus interactions (Sijmons et al., 2015).

When HCMV clinical isolates are propagated in fibroblasts a mutation in one of the UL128, UL130 or UL131A genes (the UL128 locus; UL128L) is rapidly selected (Akter et al., 2003, Dolan et al., 2004). To address the selection of mutations following passage *in vitro*, the HCMV strain Merlin genome, was cloned into a self-excising bacterial artificial chromosome (BAC). Mutations in the RL13 and UL128 loci were acquired during even the limited replication before cloning (Stanton et al., 2010). This allows for phenotypically wild type virus to be produced by placing wildtype RL13 and UL128L under a conditional promoter. Variants of the Merlin BAC allow researchers to work with a virus that is as

genetically-intact as practical, so that any observations made *in vitro* can be put into better context with clinical virus.

Aside from protein coding genes, HCMV encodes several microRNAs which are scattered across both strands of the genome. So far 23 miRNAs have been identified, though function has been ascribed to only 7 (Mocarski et al., 2013). HCMV also encodes polyadenylated RNA transcripts such as RNA2.7, a 5kb stable intron (RNA5.0) and a 1.2kb RNA (RNA1.2). Of all HCMV transcripts, RNA2.7 was shown to be the most abundantly transcribed and highly conserved (>99%) amongst clinical isolates, although it is dispensable for replication *in vitro* (McSharry et al., 2003). RNA2.7 was shown to target mitochondrial complex 1, thereby preventing apoptosis, but also maintaining ATP production in HCMV infected cells (Reeves et al., 2007).

A comprehensive study of HCMV encoded open reading frames was undertaken by Stern-Ginossar and colleagues (Stern-Ginossar et al., 2012). By combining next generation sequencing and ribosome profiling it was shown that HCMV may encode over 751 ORFs. This study showed that many small polypeptides are encoded by HCMV, with the authors suggesting that these may have a regulatory or immunological function. A similar approach was used to assess how the transcription of host proteins alters during HCMV infection in fibroblasts (Tirosh et al., 2015). The authors compared certain changes in host and viral RNA and correlated their data with published proteomic data. Genes which were transcriptionally upregulated but reduced at the whole cell protein level revealed proteins targeted for degradation such as BTN2A1 (butyrophilin subfamily 2 member A1) and IGSF8 (Immunoglobulin Superfamily Member 8), which have immune functions. This showed how whole cell ‘omics’ approaches can be used to predict host-cell interactions and combined to predict novel immune regulators.

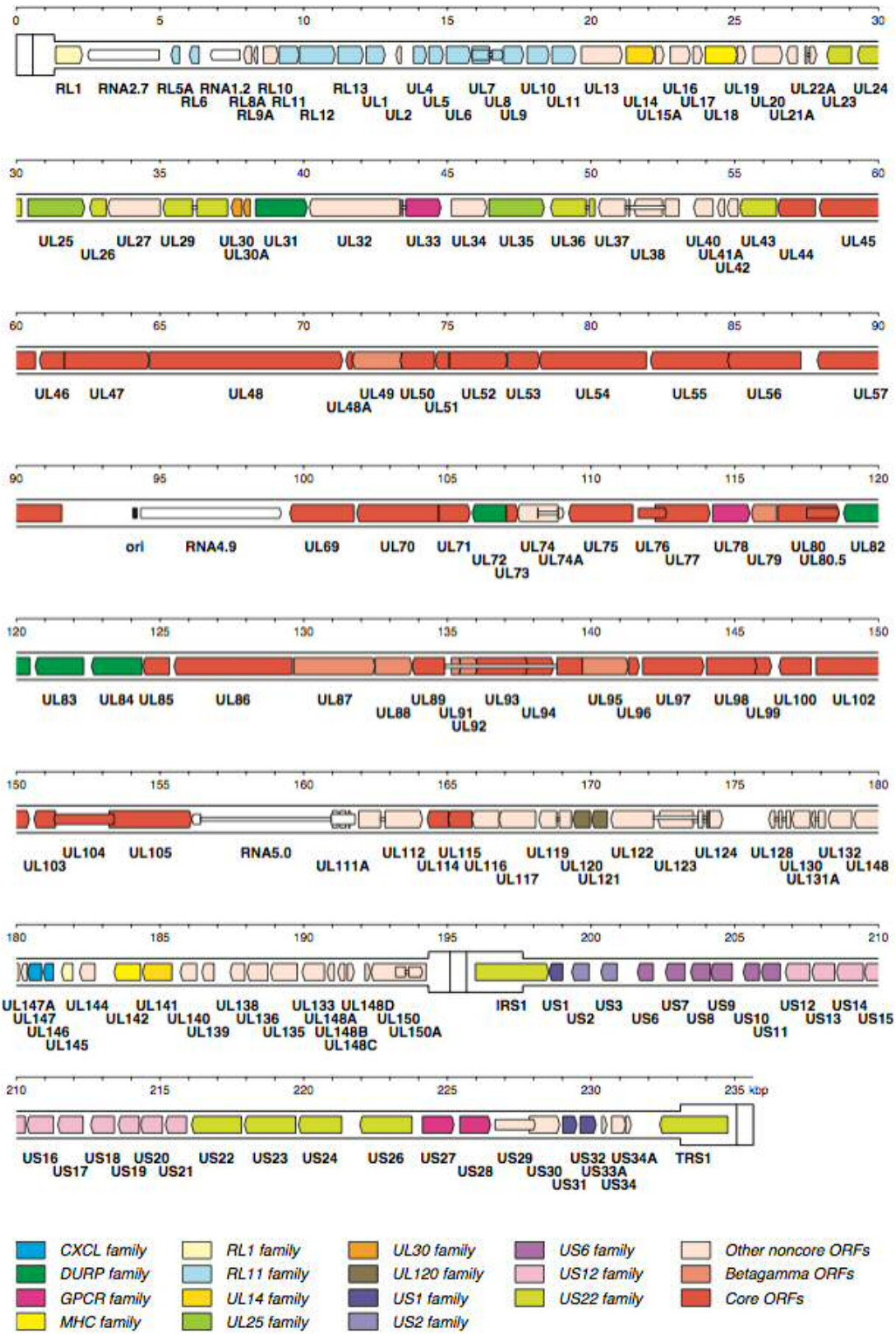

Figure 1.1 Schematic of the Merlin genome. The genome is shown from 5' to 3'. Core genes are in red. 'Betagamma ORFs' refers to genes conserved between other betaherpesviruses. The gene families are colour code as in the legend. Non-coding RNAs are shown in white. US-unique short; UL-Unique long; GPCR G-protein coupled receptor; DURP-deoxyuridine triphosphatase-related protein; RL- repeat long; TRS-terminal repeat short; IRS-internal repeat short. Figure was kindly provided by Professor Andrew Davison (Centre for Virus Research, Glasgow).

1.4 Tropism of HCMV

HCMV can be detected in a very wide range of tissues and cells *in vivo*. In healthy individuals, HCMV is found in CD14+ monocytes (Taylor-Wiedeman et al., 1991, Taylor-Wiedeman et al., 1994). From immune deficient patients with active disease, HCMV has been detected in the lung, colon, duodenum and stomach. In these patients, a range of cells were positive for HCMV including epithelial, smooth muscle, mesenchymal, endothelial cells and macrophages (Sinzger et al., 1995).

The core glycoproteins for entry of herpes viruses into cells comprises of gB, gH and gL, in addition to other accessory glycoproteins (Ryckman et al., 2008). The trimeric complex of gH (UL75), gL (UL115) and gO (UL74) allows for entry into fibroblasts. In HCMV virions, the glycoprotein complex gH, gL, UL128, pUL130, UL131 make up the pentameric complex, which was shown to be essential for entry of virus into epithelial and endothelial cells and cells of the myeloid lineage (Hahn et al., 2004, Wang and Shenk, 2005). Passaging of HCMV in fibroblasts results in mutations that affect RL13, UL128 and the U_L/b' region, and thus allows for greater entry of the virus into fibroblasts (Dargan et al., 2010). Additionally, UL148 was found to influence tropism by interacting with proteins from the pentameric complex and influencing the number of gH/gL complexes (Li et al., 2015a).

A genetically intact UL128 locus is required for entry into dendritic cells. Recently a co-culture system was developed which showed that dendritic cells could be infected with HCMV via cell to cell transfer from infected fibroblasts (Murrell et al., 2017). Whilst neutralising antibody was efficient at preventing cell free infection, cell-cell spread of Merlin was over 400 times more resistant to neutralising antibody. A further comparison was performed between HCMV strains TB40-BAC4 and Merlin, with higher levels of pentameric complex in the latter conferring resistance to neutralising antibody (Murrell et al., 2017). These studies show that wildtype HCMV spreads by cell-cell contact, which aids in evading the humoral immune system.

1.5 HCMV life cycle

1.5.1 Viral entry

The first step of the HCMV life cycle is entry into the cell. Heparan Sulphate proteoglycans were shown to be essential for the entry of HCMV *in vitro*, a function common to herpes viruses (Compton et al., 1993). Another requirement for cell entry in fibroblasts, is platelet derived growth factor-alpha receptor (PDGFRa). In PDGFRa null

cells, HCMV is not detected, and infectivity can be completely restored upon addition of the PDGFRa gene (Soroceanu et al., 2008). However, monocytes do not express PDGFRa, and instead epidermal growth factor receptor (EGFR) can substitute as the receptor required for the entry of strain TB40/E into monocytes (Chan et al., 2009). This suggests the virus may have evolved to utilise different cell receptors to infect multiple cell types. Fusion of the viral envelope with the plasma membrane results in the release of capsids into the cytoplasm. In endothelial cells and epithelial cells this occurs after endocytosis of the virion. Using cytoplasmic filaments, the nucleocapsid translocates to the nucleus and then interacts with nuclear pores allowing the viral genome to be released into the nucleus (Mocarski et al., 2013).

1.5.2 Gene expression

The major immediate early genes of the HCMV genome are the first transcribed and include the alternate transcripts IE1 (UL123) and IE2 (UL122), which encode a 72 and 86kDa protein respectively (Wilkinson et al., 1984). These two genes auto-regulate the major immediate early promoter (MIEP). IE1 acts synergistically with a transactivator encoded by IE2 to stimulate gene expression from viral and cellular promoters (Wilkinson et al., 1998). For gene expression to occur, HCMV must overcome cellular barriers. After entering the nucleus, viral DNA localises with nuclear structures known as nuclear domain 10 (ND10), which act as a defence mechanism by sequestering viral DNA. HCMV pp71 was shown to induce degradation of Death-associated protein 6 (Daxx), which is a component of ND10 (Woodhall et al., 2006). Once IE1 is expressed, it causes dispersal of ND10, which releases suppression and allows for gene replication and virus production (Kelly et al., 1995, Wilkinson et al., 1998). Histone deacetylases (HDAC) are enzymes which remove acetyl groups and allow histones to tightly wrap DNA. Using conditionally permissive cells, inhibition of MIEP expression was shown to involve recruitment of histone deacetylases (HDAC3) to the viral MIEP (Murphy et al., 2002). Fibroblasts fully permissive to HCMV contained relatively little HDAC3 suggesting that this is an important regulator of viral replication.

The temporal expression of HCMV gene expression can be described as immediate early (α), delayed early (β) and late genes (γ). Immediate early genes are those which are expressed in the absence of other viral genes, and include IE1/IE1, UL36, UL37, UL38, TRS1, IRS1 and US3 (Wilkinson et al., 1984). These genes can act synergistically to transactivate other viral and cellular gene expression (Colberg-Poley et al., 1992). The delayed early genes constitute the majority of HCMV genes and require prior *de novo* expression of viral IE genes. Delayed early genes are involved in viral DNA synthesis, assembly of virus particles and support late gene expression (White and Spector, 2007).

Late genes are expressed following the onset of viral DNA replication and form viral structural proteins and control DNA encapsidation (Mocarski et al., 2013).

The temporal expression of host and viral proteins over the course of a productive HCMV infection in fibroblasts has been quantified (Weekes et al., 2014). The approach involved multiplexed tandem mass tag-based mass spectrometry of peptides derived from HCMV infected fibroblasts at different stages of the lytic cycle and was named Quantitative Temporal Viromics (QTV). QTC quantified changes in >8000 cellular proteins and over >80% of HCMV canonical genes. Analysis of the temporal expression of HCMV genes allowed for a new system of classifying the temporal expression of genes termed Tp1, Tp2, Tp3, Tp4 and Tp5 (Figure.1.2). Tp1 genes are expressed within 24h after infection and then decrease afterwards. Tp2 genes increase within the first 24h and are maintained thereafter. The expression of Tp3 genes gradually increases over the course of a lytic infection. Tp4 genes peak at 48h and then decrease. Tp5 genes exhibit a delayed expression profile, whereby the expression increases, but only after 48hpi.

From an immunological stand point, QTV predicted possible novel immune ligands which could be regulated by HCMV infection, such as FAT1 which was suggested to be a novel NK activating ligand. Immune evasion genes were shown to be expressed with all five temporal profiles, providing protection from the cellular immune system throughout the replication cycle (Figure.1.2).

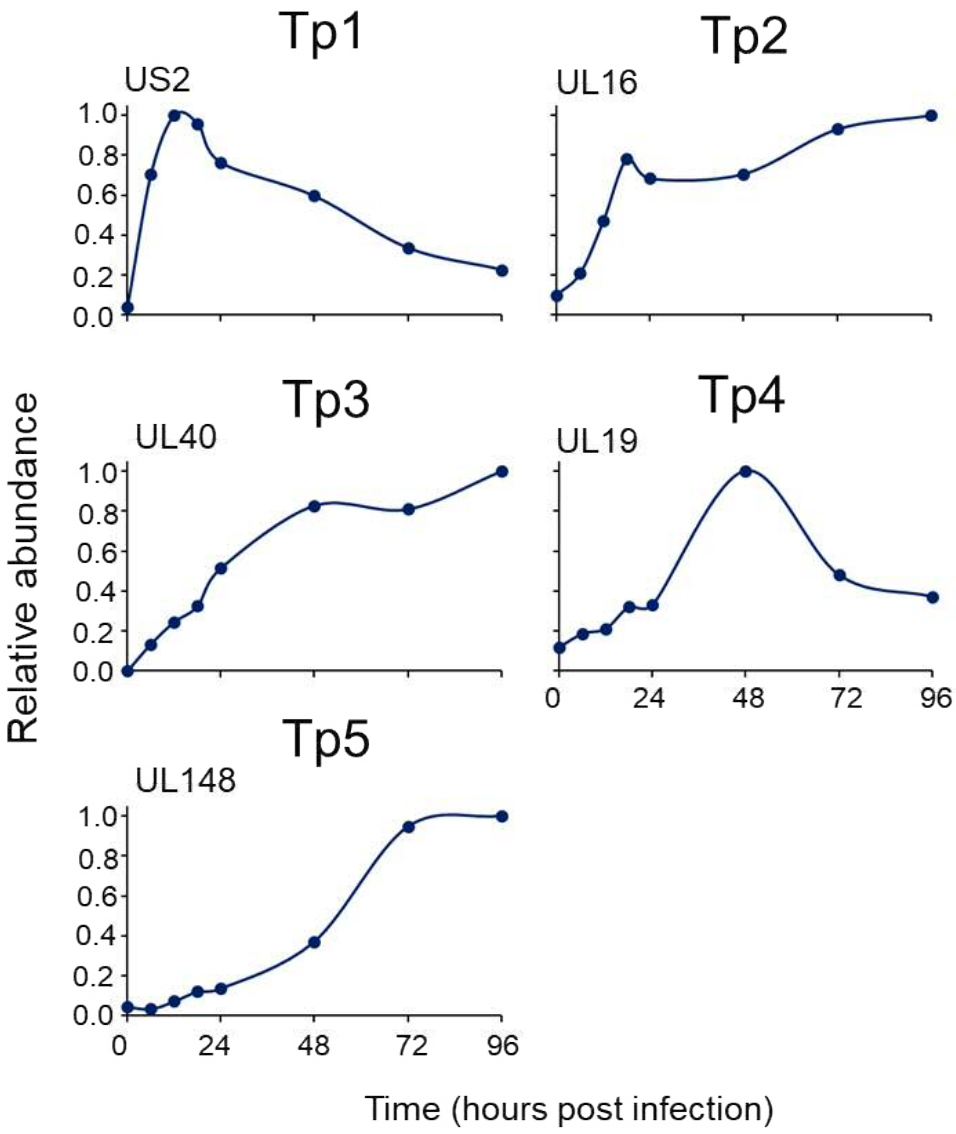

Figure.1.2 Temporal expression of HCMV genes as assessed by proteomic analysis of whole cell lysates. Data was generated from the resource paper Weekes et al. (2014). The data shows the relative amounts of HCMV proteins, which are published immune evasion proteins (other than UL19). Tp1 genes are expressed shortly after infection, with expression reducing thereafter. Tp2 genes are also expressed shortly after infection, but the expression is maintained. Genes exhibiting Tp3 kinetics increase gradually over the course of the infection. Genes expressed with Tp4 kinetics peak in abundance at 48hpi, but expression then decreases. Tp5 genes have delayed kinetics, with expression increasing after 24hpi.

1.5.3 DNA replication and egress

The core machinery of HCMV gene replication includes UL44 (polymerase accessory protein), UL54 (viral DNA polymerase), UL57 (single-stranded binding protein, UL102 (primase-associated factor) and the DNA helicase complex trimeric complex which is comprised of UL105, UL70 and UL102. These components make up the replisome. HCMV contains a single origin for DNA replication (oriLyt). This is located upstream of UL57, the single-stranded DNA binding protein. Viral DNA circularises after entry to the nucleus prior to replication. Initiation of DNA replication is dependent on transcription from orilyt promoter activated by an ppUL84:ppUL122(IE2) complex. Four proteins are produced via alternate splicing from UL112-113. Four proteins produced via alternate splicing from UL112-113 (pp34, pp43, pp50 and pp84) are required to recruit the replisome to the viral genome (Pari, 2008).

Formation of nucleocapsids occurs in the nucleus, which then egress to the cytoplasm. Nucleocapsids transiently acquire an envelope during budding through the inner nuclear membrane that is then lost when budding through the outer nuclear membrane, thereby releasing the nucleocapsid into the cytoplasm. Virus assembly takes place in the assembly complex, a highly vacuolated part of the cytoplasm. The assembly complex is comprised of the Golgi and trans-golgi network, and early endosomes, which form nested cylindrical layers (Das et al., 2007, Alwine, 2012). The nucleus surrounds the assembly complex in a kidney bean shape. As nucleocapsids emerge from the nucleus, they move to the centre of the assembly complex. The HCMV virion is then released by exocytosis to the extracellular space. Using green fluorescent tagged (GFP) tagged virus it was shown that the release of TB40 virions from fibroblasts is a rare event with a release rate of 1 infectious unit per hour per cell (Sampaio et al., 2005).

1.5.4 Latent infection

A fascinating property of HCMV, as with all herpes viruses is the ability to establish lifelong persistence. One form of viral persistence is latency. Viral latency is the ability of a virus to keep dormant within a cell with minimal viral gene expression (Sinclair and Sissons, 2006). By performing polymerase chain reaction (PCR) for HCMV DNA combined with cell sorting, CD14 monocytes were found to be a major site of latency (Taylor-Wiedeman et al., 1991, Larsson et al., 1998). Progenitor cells expressing CD34, which give rise to cells of the myeloid lineage, are also sites of latency. The level of latently infected cells is low, with an estimated 1 in 10000 cells containing HCMV genomes (Slobedman and Mocarski, 1999). As CD34+ progenitors differentiate, the virus is selectively carried down the myeloid lineage only, as HCMV genomes are not

detectable in T or B cells (Taylor-Wiedeman et al., 1991). Latently infected cells can be identified by the presence of certain HCMV transcripts including UL138, UL111A, US28 and UL81-82 and UL144 (Reeves and Sinclair, 2013). However recent work assessing the HCMV transcriptome in natural and experimental latent HCMV infection showed that the expression of HCMV transcripts in latently infected cells is similar to that observed in the late stage of lytic infection, albeit at lower levels (Shnayder et al., 2018). This data suggests that the state of latency may be based on the quantity of HCMV transcripts, rather than the detection of specific viral transcripts.

Reactivation of latent virus occurs when CD34+ cells differentiate into dendritic cells (DCs) or macrophages (Soderberg-Naucler et al., 1997, Reeves et al., 2005). During latency, the viral MIEP remains in a transcriptionally silent chromatin conformation and is associated with the silencing protein HP1. Upon differentiation, this association with HP1 is lost allowing for gene transcription. HDAC1, a transcriptional corepressor, is reduced in during differentiation to monocyte derived DCs, showing the importance of HDACs in viral repression (Reeves et al., 2005).

1.6 Clinical Virology

1.6.1 Epidemiology

HCMV is one of the most widespread pathogens infecting humans, with over 95% prevalence in some populations. The two main correlators of HCMV infection are age and socioeconomic development. In the United States, the prevalence of HCMV increased from 36.3% in children to over 90% in those >80 years old (Staras et al., 2006). There was an increased incidence in ethnic minorities compared to Caucasian individuals. Though minority groups are often less affluent than their Caucasian compatriots, this increased prevalence remains even after correcting for income, family size, geography and country of birth (Staras et al., 2006). This suggests there may be other factors affecting the transmission of HCMV such as nutrition status and genetics. In women of child bearing age, the prevalence of HCMV is 70-80% in South East Asia, but only 40-50% in France, further showing that socioeconomic development is not the only determinant of prevalence (Manicklal et al., 2013).

Genetic correlations have been found between genes of the human leukocyte antigen (HLA) family and HCMV infection. One study in Iran showed that the gene HLA-B8 may have protective roles in preventing HCMV disease in patients who had received a renal transplant (Futohi et al., 2015). A study of patients in Ireland found that genes HLA-A1 and -B8 were significantly associated with CMV seronegativity (Hassan et al., 2016).

This is the most common haplotype in the Irish population and it was suggested that this may explain the lower incidence of CMV amongst women in Ireland, compared to other developed countries.

Polymorphisms in non-classical HLA molecules could also influence HCMV disease, as these act as ligands for NK cell receptors. In a German study assessing kidney transplant patients, HLA-E*01:03 was shown to increase susceptibility to HCMV and reduce infection free survival (Guberina et al., 2017a). In a similar cohort, HLA-G +3142 CC genotype was correlated with significantly reduced allograft survival, compared to those with the GG genotype (Guberina et al., 2017b). These data suggest that genotyping of non-classical as well as classical HLA molecules would provide useful information in finding correlatives of HCMV disease.

1.6.2 Neonatal infections

HCMV infection can only occur through transfer of bodily fluids and organs. Cannon et al. (2011) performed a meta-analysis of studies investigating shedding of virus and found that children who attend day care shed virus more frequently than those that do not. Importantly, peak shedding occurs in children 1-2 years of age, which shows that young children are important vehicles for viral transmission to seronegative parents. Seroconverting adults can shed virus for months after initial CMV infection in saliva and genital secretions (Gianella et al., 2015a, Gianella et al., 2015b). Risk factors associated with an increase in viral shedding, include those who attend sexually transmitted disease (STD) clinics and those with a previous congenital infection. In neonates, transmission of HCMV via breast milk is believed to be the most common route for infection. CMV is excreted from breast milk 4-8 weeks post-partum. Risk factors for developing postnatal HCMV disease include a very low birth weight and being premature (Lanzieri et al., 2016).

A meta-analysis showed that in developed countries 0.7% of all neonates are congenitally infected with HCMV, making it the most common congenital and perinatal infection (Dollard et al., 2007). Symptomatic congenital disease may include intrauterine growth defects, thrombocytopenia, prematurity, hepatosplenomegaly, pneumonia, intracranial calcifications, microencephaly, jaundice, chorioretinitis, hearing loss and psychomotor retardation (Kurath et al., 2010). Nearly 90% of symptomatic neonates have one or more abnormality caused by damage to the central nervous system (CNS) or perception organs (Fowler et al., 1992). Neonates from recurrently infected mothers, are largely asymptomatic, however this still causes substantial morbidity. In one study between 40-58% of symptomatic congenitally infected neonates had permanent

sequelae, whilst the equivalent percentage for asymptomatic congenitally infected neonates was 13.5% (Dollard et al., 2007).

1.7 Transplant recipients

HCMV disease is one of the most dangerous infections that can arise following transplantation of solid organs or haematopoietic stem cells. In these two types of transplant, the donor and recipient status for these two types of transplantation differentially affects the outcome. Following solid organ transplants, there are three types of HCMV infection that can occur. Primary infection occurs when the donor is seropositive, and the recipient is seronegative (D+/R-). The virus is transferred in latently infected cells in the allograft. The second type, known as reactivation, occurs when the recipient is seropositive, and the virus reactivates within the host following transplantation from a seronegative donor (D-/R+). This occurs due to the high level of immunosuppressive agents that are taken by the patient. The third type, known as superinfection, occurs when both donor and recipient are seropositive but the reactivated virus is of donor origin, or when the individual is infected with multiple HCMV strains (Pereyra and Rubin, 2004).

Disease usually occurs within the first 6 months following transplantation. Among the risk factors for developing disease is immunosuppression, which can include calcineurin inhibitors, corticosteroids, mycophenolate, and anti-thymocyte globulin, a T-cell depleting agent. HCMV disease itself is also a major risk factor in graft rejection and worse disease outcomes following transplantation. In a large Spanish study including 1427 patients who had received either a kidney, liver, heart or double transplant, 7.2% developed CMV disease, with rejection and mortality being significantly higher in those patients with HCMV disease (Linares et al., 2011).

In haematopoietic stem cell transplant (HSCT) patients, the biggest risk factor for developing HCMV disease is the serology of the recipient. In D-/R- there is almost no risk of CMV disease. In patients with intermediate risk (D+/R-), there was a 10% incidence in CMV disease. In D+/R+ situations, there is little risk as the recipient receives a graft with antigen-experienced HCMV specific T-cells. The most problematic scenario occurs in D-/R+ patients because of the risk of HCMV becoming reactivated in the recipient. This occurs due to a HCMV naïve immune system derived from the graft of a seronegative donor, which is unable to suppress the latent infection in the recipient. In Australia 53% of seropositive HSCT recipients experienced CMV reactivation, despite prophylactic ganciclovir (George et al., 2010). In HSCT patients, HCMV pneumonitis

occurred in 10-15% of recipients and was fatal in 80% of these cases, prior to the advent of anti-viral therapy (Sissons and Carmichael, 2002). However, since the 1990's there has been remarkable progress in reducing mortality due to prophylactic treatment, improved diagnosis and the incidence of HCMV disease in HSCT is <5% (de la Cámara, 2016).

1.7.1 HIV patients

In the decade following the discovery of human immunodeficiency virus (HIV), HCMV end organ disease was one of the most serious complications of AIDS, occurring in up to 44% of patients (Gallant et al., 1992). HCMV disease occurred commonly in patients with advanced HIV AIDS. Historically the most common complication of HCMV in HIV patients was retinitis, which accounted for 75-85% of HCMV disease (Kempen et al., 2003a). Since the introduction of highly active ant-retroviral therapy (HAART), retinitis rates have decreased by 75%, and additional HCMV treatment further improves survival (Kempen et al., 2003b). Co-exposure of HCMV in HIV+ neonates affects development in utero. In the USA, HCMV co-infection in the first 18 months was associated with an increased rate of disease progression and CNS disease, compared to those infected with HIV alone (Kovacs et al., 1999). In Zambia, a sub-Saharan country where HIV-2 is prevalent, a cohort study showed that being an HCMV seropositive HIV exposed neonate correlated with increased growth stunting at 18 months (Gompels et al., 2012). Thus, HCMV is a significant cause of morbidity at all stages of HIV infection, and interventions that reduce HIV disease will reduce the burden of HCMV disease.

1.7.2 Treatment

Current treatment of CMV disease is with antiviral chemotherapy with ganciclovir, valganciclovir, maribavir, foscarnet and cidofovir. In HCMV infected cells ganciclovir is initially phosphorylated by the virally encoded protein kinase UL97. Further phosphorylation occurs by cellular kinases. Ganciclovir triphosphate is then metabolised intracellularly. The inhibitory effects of ganciclovir are mediated by inhibition of viral DNA synthesis by either competing with deoxyguanosine triphosphate for incorporation into the viral DNA polymerase, or by incorporation of ganciclovir triphosphate into viral DNA, which causes termination or limited chain elongation. Maribavir inhibits UL97, preventing its action (Chou, 2008). Valgancyclovir is a prodrug of ganciclovir with an L-valyl ester side chain. Following oral administration, the valine side chain allows valganciclovir to be absorbed by sodium dependent amino acid transporters. Once in the blood stream, hepatic esterases release the valine chain, releasing the pharmacologically active ganciclovir. Resistance to these drugs occurs through mutations in either UL97

(M460V/I, H520Q, C592G, A594V, L595S, C603W, M615V) or the viral polymerase subunit UL54 (Foulongne et al., 2004). Cidofovir is a monophosphate nucleoside analogue. Unlike ganciclovir, phosphorylation to the diphosphate is performed by cellular phosphatases. Foscarnet is another drug that targets HCMV DNA replication, though unlike ganciclovir and valganciclovir, it can inhibit the HCMV polymerase without requiring phosphorylation. As with the other antiviral drugs, mutations in UL54 can also impair efficacy of foscarnet (Erice, 1999).

1.8 T-cells and HCMV

1.8.1 Overview of the adaptive immune system

Anatomical and physiological barriers prevent pathogens from entering the systemic circulation. Once these are breached, the pathogen faces the innate immune system. The major cell types of the innate immune system include macrophages, neutrophils, natural killer (NK) cells and DCs (Chaplin, 2010). These cells recognise pathogens through pattern recognition receptors (PRRs), which recognise pathogen associated molecular patterns (PAMPs). Macrophages and DCs possess bridging functions as they can activate elements of the adaptive immune system too. Include lymphoid cells include natural killer (NK) cells, NKT cells and gamma-delta T-cells (Vermijlen and Prinz, 2014).

Cells of the adaptive immune system include B and T lymphocytes. Antigen specificity is a key feature of the adaptive immune system. Unlike cells of the innate immune system, where the receptors are germ line encoded, the B and T-cell receptors exhibit a very high level of variation due to recombination of T and B cell receptor genes. When naïve B or T-cells interact with the antigen for which they are specific, they undergo clonal expansion and form immunological memory. Upon re-challenge of the pathogen, memory cells that recognise the pathogen will perform effector functions with a shorter lag time compared to the primary infection and the production of antibodies by B-cells and cytotoxic granules and cytokines by T-cells will be greater. This results in more efficient clearance of the pathogen.

The B-cell receptor is a membrane bound immunoglobulin on the surface of B-cells, which is able to recognise proteins from extracellular pathogens. These receptors are then internalised peptides from the protein are presented via HLA-II molecules. Unlike HLA-I molecules which are found on all nucleated cells, HLA-II molecules are found on thymic epithelial cells and professional antigen presenting cells such as B-cells, macrophages and DCs (Reith et al., 2005). HLA-II presents peptides to CD4+ T-cells and once activated, provide cytokines to help the B-cell proliferate. The clearance of

viruses is largely mediated by CD8+ T-cells, which recognise shorter peptide fragments presented by HLA-I expressing cells.

1.8.2 T-cell development

T-cells are derived from haematopoietic stem cells in the bone marrow which then migrate to the thymus. Upon entry of the thymus, T-cells do not express CD4 or CD8 co-receptors (double negative thymocytes). It is during this stage that re-arrangement of T-cell receptor (TCR) genes occurs and T-cells acquire their antigen specificity. The T-cell receptor is composed of an alpha chain and a beta chain, each consisting of a cytoplasmic domain, a constant domain and a variable domain. The variable domain of the TCR determines the specificity of the T-cell, and which antigens it will be able to detect. It is composed of three regions (V, D and J) and recombination of the genes encoding these allows for enormous potential diversity ($10^{15\text{-}18}$) in TCRs in an individual, although only 10^{7} clonotypes may be present in any one individual (Laydon et al., 2015). Following VDJ rearrangement, T-cells become double positive and express both CD4 and CD8. During this stage, cells are selected for their ability to recognize host HLA molecules, ensuring that T-cells can successfully sample HLA (positive selection), becoming CD4+ or CD8+ depending on whether they recognise HLA-II or HLA-I, respectively. During the single positive phase, T-cells are selected for their inability to bind HLA with host peptides with high affinity (negative selection). This ensures host cells are less likely to mount an immune response against host tissue, which could lead to autoimmune disease. Positive, and then negative selection eliminates 98% of T-cells by apoptosis. Mature T-cells can bind host HLA, but not HLA with commonly expressed host peptides. These naïve cells are then released into the periphery (Koch and Radtke, 2011).

1.8.3 Antigen presentation

Once naïve T-cells leave the thymus, they may be activated by professional antigen presenting cells such as dendritic cells, macrophages and B-cells. DCs possess the range of co-stimulatory molecules required to activate a naïve T-cell (Banchereau et al., 2000). The first signal required by T-cells for activation is the binding of the TCR to peptide-HLA (pHLA). For HLA-I, the proteasome continually produces peptides from intracellular proteins. Heat shock proteins transport these peptides to the ER where they are transferred by the transporters of antigenic peptide (TAPs) to the luminal side of the ER. HLA molecules are held in a semi folded state by calnexin in the ER. When beta-2-microglobulin binds to HLA-I, calnexin dissociates and binds to a TAP transporter protein. Chaperone molecules in the ER load peptides into the groove of mature HLA-I

molecules. The HLA peptide complex is then transported via the transgolgi network to the surface of the cell, where they can be inspected by CD8+ T-cells (Figure 1.3).

HLA-II presents antigenic molecules to CD4+ T-cells. Bacteria, parasites and virus particles are taken up by professional antigen presenting cells such as cells of the myeloid lineage and B-cells. Proteins are degraded by early endosomes, following fusion with acidic lysosomes, resulting in the production of peptides. As with HLA-I molecules, HLA-II molecules are held by calnexin in the ER. They associate with the invariant chain (Li) a portion of which (class II associated invariant chain) protects the peptide binding groove of the HLA-II molecule until it moves to the class II loading compartment. Following ER and endosome fusion the invariant chain is degraded by acid proteases, which allows peptides from the degraded antigen to bind into the class II groove. The class II endosome then fuses with the plasma membrane allowing delivery of the HLA-II peptide complex to the cell surface (Parkin and Cohen, 2001, Antoniou et al., 2003, Klein and Sato, 2000a, Klein and Sato, 2000b).

Recognition of the pHLA by a T-cell is mediated by the T-cell receptor. For activation of the T-cell to occur, a threshold of activation needs to be acquired in order to fully activate. Viola and Lanzavecchia (1996) showed that approximately 8000 T-cell receptor-HLA interactions were required to activate a T-cell. Each binding of the TCR provides a signal via phosphorylation of the CD3 molecule and once the threshold of activation has been achieved a range of transcription factors initiate gene transcription. Binding of pHLA and TCR allows for the formation of the immunological synapse. The TCR forms at the centre of this and is surrounded by a ring of adhesion molecules such as LFA-1 (lymphocyte adhesion molecules) and CD2 which interacts with ICAM-1 (intracellular adhesion molecule) and CD58 respectively. These, along with other co-stimulatory molecules form the supramolecular adhesion complex (SMAC) which regulates the secretion of cytokines and cytotoxic granules (Dustin, 2014).

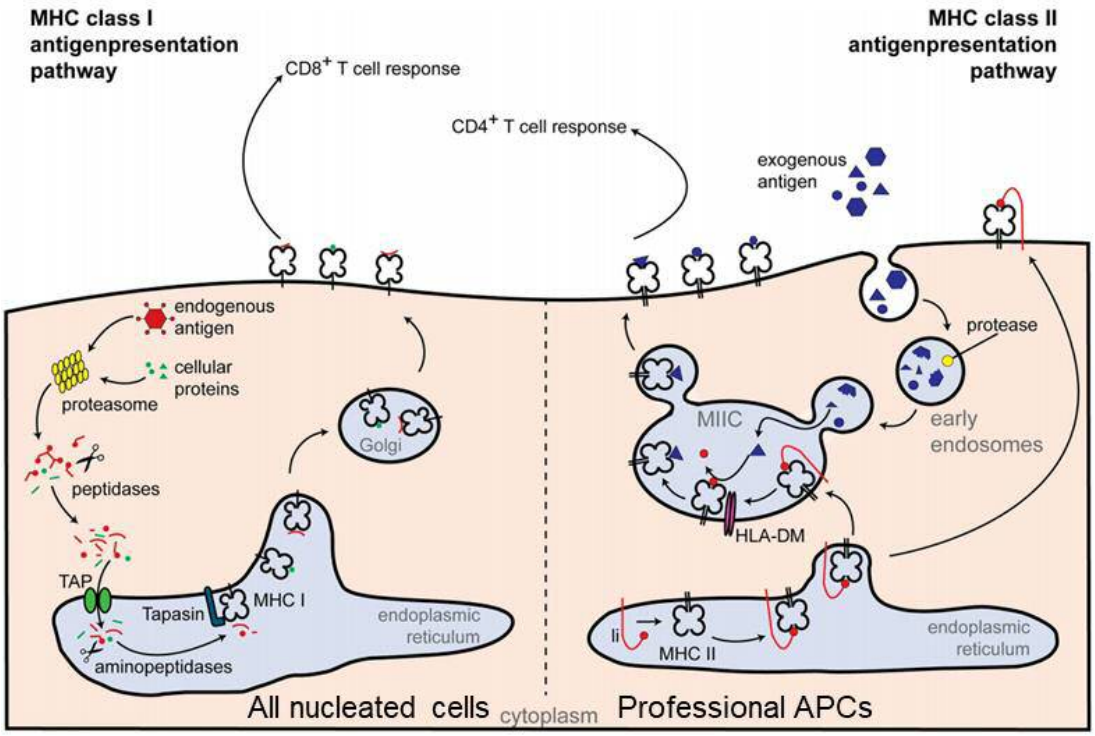

Figure 1.3 Mechanism of antigen presentation to T-cells by HLA-I and HLA-II molecules. Foreign intracellular proteins of viral, tumoural or bacterial origin are degraded by the proteasome and transported into the endoplasmic reticulum via TAP (left). Aminopeptidases further degrade peptides to shorter length (between 8-12 amino acids). In the ER peptides fit into the class 1 binding groove and are then transported to the surface. Foreign proteins such as bacteria and viruses can be endocytosed or phagocytosed by APCs (right). These are degraded by acidic lysosomes forming antigenic peptides between 12-18 amino acids in length. HLA-II molecules are assembled with the invariant chain, which covers the peptide binding groove. Following fusion with the endosome, the invariant chain is degraded and is replaced with peptide. HLAII molecules are delivered to the surface following fusion of the class II compartment with the plasma membrane. Adapted from Neerincx et al. (2013)

1.8.4 Co-stimulation of T-cells

The activation of T-cells is not solely dependent on the recognition of peptide-HLA (pHLA) by T-cells. Whilst this is the primary signal, the interaction between co-signalling (both activating and inhibitory) molecules on the T-cells and APC are essential for the determination of the outcome of TCR signalling (Chen and Flies, 2013). This is referred to as signal 2. Most molecules involved in this process are members of the immunoglobulin superfamily (IgSF) or the tumour necrosis factor receptor super family (TNFRSF). The IgSF co-signalling molecules includes CD28, ICOS, CTLA-4, PD1, TIGIT, BTLA and CD2 (Chen and Flies, 2013). TNFRSF co-signalling molecules include GITR, DR3, 4-1BB, TNFR2, OX40 and CD30 (Ward-Kavanagh et al., 2016). The ligands for these receptors are found on, or released as soluble proteins by, antigen presenting cells. A range of co-signalling molecules are shown in Figure 1.4 and displays a complex relationship, with some of the molecules present on both the T-cell and APC.

Binding of CD28 on T-cells to B7-1(CD80) or B7-2 (CD86) on APCs is essential for full naive T-cell activation (Esensten et al., 2016, Hathcock et al., 1994). CD28 family co-stimulation reduces the threshold for TCR triggering. In the absence of CD28-B7, pMHC to TCR interactions result in anergy/apoptosis. Co-stimulation of T-cells leads to proliferation, cytokine production, memory formation and survival whereas co-inhibition of T-cells (such as binding of B7 family members to CTLA4) results in cell cycle inhibition, tolerance, exhaustion and apoptosis (Chen and Flies, 2013).

Co-stimulation reduces the number of pHLA-TCR interactions required for activation from 8000 to 1500 (Viola and Lanzavecchia, 1996). Following signal 1 and signal 2, signal 3 is provided by inflammatory cytokines, such as interleukin-12 (IL-12) and interferon α/β (IFNα/β). In the absence of these cytokines, T-cells do not develop optimal effector functions and are less viable. These cytokines allow for proliferation, and the development of memory due to increased gene expression downstream of receptor signalling (Curtsinger and Mescher, 2010). Following activation of a naïve cell there is a 10^4-10^5-fold expansion in a specific clone accompanied by tumour necrosis factor (TNF), IFNγ, perforin and granzyme production and the ability to enter nonlymphoid tissue (Wherry and Ahmed, 2004).

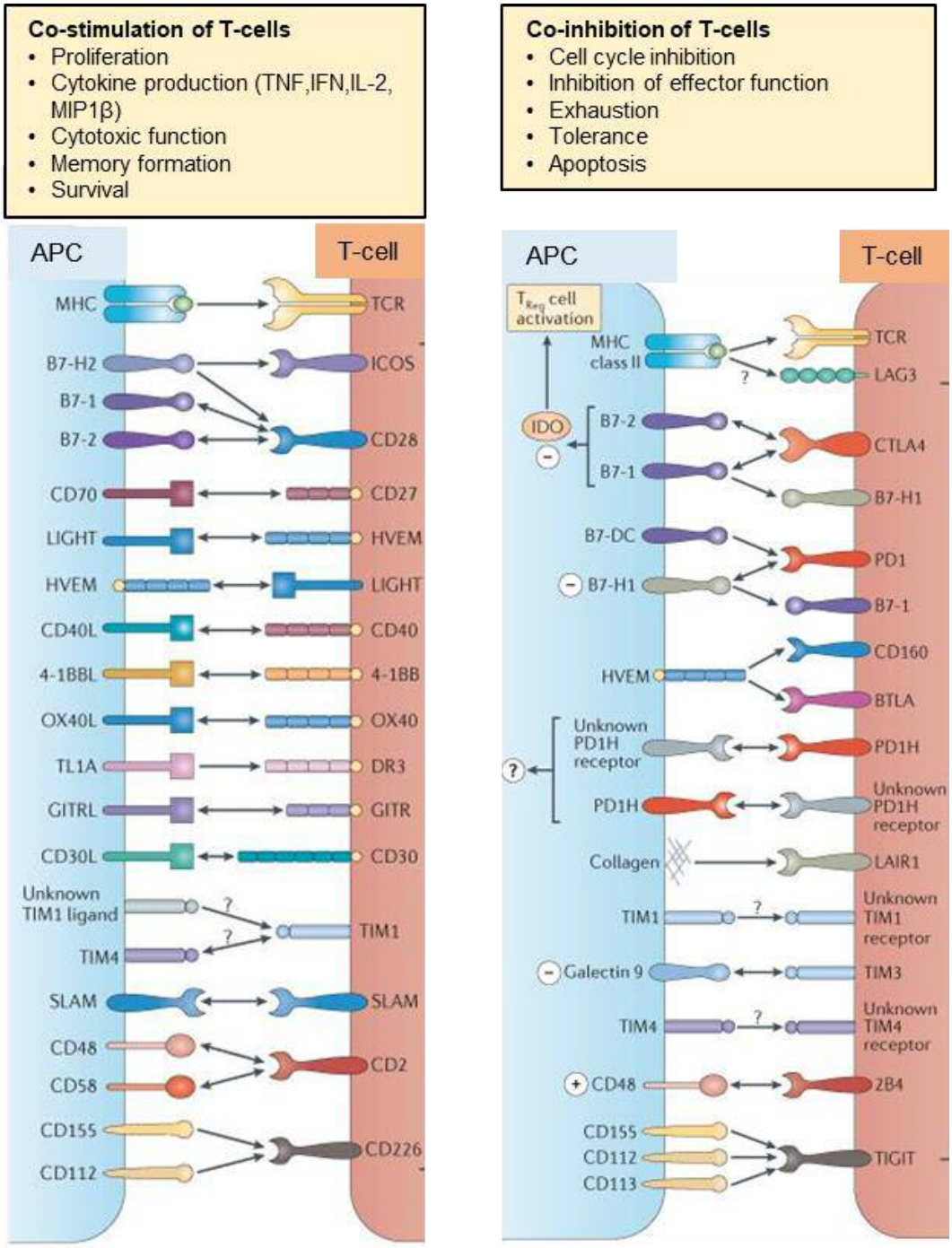

Figure 1.4 Co-signalling of T-cells. The left shows co-stimulatory ligands and their receptors on the T-cells. Some of the molecules are bi-directional and are found on the APC and T-cell. The right shows co-inhibitory signalling molecules. Because members of the B7 family can bind to multiple receptors, there is competition between members of the B7 family ligands (B7-1, B7-2, B7-H1, B7-H2, B7-DC) for CD28 family receptors (CD28, CTLA-4, PD-1, ICOS). The fate of the T-cell will depend on the dominance of the inhibitory signals versus the activating signals. ICOS inducible T-cell co-stimulator, LIGHT homologous to lymphotoxin, exhibits inducible expression and competes with HSV glycoprotein D for binding to herpesvirus entry mediator, a receptor expressed on T lymphocytes; HVEM- Herpes virus entry mediator; TL1A- TNF-like protein 1A; DR3- Death receptor 3; GITR-glucocorticoid-induced TNFR family related gene; TIM- T-cell

immunoglobulin domain and mucin domain; SLAM-signalling lymphocytic activation molecule; LAG3-Lymphocyte-activation gene 3; CTLA4- Cytotoxic T-lymphocyte associated antigen 4; PD-1 Programmed cell death protein 1; BTLA-B- and T-lymphocyte attenuator; LAIR1 Leukocyte-associated immunoglobulin-like receptor 1; TIGIT T-cell immunoreceptor with Ig and ITIM domains. Figure was adapted from Chen and Flies (2013).

1.8.5 Development of T-cell memory

The division of naïve CD8+ cells results in extensive expansion of CD8+ T-cell numbers following interaction with an antigen bearing APC. This is known as clonal expansion and results in a few antigen specific T-cells dominating the T-cell compartment for several days following the initial antigen encounter. Following activation and clonal expansion of T-cells, 5-10% will survive and form immunological memory (Wherry and Ahmed, 2004). This occurs due to activation induced cell death (AICD) of most T-cells via extrinsic and intrinsic apoptosis pathways, showing that even in antigen limited conditions, memory persists and provides immunity upon re-challenge (Lau et al., 1994, Kaech and Ahmed, 2001). Even though the initial priming of CD8+ T-cells is independent of CD4+ T-cells, CD4+ T-cells are essential for the formation of memory and rapid recall upon re-challenge (Shedlock and Shen, 2003).

CD45 is a very abundant surface glycoprotein, accounting for 10% of the cell surface proteome of T-cells (Thomas, 1989). Naïve T-cells are CD45RO-, CD45RA+ and memory T-cells are CD45RA- and CD45RO+. CD45RA- Memory cells can be further categorised to CCR7+ (central memory) and CCR7- (peripheral memory) as CCR7 is a chemokine receptor that directs homing back to lymph nodes. Memory T-cells remain specific to the antigen from which they first responded and can be found preferentially compartmentalised at the site of the initial encounter between the naïve T-cell and the antigen presenting cell (Farber et al., 2014).

1.8.6 T-cells in HCMV patients

Memory T-cells are defined by CD45RO surface expression; however, phenotyping showed a large proportion of HCMV specific T-cells express CD45RA and are therefore referred to as T_{EMRA} cells (effector memory expressing CD45RA)(Wills et al., 1999, Gillespie et al., 2000). Using tetramer technology, it was shown that a significant proportion of HCMV specific CD8+ T-cells expressed both CD45RO and CD45RA and that upon stimulation these cells could produce large amounts of effector cytokines such as IFNγ, MIP-1β, TNF and perforin. Following primary infection in a symptomatic patient, the percentage of CD45RA cells increases between 3 and 8 weeks after onset of symptoms, though this correlates with a reduction in total CD8+ cells and reduced ex-vivo cytotoxicity of peptide pulsed target cell (Wills et al., 1999). Also the cells lose the co-stimulatory molecule CD28 and are absent for CCR7 (Gillespie et al., 2000, Khan et al., 2002). These cells accumulate in the elderly, with increased proportions of tetramer specific cells in the very elderly (Ouyang et al., 2003, Olsson et al., 2000). Functionally cells from older individuals are less able to produce IFNγ and less responsive to peptide

compared to younger subjects (Ouyang et al., 2004). It has been hypothesised that this fills the 'immunological space' and reduces the repertoire of T-cells for novel antigens (Ouyang et al., 2003).

1.8.7 Antigen specificity of CD8+ T-cells against HCMV

It has long been shown that HCMV specific cells could be grown out from the PBMCs of healthy HCMV seropositive patients (Borysiewicz et al., 1983). This suggested that despite being a latent virus, the initial HCMV infection is enough to generate a memory response, or that low levels of antigen are being produced from HCMV infected cells. Follow up studies showed that IE1, and the tegument protein phosphoprotein 65 (pp65) were dominating (70-90%) the specificity of HCMV-specific cytotoxic CD8+ T-cells (McLaughlin-Taylor et al., 1994, Wills et al., 1996). Using peptide libraries, the first antigenic peptide sequences were identified and showed that 70-90% of HCMV specific T-cells could be pp65 specific in some subjects.

HCMV produces the strongest immune response of all known human viruses. This was exemplified in a longitudinal study which followed immunocompetent patients following a primary HCMV infection. In one of the patients HCMV specific cells accounted for 20% of the entire CD8 compartment. Eight weeks following infection, the activity of the cells had reduced amongst CD45RO expressing cells. Using BAC cloning of TCR's it was shown that the initial response to HCMV was made of a diverse range of TCR$\alpha\beta$ segments, though over the next year, clonal focussing of the response was observed, and a dominant TCR prevailed following resolution of the primary infection. In a broader study assessing the response to the whole HCMV genome, it was shown that HCMV specific T-cells can make up 30% of the CD8+ compartment (Sylwester et al., 2005). Of the HCMV ORF's in AD169, 81 ORFs were recognized by CD4+ T-cells and CD8+ T-cells and 26 ORFs were recognised by CD8+T-cells alone. Whilst some HCMV genes are variable (Davison et al., 2003a), HCMV genes with low strain variation have the highest number of responders, which indicates that conserved genes produce proteins which trigger stronger immunological recognition (Sylwester et al., 2005). T-cells specific to three genes products (UL48, UL83, UL123) are recognized by T-cells from more than half of HCMV seropositive subjects, indicating the immunodominance of these genes.

1.8.8 The role of T-cells in HCMV disease

HCMV disease occurs in the absence of a competent immune system. A historical study showed that 43 out of 58 bone marrow transplant recipients developed HCMV disease, and of these, 12 were fatal (Quinnan et al., 1982). From patients who survived the infection, the T and NK cell activity was higher than in those who succumbed to the

infection, as measured by specific lysis of target cells (Quinnan et al., 1982). The biggest threat of disease in HSCT patients is with D-/R+ transplantation as the bone marrow graft does not contain HCMV specific T-cells, and reactivation in the donor may occur. Using a range of HLA-A and HLA-B tetramers, the absence of HCMV re-activation significantly related to the reconstitution of at least 1 HCMV specific T-cell per 1μL of blood (Borchers et al., 2012). In solid organ transplantation the opposite situation arises, where D+/R- patients are at risk of serious disease due to HCMV being transferred into a patient who has had no prior exposure to HCMV and is on immunosuppressive drugs.

CD4+ T-cells are essential in maintaining the memory CD8+ compartment and can themselves produce antiviral cytokines. In CMV+ AIDS patients, CD4+ T-cell counts of <50, 50-100 and >100 cells/mm^3 correlated with end organ disease rates of 25%, 5.5% and 1.3% respectively underscoring the role of HCMV as an opportunistic pathogen (Gerard et al., 1997). In the pre-HAART era (1984-1996), mean CD4+T-cell count in HIV patients was 390 cells/mm3, compared to the 432 cells/mm3 in the post HAART analysis between 1997-2005 (Kim et al., 2006). The immune reconstitution resulted in a reduction in HCMV disease, and survival of patients with HCMV retinitis increased 93% (Murphy et al., 2001, Springer and Weinberg, 2004). Using tetramers CD8+ T-cells were profiled in HCMV and HIV co-infection. One study showed that HCMV specific T-cells increased in number in chronic HIV and increased further for patients receiving HAART, though the functional response was not assessed (Naeger et al., 2010). In co-infected babies, HCMV infection increased the CD8+ count, compared to HCMV-/HIV+ babies, but this had no bearing on long term complications as co-infected babies had much lower CD4 counts and worse disease progression (Kovacs et al., 1999).

T-cells from HCMV positive Gambian babies showed a significantly higher proportion of cells that were CD45RO+, CD95+, CD28-, CD27-, Bcl2-, which indicated a more activated T-cell profile compared to HCMV negative babies. HCMV specific tetramer positive cells were detected in up to 7.5% of total CD8+ T-cells indicating a degree of expansion (Marchant et al., 2003). This was also shown in longitudinal study comparing T-cells between congenitally infected infants and primary infection in pregnancy. Compared to adults, T-cells in HCMV infected neonates displayed fewer HCMV specific CD8+ and CD4+ T-cells and reduced polyfunctionality suggesting that T-cell activity was correlated with the absence of HCMV disease.

The importance of T-cells in controlling HCMV disease is highlighted by the success of adoptive immunotherapy strategies that seek to reconstitute T-cell immunity to HCMV by transfer of HCMV specific T-cells to transplant patients. In one study HCMV positive,

HLA-matched donor blood was stimulated ex-vivo with whole pp65 antigen and reintroduced to the patients. In 83% of patients who received treatment, HCMV infection was cleared or the viral burden was significantly reduced, as measured by CMV copy number (Feuchtinger et al., 2010). In another study, DCs stimulated with viral lysate were used to stimulate T-cells *ex vivo*, and HSCT recipients experienced large *in vivo* T-cell expansions and a significant reduction in recurring and late HCMV infection (Peggs, 2009).

1.9 Evasion of the cellular immune response by HCMV

Herpes viruses arose from a common ancestor approximately 350-400 million years ago. The family of herpes viruses are incredibly successful, being found in a huge range of vertebrates. Host specificity indicates that they have co-evolved with their host over a long time (Davison et al., 2003a). The success of HCMV as a lifelong pathogen is attributed at least in part to the broad range of encoded immune evasion molecules that inhibit the cellular immune response. Indeed, HCMV has become a paradigm for immune evasion, the study of which has revealed several basic immunological processes.

1.9.1 Immune evasion of T-cells

Whilst HCMV has a large genome of 226kb, most of these genes are not core genes and are dispensable for replication *in vivo.* So far, many of these dispensable genes have been found to be involved in immune evasion particularly of T and NK cells, which have essential roles in the clearance of virally infected cells. Many genes have evolved to combat different aspects of T-cell recognition, but despite this, HCMV still induces a remarkable immune response. This has been proposed to be due to the ability of DCs to cross present antigens, allowing non-infected DCs to activate T-cells (Sinclair, 2008).

1.9.1.1 Downregulation of HLA-I

The main way by which HCMV infected cells are able to by-pass immune surveillance by CD8+ T-cells is by prevention of antigenic peptide presentation, which reduces pHLA-TCR signalling events. The first report by Barnes and Grundy (1992) showed a gradual decrease in surface HLA-I when fibroblasts were infected with strain AD169, which was then shown to occur in whole cell lysates, indicating that the effect was not limited to surface protein (Yamashita et al., 1993). This downregulation occurs early in the HCMV cycle and is not due to reduced synthesis of HLA-I, but due to degradation of HLA-I heavy chains (Beersma et al., 1993, Yamashita et al., 1994). This was shown to be functionally relevant when in-vitro T-cell assays showed that HCMV infected cells became resistant to T-cell mediated lysis (Warren et al., 1994).

HLA-I is targeted through different mechanisms by several genes within the U_s region of the HCMV genome (Jones et al., 1995). Shortly after the identification of HLA-I downregulation by HCMV, the precise mechanism of how genes in the US2-US11 region downregulated HLA-I was uncovered. US3 binds HLA-I heavy chains and inhibits their maturation by preventing egress from the endoplasmic reticulum (Jones et al., 1996). US2 increases the degradation of HLA-I by utilizing the cellular E3 ligase translocation in renal cancer from chromosome 8 (TRC8) (Jones and Sun, 1997, Stagg et al., 2009). US11 causes degradation of HLA-I, but unlike US2, it direct HLA-I to endoplasmic reticulum associated protein degradation (ERAD) by utilising the pseusoprotease Derlin-1 (Wiertz et al., 1996, Lee et al., 2005, van den Boomen et al., 2014). Synergism between these genes has been reported. Co-expression of both US2 and US3 results in increased downregulation and degradation of HLA-I, by increasing the association of US2 and HLA-I (Noriega and Tortorella, 2009).

Aside from interfering with the HLA-I heavy chain, HCMV reduces peptide translocation into the endoplasmic reticulum, which is required for HLA-I presentation (Hengel et al., 1996). US6 does not target HLA-I molecules directly. Instead, it prevents peptide transport by binding to TAP inside the ER lumen (Ahn et al., 1997). The peptide transport is inversely correlated with US6 expression, which peaks at 72hpi during a lytic cycle. This results in a reduction in the level of surface HLA-I expression correlating with a reduction in CD8+ T-cell mediated lysis of target cells (Lehner et al., 1997). Orthologs of US6 are found in herpes simplex virus, Epstein-Barr virus and varicella-zoster virus (HSV, EBV and VZV), with all serving a common purpose; to prevent the transport of antigenic peptide to HLA-I molecules. This is a fascinating example of convergent evolution which shows the importance of inhibiting peptide transport for life long viral infection (Verweij et al., 2015). More recently the microRNA US4-1 was found to specifically downregulate ERAP1, a peptidase which trims long peptides to 8-9 amino acids in length. miRNA US4 reduces ERAP1 expression in HCMV infected cells, and miRNA US4-1 can impair the generation of antigenic peptides and subsequent lysis of HCMV infected cells by T-cell clones (Kim et al., 2011).

Aside from genes in the U_s region of the HCMV genome, other gene products have been found to impair T-cell mediated killing. The trafficking of mature HLA-I molecules is reduced by the tegument protein pp71, encoded by UL82 (Trgovcich et al., 2006). When expressed in isolation, pp71 does not affect HLA-I transcript levels or whole cell protein level, but only the surface expression. The precise mechanism remains unclear, though it can be concluded that pp71 affects the tracking from the ER to the surface of mature HLA-I. pp65 (pUL83), another tegument protein was also shown to affect T-cell mediated

killing. By expressing UL83 and UL121 in isolation and in combination, it was shown that pp65 had a large effect on the ability of IE1 specific T-cells to kill IE1 expressing cells (Gilbert et al., 1996). This was not the case for pp150, which suggested that pp65 selectively prevents the processing of IE1, an early immunogenic antigen. Thus, tegument proteins derived from the virion provide a level of immune suppression in the interim period between infection of the cell and translation of other HLA-I downregulating genes.

The fact that no fewer than five HCMV genes (US2, US3, miRNA-US4, US6, US11) are dedicated to reducing the presentation of antigenic peptide by HLA-I shows the importance of this pathway for allowing HCMV to maintain virulence.

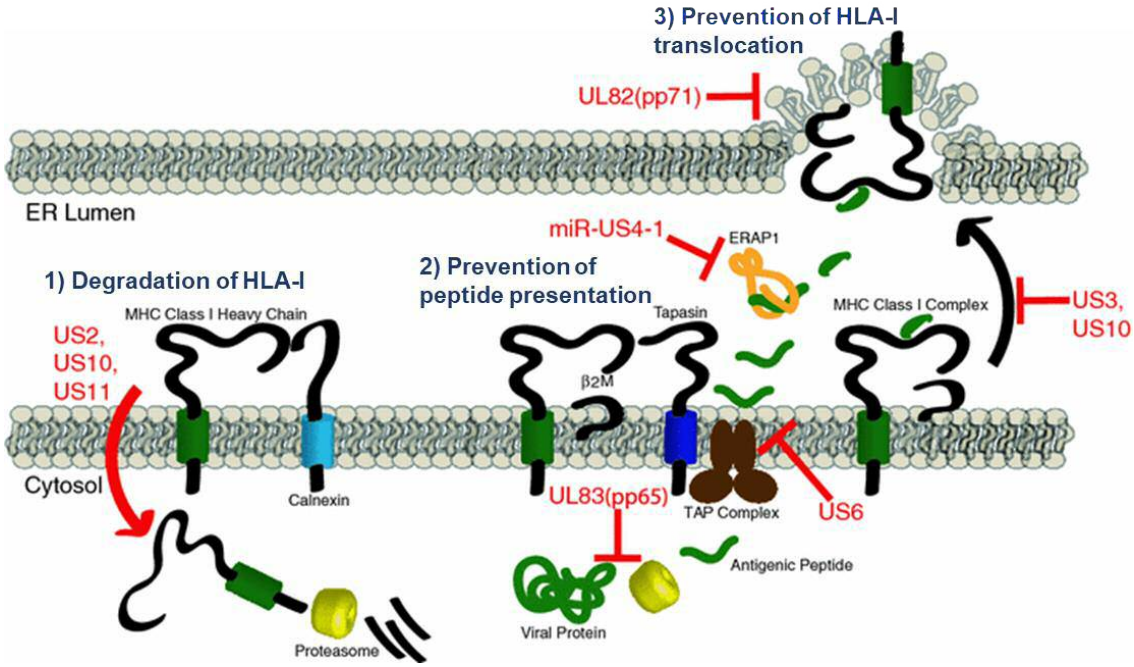

Figure 1.5 Impairment of antigenic peptide presentation in HCMV infected cells. The production of mature pHLA-I is imparied in three steps; first by targetting the HLA chains for proteosomal degradation; secondly, by preventing the availability of antigenic peptide; and thirdly by preventing translocation of pHLA-I from the ER to the cell surface. Figure was adapted from Noriega et al. (2012).

1.9.1.2 Downregulation of other HLA molecules

Whilst there is a significant investment by HCMV in combatting the main signal for CD8+ T-cell activation, many of these genes are also active in the downregulation of HLA-II molecules, which present peptides to CD4+ T-cells. In macrophages US2 causes the degradation of HLA-II molecules (Tomazin et al., 1999). This was not shown on immature or mature DCs, suggesting that HLA-II downregulation by HCMV may be more efficient in certain cell types (Beck et al., 2003). As a downstream effect of impairing interferon signalling, HCMV interferes with the IFNγ induced JAK/STAT and class II transactivator (CIITA) production (Miller et al., 1998). This impairs the production of de novo HLA-II molecules.

Unlike classical HLA molecules, HLA-G expression is generally restricted to foetal trophoblasts, and the thymus (Crisa et al., 1997). As a homodimer, HLA-G binds to co-inhibitory molecules leukocyte immunoglobulin-like receptor-1 (LIR-1), LIR-2 and KIR2DL4 on NK and T cells. Park et al. (2010) showed that HLA-G interacts with US2, resulting in degradation, similar to how US2 targets HLA-I heavy chains. HLA-G is destabilized by US10 in a proteasome dependent matter, resulting in its degradation. US10 specifically targets HLA-G via the C-terminal tail, as an HLA-G variant with the cytoplasmic domain of HLA-A2 was not degraded by US10 (Park et al., 2010).

1.9.1.3 Regulation of other T-cell co-stimulatory molecules by HCMV

Mature DCs are the best activators of naive T-cells and can activate both CD4+ and CD8+ T-cells due to their expression of both HLA-I and HLA-II molecules. Upon maturation, DCs upregulate the co-stimulatory molecules CD80 (B7-1) and CD86 (B7-2), which bind CD28 and are essential for complete naïve T-cell activation. Mature and immature DCs were infected with endothelial cell adapted clinical HCMV strains and flow cytometry was performed. When immature DCs were infected, CD80 was partially down regulated, though CD86 was unchanged (Beck et al., 2003). Mature DCs also showed this pattern, suggesting that the regulation of CD80 may be a target for HCMV immune evasion.

CD40 is found on the surface of APCs and binds to CD40L on T-cells, as well as B-cells (Elgueta et al., 2009). The signalling of CD40 leads to the maturation of DCs and the receptor is vital for immune function as demonstrated in patients with a mutation in the CD40 gene, who exhibit a defect in T-cell immunity (Fontana et al., 2003, Schneider et al., 2008). Although CD40 is downregulated following HCMV infection in mature DCs, in endothelial cells and fibroblasts HCMV infection stimulates CD40 expression (Weekes

et al., 2014, Maisch et al., 2002). HCMV has differential effects on CD40 depending on the cell type that is being infected, which could influence immune cell activation.

1.9.1.4 Regulation of T-cell signalling by HCMV

CD45 is a tyrosine phosphatase essential for T-cell signalling. UL11 is a is member of the RL11 family that encodes a surface glycoprotein that binds CD45 on T-cells to suppress proliferation and signalling by CD4+ T-cells (Gabaev et al., 2011). GpUL11stimulates the production of the anti-inflammatory and immunosuppressive cytokine IL-10 from CD4+ T-cells, which resulted in reduced IFNγ production by T-cells. The effect of HCMV UL11 expression is thus immunosuppressive by affecting the proliferation of certain subsets of T-cells (Zischke et al., 2017). The original work was performed on CD4+ T-cells, however using a similar experimental set up UL11-Fc did not affect IFNγ production by HCMV specific CD8+ T-cells, even though the soluble protein was shown to bind to them (Gabaev et al., 2014).

UL10, also a member of the RL11 gene family was shown to bind to a wide range of leukocytes specifically CD4, CD8, B B-cells, NK-cells, monocytes and neutrophils. GpUL10 binding significantly affected production of multiple cytokines from CD4+ T-cells, though a functional effect of CD8+T-cells was not ruled out as the number of IL-17 producing CD8+ T-cells was significantly reduced (Bruno et al., 2016).

1.9.2 Immune evasion of Natural Killer cells

A landmark case report came from America and described an adolescent girl who had functional deficiency of NK cells. The girl was hospitalised multiple times for herpes virus infections including varicella and cytomegalovirus, showing the importance of NK cells in preventing HCMV disease occurring in seropositive individuals (Biron et al., 1989). In total, there have been at least 19 individuals reported with classical NK cell deficiency (CNKD). Of these, 10 experienced severe consequences of herpesvirus infection (Orange, 2013).

Unlike T and B cells, the receptors of NK cells are germline encoded and not subject to rearrangement. These receptors can be inhibitory or activating. NK cells function according to the ‘missing self’ hypothesis which states that they respond to cells that display a lack of ‘self’ (HLA-I molecules); an abnormal situation as the large majority of nucleated cells express MHC-I (Shifrin et al., 2014). Because HCMV impairs HLA-I expression to avoid detect by CD8+ T-cells, HCMV infected cells should trigger NK activation. To counter this HCMV has developed a range of strategies to subvert NK cell response. A summary of NK evasion functions is shown in (Figure 1.6).

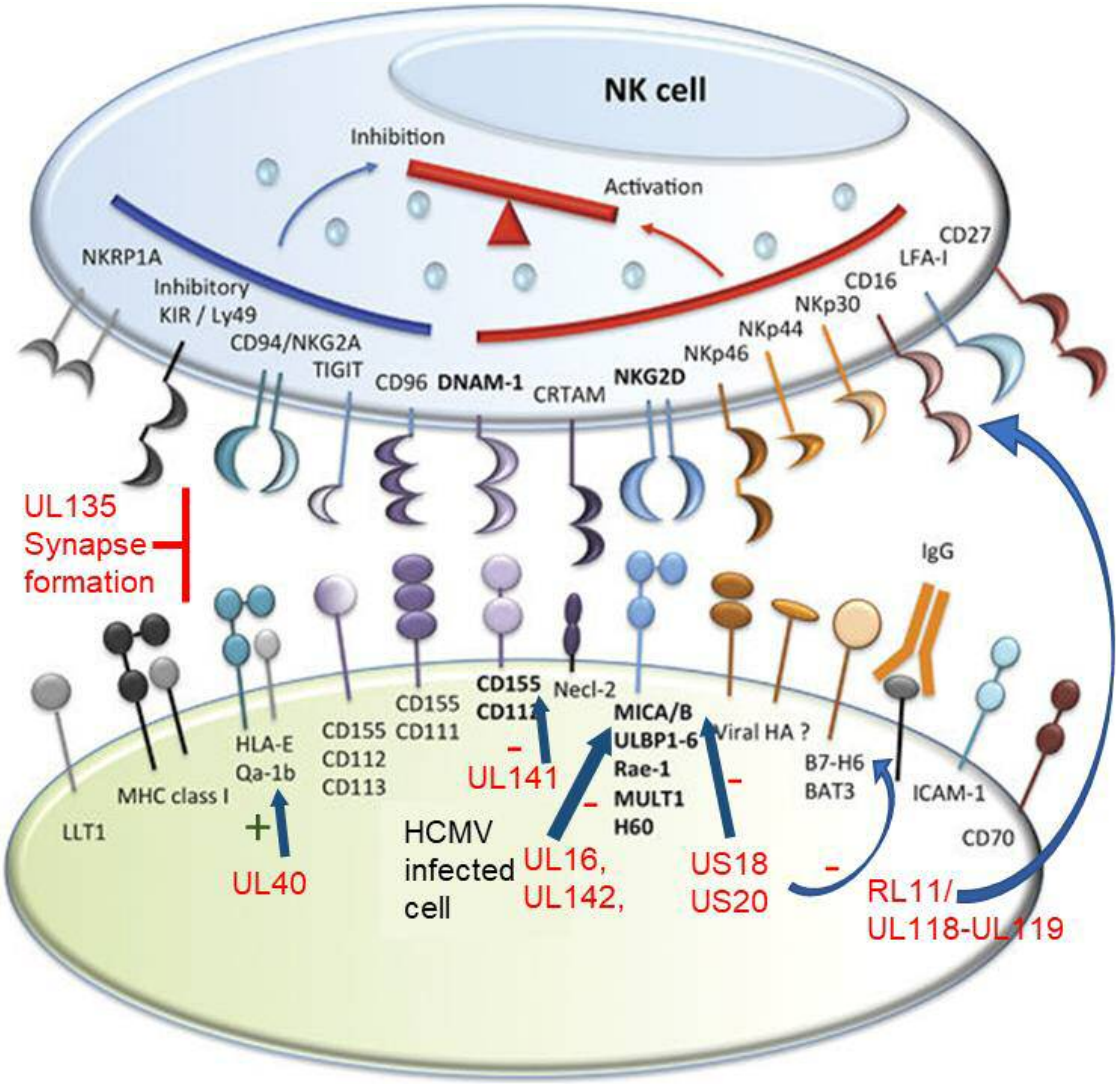

Figure 1.6 Relationship between NK ligands and receptors, and HCMV genes which affect them. The diagram shows common NK cell activating and inhibitory receptors. UL141, UL16, UL142, US18 and US20 act by downregulating NK cell activating receptor ligands. UL40 increases an NK cell inhibitory ligand HLA-E. RL11 and UL118-UL119 were shown to inhibit NK cell function by impairing the function of Fc antibody receptors which affect ADCC (antibody dependant cellular cytotoxicity) (Corrales-Aguilar et al., 2014). NKRP1A- Natural killer receptor P1A, KIR- Killer immunoglobulin like receptor; NKG2- natural killer group 2; TIGIT- T cell immunoreceptor with Ig and ITIM domains; DNAM1- DNAX Accessory Molecule-1; CRTAM- cytotoxic and regulatory T cell molecule; LFA-lymphocyte function associated antigen; ICAM- intercellular adhesion molecule; LLT1- lectin like transcript 1; Necl- nectin like molecule. Adapted from Chan et al. (2014)

1.9.2.1 Regulation of NKG2D ligands

Natural-killer group 2, member D (NKG2D) is an activating receptor expressed on NK and T-cells and binds to MHC-I related proteins (MIC) such as MICA, MICB as well as the UL16 binding proteins (ULBPs). ULBPs are named so, as they bind HCMV UL16 and were shown to activate NK cells (Kubin et al., 2001, Cosman et al., 2001). UL16 sequesters some of these proteins intracellularly and stabilises them in the ER and Golgi (Dunn et al., 2003a). This was later validated in the context of a HCMV infection using ΔUL16 viruses and showed that UL16 counteracts upregulation of MICB and ULBPs following viral infection (Rölle et al., 2003, Odeberg et al., 2003).

Whilst UL16 binds ULBP1-2 and MICB, other NKG2D ligands such as ULBP3 and MICA were unaffected, even though HCMV infection was shown to downregulate MICA (Cosman et al., 2001). Using a series of block deletions, downregulation of MICA was mapped to the US18-22 region of the HCMV genome (Fielding et al., 2014). Whilst deleting US18 and US20 individually has small effects on surface MICA, deleting both causes a large increase in surface MICA indicating that these two genes act synergistically to prevent the surface upregulation of MICA. Microscopy of HCMV infected cells shows that MICA is trafficked to the lysosome, and functionally US18 and US20 impair NK cell recognition of HCMV infected cells.

Using UL142 sequences from high and low passage HCMV strains, and ORF prediction tools, the structure of UL142 was predicted to have homology to HLA-I (Wills et al., 2005). Cells which expressed UL142 were more resistant to NK cell mediated killing, although this was not the case with all PBMC donors. Whilst ectopic expression of UL142 provides protection against NK cells by downregulating MICA and sequestering it in the cis-Golgi (Chalupny et al., 2006, Ashiru et al., 2009) this function does not explain why UL142 acts in a donor-specific manner.

UL142 is a highly polymorphic HCMV gene in clinical HCMV isolates (Chalupny et al., 2006), and it has been proposed that this is to accommodate for the diversity in MIC alleles. Indeed, MICA*008, the most common MICA allele (25.3%), was found to be resistant to UL142 mediated downregulation (Wilkinson et al., 2008, Chalupny et al., 2006). The resistance of MICA*008 to UL142, US18 and US20 can be compensated for by US9, which specifically targets MICA*008, without effecting other MICA or HLA molecules (Seidel et al., 2015).

To assess the function of HCMV encoded miRNAs, Stern-Ginossar et al. (2007) used an algorithm for the prediction of mRNA targets, with miRNA-UL112 predicted to duplex with MICB. Ectopic expression of miRNA-UL112 reduced NKG2D binding and resulted in

reduced NK-cell mediated killing. It was later shown that host miRNAs (miRNA-376A and miRNA-433) can also reduce MICB expression and that miRNA-UL112 synergises with miRNA-376A to downregulate MICB expression (Nachmani et al., 2010). These data show that HCMV has evolved mechanisms to prevent NKG2D mediated cell activation both at the protein and transcriptional level. The latter is of relevance as ectopic expression of IE1 and IE2 can increase whole cell levels of ULBP molecules and MICA/B (Fielding et al., 2014). HCMV has evolved multiple mechanisms that act in concert to systematically combat the array of NKG2D stress ligands stimulated during virus infection

1.9.2.2 Upregulation of HLA-E

NK cell activation can be regulated via the HLA-E/CD94 axis. CD94 heterodimerises with NKG2A, to form an inhibitory receptor, whereas CD94/NKG2C functions as a lower affinity activating receptor (Beziat et al., 2012). HLA-E, like other non-classical HLA molecules binds peptides. Unlike the vast polymorphism of classical HLA molecules (HLA-I and HLA-II), HLA-E exhibits limited polymorphism, and is restricted to 13 alleles, though only two of these contribute to HLA-E function; HLA-E*01:01 and HLA-E*01:03 (Kraemer et al., 2014). To be expressed at the surface of the cell, HLA-E must first bind with a nonameric peptide derived from the leader sequence of classical HLA molecules. This was originally determined as VMAPRTVLL although variations at position 8 occurs depending on the haplotype of the HLA molecule (Braud et al., 1997, Braud et al., 1998a, Braud et al., 1998b). The conserved interaction between HLA-E and CD94/NKG2A inhibits NK cell activity when cells express normal levels of HLA-I.

Comparison of amino acid sequences found that the N-terminus of HCMV UL40 from strain Merlin was homologous to the HLA-A2 leader sequence, VMAPRTLIL, as was the sequence from Toledo (Tomasec et al., 2000). UL40 to increases surface expression of HLA-E and decreases NK cell mediated killing. Despite the inhibition of TAP by US6, the UL40 peptide can be loaded to HLA-E. UL40 peptide was loaded to HLA-E and presented on the surface of TAP deficient cells indicating a TAP independent mechanism for the loading of peptide to HLA-E (Ulbrecht et al., 2000). The effect of UL40 was further shown in the context of a HCMV infection when it was deleted from AD169 resulting in increased killing by CD94+ NK cells. Blocking of CD94 increased NK killing, and PBMCs depleted for CD94+ cells did not kill HCMVΔUL40 infected cells (Wang et al., 2002). A further example of synergistic action between HCMV proteins was noted when UL40 was found to upregulate surface UL18. Further analysis showed that UL40 contains two transcriptions start sites with the first being translated to generate a signal peptide

capable of upregulating both HLA-E and UL18 and the second shorter signal peptide which can upregulate HLA-E only (Prod'homme et al., 2012).

HCMV infections are characterised by large expansions of NKG2C+ NK cells, which display an altered receptor profile and are referred to as adaptive NK cells (Guma et al., 2004). These cells are named such as they display rapid recall response and provide protective immunity against HCMV(Sun et al., 2009). To assess if sequence variation of the UL40 peptide could influence adaptive NK cell responses, UL40 variants from multiple HCMV strains were used to coat HLA-E and present to NKG2C+ NK cells. It was found that UL40 sequence VMAPRTLFL induced greater activation of NK cells compared to other UL40 sequences and could drive expansion of NKG2C+ NK cells in HCMV seronegative subjects (Hammer et al., 2018). Regardless, the presence of HLA-E restricted CD8+T cells can be detected in a third of HCMV seropositive hosts and are active against cells expressing the UL40 peptide and HLA-E (Pietra et al., 2003, Jouand et al., 2018).

1.9.2.3 Homology to HLA-I

Before the discovery that HCMV downregulates HLA-I, gpUL18 was identified as an HLA-I homolog (Beck and Barrell, 1988). When both UL18 and β2-microglobulin were expressed in combination, both proteins were precipitated together showing an interaction similar to that between β2-microglobulin and HLA-I molecules. There was also an increase in the surface expression of UL18, indicating that UL18 requires β2-microglobulin for surface expression. Initially it was suggested that HCMV UL18 was sequestering β2-microglobulin in an attempt to prevent mature HLA-I/β2-microglobulin heterodimers (Browne et al., 1990), though this was later ruled out as high levels of free β2-microglobulin were found on the surface of HCMV infected cells (Beersma et al., 1993). UL18 is also able to bind peptides derived from host proteins (Fahnestock et al., 1995). Significance of this homology to HLA-I was revealed when it was shown that gpUL18 inhibited NK-cell function when HLA-I deficient cells were transfected with UL18 (Reyburn et al., 1997).

The ligand for gpUL18 was identified as leukocyte immunoglobulin-like receptor 1 (LIR-1, CD85j) (Cosman et al., 1997). Surface plasma resonance revealed that LIR-I has a greater than 1000-fold higher affinity for strain AD169 gpUL18 compared to HLA-I (Chapman et al., 1999). A complication in understanding gpUL18 function was that the inhibition of NK cells by UL18 was donor specific, with only some showing a response against gpUL18 expressing cells. The issue was resolved by application of a CD107 mobilisation assay which showed that whilst gpUL18 decreased the activation of LIR1+

NK cells, this effect was offset by an activation of LIR1- NK cells (Prod'homme et al., 2007). Despite exhibiting homology to HLA-I, gpUL18 is resistant to the HLA-I downregulating genes US2, US3, US6, and US11 (Park et al., 2002). GpUL18 can also decrease activation of LIR1 expressing CD8+ T-cells (Wagner et al., 2007). UL18 restricted CD8+ T-cells have also been reported which can lyse HCMV infected cells independently of CD3/TCR engagement, and therefore UL18 can activate and inhibit both NK and T cells (Saverino et al., 2004).

1.9.2.4 Downregulation of other NK activating ligands

Decreased activation of NK-cells had been reported against cells infected with HCMV containing an intact U_L/*b*' region compared to AD169 or Towne, which lacked this region. Using primary NK cells and NK clones, it was found that UL141 was an NK cell evasion gene (Tomasec et al., 2005). Screening for changes of different NK cell activating ligands on the surface of HCMV infected cells revealed that UL141 downregulates surface CD155 (poliovirus receptor/ nectin-like molecules 5) by binding and sequestering it inside the cell (Tomasec et al., 2005), thereby impairing signalling through its activating receptor, DNAM-1.

CD112 is a second ligand for DNAM-1 and is also downregulated upon Merlin infection and was also rescued by deletion of UL141 (Prod'homme et al., 2010). This was due to proteasomal degradation. Plasma membrane profiling of cells infected with HCMV lacking each of the HLA-I downregulating genes (US2, US3, US6 and US11) revealed that US2 also downregulated CD112 by promoting TRC88 dependent degradation, the same mechanism by which it reduces HLA-I heavy chain degradation (Hsu et al., 2015). This further exemplifies how genes involved in T-cell regulation can also be involved in regulation of NK ligands. Further still, UL141 downregulates death receptors 4 and 5, which results in a reduction of TRAIL mediated killing (discussed in section 1.10.4.3).

To determine if the US12 gene family had a larger role in immune modulation, proteomic analysis was performed on cells infected with HCMV deletion mutants within the US12 family. An initial experiment with a ΔUS12-21 mutant revealed that these genes are responsible for regulating many proteins on the plasma membrane and in whole cell lysates (Fielding et al., 2017). One of the proteins that was upregulated upon deletion of US12-21 was B7-H6 which has been identified as a ligand for the natural cytotoxicity receptor (NCR) NKp30 (Brandt et al., 2009). To identify the individual genes, expanded and proteomic analysis was performed with individual knockout viruses within the US12-21 region, which revealed that US18 and US20 target B7-H6 for lysosomal degradation in addition to their previously described action on MICA (Charpak-Amikam et al., 2017,

Fielding et al., 2017). This supports earlier findings that many HCMV proteins target multiple host proteins to aid in immune evasion. A range of immune modulatory molecules were shown to be regulated by US12-21 genes, including T-cell costimulatory molecules such as ICOS-L.

1.9.2.5 Modification of the actin cytoskeleton

A systematic screen of genes in the U_L/*b*' region showed that UL135 impaired the degranulation of NK and T cells (Stanton et al., 2014). Cells infected with MerlinΔUL135 were less rounded and more spread out compared to Merlin, when assessed by microscopy indicating that UL135 has an important role in the characteristic morphological changes following HCMV infection. UL135 also reduced the number of fibroblast-NK cell complexes. In a HCMV infection f-actin was lost from the center of the cell, but following MerlinΔUL135 infection, a proportion of actin remained in the center of the cell indicating that UL135 remodels the actin cytoskeleton. Using SILAC-IP and a range of RAd-UL135 variants, it was shown that UL135 interacts with AB1/AB2, which are involved in the formation of the WAVE regulatory complex that regulates the actin nucleator Arp/2 (Takenawa and Suetsugu, 2007). This interaction is critical for the immune evasion elicited by UL135 when assessed by NK cell degranulation and adhesion (Stanton et al., 2014).

In summary, the study of NK cell evasion by HCMV has revealed the importance of basic immunological processes and the discovery of novel immune ligands. These include HCMV encoded genes which activate of inhibitory pathways (LIR1, HLA-E) and the downregulation of activating ligands (MIC, ULBP, DNAM1, B7-H6).

1.10 Modulation of the Tumour Necrosis Factor Receptor Superfamily and HCMV

1.10.1 Overview of the Tumour Necrosis Factor Superfamily

The ligands and receptors of the tumour necrosis factor (TNF) superfamily regulate many cellular processes such as organogenesis, apoptosis, cell differentiation and cytokine proliferation and co-stimulation. There are at least 26 known receptors and 31 known ligand receptor pairs (Figure 1.7, (Lang et al., 2016). The tissue expression of receptors varies greatly. For example, TNFR1 is found on most nucleated cells, whilst others have a more defined pattern of expression such as RANK, which is found on osteoclast precursor cells (Boyce and Xing, 2007) while 4-1BB is found predominantly on activated T-cells (Wen et al., 2002).

Based on intracellular adaptor proteins, the family of receptors can be divided into three groups. The first group includes receptors whose activation causes recruitment of intracellular signalling molecules that express death-inducing domains such as TNFR associated death domain (TRADD) and first apoptosis signal (FAS)-associated death domain (e.g. FAS, TNFR1, and death receptor 3). The second group includes receptors which recruit TNF-receptor associated factor (TRAF) (e.g. TNFR2, CD40, CD27). The third group of receptors includes those that do not signal, but compete with other receptors for ligands, such as osteoprotegrin (OPG) which can bind to RANKL.

The ligands of the family can be secreted as is the case for lymphotoxin (LT), though most function as transmembrane proteins that can act locally such as CD95L, TRAIL, GITRL, CD40L. These ligands have pleiotropic properties due to the fact they can bind to more than one receptor or may have different effector functions depending on where the receptor is expressed. A notable example is lymphotoxin which can cause necrosis of tumours but also is crucial in the organogenesis of secondary lymphoid organs (Carswell et al., 1975, De Togni et al., 1994).

Despite the pleotropic nature of receptor ligand interactions, different TNFRSF receptors/ligands show high levels of amino acid homology. The majority of ligands of the TNFRSF are type II transmembrane proteins, which means they have intracellular N-terminus and extracellular C terminus domains. Ligands have a conserved C-terminal domain termed the TNF homology domain (THD), which is a framework of aromatic and hydrophobic amino acids. This domain is responsible for receptor binding and there is 20-30% sequence homology between family members. Additionally, there is similarity in how ligands bind to receptors. Crystal structure of TNF bound to TNFR1 showed that TNF binds as a trimer to three receptors (Banner et al., 1993). This 3:3 stoichiometry was also observed for TRAIL binding to DR5 (Cha et al., 2000). Work by Wyzgol et al. (2009) showed that stabilisation of ligand trimers of CD27L, CD40L, 4-1BBL and GITRL improved the activity of these soluble trimers, further showing that ligand trimerization of TNFRSFs improves function.

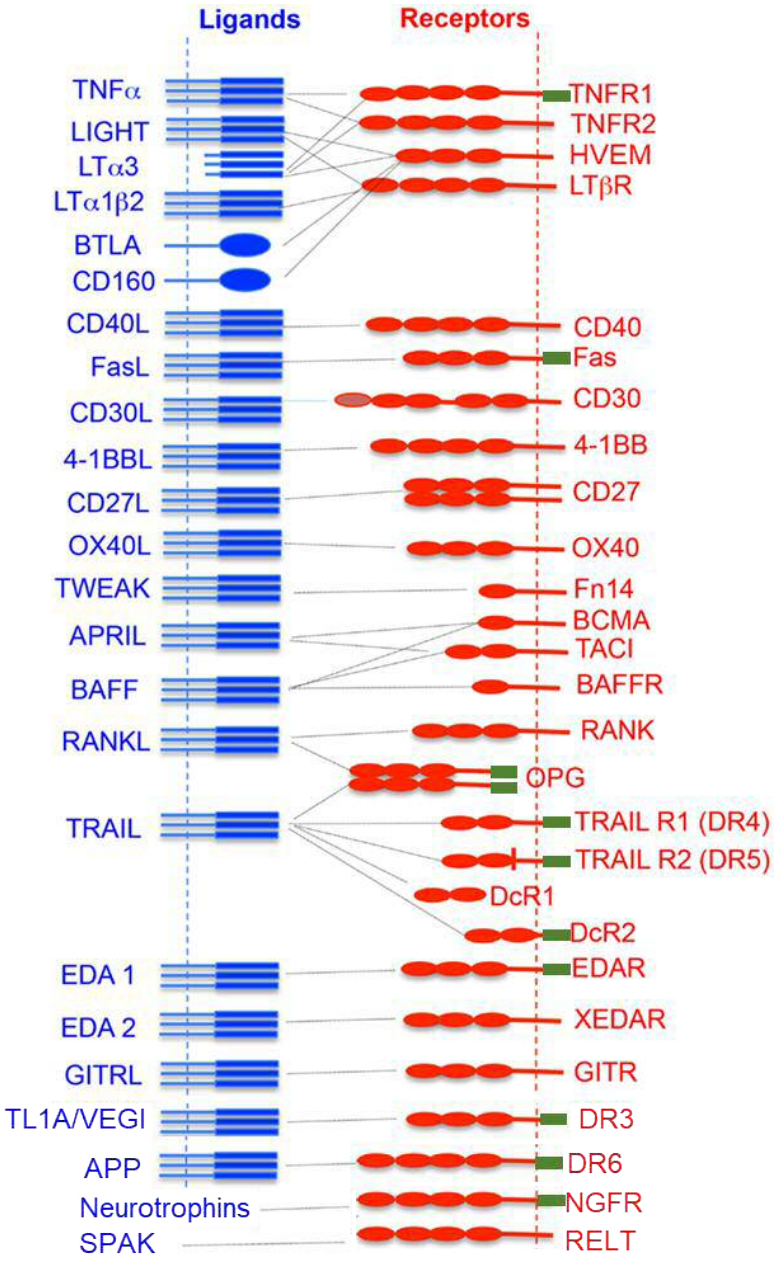

Figure 1.7 The tumour necrosis family super family of receptors and ligands. Ligands are shown in blue and receptors in red. The vertical dotted line represents the cell membrane where ligands or receptors are attached. The number of red ovals represents the number of cysteine rich domains. The green rectangles represent the presence of a death domain. TNF Tumour necrosis factor; LT lymphotoxin; BTLA B and T Lymphocyte Associated; TWEAK- TNF related weak inducer of apoptosis; EDA Ectodysplasin A; GITR; glucocorticoid-induced TNFR-related protein; APP-amyloid precursor protein; SPAK-Ste20-related proline-alanine-rich kinase; RELT-Receptor expressed in lymphoid tissues; LTβR- Lymphotoxin β receptor; Fn14- Fibroblast growth factor-inducible 14; BCMA- B-cell maturation antigen; TACI- transmembrane activator and CAML interactor; BAFFB cell-activating factor; OPR- osteoprotegrin; TRAIL TNF related apoptosis inducing ligand; DcR decoy receptor; XEDAR- X-linked ectodysplasin-A2 receptor; NGFR- Nerve growth factor receptor; DR- Death receptor. Adapted from Sonar and Lal (2015).

1.10.2 Overview of TNF and TNFR1/2

As early as the 1800s, patients undergoing cancer regression were found to have concurrent bacterial infections and in 1893 William Coley tried to replicate this by using a mixture of live and dead bacteria to treat tumours (Nauts and McLaren, 1990). It wasn't until 1975 when Lloyd Old's group showed that the tumour necrotizing effects induced by LPS were not direct but were mediated by a soluble factor causing necrotic degeneration of tumours (Carswell et al., 1975). A decade later, the cDNA of tumour necrosis factor (TNF) was cloned and expressed. Both recombinant and natural human TNF were found to produce substantial necrotic responses, verifying the earlier reports of LPS induced tumour necrosis factor (Pennica et al., 1984, Shirai et al., 1985).

The TNF (and LT) gene are found within the MHC III region on chromosome 6p21, between the MHC class I and class II genes (Carroll et al., 1987, Nedwin et al., 1985). TNF has two forms; the 17kDa soluble form and the 26kDa membrane bound form, suggesting that the soluble molecule may need to be produced by cleavage of a receptor bound molecule (Kriegler et al., 1988). TNF was shown to be cleaved by a metalloproteinase at the cell surface, which releases the ectodomain of TNF into the supernatant. The enzyme, tumour necrosis factor activating enzyme (TACE) also known as A Disintegrin And Metalloproteinase (ADAM17), is a zinc metalloproteinase which is present on most immune cells (Mohler et al., 1994, Gearing et al., 1994, Black et al., 1997, Moss et al., 1997). ADAM17 has been shown to be responsible for the shedding of other TNFRSF receptors and ligands (Scheller et al., 2011).

After its characterisation in 1984-85, the true importance of TNF was realised as it was found to orchestrate a range of cellular functions including cell death, survival, differentiation, proliferation and cytokine production (Ashkenazi and Dixit, 1998, Waters et al., 2013). Upon activation of lymphocytes, TNF is one of the earliest genes to be transcribed with levels of TNF mRNA within lymphocytes peaking at 30min post stimulation (Goldfeld et al., 1992). Its rapid production shows its importance as an early effector molecule against pathogens.

1.10.3 Signalling of TNF receptors

The two specific receptors for TNF share homology in the extracellular region but differ in their cytoplasmic motifs. TNFR1 is found on most nucleated cells, whereas the expression of TNFR2 is limited primarily to lymphocytes, endothelial cells and cells of the myeloid lineage such as DCs and macrophages, which are reservoirs for HCMV (Carpentier et al., 2004). TNFR1 possesses a death domain and can activate apoptotic pathways following the binding of TNF to TNFR1. TNFR1 signalling can also promote

cell survival by increasing transcription of cellular inhibitors of apoptosis (cIAP), which inhibit caspase 3 activation. The contrasting outcomes of apoptosis and survival was uncovered when Micheau and Tschopp (2003) showed that TNFR1 signalling involves two signalling complexes; complex 1 and complex 2.

Death receptor signalling is complex with regards to the enzymes, and ubiquitination, which regulates the activation and degradation of signalling molecules (Wertz and Dixit, 2010). The following is a simplified description of the TNF signalling pathway (Figure 1.8). Upon binding of TNF to TNFR1, the adapter molecule TRADD (TNF receptor associated death domain) is recruited. TRAF2 (TNF receptor associated factor) and RIPK1 (receptor interacting protein kinase1) then bind to TRADD. TRAF2 is then able to bind cIAPs (cellular inhibitors of apoptosis) that catalyse ubiquitination of RIPK1. This collection of molecules is referred to as complex 1. Polyubiquinated RIP1 recruits NEMO to the IκB kinase (IKK) complex. Activated IKK phosphorylates inhibitor of kappa B (IκB), which is bound to nuclear factor kappa-light-chain-enhancer of activated B cells (NF-κB), leading to IκB ubiquitination and degradation. The NF-κB heterodimer enters the nucleus. This allows NF-kB to bind to specific sites and increase the transcription of proinflammatory and anti-apoptotic genes. TNFR1 also activates p38-Mitogen Activated Protein Kinases (MAPK) and c-Jun N-terminal Kinases (JNK) which activate Activating Transcription Factor 2 (ATF2) and Activator Protein 1 (AP-1). These signalling pathways can potentially alter the expression of 500 genes which initiates a wide range of effector functions (Faustman and Davis, 2010).

The other mechanism of signalling is via complex 2, which results in apoptosis following binding of TNF to TNFR1. As with complex 1, TRADD is recruited to the cytoplasmic domain of TNFR1. However, modification occurs and TRADD dissociates from TNFR1 and the death domain becomes available to bind FADD (Fas associated death domain), which in turn recruits caspase 8/10. One of the genes transcribed downstream of NF-kB signalling, is FAD-like IL-1beta-converting enzyme (FLICE) inhibitory protein (FLIP) and is a master regulator of apoptosis (Kreuz et al., 2001, Safa, 2012). FLIP binds to FADD, caspase 8/10, cleaves RIPK1/3, and also forms an apoptosis inhibitory complex, preventing complex 2 formation. Therefore, TNF mediated apoptosis can be subject to a checkpoint, dependent on the lack of complex-I mediated FLIP production downstream of NF-kB (Kreuz et al., 2001). TNFR1 is predominantly proinflammatory as long as the protective mechanisms of NF-kB are not impaired (Wajant, 2015).

Unlike TNFR1, TNFR2 does not have a death domain, and as such it is not considered to directly activate cell death pathways (Cabal-Hierro and Lazo, 2012). TNFR2 can

recruit TRAF2 and TRAF1, cIAP1 and cIAP2 upon activation. TRAF signalling can then occur as with TNFR1 with transcription factors NF-κB MAPK and AP1 entering the nucleus, resulting in pro-inflammatory gene expression. TNFR2 signalling can result in TRAF2 ubiquitination and subsequent proteasomal degradation. This suggests that TNFR2 signalling is controlled by an autoregulatory loop (Cabal-Hierro and Lazo, 2012). TNF receptors are important on myeloid cells such as macrophages and DCs, which express both receptors. Despite the conventional theory about TNFR2 and non-cell death pathways, TNFR2 activation sensitized cells to TNFR1 mediated necroptosis, a cell death pathway that occurs when caspase enzymes are inhibited (Siegmund et al., 2016). Crossover of function has been reported, with increased cell death when both TNFR1 and TNFR2 were stimulated, compared to TNFR1 alone (Bigda et al., 1994).

Whilst the two receptors share homology in their extracellular regions, the affinity of binding by TNF is different. Determination of the dissociation constant at 37˚C revealed significantly higher affinity of soluble TNF (sTNF) for TNFR1 rather than TNFR2, which has designated TNFR1 as the main transducer of sTNF signalling. Binding studies have shown that TNF has a very high binding affinity to TNFR1 ($Kd = 1.9 \times 10^{-11}M$) and a significantly lower affinity for TNFR2 ($Kd = 4.2 \times 10^{-10}M$) (Grell et al., 1998). Whereas sTNF primarily exerts its biological activity through TNFR1, multimeric TNF (mTNF) can activate both TNFR1 and TNFR2 (Grell et al., 1995).

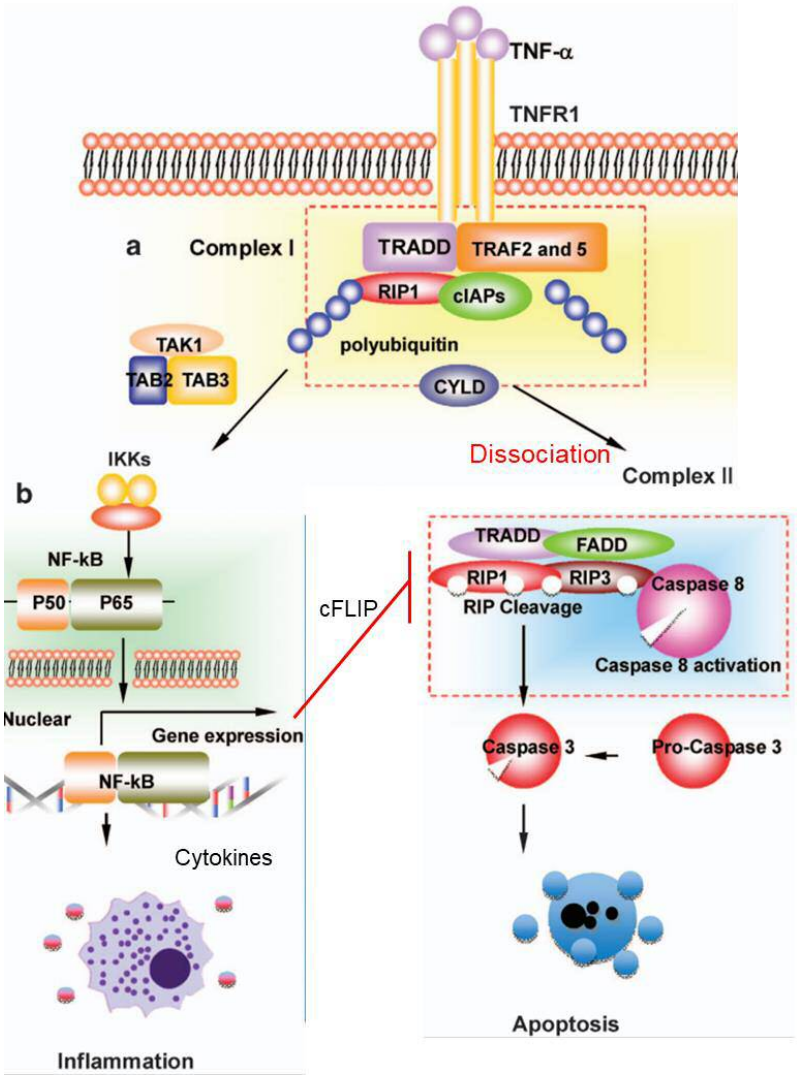

Figure 1.8 The TNF signalling pathway. TNF binding to TNFR1 causes conformation changes that allow binding of TRADD to the death domains of TNFR1.TRADD recruits TRAF2/5, RIP-1 and cIAPs to form complex-1. The signalling complex with RIP-1 ubiquitination initiates activation of IKK complex, consisting of IKKα and IKKβ, regulates IKKγ. IKKγ phosphorylates IκBα, leading to its ubiquitination and subsequent degradation. This allows NF-kB, consisting of p65 and p50 to translocate to the nucleus and bind to NF-κB binding sites. This initiates the production of pro-inflammatory genes. When complex 1 fails to activate the NF-κB pathway, and cFLIP is not produced, TRADD and RIP dissociate from the cytoplasmic domain of TNFR1. FADD and Caspase 8 are recruited to complex II. This results in the apoptosis cascade and cell death. TRADD- Tumor necrosis factor receptor type 1-associated DEATH domain; TRAF- TNF receptor associated factor; RIP- Receptor-interacting serine/threonine-protein kinase 1; CYLD Ubiquitin carboxyl-terminal hydrolase; cIAP- cellular inhibitor of apoptosis; FADD Fas-associated protein with death domain; TAK1 Transforming growth factor beta-activated kinase 1; TAB- TAK1-binding protein; NF-κB - nuclear factor kappa-light-chain-enhancer of activated B cells. Adapted from Zhao et al. (2015).

1.10.4 Regulation of TNFRSF members by HCMV

TNF has a crucial role in viral infection. This is manifested by increased viral reactivation in patients taking anti-TNF therapy (Ali et al., 2013). Given that many members of the TNFRSF are co-stimulatory molecules and influence cell death/survival, this makes them prime targets for immune evasion and inhibition of apoptosis. Herpes viruses and HCMV have evolved many ways to regulate the TNF pathway, aside from modulation of the receptors themselves. The next section discusses the advances made relating to HCMV and TNFRSF members.

1.10.4.1 Tumour necrosis factor receptor 1 (TNFRSF1A)

Initial work with AD169 showed that TNFR1 was downregulated over the course of a HCMV infection (Baillie et al., 2003). When TNFR regulation was examined using viruses containing intact U_L/*b*' regions, a gene responsible for the upregulation of TNFR1 was mapped to a gene contained within U_L/*b*': UL138 (Montag et al., 2011, Le et al., 2011). Functionally, UL138 expressing cells were shown to increase TRAF1 expression and increased HCMV IE1 expression upon TNF challenge. This suggested that UL138 could increase sensitivity to TNF mediated viral gene expression (Montag et al., 2011). It was also shown that HCMVΔUL138 infected cells partially recovered IκBα expression when challenged with TNF, which is normally completely degraded in mock infected cells upon TNF challenge. UL138 is expressed in latent infection and was shown to increase TNFR1 in CD34+ THP1 cells (Weekes et al., 2013).

1.10.4.2 Fas (TNFRSF6)

Fas can signal to cause apoptosis following ligation with Fas ligand (CD95L), which plays a crucial role in controlling virally infections. Our lab demonstrated that HCMV starts downregulating Fas at 24hpi (Seirafian et al., 2014). Infecting cells with a range of HCMV strains causes Fas downregulation, though this does not occur with irradiated virus indicating that Fas downregulation requires *de novo* gene synthesis (Seirafian et al., 2014). Efforts to map the HCMV function modulating Fas using a series of HCMV block deletion mutants and a bank of replication deficient adenoviruses encoding all HCMV canonical genes were not successful (Seirafian, 2012). However Fas regulation could be a product of multiple HCMV genes acting together. In CD34+ myeloid cells, subversion of Fas induced apoptosis is mediated by the host anti-apoptotic factor PEA-15 (Poole et al., 2015). Moreover, the inhibition of Fas-mediated apoptosis occurs in both lytic and latent HCMV infected cells. FasL is increased in human retinal pigment epithelial (HRPE) cells infected with HCMV, and soluble FasL secreted from HCMV infected cells is capable of inducing apoptosis of immune cells (Chiou et al., 2001). Therefore, the

regulation of Fas-FasL signalling is manipulated by HCMV both at the ligand and receptor level.

1.10.4.3 TRAIL-R1/2 (TNFRSF10A, TNFRSF10B)

TNF-related apoptosis inducing ligand (TRAIL) receptors 1 and 2 are able to transmit apoptotic signals to the cell by using similar adapter molecules leading to caspase activation. The ligand for these receptors is TRAIL/Apo2L. Following TRAIL ligation, FADD is recruited, followed by caspase 8 and caspase 10, which activates the caspase cascade (Mahalingam et al., 2009). TRAIL binds to TRAIL-R1/2, which possess death domains, but it can also bind to decoy receptors such as TRAIL-R3/4 and osteoprotegrin, which may function to antagonise apoptosis signalling (Wang and El-Deiry, 2003). Our laboratory showed that the glycoprotein encoded by UL141 is responsible for downregulation of both TRAIL-R1/2 (Smith et al., 2013, Nemčovičová et al., 2013). Microscopy showed that TRAIL receptors were localised to the endoplasmic reticulum by UL141. Apoptosis assays showed that cells infected with HCMVΔUL141 were more resistant to TRAIL-dependent NK cell effector function, which expanded on the previously identified role of UL141 as a NK evasin targeting CD155 and CD112 (Smith et al., 2013).

1.10.4.4 Herpes virus entry mediator (HVEM)

The herpes virus entry mediator (HVEM) is a TNFRSFR that has multiple ligands including LIGHT, CD160, B- and T-lymphocyte attenuator (BTLA) and LT. HVEM also acts as a receptor for the entry of herpes simplex virus (Steinberg et al., 2011). Signalling results in the recruitment of TRAF molecules and subsequent NF-kB activation. UL144 was shown to encode a HVEM homologue (Benedict et al., 1999). Treatment of HCMV infected cells with LT and LIGHT, ligands for HVEM, resulted in reduced spread of HCMV, following a low MOI infection (Benedict et al., 2001). Interestingly, human TNFRSF ligands do not bind to UL144, but instead UL144 causes NF-kB activation in isolation via recruitment of TRAF-6 to the cytoplasmic domain of UL144 (Poole et al., 2006).

Significantly reduced proliferation of CD4+ T-cells was reported in the presence of plate bound UL144 (Cheung et al., 2005). This was attributed to the binding of UL144 to BTLA, a member of the Ig family of co-stimulatory receptors and demonstrated how virally regulated TNF receptor homologs can influence T-cell proliferation. Different genotypes of UL144 were identified from the amniotic fluid of HCMV infected mothers, though they did not carry any prognostic value in infected foetuses (Picone et al., 2005).

1.10.4.5 CD40

CD40L (CD154) is found on the surface of T-cells and binds to its cognate receptor CD40 (TNFRSF5), which is found on APCs. This interaction leads to the activation of B-cells and allows them to become antibody producing plasma cells. On T-cells CD40 is important for co-stimulation and is essential for the generation of memory CD8+ cells by receiving help from the CD40L expressing CD4+ T-cells (Bourgeois et al., 2002). Upon infection of mature DCs with HCMV, CD40 is downregulated (Beck et al., 2003, Moutaftsi et al., 2002). This results in decreased production of the inflammatory cytokines IL-12 and TNF when the HCMV infected cells are challenged with CD40L. Proteomic analysis of HCMV infected fibroblasts was able to show that CD40 was increased on the cell surface upon infection with strain Merlin (Weekes et al., 2014). Thus, the regulation of CD40 by HCMV may differ depending on the cell type it infects.

1.10.4.6 Proteomic analysis of other TNFRSF receptors

Plasma membrane profiling revealed that a range of other TNFRSF members are subject to large changes in expression following HCMV infection of fibroblasts (Figure 1.9). The increase in TNFR1 correlated with cellular levels of UL138, which exhibits Tp1 kinetics. TNFR2 was shown to be increased dramatically on the cell surface relative to uninfected cells. The decoy receptors TRAIL-R3 and TRAIL-R4 were shown to be decreased, along with TRAIL-R1 and TRAIL-R2 (1.10.4.3). Whilst these findings are to be followed up, proteomic analysis of cells infected with deletion mutants from the US12-21 region did reveal that TWEAKR (TNFRSF12) and CD30 (TNFRSF8) involved US18 and US20 (Fielding et al., 2017). The downregulation of LTBR was also shown to require US12 family members US16 and US18, although this was not validated by flow cytometry. The functional relevance of many TNFRSF members in HCMV infection remains to be investigated.

1.10.4.7 Inhibition of death receptor signalling

HCMV encodes genes that can prevent apoptosis itself, downstream of FAS, TNFR1 and TRAIL-R1/2 signalling. In HCMV, UL37 localises to the mitochondria and rescues cells from Fas mediated apoptosis (Goldmacher et al., 1999). Bax, a mitochondrial permeabilising protein, is relocated by UL37 to the mitochondrial associated membrane (MAM). This results in increased ubiquitination and degradation of Bcl-2 associated C-protein (Bax), preventing release of apoptosis inducing molecules from the mitochondria (Zhang 2013). The adjacent gene, UL38, is also a known apoptosis inhibitor, as well as being responsible for growth of the virus. Fibroblasts infected with AD169ΔUL38 were shown to be more susceptible to cell death, which was rescued by

ectopic UL38 expression (Terhune 2007). UL36 prevents apoptosis by inhibiting Fas mediated apoptosis by forming a complex with pro-caspase-8 and is therefore termed viral inhibitor of caspase-8 induced apoptosis (vICA) (Skaletskaya et al., 2001). The genes UL36-38 all exhibit immediate early kinetics, and therefore shows that subverting apoptosis is a crucial function early in the HCMV lytic cycle and allows the replication cycle to initiate without the threat of apoptosis. Aside from these genes, IE2 can bind to the c-FLIP promoter and increase cellular levels of c-FLIP, an inhibitor of caspase activity (Chiou et al., 2006).

As with the range of NK and T cell evasion mechanisms, the prevention of apoptosis signalling affords HCMV the ability to complete the replication cycle and contributes to viral pathogenesis.

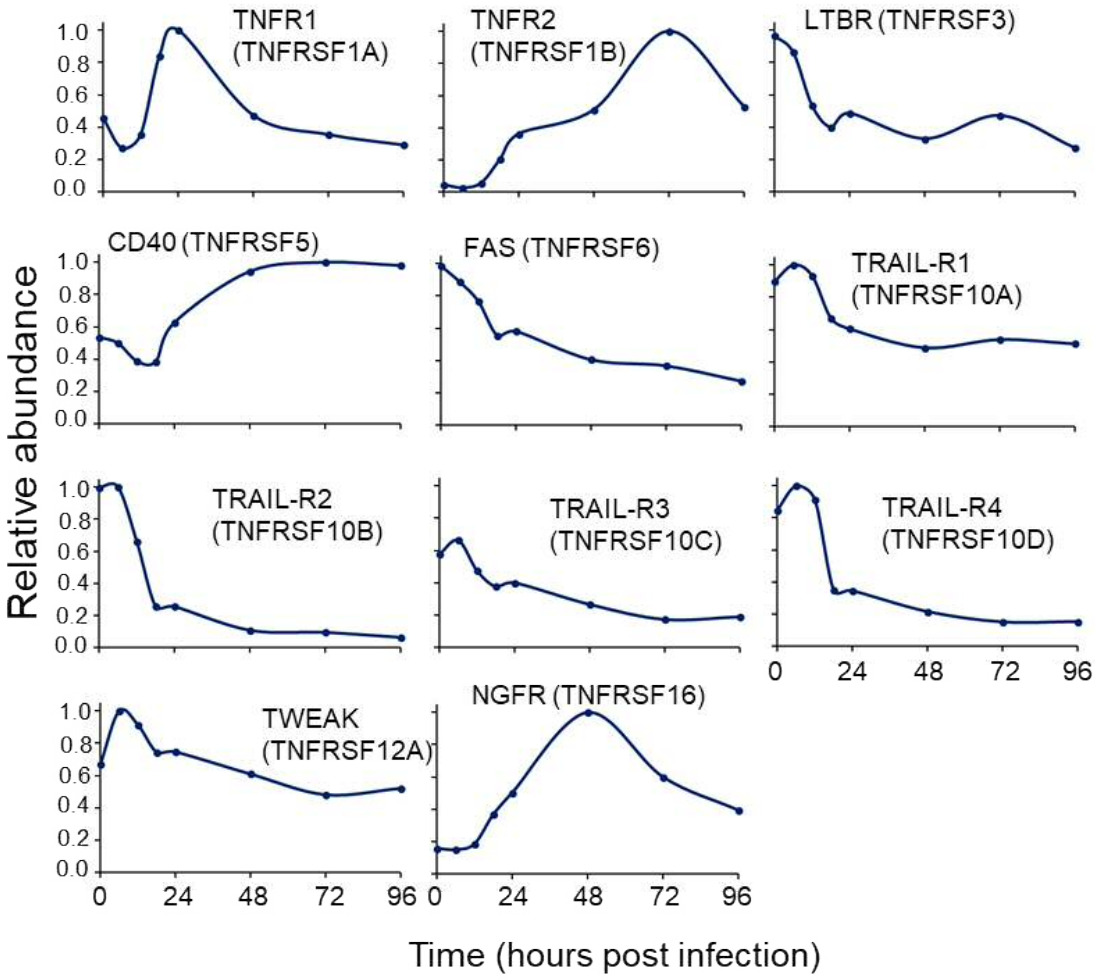

Figure 1.9 Regulation of TNFRSF members by HCMV. Data was generated from the source paper Weekes et al. (2014). The relative amounts of protein at the plasma membrane are shown, with the maximum amount plotted as 1, with other values plotted as a relative value. A minimum of 3 peptides was detected for each protein, except for TRAIL-R1 (1 peptide).

1.11 Hypothesis and Aims

My thesis explores and tests 2 major hypotheses. The first is that there are genes located within the HCMV genome, other than in the US2-11 region, that impair the activation of HCMV specific CD8+ T-cells. Given the wide range of co-signalling molecules (Figure 1.4), we believed there would be HCMV-encoded genes that could target these. The second hypothesis is that HCMV will also target pathways triggered by effector cytokines, in this case TNF. Of all the TNFRSF members detected by proteomic analysis, the largest change in relative expression was observed with TNFR2 (Figure 1.9). It would be predicted this receptor should have a role in altering the response to TNF. Thus, uncovering the regulation of TNFR2 will help further define the response of HCMV to inflammatory cytokines.

Aims

1) To identify novel immune regulatory genes encoded by HCMV that impair the activation of CD8+ T-cells.
2) Identify potential genes and the mechanisms that underpin the increase in TNFR2 during a HCMV lytic infection.
3) Assess the functional significance of increased TNFR2 on HCMV infection.

2 Methods and materials

Ethics Statement

Healthy adult volunteers provided blood and dermal fibroblasts for this work with informed consent, and sample usage was recorded following Human Tissue Act 2006 legislation. The study was approved by the Cardiff University School of Medicine Research Ethics Committee (SMREC), applications 10/20 and 16/52.

2.1 Reagents

Unless stated otherwise, reagents required for tissue culture media were from Gibco (Thermo Fisher Scientific). Analytical grade chemicals were acquired from Fisher (Thermo Fisher Scientific) or Sigma.

2.1.1 Antibodies

Antibodies were used according to the manufacturers' instructions unless otherwise stated. For flow cytometry, all antibodies were diluted in FACS buffer unless stated otherwise.

Table 2.1 Antibodies used.

Target protein and fluorophore	Company and product code	Clone	Dilution and use
α-CD8-APC	Biolegend 301049	RPA-T8	1/100 (FC)
α-CD8-PE/Cy7	Biolegend 301012	RPA-T8	1/100 (FC)
α-CD8-APC/H7	BD Pharmingen 560273	SK1 (RUO)	1/100 (FC)
α-CD3-PE/Cy7	Biolegend 300316	HIT3a	1/100 (FC)
α-CD3-FITC	Biolegend 300440	HIT3a	1/100 (FC)
α-CD107a-PerCP/Cy5.5	Biolegend 328616	H4A3	1/100 (FC)
α-CD107a-FITC	BD-Pharmingen 555800	H4A3	1/100 (FC)
α-CD120b-PE	Miltenyi 130-107-705	REA520	1/100 (FC)
α-CD120b-Biotin	BD Pharmingen 552477	hTNFR-M1	1/100 (FC)
α-CD120a-Biotin	BD Pharmingen 550900	MABTNFR1-B1 (RUO)	1/100 (FC)
α-CD120a-PE	Miltenyi	REA252	1/100 (FC)
α-CD120b	Abcam ab109322	EPR1653	1/10000 (WB)
α-CD120b	Hycult HM2022	80M2	2µg/ml (F)
α-CD120b	BioRad 0100-0288	22221(2/220)	10µg/ml (F)
α-HLA-1-AF647	Biolegend 311414	W6/32	1/100 (FC)
α-HLA-1-PE	Biolegend 311406	W6/32	1/50 (FC)
α-HLA-1-FITC	BD Pharmingen 555552	G46-2.6	1/20 (FC)
α-V5-FITC	Invitrogen 46-0308	Polyclonal	1/500 (FC)
α-CD158b-PE	BD Pharmingen 559785	CH-L	1/100 (FC)
α-RHBDF1	Invitrogen PA5-43410	Polyclonal	1/2000 (WB)
α-RHBDF2	Invitrogen PA5-48602	Polyclonal	1/2000 (WB)
α-ADAM17	Abcam ab39162	Polyclonal	1/2000 (WB)
α-ADAM17	Abcam ab39161	Polyclonal	1/1000 (WB)
α-ADAM17	R&D systems MAB9301	111633	1/200 (FC)
α-ADAM17	Abcam ab215268	D1(A12)	100nM (F)
α-TNF-APC	Biolegend 502912	MAb11	1/100 (ICS)
α-IL2-BV421	Biolegend 500328	MQ1-17H12	1/100 (ICS)
α-IFNγ-FITC	BD Pharmingen	B27	1/100 (ICS)
goat-anti adenovirus	Abcam ab1056	Polyclonal	1/500 (IF)
α-mouse IgG-AF647	A21237 Thermo	AB_2535806	1/100 (FC)
α-mouse-IgG-HRP	BioRad 1721011	Polyclonal	1/2000 (WB)
α-rabbit-IgG-HRP	BioRad 1706515	Polyclonal	1/2000 (WB)

α-mouse IgM-PerCP/Cy5.5	Biolegend 406511	RMM-1	1/100 (FC)
α-mouse-IgG2A-FITC	Biolegend 407106	RMG2a-62	1/200 (FC)
Streptavidin-APC	Ebiosciences 17-4317-82	-	1/300 (FC)
Streptavidin-PE	Invitrogen 5866	-	1/100 (FC)
α-ICAM-1-PE	Biolegend 353105	HA58	1/100 (FC)
α-VCAM-1-APC	Biolegend 305809	STA	1/100 (FC)
α-LIR1-PE	BD pharmingen 551053	GHI/75	1/100 (FC)
α-NKG2D-PE	Ebioscience12528971	1D11	1/100 (FC)
α-DNAM1-PE	Biolegend 338306	11A1	1/100 (FC)

FC - Flow cytometry, WB - Western blot, F - functional, ICS – intracellular staining, IF – immunofluorescence

2.1.2 Tissue culture media

All tissue culture media were warmed to 37˚C prior to use on cells.

Table 2.2 Table of media used for tissue culture.

Cell culture media	Constituents
DMEM	Dulbecco's Modified Eagles Medium (4.5ml/L glucose)
DMEM X 2 (500ml)	250ml of sterile water ddH_2O, 100ml 10x Minimal essential media, 100ml FCS, 30ml sodium bicarbonate 7.5% solution, 20ml Pen/Strep (10000u/ml), 10ml L- glutamine (200mM)
DMEM10	DMEM+10% FCS, 1% L-glutamine (200mM), 2% penicillin/streptomycin (10000iu/ml)
Freezing media	90% FCS, 10% DMSO.
RPMI	Roswell Park Memorial Institute medium
RPMI10	RPMI+10% FCS, 1% L-glutamine (200mM), 2% penicillin/streptomycin (10000iu/ml)
RPMIAB	RPMI10 + 2% AB serum
Serum free DMEM	DMEM+1% L-glutamine (200mM), 2% penicillin/streptomycin (10000iu/ml)

2.1.3 Buffers and Solutions

Table 2.3 Table of buffers and solutions and their constituents. All buffers and solutions were used at room temperature unless stated otherwise. ddH_2O was obtained from Nanopore Diamond (Barnstead).

Buffer/Solution/ Media	Constituents
Agarose Gel 0.7%(50ml)	50ml 1xTAE buffer, 0.35g agarose. Mixture was microwaved until fully dissolved.
Avicel 2%	20g of Avicel and 1000ml water was mixed thoroughly until homogeneous, and then autoclaved
Concanavalin A elution buffer	250µl 4x LDS buffer, 50µl 1M DTT, 300µl 50% sucrose, 400µl ddH_2O
Concanavalin A Lysis Buffer	1% NP40, 10mM 1,10-phenanthroline, 50mM Tris-HCL, 300mM NaCl, 5mM EDTA, 1 mM MgCl2, 1 mM CaCl2.
Crystal violet/ formaldehyde fix/stain 100ml	10ml 37-40% Formalin, 90ml water, 0.4g NaH_2PO_4, 0.65 Na_2HPO_4, 0.1g crystal violet
CsCl heavy solution	1.45g/ml CsCl. (3.6M) solution in 5mM Tris-HCL, pH 7.8
CsCl light solution	1.33g/ml CsCl (2.6M) solution in 1mM EDTA, 5mM Tris-HCL, pH 7.8
Dialysis buffer	1mM $MgCl_2$, 135mM NaCl, 10mM Tris HCl, 10% glycerol, pH7.8
DNA Loading buffer	30% (v/v) glycerol, 0.25% (w/v) bromophenol blue, 0.25% (w/v) xylene cyanol FF
FACS buffer	PBS+1% FCS
Luria-Bertani (LB) agar (500ml)	10g LB powder, 7.5g agar, 500ml ddH_2O. Mixture was autoclaved
LB Broth (500ml):	10g LB powder, 500ml ddH_2O, 500µl chloramphenicol (12.5mg/ml stock). Mixture was autoclaved.
Negative selection plates (500ml)	500ml liquid LB agar, 500µl chloramphenicol (12.5mg/ml stock), 1ml streptomycin, 1ml IPTG (100mM stock), 1ml X-Gal (40mg/ml stock).
PBST	PBS+0.1%Tween20 and 0.1%TritonX

Positive Selection Plates (500ml)	500ml liquid LB agar, 500µl chloramphenicol (12.5mg/ml stock), 300µl Kanamycin (15mg/ml stock), 1ml IPTG (100mM stock), 1ml X-Gal (40mg/ml stock).
50xTAE buffer	Tris (hydroxymethyl) aminomethane: 2M, Acetic Acid: 1M EDTA, Disodium Salt Dihydrate: 50mM (Melford)
TAE buffer 1x (5L)	50ml of 50xTAE buffer, 4950ml ddH_2O
Transfer buffer (500ml)	50ml NuPage transfer buffer, 50ml methanol, 400ml ddH_2O

2.2 Cell culture

2.2.1 Preparation of Human AB serum

Serum from AB donors was obtained from the Welsh Blood Transfusion Service and stored at -80˚C until preparation. Plastic Sorvall tubes (11529944, Fisher Scientific) were sterilised by autoclaving and 30ml of serum was pipetted into each tube. The tubes were balanced to within 0.01g. The tubes were inserted into a JA-25.50 rotor (Beckman Coulter) and were centrifuged at 53300x *g* at 4˚C for 1h. In a class II tissue culture hood, the layer of fat was moved aside, and the serum was removed from the centrifuge tubes. Sera from tubes were pooled and filtered through 0.45µm bottle top filters (Millipore Durapore™ 0.45 µm). Filters were changed if clogging occurred. Filtration was repeated with 0.22µm filters (Millipore Express ™ Plus 0.22µm). Filtered sera were aliquoted into 10ml volumes and heat inactivated in a water bath at 56˚C for 30min. Tubes were stored at -20˚C.

2.2.2 Established adherent cell lines

Human foetal foreskin fibroblasts were provided by Dr Graham Farrar (Porton Down) and were immortalised using human telomerase reverse transcriptase (hTERT) by Brian McSharry as previously described (McSharry et al., 2001). These are referred to as HF-TERT cells. Transduction of HF-TERT cells with a retrovirus expressing the Coxsackie adenovirus receptor was carried out by Brian McSharry (McSharry et al., 2008) and referred to as HF-CAR cells throughout. Donor derived skin fibroblasts (SFi) were generated from skin biopsies taken by Dr Stephen Siebert or Dr Tom Pembroke. Cell lines were established by Dr Eddie Wang and immortalisation by Sian Llewellyn-Lacey or Dawn Roberts as previously described (McSharry et al., 2001). Adenovirus transformed human embryonic kidney cells (HEK-293) cells (Graham et al., 1977), stably expressing the tetraycline (Tet) repressor were purchased from Invitrogen (T-REx™-293, Cat No. R71007). MRC-5 fibroblasts were purchased from the European Collection of Authenticated Cell Cultures.

2.2.3 Passage of adherent cells

Unless stated otherwise, adherent cells were maintained in DMEM10. All cells were stored in an incubator at 37˚C with 5% CO_2. Once cells had reached 90% confluency, the media was aspirated, and cells were washed in PBS. Trypsin was added (4ml for T150, 2ml for T75 and 1ml for T25) and incubated at 37˚C for 3-5min until all cells had detached. The trypsin was neutralised with DMEM10 and a proportion of cells were

discarded to maintain 30-40% confluency. HF-TERT cells were passaged at 1/3-1/4, HF-CAR cells 1/4-1/6, SFi cells 1/2-1/3 and TREX-293 cells 1/6-1/8.

2.2.4 Cryopreservation of cells

Adherent cells were washed and detached with trypsin before being centrifuged at 470x *g* for 3min. Cells were then resuspended in freezing media at a density of 0.5-1x10^6/ml and aliquoted into cryovials. Cryovials were placed in Mr Frosty freezing pots (Nalgene) and stored at -70˚C to reduce the temperature by 1˚C per minute. The following day cells were transferred in to liquid nitrogen storage. To recover cells from liquid nitrogen, vials were thawed in a water bath at 37˚C. To wash off freezing media, cells were transferred to a Falcon tube and 10ml of media (DMEM10 for adherent cells and RPMI10 for T-cells) was added to cells dropwise. Cells were centrifuged at 209 x *g* for 5min. Media was removed, and the cells were resuspended in the appropriate media and seeded into a T25 flask for adherent cells or a 24 well plate for T-cells.

2.2.5 Counting of cells

Following detachment and neutralisation with DMEM10, cells were mixed with a stripette to ensure a single cell homogenous suspension. T-cells were resuspended with a pipette. For both adherent and non-adherent cells, 10µl of cells were added to the chamber of a Neubauer haemocytometer. The number of cells within each of at least 3 large grid squares were counted and the average was taken. This number was then multiplied by 10^4 to give the number of cells per ml of suspension. Where viability staining was required, an equal volume of cells and Trypan Blue (Sigma) was mixed and 10µl of this suspension was added to the haemocytometer chamber. Dead cells appeared dark blue under white light due to uptake of the Trypan Blue.

2.3 Generation of HCMV specific T cells lines.

2.3.1 Isolation of PBMCs

Blood from donors was transferred into a Falcon tube and 10iu of heparin was added to each 1ml of blood. Blood was carefully layered onto histopaque 1.077g/ml (Sigma). Blood was centrifuged at 470 x *g* for 20mins without brake. The buffy coat (PBMCs) was transferred into a Falcon tube and 20ml of PBS was added to each tube as a washing step. PBMC's were centrifuged at 470 x *g* for 7 mins. The cells were then washed twice in 15ml of PBS at 209 x *g* for 5min. Cells were maintained in RPMI10.

2.3.2 Generation of $CD8^+$ T cell lines

Immortalised skin fibroblasts were trypsinised, washed and resuspended in DMEM10. Cells were irradiated at 6000Gy and then coated in peptide (Severn Biotech) at 10 µg/ml in DMEM10 for 1h at 37°C. Peptides were of at least 90% purity as stated by the manufacturer. PBMC's were co-cultured with peptide coated fibroblasts at a 10:1 ratio in RPMI10 + 2% AB serum (RPMIAB), 25iu/ml IL-15 (Peprotech), and 30iu/ml IL-2 (Roche) at a density of $2\text{-}3x10^6$ PBMC per well of a 24-well plate. Cells were split based on cell density and media discolouration, with media becoming yellow upon acidification. Cytokines were added every 3-4 days keeping total concentration of IL-15 at 25iu/ml and IL-2 at 30IU/ml. When passaging was required on non-feed days, RPMIAB was used, without cytokines. Growth of peptide specific CD8+ T cells was measured by flow cytometry. Functional responsiveness was measured by CD107a degranulation assay against peptide coated autologous fibroblasts.

Table 2.4 HLA class I restricted HCMV epitopes used to generate T-cell lines (Wills et al., 2013).

Donor[a]	HLA-restriction	HCMV antigen	Epitope sequence
D3, D43	HLA-A11	pp65	501-ATVQGQNLK-509
D7	HLA-A2	IE1	316-VLEETSVML-324
D7, D8	HLA-A2	pp65	495-NLVPMVATV-506
D9	HLA-A1	pp50	245-VTEHDTLLY-253
D9	HLA-B8	IE1	198-ELRRKMMYM-207
D9	HLA-A24	pp65	341-QYDPVAALF-349
D43	HLA-B15	pp65	215-KMQVIGDDQY-223

[a] Number designates identity of the donor

[b] Numbers show start and end positions of the peptide sequence within the antigen

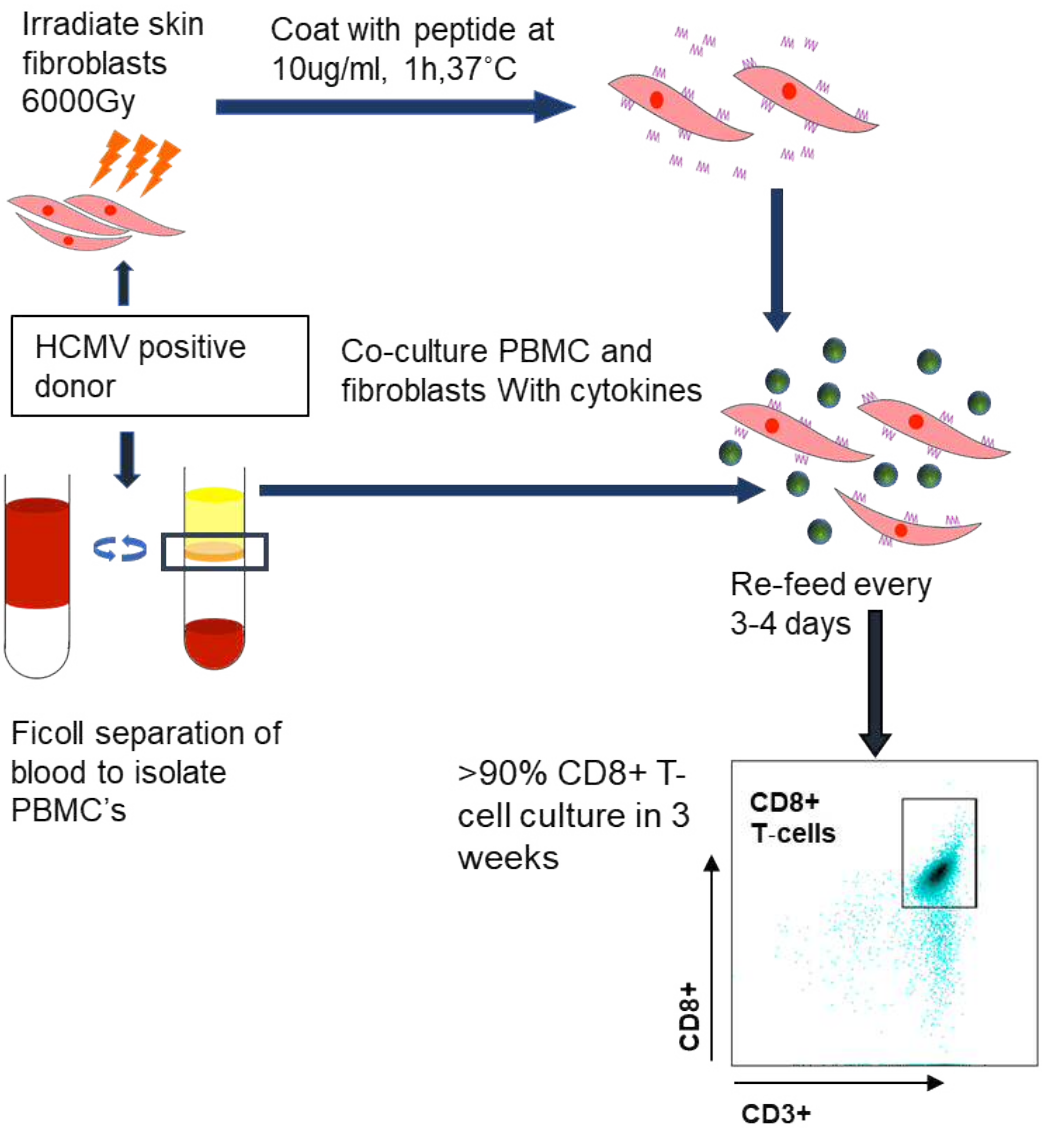

Figure 2.1 Schematic showing the generation of HCMV specific T-cells.Immortalized skin fibroblasts and PBMCs were generated from HCMV positive donors. Skin fibroblasts were irradiated and coated with peptide, prior to co-culture with PBMCs. Culture was refed with cytokines every 3-4 days. Flow cytometry was performed periodically to check proportion of CD8+ cells.

2.4 HCMV culture

2.4.1 Generation of recombinant HCMV from HCMV bacterial artificial chromosomes (BAC)

All HCMV manipulation was performed under class II conditions. HF-TERT cells were trypsinised, and 10^6 cells were put into a 15ml tube and centrifuged at 75 x *g* for 5 mins. Medium was removed to form a dry pellet. Nucleofector Solution (VPI-1002) was warmed and HF-TERT cells were resuspended in 100µl of Nucleofector Solution. Cells were put into a cuvette provided with the kit. BAC DNA (3000µg) was added to the cuvette and gently mixed. Less (2000µg) was used if the concentration of BAC was low. Cells were electroporated using the Nucleofector II (Amaxa). Cells were recovered in 5ml of DMEM10 and transferred to a T25 flask. The following day, $5x10^5$ HF-TERT cells were added to the flask to ensure a confluent monolayer. Cells were fed every 3-4 days with fresh DMEM10 as plaques enlarged. Medium (passage 1 of virus) was collected and stored at -80˚C once there was complete infection of the monolayer.

2.4.2 Growth of HCMV stocks

HF-TERT cells from 4 confluent T150 flasks was seeded into a Nunc™ EasyFill™ Cell Factory™ (ThermoFisher Scientific) with DMEM10. Once 70-80% confluency was reached, cells were infected at a MOI of 0.003. The factory was re-fed every 3-4 days with fresh DMEM10. Once the entire monolayer had become infected, the supernatant was collected, and the virus was pelleted at 29416x *g* for 2h. The pellet was resuspended in 1ml of DMEM10 and a syringe (22-gauge) was used to release virus from the cellular debris. Cellular debris was removed by centrifugation at 836 x *g* for 2min and the virus containing supernatant was frozen at -70˚C. This was repeated every alternate day until the monolayer was dead. The virus stocks from different days were thawed, then pooled and and stored at -80˚C in 300µL.

2.4.3 Titration of HCMV stocks by plaque assay.

HF-TERT cells were seeded into a 6-well plate in serum free DMEM at a density of $2.5x10^5$ cells per well. The following day, 10^{-4},10^{-5} and 10^{-6} virus dilutions were made in serum free DMEM. Medium was removed from the plate and 100µl of each virus dilution was added to each well in duplicate and 900µl of serum free medium was added. The plate was put on a rocker (Stuart See-saw rocker SSl-4) at 10 RPM, in an incubator at 37˚C in 5%CO_2 for 2h. Overlay medium was made by mixing 2 % Avicel and 2x medium at a 1:1 ratio. Following the 2h incubation the virus inoculum was removed, and 8ml of overlay medium was added to each well. The plate was incubated at 37˚C in 5%CO_2.

After 14 days the overlay medium was removed, and the monolayers were washed well with PBS. 2ml of crystal violet. Plaques were counted, and the titre was calculated.

2.4.4 HCMV infections

Fibroblasts were seeded in serum free DMEM at $10^6/25cm^2$ flask. This number was adjusted based on the surface area of other flasks used. The following day, virus aliquots were thawed in a water bath at 37˚C and cells were infected with virus in serum free DMEM for 2h on a rocker at 37˚C in 5%CO_2. The inoculum was then replaced with DMEM10. Cells were infected at a MOI 10, or 20 for viruses which infected less efficiently.

Table 2.5 HCMV variants used and contributions by other lab members.

HCMV number	Strain	Deletions/mutations	Creator
1111	Merlin (Tomasec et al., 2000)	Mutations in RL13 and UL128 locus (present in all Merlin derived viruses used in this work). Stanton et al. (2010)	N/A
1819	Merlin	ΔUL131A	Eva Ruckova
1821	Merlin	ΔUL132	Eva Ruckova
1823	Merlin	ΔUL133	Eva Ruckova
1151	Merlin	ΔUL135	Virginie Prod'homme
1825	Merlin	ΔUL136	Eva Ruckova
1847	Merlin	ΔUL138	Eva Ruckova
1849	Merlin	ΔUL139	Eva Ruckova
1851	Merlin	ΔUL140	Eva Ruckova
1149	Merlin	ΔUL141	Virginie Prod'homme
1812	Merlin	ΔUL142	Eva Ruckova
1853	Merlin	ΔUL144	Eva Ruckova
1835	Merlin	ΔUL145	Eva Ruckova
1837	Merlin	ΔUL146/US11	Eva Ruckova
1814	Merlin	ΔUL147	Eva Ruckova
1855	Merlin	ΔUL147A	Eva Ruckova
2035	Merlin	ΔUL148	Ceri Fielding
1839	Merlin	ΔUL148A	Eva Ruckova
1841	Merlin	ΔUL148B	Eva Ruckova
1843	Merlin	ΔUL148	Eva Ruckova
1845	Merlin	ΔUL148D	Eva Ruckova
1857	Merlin	ΔUL150a	Eva Ruckova
1267	Merlin	ΔUL16+GFP upstream of UL32	Rich Stanton
1642	Merlin	ΔUL18+GFP upstream of UL32	Rich Stanton
1278	Merlin	ΔUL18+UL16, GFP upstream of UL32,	Rich Stanton
1332	Merlin	ΔUL18+UL16, GFP upstream of UL32, ΔRL1-RL6	Rich Stanton
1333	Merlin	ΔUL18+UL16, GFP upstream of UL32, ΔRL10-UL1	Rich Stanton
1293	Merlin	ΔUL18+UL16, GFP upstream of UL32, ΔUL2-UL11	Rich Stanton
1294	Merlin	ΔUL18+UL16, GFP upstream of UL32, ΔUL13-UL20	Rich Stanton

1295	Merlin	ΔUL18+UL16, GFP upstream of UL32, ΔUL22A-UL25	Rich Stanton
1528	Merlin	ΔUL18+UL16, GFP upstream of UL32, ΔUS1-US11	Dan Sugrue
1297	Merlin	ΔUL18+UL16, GFP upstream of UL32, ΔUS12-US17	Rich Stanton
1318	Merlin	ΔUL18+UL16, GFP upstream of UL32, ΔUS18-US22	Rich Stanton
1299	Merlin	ΔUL18+UL16, GFP upstream of UL32, ΔUS27-US28	Rich Stanton
1300	Merlin	ΔUL18+UL16, GFP upstream of UL32, ΔUS29A-US34A	Rich Stanton
2393	Merlin	ΔUL148+UL148D	Mihil Patel
2445	Merlin	V5 tag at C-terminus of UL148	Mihil Patel
2474	Merlin	V5 tag at C-terminus of UL148, His Tag N-terminus UL148D	Mihil Patel
2193	Merlin	ΔRL11	Sepehr Seirafian
2194	Merlin	ΔRL12	Sepehr Seirafian
2199	Merlin	ΔUL19	Sepehr Seirafian
2209	Merlin	ΔRL11-UL11	Hester Nichols
N/A	AD169-varUK (Rowe et al., 1956)	Mutated: RL5A, RL13, UL36, UL131A. Deleted: UL133-UL150 (Bradley et al., 2009)	N/A
N/A	Towne (Plotkin et al., 1975)	Mutated: RL13 Deleted: 13kb deletion UL133-UL145, UL148-UL150/A	N/A
N/A	Toledo (Quinnan et al., 1984)	Mutations in RL13 and UL128 locus. Frame shift in UL140, UL141, UL145, UL150 (Dolan et al., 2004)	N/A

2.5 Adenovirus Culture

2.5.1 Growth of adenovirus

TREx-293 cells were seeded into each of 5 x T150 Cellbind flasks ($6x10^6$ per flask). At 90% confluency, cells were infected at an MOI of 0.2. Media was changed when the pH was low, as determined by yellowing of DMEM10. Sodium bicarbonate was added to buffer acidic conditions. When all cells displayed cytopathic effect (between 48-120hpi), cells were harvested by banging the flask. The cell pellet was formed by centrifuging in a 50ml Falcon tube at 470 x *g* for 5min. The supernatant was discarded, and cells were washed by resuspending in PBS and pelleting at 470x *g* for 5min.The PBS was discarded, and the cell pellet was frozen at -70˚C.

2.5.2 Purification of adenovirus on caesium chloride gradient

Cell pellets were thawed and resuspended in PBS. An equal volume of tetrachloroethylene was added. Suspensions were shaken vigorously for 30s, forming a single phase to lyse and release virions from the cells. Falcons were centrifuged at 836 x *g* for 20 min, creating two phases, with the upper aqueous phase containing virions. The upper layer was carefully pipetted off. To prepare the CsCl gradient, 1.6ml of CsCl heavy solution was pipetted into 14x89mm ultraclear Beckman centrifuge tubes and 3ml of a less dense CsCl solution light solution was carefully overlayered. Extracted virus was carefully laid on top of the gradient and PBS was added until the tubes were filled to within 2.5mm of the top. Tubes were loaded into a SW41 Ti rotor and centrifuged at 90000 x *g* for 2h at room temperature in an Ultra Beckman L8-M ultracentrifuge (Beckman). After 2h the virus appeared as an opalescent layer resting between the higher and lower density CsCl solution. The virus was harvested by puncturing the tube just beneath the virus band with a 21-gauge needle (BD) and gently pulling the virus into a 2ml syringe (BD).

2.5.3 Dialysis of purified virus

CsCl extracted virus was made up to 2ml with dialysis buffer. Dialysis tubing (Medicell International Ltd, DTV12000.01.000) was sterilised beforehand by submerging in boiled dialysis buffer and allowing to cool. Tubing was flushed with dialysis buffer and then tied at one end before loading with virus solution. The other end of the tubing was tied, and the tube was placed in one litre of dialysis buffer. The beaker was dialysed at 4˚C overnight with one change of dialysis buffer in between. Dialysed virus was removed from the tubing the next morning by cutting the dialysis tubing below the knot and then decanting into a 15ml tube. Virus was aliquoted and stored at -80˚C.

2.5.4 Titration of adenovirus by immunofluorescence

A 12 well plate was seeded with TREx-293 at $5x10^5$ cells/well in a 1ml volume and allowed to adhere overnight. The next day serial dilutions were used to prepare 10^{-4} and 10^{-5} virus, and 100µl of each dilution was added to a well in duplicate. At 48hpi, the media was aspirated and the plate was allowed to dry. Ice cold 50/50 v/v acetone and methanol (1ml/well) was added to each well and incubated at -20˚C for 10min. The acetone/methanol was aspirated and washed 3 times in PBS+1% BSA. To each well, 500µl of 1/500 goat-anti adenovirus was added and incubated on a rocker (10 RPM) at 37˚C. The antibody was aspirated and washed 3 times in PBS+1% BSA. To each well, 0.5ml of 1/500 donkey anti-goat HRP was added, and the plate was incubated on a rocker at 37˚C at 10 RPM. The antibody was discarded and washed 3 times with PBS+1% BSA. DAB (3, 3'-diaminobenzidine) substrate kit for peroxidase (Vector Laboratories SK-4100) was used to prepare a working stock of DAB solution as per manufacturer's instructions. To each well, 1ml of DAB solution was added and incubated at room temperature for 10min. Adenovirus infected cells (PFU) appeared brown under white light. The titre of adenovirus stock was calculated using the below formula.

Titer (PFU/ml) = (average number of infected cells per field of view x number of fields per well) / (virus volume used (ml) x dilution factor)

2.5.5 Infections with adenovirus

Fibroblasts were seeded in DMEM10. The following day, virus aliquots were thawed on ice and cells were infected with virus in DMEM10 for 2h on a rocker at 37˚C in 5%CO_2. The inoculum was then replaced with DMEM10. Cells were infected at MOI 10 for HF-CAR cells or reduced to MOI 5 if toxicity occurred. Skin fibroblast cells were infected at a MOI of 500. For reconstitution experiment, adenovirus and HCMV was added to the same inoculum. MRC-5 fibroblasts were infected at MOI of 20. These were based on titrations using RAd-GFP (Figure 2.2) and previous work performed by other lab members ((Seirafian, 2012, Aicheler, 2005)). Adenoviruses used in this thesis were recombineered by Dr Sepehr Seirafian, Dr James Davies and Dr Richard Stanton. All Merlin derived HCMV genes had previously been clones into the AdZ vector with HCMV genes being downstream of the HCMV MIE promoter, resulting in constitutively driven transgene expression (Seirafian, 2012). Adenoviruses used in this work were recombineered by Dr Sepehr Seirafian, Dr James Davies and Dr Richard Stanton.

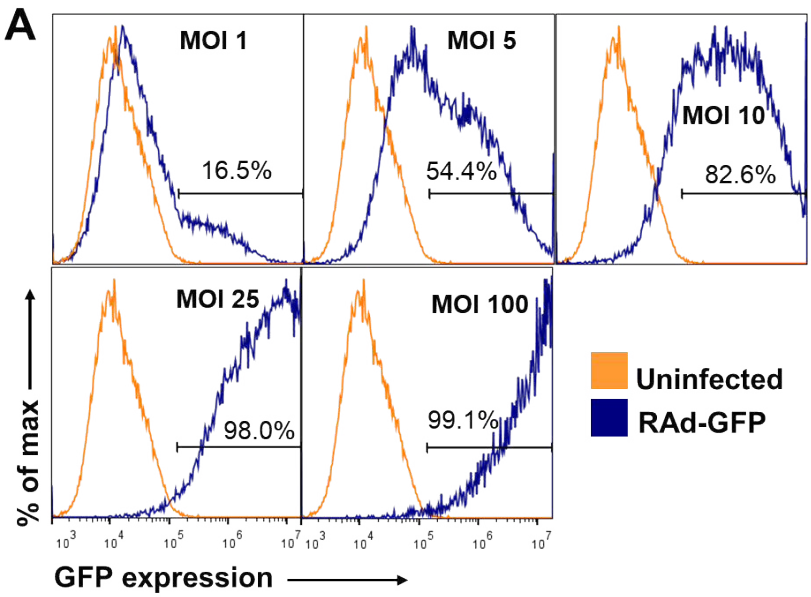

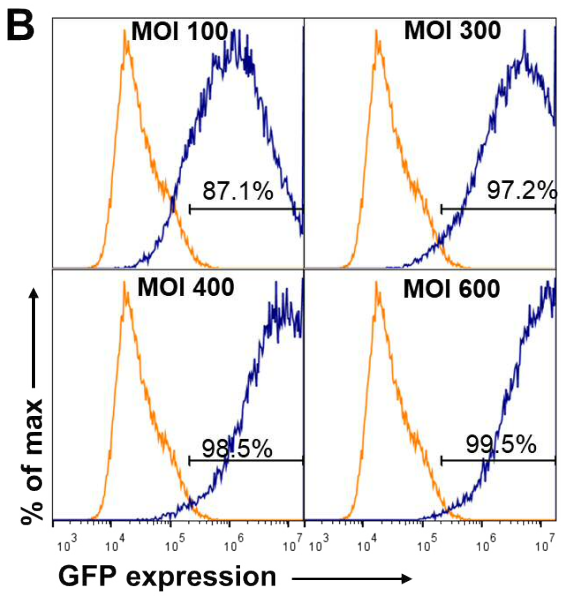

Figure 2.2 Infection efficiency of GFP expressing adenovirus. (A) MRC5 and (B) D7 skin fibroblasts were infected at different MOIs. The proportion of GFP positive cells is shown. Cells were incubated for 48hpi and then harvested, fixed and analysed by flow cytometry. Experiments were performed for D8 and D9 fibroblasts with comparable results to (B) (data not shown).

2.6 Standard molecular biology techniques

2.6.1 Polymerase Chain Reaction

Recombineering relied on the incorporation of the ribosomal S12 protein gene, which confers streptomycin resistance from *M. tuberculosis* (referred to as rpsL cassette). Amplification of the rpsL cassette was performed using Roche-Expand Hi-Fi. Primer mixes were made as follows - per 50µl; 40µl H_2O, 5µl 10x buffer 2, 1µl dNTPs, 1.5µl DMSO, 2.5µl of primer mix (1/10 of each forward and backward primer, 100mM stock), 1µl of cassette, 0.5µl of Roche-Expand Hi-Fi polymerase. The forward and backward primer were designed with arms of homology to the regions of insertion in the HCMV BAC. The following program was used for expansion using BioMetra T3000 Thermocycler.

95ºC: 2min.

95ºC: 30s, 55ºC 30s, 68ºC 4m30s (10 cycles)

95 ºC:30s, 55ºC 30s, 68ºC 4m30s+20s/cycle (25 cycles)

68ºC:15min

4ºC Hold

2.6.2 Electrophoresis of DNA

DNA was separated on a 0.7% Agaraose-TAE gel (Tris-acetate-EDTA). To stain DNA, 2.5µl of ethidium bromide (10mg/ml) was added per 50ml of liquid agarose gel. The mixture was then poured into a cassette with a comb and allowed to cool. Once solidified, the gel was placed into a tank of TAE buffer. HighRanger 1 kb DNA Ladder (Norgen Cat. 11900) was added to the first well. Loading buffer (1/6) was added to each sample and then mixed. The sample was loaded into wells of the agarose gel with gel filling tips. DNA was electrophoresed at 100V for 45-60min.

2.6.3 Purification of DNA

Following resolution of DNA, the gel was visualised under UV light. The relevant band was cut out and placed into a 1.5ml Eppendorf tube. Geneflow Q-Spin Gel Extraction/PCR Purification Kit was used to isolate DNA. The gel fragment was weighed and an equivalent amount (volume per weight) of DNA binding buffer was added (e.g. 100µl per 100mg of gel). The gel fragment was incubated and vortexed occasionally for 5-10min in a water bath (50-65˚C) until the gel was completely dissolved. The mixture was added to the spin column and incubated at room temperature for 2min.The solution

was centrifuged for 1min (16000 x g) and the flow-through was discarded. The column was washed twice with wash solution and then transferred to a 1.5ml Eppendorf tube and 30µl was added to the centre of the membrane of the column and incubated for 2min at room temperature. DNA was eluted by centrifuging the column for 1min at 16000 x g. DNA was stored at -20˚C.

2.6.4 Determination of DNA concentration

A NanoDrop ND1000 spectrophotometer was used for determining DNA concentration. Prior to running samples, ddH_2O was run through. The instrument was calibrated by running the DNA solvent (elution buffer or 10mM TRIS-HCl). DNA samples were thawed and equilibrated to room temperature and 2µl was used for measurement. The instrument was cleaned between each sample with microfibre paper. Absorbance was measured at 260/280nm.

2.6.5 Isolation of Virus DNA

Viral DNA was extracted using QIAamp® MinElute® Virus Spin kits (Quigen) as per manufacturers specifications. Briefly, virus was thawed (200µl) and mixed with 25µl of protease to breakdown viral proteins. Lysis was carried out by adding 200µl of buffer AL and mixing. The mixture was incubated at 56˚C for 15min. Ethanol was added, and the mixture incubated for 5min at room temperature. Lysate was added to the QIAamp MinElute column and centrifuged (16000 *x g*). Buffer AW1, AW2 and ethanol were added and then centrifuged (16000 *x g*) with the flow through being discarded each time. The membrane was dried and the 50µl of Buffer AVE was added to the membrane. The column was centrifuged (16000 x *g*) 1min with the flow through being frozen for analysis.

2.6.6 Sequencing of DNA

Sequencing of DNA was performed using the Mix2Seq kit (Eurofins). Recombineered sequences were amplified by PCR, gel purified and quantified as described as per the sections above. DNA was diluted to 10ng/ml with ddH_2O and 15µl was added to each tube along with 2µl of either the forward or reverse primer (100µM). Tubes were sealed, vortexed briefly and pulse centrifuged. Tubes were sent to Eurofins Genomics for sequencing. For whole genome sequencing, viral DNA was extracted as described in 2.6.5 and sent to Professor Andrew Davison (Centre for Virus Research, Glasgow).

2.7 Recombineering of HCMV BAC

2.7.1 Cassette insertion-First round

The rpsL cassette was amplified by PCR and gel purified as described in the section 2.6.1. SW102 *Escherichia Coli* were inoculated into 5ml of LB broth. Bacteria were incubated overnight in at 32˚C shaking incubator (200 RPM). The next day 0.5ml of overnight culture were seeded into 25ml of fresh LB broth and incubated at 32˚C in a shaking incubator to an optical density (OD) of 0.6. When O.D of 0.6 was reached, bacteria were put into a 42˚C water bath for 15min to activate the Lambda red genes. The Falcon tube was shaken on ice for 15min to cool. Bacteria were pelleted (3345x g, 5min, 0°C) and washed twice in ice cold ddH_2O. After the last wash, bacteria were resuspended to 400µl of ddH_2O and 25µl was transferred to a 1.5ml Eppendorf tube and mixed with 4µl of PCR product or H_2O as a negative control. Bacteria and PCR product was transferred to a pre-chilled cuvette and allowed to stand for 5min. Cuvettes were electroporated at 2.5kV. Bacteria were recovered in 1ml of LB for 1h at 32˚C (200RPM). Bacteria were pelleted, resuspended in 150µl LB and spread onto LB plates with kanamycin, IPTG, X-Gal and chloramphenicol (positive selection plates). Where bacterial uptake of cassette had occurred, blue colonies formed. Colonies (6-8) were then streaked on to positive selection plates and negative selection plates. Colonies which grew only on positive selection plates, but not on negative selection plates, were seeded as overnight cultures for mini-prepping and PCR.

2.7.2 Minipreparation of BAC DNA

Qiagen Spin miniprep kits were used for miniprep DNA generation, with solutions being prepared as per manufacturers' instructions. Overnight cultures were pelleted, and a dry pellet was formed. The pellet was resuspended in 250µl of resuspension buffer P1 and transferred to a 1.5ml tube. Lysis buffer P2 (250µl) was added and mixed, to release DNA and incubated for 5min followed by 250µl of wash buffer N3. After mixing, the tube was centrifuged for 16000 x *g* for 10min and the supernatant was transferred to a new tube. DNA was precipitated by adding and mixing of 750µl isopropanol. The DNA was centrifuged at 16000 x *g* for 10min at 4˚C. The supernatant was discarded and 500µl of 70% ethanol was added. The tube was centrifuged for 10min at 16000 x g. The supernatant was removed, and the tube was air dried for 20min, leaving a dry DNA pellet. The DNA pellet was dissolved in 30µl of 10mM TRIS-HCl pH8.

2.7.3 Restriction Digest

To confirm the recombineering process had not affected the integrity of the HCMV BAC, DNA was digested and compared against a reference HCMV BAC. In a PCR tube, 8µl of miniprepped DNA, 1µl of NE buffer 2 (New England Biolabs) and 1µl of *Hind*III (NE Biolabs) was added, pulse vortexed and pulse centrifuged. The tube was incubated for 1h at 37˚C. Loading buffer (1/6) was added and the 12µl was loaded onto a 0.7% agarose gel. The gel was electrophoresed at 100V for 45min. The gel was visualised under UV light. Recombineered BAC was compared alongside a positive control (1111 BAC).

2.7.4 Second round of recombineering

Colonies that gave the correct digest pattern and PCR product were selected for a 2nd round of recombineering. PCR products had a higher molecular weight due to the presence of the cassette when compared to the negative control (Figure 2.3). Overnight cultures were set up as before with SW102 bacteria containing HCMV BAC with the cassette. Production of competent bacteria was carried out as per 1st round of recombineering (2.7.1) and 25µl of bacteria and 1µl of oligo was mixed in a 1.5ml tube before transferring to a cuvette and electroporating. Bacteria were recovered in 5ml LB for 4h at 32˚C. Bacteria were pelleted (3345x g, 5min, 0°C), resuspended in 150µl of LB and spread on to positive and negative selection. If the proportion of white colonies to blue colonies was greater on streptomycin containing plates, then the removal of the cassette was likely successful. Colonies from these plates were grown over night and then miniprepped the next day. The DNA was digested with *Hind*III. If the pattern was correct, the region of interest was amplified by PCR and the number of base pairs was assessed by gel electrophoreses. If the region gave the correct PCR product size (fewer base pairs for knockout viruses, compared to control), then the PCR product was gel purified and sequenced. If the correct sequence was present than the BAC was maxi-prepped.

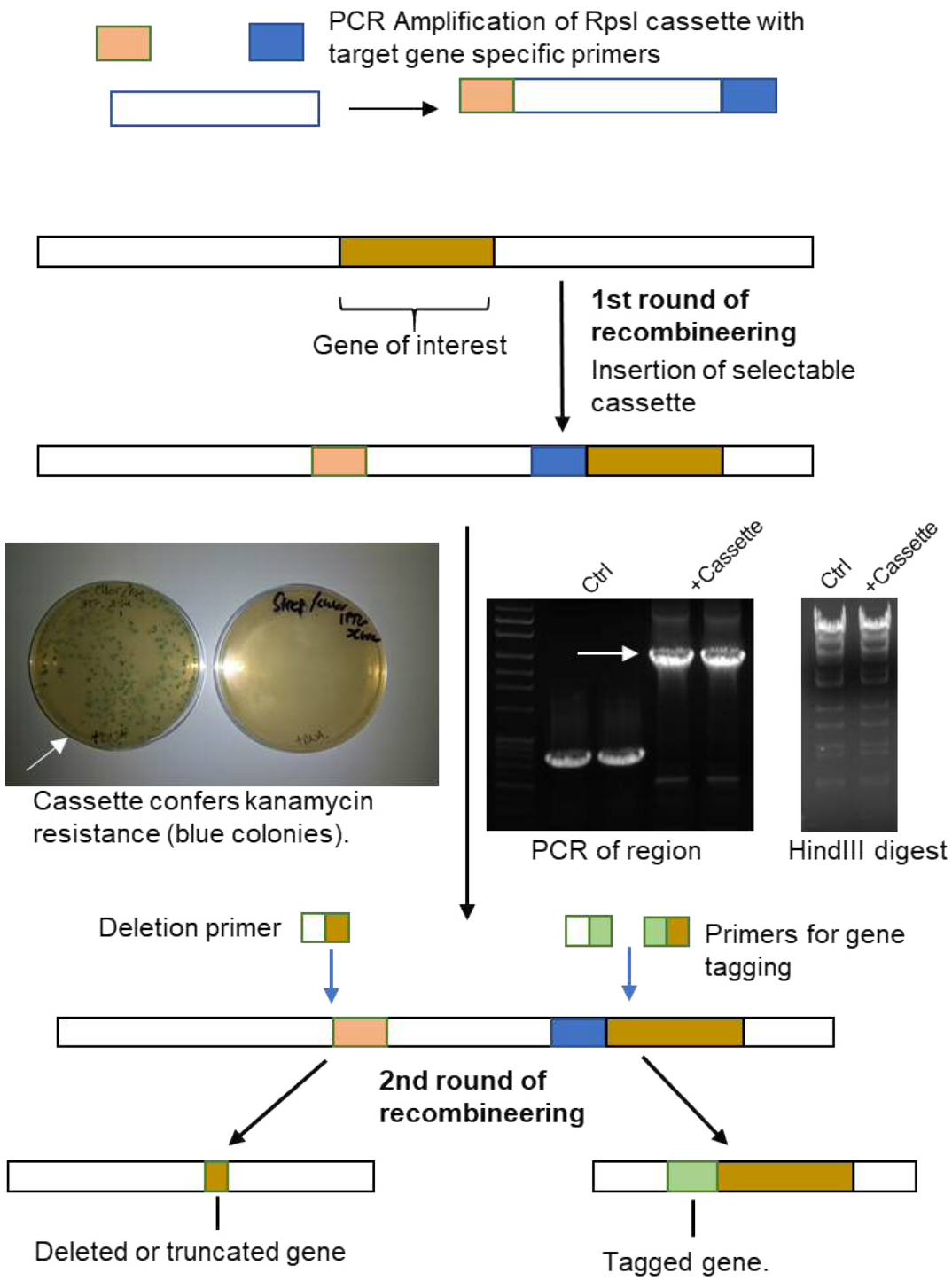

Figure 2.3 Principle of recombineering the HCMV BAC.By PCR, the rpsL Cassette was amplified with primers having homology toward the ends of the cassette and the gene of interest. Success of 1st round recombineering, was verified by picking a blue colony from the positive selection plate and then ensuring the PCR product was larger than that of a control, unmodified virus and exhibiting the correct DNA digest pattern. Primers for deleting or tagging, were used for the second round, with removal of the cassette being verified by PCR, DNA digest and sequencing.

2.7.5 Maxipreparation of BAC DNA

Large scale preparation of BAC DNA suitable for transfection, was maxi-prepped using the Nucleobond BAC100 kit (Macherery Nagel). Following overnight growth of bacteria (those shown to be correct following two rounds of recombineering) in 500ml of LB + chloramphenicol. Bacteria were pelleted at 6000g for 15min at 4˚C. Cells were lysed by resuspending the pellet in 24ml of resuspension buffer S1 followed by 24ml of lysis buffer S2. The suspension was incubated for 3min, after which 24ml of chilled neutralisation buffer S3 was added. The flocculate was inverted 8 times until a homogenous suspension was formed with an off-white flocculate. The Nucleobond column was equilibrated with 6ml of equilibration buffer N2 and allowed to empty by gravity. A funnel was placed above the column with some filter paper wetted with buffer N2. The lysate was loaded on to the column and allowed to empty by gravity. Washing was performed twice with 18ml of wash buffer N3. DNA was eluted with 15ml of elution buffer N5 which had been pre-heated to 50˚C to aid elution. DNA was precipitated with 11ml of isopropanol followed by mixing and centrifugation at 5000g for 30min at 4˚C. The supernatant was discarded, and the DNA pellet was washed with 5ml of 70% ethanol and centrifugation at 5000 x *g* for 10min. The ethanol was carefully removed, and the DNA pellet was dissolved in 100µl 10mM TRIS-HCl (pH 8.1) overnight at 4˚C. The next day the DNA was transferred to a sterile tube and stored at -20˚C.

2.8 Flow cytometry

All flow cytometry was performed on a BD Accuri (BD) or Attune NxT Flow Cytometer (Thermo Fisher Scientific). Compensation was performed manually for experiments analysed using the BD Accuri. For experiments using Attune NxT, compensation was automatically calculated by Attune NxT software.

2.8.1 Surface staining procedure

Cells were detached from the plate/flask using HyQTase™ (GE Healthcare) or TrypLE Express (Thermo), in place of trypsin, which can cleave surface proteins. Detachment reagent was neutralised with DMEM10 and cells were kept on ice. Cells were transferred to 96 well V-bottom plates and washed by centrifuging (470x *g* for 2min) in cold FACS buffer. Cells were resuspended in 100µl of antibody solution and staining was carried out for 20min at 4˚C in a darkened environment. Cells were washed 3 times with FACS buffer (470x *g* for 2min, 4°C). The process of staining and washing was repeated if a secondary antibody was used. Fixing was performed with 4% paraformaldehyde (10min).

2.8.2 Intracellular Staining

Cells were harvested as with surface staining and washed in PBS (470x *g* for 2min). For live/dead cell staining, cells were incubated with 100µl of 1/1000 Live/dead EF660 stain (eBioscience). After 15min and cells were washed twice (470x *g* for 2min) and resuspended with 100µl BD CytoFix/CytoPerm solution. Cells were incubated for 20 mins at 4˚C. The cells were washed once in 100µl 1x BD Perm/Wash Buffer, made fresh on the day. Antibodies for intracellular staining were diluted in 1x BD Perm/Wash and 100µl of antibody master-mix was added to each well. Cells were incubated for 30min at 4˚C. Washing was carried out twice in 1xBDPerm/Wash and cells were resuspended in 200µl of PBS before flow cytometry.

2.8.3 Gating strategy for T-cells

T-cells were gated using FSC-area vs SSC-area gate. Doublets were excluded by comparing FSC-height vs FSC-area of cells. Whenever used, a live/dead gate was applied to these cells, with cells having incorporated the dye being excluded from further analysis. Cells which were CD8+ and CD3+ were analysed.

2.8.4 Gating strategy for fibroblasts

Fibroblasts were gated by forward scatter (FSC) area vs Side scatter (SSC) area. When using the NxT Attune flow cytometer, the forward scatter voltage was lowered and SSC Area vs FSC height was used to gate on HCMV-infected fibroblasts due to the enlargement of cells. Anti-HLA-I antibody was used to distinguish infected cells from non-infected cells.

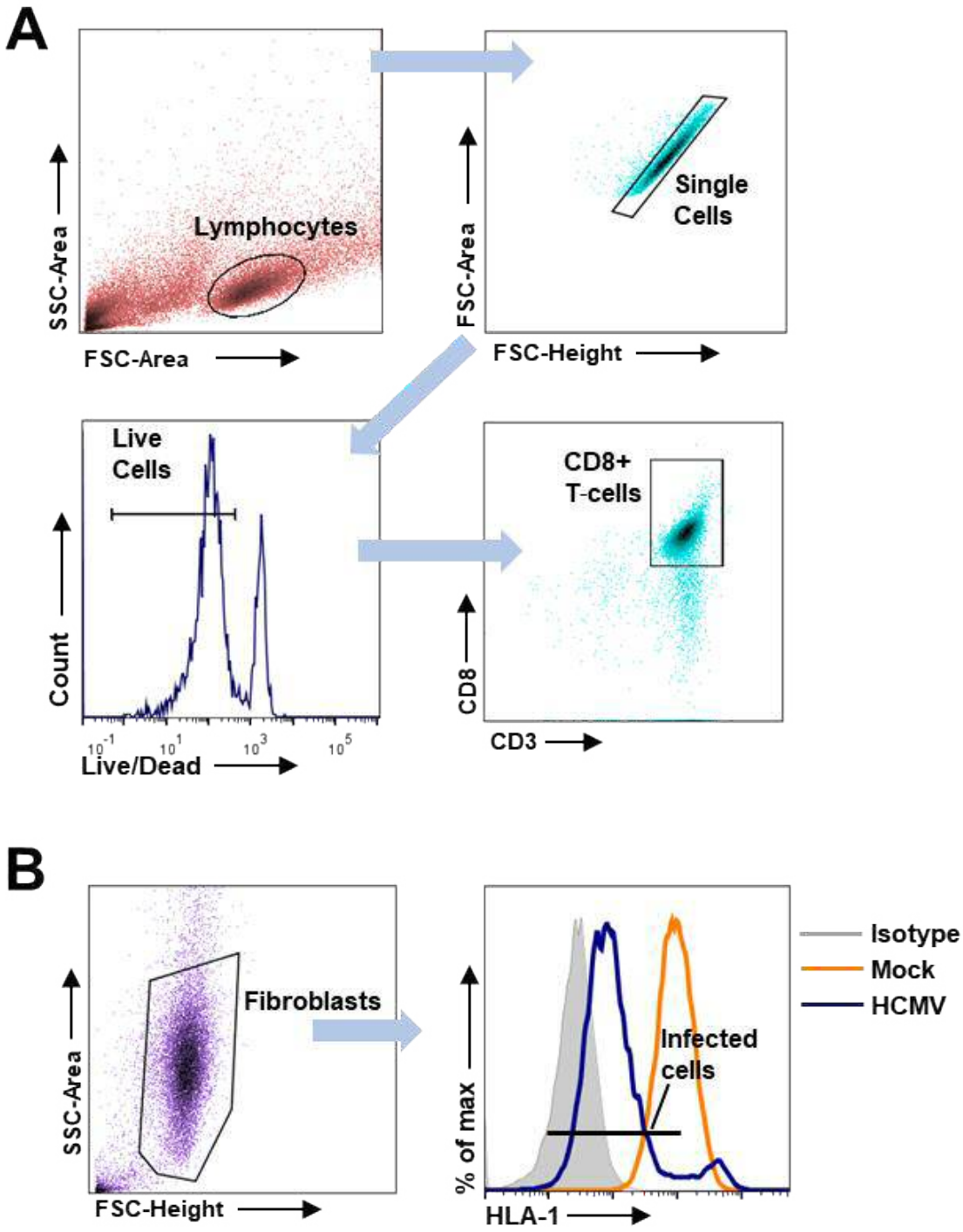

Figure 2.4 Flow cytometry gating strategy. (A) Gating of CD8+ T-cells. Cells were gated by side scatter vs forward scatter. Doublet cells were eliminated by gating on cells which proportionally increased FSC-area, compared to FSC-height. Viable cells were then selected through exclusion of a live/dead dye. Cells positive for CD8 and CD3 were analysed. (B) Fibroblasts were gated on by comparing SSC-Area vs FSC-Height. Infection efficiency was determined by performing HLA-I staining with HLA-I low cells deemed infected.

2.9 Proteomic analysis of cellular proteins by mass spectrometry

All sample preparation was performed by Dr Peter Tomasec. Mass spectrometry was performed by Dr Michael Weekes (Cambridge) as described in (Weekes et al., 2014).

2.10 Immunoblotting of cell proteins

2.10.1 Preparation of lysates

$1.5x10^6$ HF-TERT cells were infected or mock infected with HCMV. At 72hpi, cells were washed in ice cold PBS, and then ice cold PBS+ 10mM-phenanthroline. Cells were scraped into a 15 ml Falcon tube. In a chilled centrifuge, cells were pelleted at 470g to form a dry pellet. Cells were lysed in 100µl of 25% NuPage LDS lysis buffer + 1% complete protease inhibitor (Sigma). Cell lysates were sonicated to break up the chromosomal DNA. Lysates were aliquoted and stored at -80˚C.

2.10.2 Enrichment of glycoproteins by concanavalin A

This method was used for detection of ADAM17 protein in cells. In $25cm^2$ flasks, $1.5x10^6$ HF-TERT cells were seeded and infected or mock infected. At harvesting point, cells were washed twice in ice-cold PBS and then lysed for 10min on a rocker (10 RPM) on ice in 1ml of Concanavalin A lysis buffer, containing 1% complete protease inhibitor (Sigma). This was added to the buffer to prevent autocatalysis of ADAM17. After 10min, cells were scraped into a 1.5ml tube and lysates were clarified at 20,000x *g* for 1min. Lysates were mixed with 50µl of Concanavalin A beads (Sigma) washed in lysis buffer. Capture of glycoproteins was performed at 4˚C on a 360˚ rotor overnight. The following morning beads were washed 3 times in lysis buffer by centrifuging at 470g for 3min, removing the supernatant with a pipette and then resuspended by adding 1ml of lysis buffer and then placing on the rotor for 5min. Glycoprotein elution was carried out by adding 60µl of ConA elution buffer and incubating for 15min at 65˚C. Samples were frozen at -70˚C until resolution by SDS-PAGE.

2.10.3 Separation of polypeptides by electrophoresis

Samples were thawed and DTT was added (1 in 10 of >97% pure DTT) for sample reduction. Samples were heated in a waterbath (65˚C for 15 min) for reduction. Samples were centrifuged at 16000 x *g* for 1min to pellet cellular debris. NuPage 10% Bis-Tris gels (Invitrogen) were assembled in the XCell4 SureLock system and submerged in MOPS buffer. Sample (20µl) was added into each well and 10µl of Novex™ Sharp

Pre-stained Protein Standard (Invitrogen) was used for determination of protein size. Resolution was carried out for 1h at 200V.

2.10.4 Transfer of proteins on to membrane

Transfer of proteins was carried out under semi dry conditions. PVDF membranes (Amersham Hybond P 0.45 PVDF) were soaked in methanol for 10min. PVDF and 2 sheets of blotting paper were then soaked in transfer buffer for 10min. From bottom up, the transfer stack was layered; blotting paper, PVDF membrane, gel, blotting paper. Air bubbles were removed by rolling a stripette over the top of the blotting paper. The remainder of the transfer buffer was poured over to ensure adequate wetting. Transfer was performed in a Novex semi dry blotter (Invitrogen) for 2h at 10V, after which the stack was deconstructed and the PVDF membrane was rinsed in ddH_2O.

2.10.5 Blotting of transferred proteins

The PVDF membrane was dried in an incubator to allow the methanol to evaporate and therefore prevent any further protein binding. After drying, the membrane was re-wetted in PBST with 1%BSA. Antibodies were diluted in PBST+1% BSA as per manufacturers' instructions and staining with primary antibody was carried out overnight at 4˚C. Washing (3 x 5min) was performed in PBST. Staining with HRP conjugated secondary antibody was carried out for 1h at room temperature. The membrane was washed (5 x 5min) in PBST. Signal generation from antibody bound proteins was visualised with a Super Signal West Pico Chemiluminescent Substrate (Pierce). Equal amounts of each component were mixed thoroughly and added on to the membrane for 5min. Signals were recorded by visualising the PVDF membrane under UV light using a GelDoc system (Syngene). Exposure was continued until bands of intermediate strength were produced, but without saturation of the signal.

2.11 Cytokine detection

2.11.1 Enzyme linked Immunosorbent Assay (ELISA)

For TNFR2 ELISA, $1.6x10^5$ HF-TERT cells were infected in each well of a 12-well plate at MOI 10. After the 2h incubation period, 1ml of DMEM10 was overlaid. For ADAM17 blocking experiments, media was replaced with 1ml of DMEM10 containing the ADAM17 blocking antibody D1(A12) or isotype control (human IgG) at 48hpi. At 72hpi, the media was removed and centrifuged at 16000 x *g* for 1min to pellet cellular debris.

Human TNFR2 Quantikine ELISA (R&D systems DRT200) was used. Dilutions of supernatant were made in calibrator diluent RD5-5 to ensure that recorded values would

fall within the range of the calibration curve. Standards were prepared as per the manufacturer's instructions and 50µl of assay diluent (RD1-6) was added to each well of the plate followed by 200µl of sample. Wells were mixed with a multichannel pipette. The plate was incubated for 2h at room temperature in the dark. The plate was then aspirated and washed 3 times with wash buffer and 200µl of human sTNFR2 conjugate was added to each well. The plate was incubated for 1h. Washing was repeated as before and 200µl of substrate solution was added to each well. The plate was incubated until differences between the calibration standards was visible, at which point 50µl of Stop Solution (2M sulphuric acid) was added to each well to quench the reaction. The wells were mixed well with a multichannel to ensure a homogenous colour. Optical density was measured on a FLUOstar Omega microplate reader (BMG-LABTECH) at 540nm and 450nm. Wavelength correction was made by subtracting values at 540nm from 450nm. A standard curve was generated using a four-parameter logistic curve fit, as per the manufacturer's instructions.

2.11.2 Cytometric bead array

In a 24-well plate, $0.8x10^5$ HF-TERT cells were seeded per well. Cells were infected with HCMV at MOI 10, or mock infected and 0.5ml of DMEM10 was overlaid after infection. At 48hpi, media was exchanged with 0.5 ml of DMEM10 containing 100nM of D1(A12) or hIgG. At 54hpi, TNF was added to wells to give a final concentration of 30ng/ml. At 72hpi, samples were collected and stored at -80˚C. A LEGENDplex (Biolgend) was used for multi-analyte quantification of cytokines in supernatant (IL-8, IL-6, GM-CSF, IL-1, CXCL-10, CCL-2, CXCL-1, RANTES). Calibration standards were prepared as per the manufacturer's instructions. Samples were defrosted and warmed to room temperature. Samples were vortexed to homogenise tissue culture supernatants and then centrifuged at 16000 x *g* for 1min to pellet debris. To each well of a V-bottom plate, 25µl of assay buffer was added and 25µl of sample or standard. Capture beads were vortexed and 25µl was added to each well. The plate was sealed in aluminium foil and placed on a plate shaker (KS 130 basic, IKA) at 400RPM for 2h at room temperature. The plate was centrifuged at 250 x *g* for 5min and the supernatant was discarded. The plate was washed with 200µl of wash buffer and centrifuges as before. Detection antibodies (25µl) was added to each well. The plate was sealed in foil and shook as before for 1h. SA-PE (25µl) was added to each well directly. The plate was sealed and shook for 30min. A washing step was performed, and the beads were resuspended in 150µl of wash buffer. Beads were analysed by flow cytometry on the Attune NxT flow cytometer, as per manufacturer's instructions. Data was analysed using LEGENDplex data analysis.

2.12 T-cell activation assay

2.12.1 Preparation of target cells

Target cells consisted of autologous skin fibroblast cells or MRC-5 cells (HLA-A2+). Cells were infected with HCMV or adenovirus and harvested at 72h or 48hpi respectively by using HyQtase. Cells were washed in DMEM10 (470 *g* x, 2 min), and the cell pellet was and resuspended in DMEM10 containing peptide at the indicated concentrations. Cells were pulsed with peptide for 1h at 37˚C. Cells were washed twice in DMEM10 (470 *g* x, 2 min) and counted. Cell suspensions were made up to a concentration of 10^5 per ml. For all assays 10^4 target cells were used per well which equated to 100µl.

2.12.2 Preparation of effector cells.

T-cells were cultured for 10 days prior to use in activation assays. The required number of cells was calculated by mixing T-cell cultures to achieve a single cell suspension and then counted using a haemocytometer, staining with Trypan blue to distinguish between live cells and dead cells. The required number of cells was transferred into a falcon tube and T-cells were washed and resuspended in RPMI10 to a concentration of 10^6/ml. Monensin (BD GolgiStop, 0.26% monensin) was added to the culture at a final dilution of 1/400. For intracellular staining, brefeldin-A solution was added at a 1 in 1000 dilution (eBioscience 00-4506-51).

2.12.3 Assay set up

For performing the assay 100µl of targets was plates into each well 4 or 5 times (1 fluorescence minus one (FMO) and 3 or 4 replicate test wells for each condition). T-cell suspensions were aliquoted such that 1 part had IgG1 added to it and anti-CD107a to the other 4 parts (or 3 parts if doing triplicates). T-cells (100 µl) plus isotype/anti-CD107a was added to each well of target cells. The outer wells were filled with sterile PBS to abrogate the effect of evaporation in the incubator. The plate was put in a plastic container and then incubated at 37˚C for 5h without being moved. After 5h, the cells were washed in cold FACS buffer in a chilled centrifuge (4˚C, 470 x g, 2min). Staining was carried out as described in section 2.12.3.

2.13 Apoptosis assays

2.13.1 Annexin-V staining

HF-TERT cells were seeded into a 12-well plate ($1.6x10^4$/well). Cells were infected with HCMV at MOI 10. At 72hpi, the supernatant was removed and replaced with 1ml

DMEM10 or DMEM10 with 30ng/ml TNF. At 120hpi, cells were washed twice and detached with TryplE Express. Detaching agent was then neutralised with DMEM10 and cells were aliquoted into a 96 well V-bottom plate. Cells were washed with Annexin V binding buffer (Biolegend 422201) and resuspended in 100µl of 1/100 Annexin V-FITC (Biolegend) and 1/1000 L/D EFlour660 (eBioscience). Cells were incubated for 15min at room temperature. Cells were then washed twice in Annexin V binding buffer and then fixed in 2% PFA. Cells were analysed by flow cytometry.

2.13.2 Caspase 3/7 Cell Event

HF-TERT cells were infected with HCMV, treated with TNF, harvested and aliquoted into a 96 well V bottom plate as per Annexin V staining (2.13.1). Cells were washed in PBS. CellEvent™ Caspase 3/7 Green Detection Reagent (Thermo) was thawed at room temperature and diluted 1/1000 in PBS. Live/Dead Eflour660 was added (1/1000) to the staining solution and 100µl of this solution was added to each well. The plate was then placed on a rocker at 10RPM at 37˚C for 1h. After the incubation cells were then washed once in PBS and the fixed in 2% PFA. Cells were analysed by flow cytometry.

3 Modulation of the CD8+ T-cell response by HCMV

3.1 Introduction

The aim was to screen the HCMV genome in order to identify novel viral genes involved in evading the CD8+ T-cell response. Given the range of co-signalling receptors that are involved with T-cell activation and inhibition, we believed that HCMV may encode immune evasion functions targeting these molecules. When this investigation began, data generated from our laboratory had shown that HCMV pUL148 targets the co-stimulatory molecule CD58 (LFA3), reducing the activation of CD8+ T-cells (Wang et al., 2018). This result indicated that CD8+ T-cell evasion mechanisms are not limited to the direct inhibition of peptide presentation by MHC-I in the host cell. The HCMV group in Cardiff has generated a panel of HCMV mutants deleted in blocks of non-essential genes to specifically facilitate the identification and mapping of novel immune evasion functions. Using this approach has recently demonstrated that US18 and US20 retain the NK cell activating ligands MICA (Fielding et al., 2014) and B7-H6 (Fielding et al., 2017) inside the infected cell and target them, and other host molecules, for lysosomal degradation. Using the block-deleted HCMVs was an attractive approach to mapping areas involved with CD8+ T-cell evasion strategies independent of HLA-I peptide presentation. By finding new viral immune evasion genes, this work could further our knowledge of how HCMV remains as a life-long pathogen.

3.2 Production of HCMV specific CD8+ T-cell lines

3.2.1 Testing peptide responses of HCMV seropositive donors

HCMV positive donors were bled and their PBMCs were co-cultured with irradiated, autologous fibroblasts, pulsed with peptide as described in the Materials & Methods. The peptide used for each individual was based on previously defined dominant peptide specificities for HLA-I haplotypes (Wills et al., 2013). Expansions of cells were assessed over a minimum period of two weeks to allow CD8+ T-cells to proliferate. Each T-cell line was identified using the donor number followed by 3 letters indicating the peptide specificity of the T-cell line, referring to the first three amino acids of the HLA-I restricted peptide. For three of the donor-peptide combinations tested, large expansions of CD8+ T-cells were recorded; D7-VLE (97% CD8+), D7-NLV (82% CD8+) and D9-VTE (94% CD8+) (Figure 3.1).

This level of CD8+ T-cell expansion did not occur with all peptide-donor combinations, suggesting some combinations were not dominant peptide responses for those donors. To provide a readout, HCMV-specific CD8+ T-cell lines were used as effector cells to screen HCMV knockout viruses using primarily CD107a recycling to measure degranulation. CD107a is a protein found in cytotoxic granules that migrates to the cell surface following CD8+ T-cell degranulation, as a result of fusion of cytotoxic vesicles with the plasma membrane. Surface exposure of CD107a can thus be used as a readout of T-cell activation. For these non-responsive T-cell lines, the level of degranulation was <8% CD107a+ of the CD8+ compartment (Appendix). The D9-ELR response had previously been detected by tetramer (Aicheler, 2005). Whilst this culture did reach 56% CD8+ T-cells at 2 weeks post stimulation (Figure 3.1), this proportion decreased afterwards, and the T-cell line contained only 35% CD8+ T-cells by 3 weeks post stimulation.

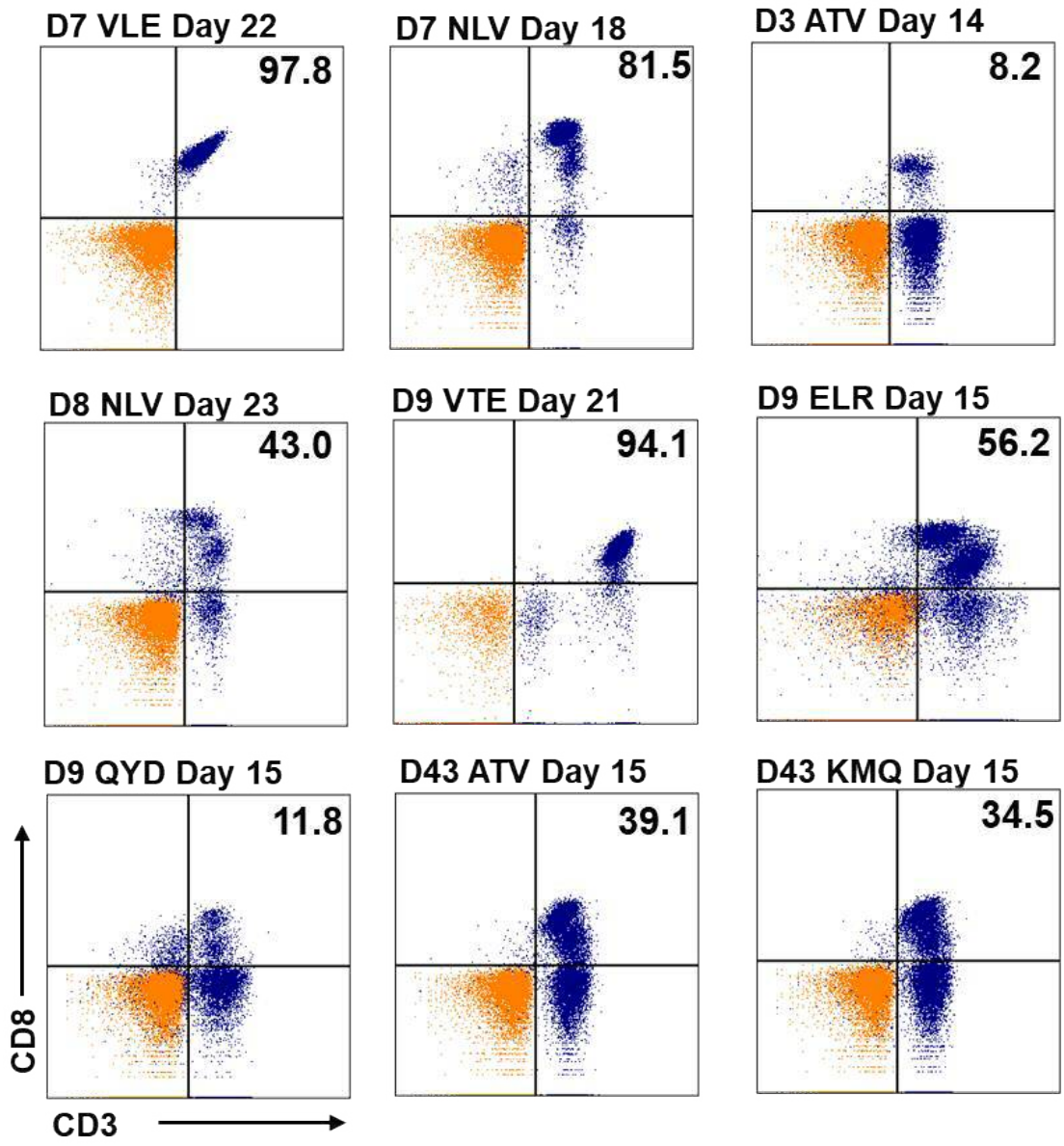

Figure 3.1. Proportions of CD8+ T-cells in lines generated from HCMV seropositive donors. PBMCs were stimulated with irradiated autologous skin fibroblasts pulsed with the indicated peptides. The proportion of CD8+ T-cells was assessed by flow cytometry between 2-3 weeks post-stimulation. Unstained cells are shown in orange, with cells stained for CD8 and CD3 overlaid in blue. Donor number, first three amino acids of peptide used for stimulation and days post stimulation are shown above the flow cytometry dot plots. Proportion of CD3+, CD8+ T-cells are shown within the plots.

3.2.2 Assessing responsiveness of CD8+ T-cell lines

T-cell receptors recognise peptide in the context of HLA-I with the strength of activation signal received by the T-cell dependent on the number of cognate peptide-HLA complexes they encounter on their targets. To determine the activation range of each T-cell line, dose response experiments were performed measuring activation as a function of exogenous peptide concentration used to coat HLA-I on autologous target fibroblasts.

Of the 5 lines tested (D7-VLE, D7-NLV, D8-NLV, D9-ELR, D9-VTE) all responded to peptide pulsed autologous fibroblasts in a dose-dependent manner, with degranulation increasing in response to increasing concentrations of exogenous peptide used for pulsing cells (Figure 3.2). The responsiveness to peptide was noticeably lower for D9-ELR, with CD8+ cells being just 15% CD107a+ when targets were pulsed with 10μg/ml of exogenous peptide.

With D8-NLV, responses plateaued at 1μg/ml of exogenous peptide such that increasing the peptide concentration to 10μg/ml did not increase degranulation. Lines D7-VLE, D7-NLV, and D9-VTE showed a s-shaped degranulation profile versus peptide concentration, though responses had not plateaued by 10μg/ml. At concentrations of peptide below 0.001μg/ml, the level of stimulation was not great enough to induce detectable surface CD107a recycling. This system for activating T-cells was the most sensitive to exogenous peptide between 0.1-1μg/ml as reflected by the steepest gradient of the curve. For D9-VTE, IFNγ and TNF production was also assessed by intracellular cytokine staining (ICS). This was performed following the acquisition of the Attune NxT flow cytometer and allowed me to determine further functionality of this T-cell line as assessed by effector cytokine production. The data showed that detection of TNF production by this T-cell line was at least as sensitive as CD107a. IFNγ was detected in a smaller proportion of CD8+ T-cells. The pattern in the increase in detection of both cytokines was similar to CD107a, with the largest increase being measured between 0.1 and 10μg/ml of peptide.

Of these T-cell lines, D7-VLE, D7-NLV, and D9-VTE were used for all experiments in this chapter as these cells were able to degranulate over a wide range of peptide concentrations. Additionally, these T-cell lines also maintained a high proportion (>80%) of CD8+ cells. D8-NLV was not used as I was unable to grow out large quantities of the cells. Neither was D9-ELR as degranulation of CD8+ cells above 15% was not achieved, even at 10μg/ml of peptide, indicating low sensitivity of this T-cell line to the targets used to stimulate it. These data indicated that coating target T-cells between 1 and 0.1μg/ml

would induce enough degranulation of T-cells to allow differences in activation across conditions to become discernible, without saturating the positive signal to T-cells, and preventing detection of increases in activation.

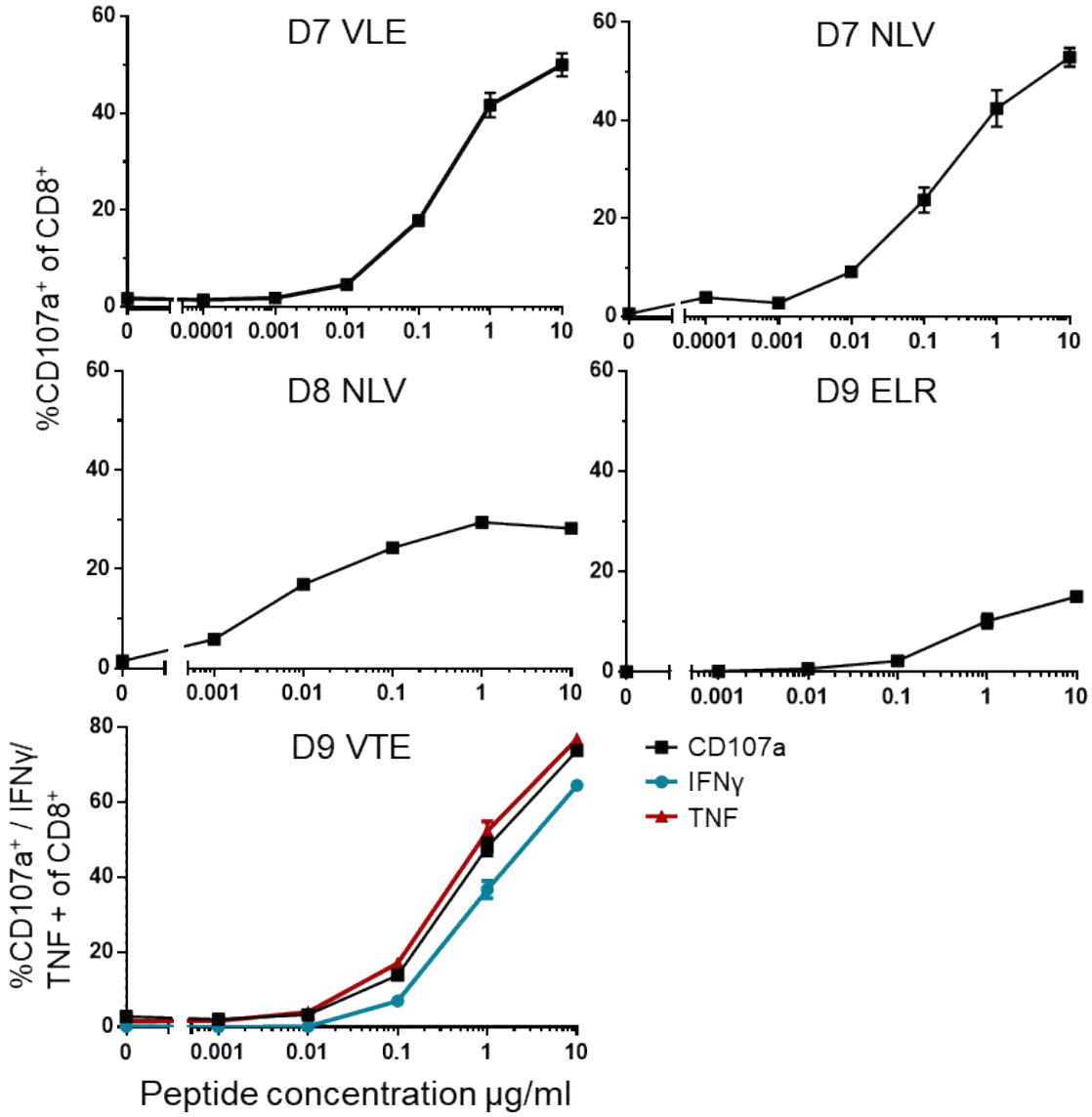

Figure 3.2 Dose response experiments assessing degranulation of HCMV-specific T-cell lines against peptide pulsed autologous fibroblasts. SFi cells (D7, D8 and D9) were pulsed with the indicated peptide concentrations. These cells were then used as targets in a CD107a degranulation assay. T-cell lines used are shown in each panel. Cytokine production was assessed with D9-VTE, with the proportion of cells producing IFNγ and TNF also being measured. Data shows mean %CD107a+ of CD8+ cells ±SEM of quadruplicate values. For D9-VTE, data shows mean %CD107a+/IFNγ+/TNF+ of CD8+ cells ±SEM of quadruplicate values.

3.3 Screening of the HCMV genome for regions involved with CD8$^+$ T-cell evasion

3.3.1 Effect of block deleted HCMV variants on CD8+ T-cell responses

Having generated functionally active peptide-specific T-cells, experiments were performed comparing responses to target cells infected with HCMV deletion variants. These variants each contained a deletion in regions of the HCMV genome not required for replication (Figure 3.3). These viruses were made so that NK cell evasion genes could be mapped to specific regions of the HCMV genome. The block deletions were made on a ΔUL16/UL18 background in order to detect additional NK evasion genes that may be masked by the suppression caused by UL16 and UL18. Both genes have been well described as NK cell evasion genes, with UL16 binding to MICA, ULBP1 and ULBP2 which are ligands for the activating receptor NKG2D (Dunn et al., 2003a) and UL18 binding to LIR1 on NK cells (Chapman et al., 1999). This was performed in order to provide an intermediate levels of NK cell degranulation, which could increase upon the deletion of NK inhibitory genes or decrease upon deletion of NK activating genes. Using this loss of function system, the first aim was to investigate whether any of these deletion variants were able to significantly alter the activation of T-cells in the absence of exogenous peptide, relative to parent virus.

Initial experiments were performed with the D7-VLE and D7-NLV lines as effector cells, against D7-SFi cells (Figure 3.4A and B. Experiments were performed by Dr Eddie Wang). An initial screen without exogenous peptide, showed no differences in CD8+ T-cell activation against mock, Merlin and AD169 infected targets, indicating that HCMV infection in itself did not increase recognition by either T-cell line. Deleting US2-11 increased degranulation to levels comparable to mock infected cells coated with peptide. This was expected as this region includes the HLA-I downregulating genes US2, US3, US6 and US11 (Jackson et al., 2011). This showed that in the absence of exogenous peptide, HCMV induced CD8+ T-cell activation is difficult to measure as assessed by CD107a expression and that recovery of peptide presentation by HLA-I greatly increased activation without the need for additional peptide pulsing.

Screening of the block deletions showed small statistically significant differences from a number of variants, but ΔRL10-UL1 was the only deletion that caused a significant increase in degranulation by both lines. This suggested that the RL10-UL1 region encodes a potential T-cell inhibitor. ΔUL22A-25 reduced the CD107a signal with the NLV

line but increased it with the VLE line. Deep sequencing would later reveal bacterial DNA incorporated into the BAC of this HCMV deletion mutant. The assay was repeated with certain mutants with both T-cell lines in parallel to further show differences between the parent HCMV and the deletion variants. In both experiments ΔUS18-22 increased activation (Figure 3.4C and D). ΔUS27-28 also increased degranulation, but only with the NLV line. These data show that in the absence of exogenous peptide, RL10-UL1 can decrease the activation of T-cells and that the US18-US22 region may also have an inhibitory effect on CD8+ T-cells.

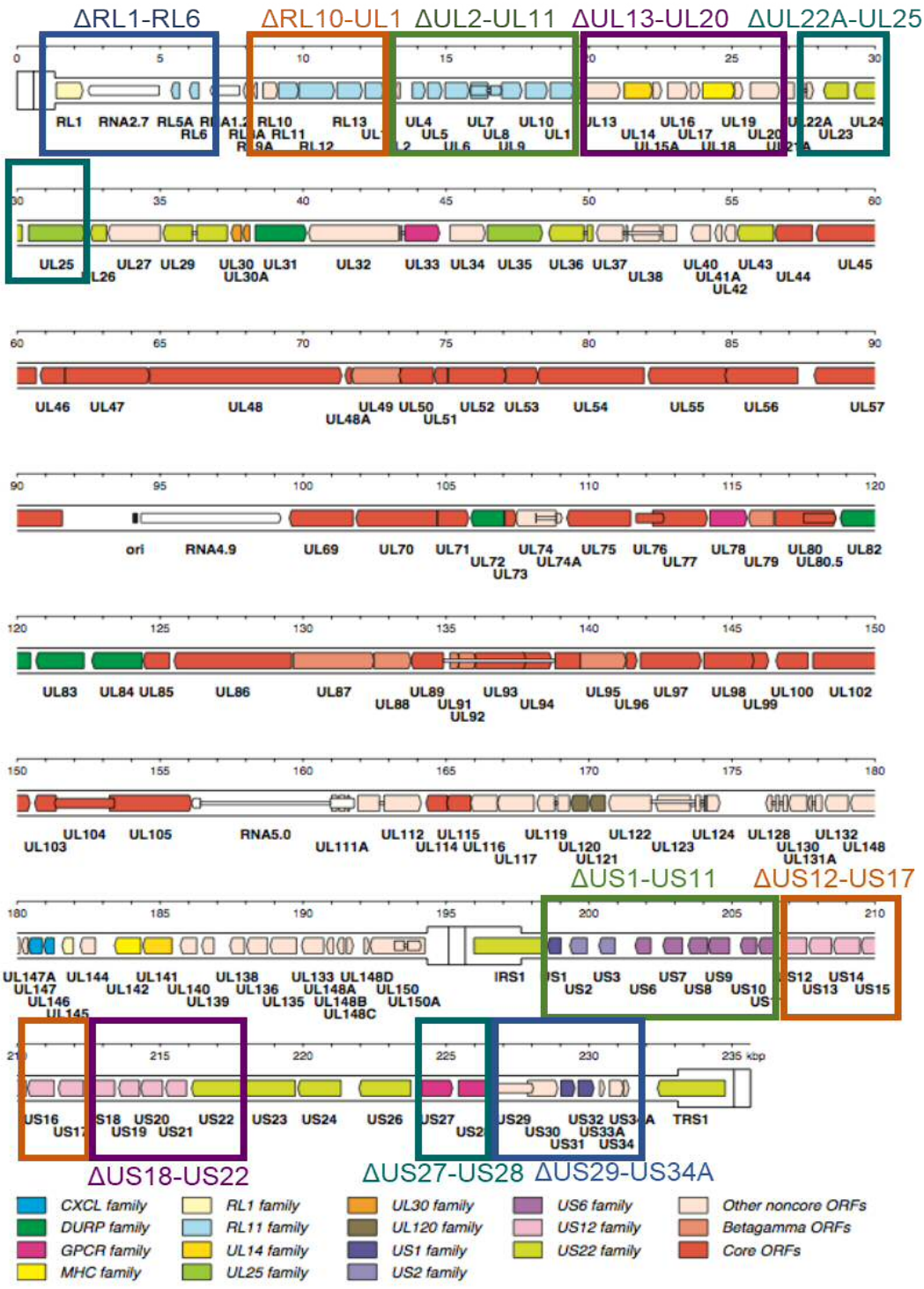

Figure 3.3 Genetic map of Merlin genome and genes missing in block deletions. Block deletions are shown in rectangles. Coloured arrows indicate protein-coding regions and direction refers to 5' to 3'. Conservation across the Herpes viruses are designated 'core' genes. Non-core genes are grouped into gene families and are colour coded. The diagram was provided by Prof Andrew Davison (MRC-University of Glasgow Centre for Virus Research, Glasgow, UK).

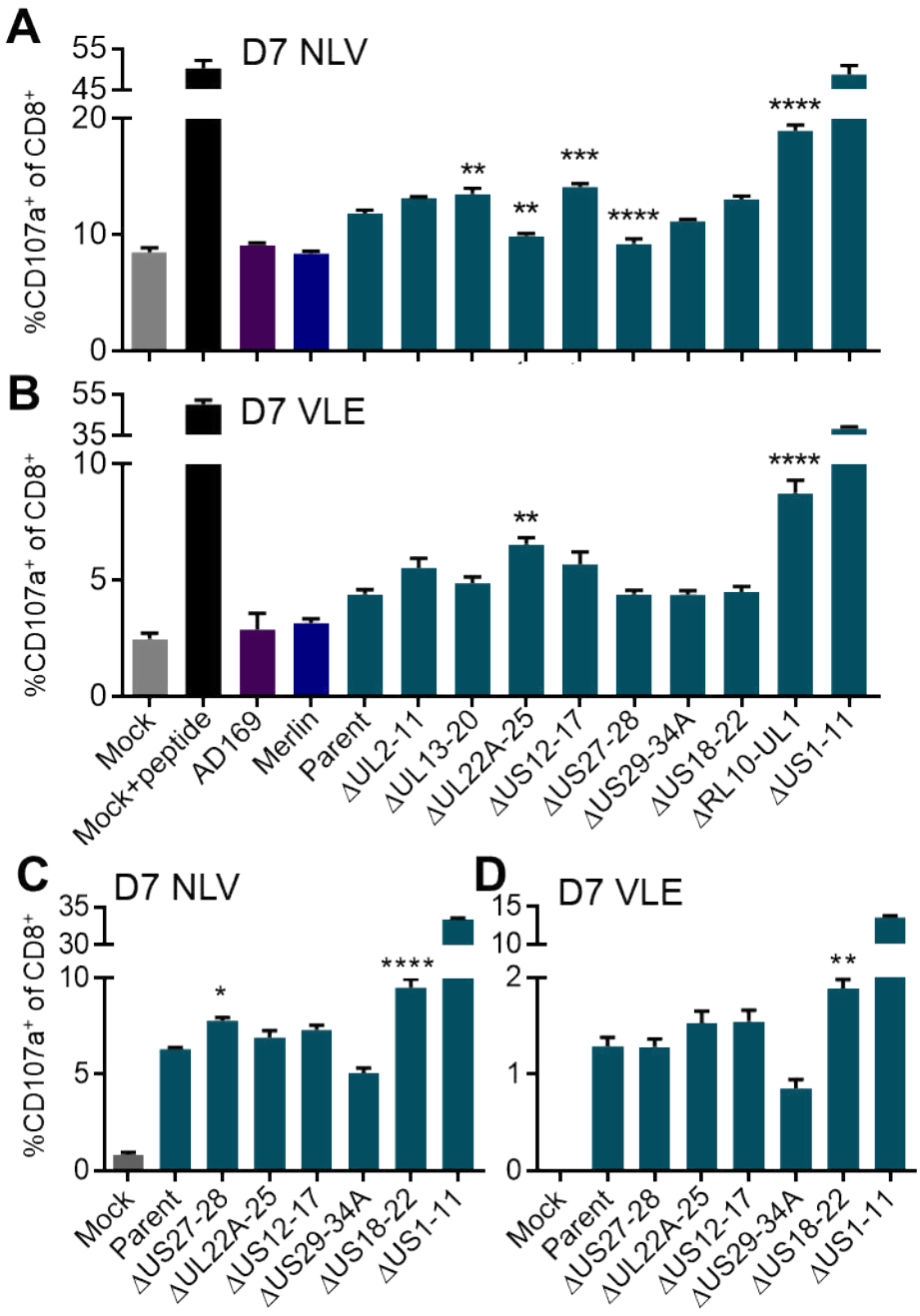

Figure 3.4 Degranulation of HCMV specific CD8+ T-cells against fibroblasts infected with HCMV block mutants. D7-SFi were infected with the indicated HCMV or mock infected. At 72hpi, D7-SFi cells were used as targets in a CD107a degranulation assay with T-cell lines (A) D7-NLV or (B) D7-VLE as effectors. A and B were performed separately. Experiments C and D were performed in parallel. Data shows mean %CD107a of CD8+ cells and +SEM of quadruplicate samples. Statistical analysis was performed comparing the HCMV 'parent' with all other block mutants except ΔUS1-11, which served as a positive control alongside mock + peptide (1µg/ml). One-way ANOVA with Tukey multiple comparison post-hoc tests showed significant differences at **** $p<0.0001$, ***$p<0.001$, **$p<0.01$, *$p<0.05$. Assays were performed without peptide pulsing.

3.3.2 Effect of block deleted HCMV variants with peptide on CD8+ T-cell responses

Measuring degranulation of HCMV specific T-cells against HCMV infected cells without exogenous peptide indicated that RL10-UL1 and US18-22 may be regions containing T-cell evasins. Using the same block deletions, the screen performed in section 3.3.1 was repeated, but with the addition of peptide. This allowed me to investigate whether increasing the strength of TCR signal could reveal functions otherwise hidden by the considerable inhibition of CD8+T-cell activation that is induced by HCMV-encoded genes targeting HLA-I surface expression and antigen processing.

With all assays performed with HCMV variants, levels of surface HLA-I were used to determine the extent of infection within target fibroblast cultures. This was particularly important in assays involving addition of exogenous peptide, as a large proportion of uninfected cells with normal levels of HLA-I would induce a false positive signal from CD8+ T-cell assays where exogenous peptide was added. Further, any functions that affected HLA-I expression would also be revealed. D7-SFi cells were infected with HCMV block deletion variants and at 72hpi, cells were stained for HLA-I (Figure 3.5A,B). The experiment showed that for the majority of HCMV deletion variants used, HLA-I expression did not alter compared to the parent HCMV, indicating no HLA-I downregulating genes in these deletion mutants. One exception was ΔUS1-US11 (a region containing multiple HLA-I downregulating functions), with cells infected with this virus unsurprisingly having more HLA-I on the surface compared to the parent strain. Another exception was ΔUS29-34A, in which a population of HLA-I high cells (showed by arrow in Figure 3.5) suggested partial infection of the fibroblast culture. For all T-cell assays where exogenous peptide was added, target cells showing less than 95% of cells with low levels of surface HLA-I were excluded, because this implied an insufficient level of HCMV infection.

In my first assay, D7-SFi cells infected with block deletions. At 72hpi, cells were were pulsed with 0.1µg/ml of VLE peptide. The HLA-I expressions from this experiment is shown in Figure 3.5. The experiment showed that deleting UL13-UL20 increased the activation of T-cells far beyond the parent HCMV (21% vs 45% CD107a+ of CD8+ cells) or any other mutants (Figure 3.6A). Other deletion mutants that significantly increased activation above parent, but to a lesser extent than ΔUL13-20, included ΔUS27-28, ΔUS18-22 and ΔUS29-34A. The assay was performed in parallel without peptide to see whether the initial findings that suggested ΔRL10-UL1 increased CD8+ T-cell activation could be repeated (3.3.1). In contrast though, no significant increases were observed

beyond the parent HCMV. Except for ΔUS1-11, the mean %CD107a of CD8+ cells induced by HCMV infected cells was <1%, which indicated the inability of this T-cell line to recognise and degranulate against cells in the absence of exogenous peptide (Figure 3.6B). This contrasted with the previous data set (Figure 3.4) which did show significant increases in degranulation against targets infected with these block mutants.

In summary UL13-20, US27-28, and US18-22 were flagged as other regions of the HCMV genome, which could encode CD8+ T-cell evasion genes once a small dose of exogenous peptide was used to coat targets.

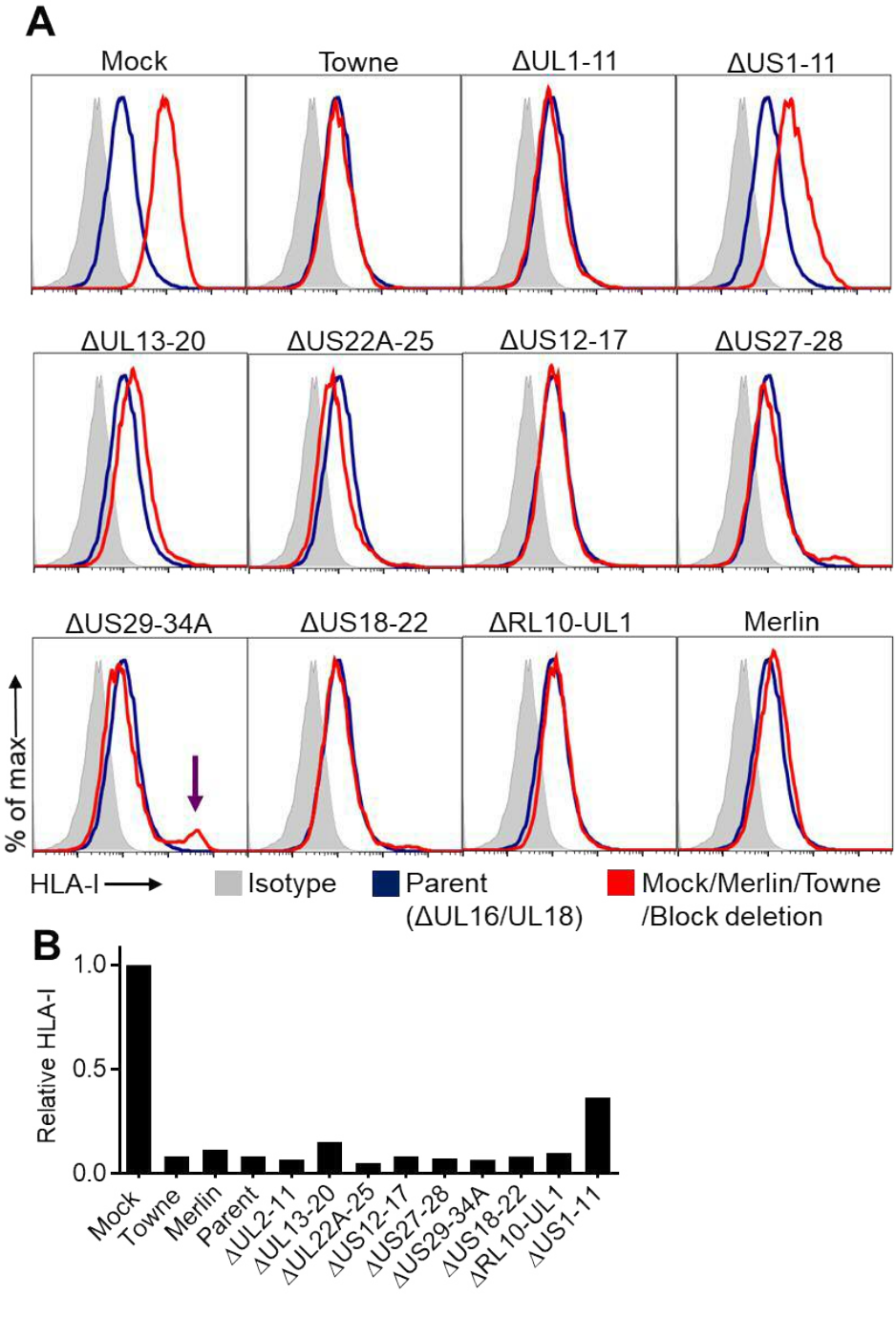

Figure 3.5 Effect of Merlin block deletions on HLA-I downregulation. D7-SFi cells were infected with HCMV block-deletion variants or mock infected. At 72hpi cells were stained for HLA-I and analysed by flow cytometry. (A) Overlay histograms comparing parent HCMV with block deletions, Towne and Merlin. (B) Data from (A) plotted as relative median fluorescence intensity (MFI). HLA-I MFI from mock infected cells was set as 1, with other values plotted as a relative value.

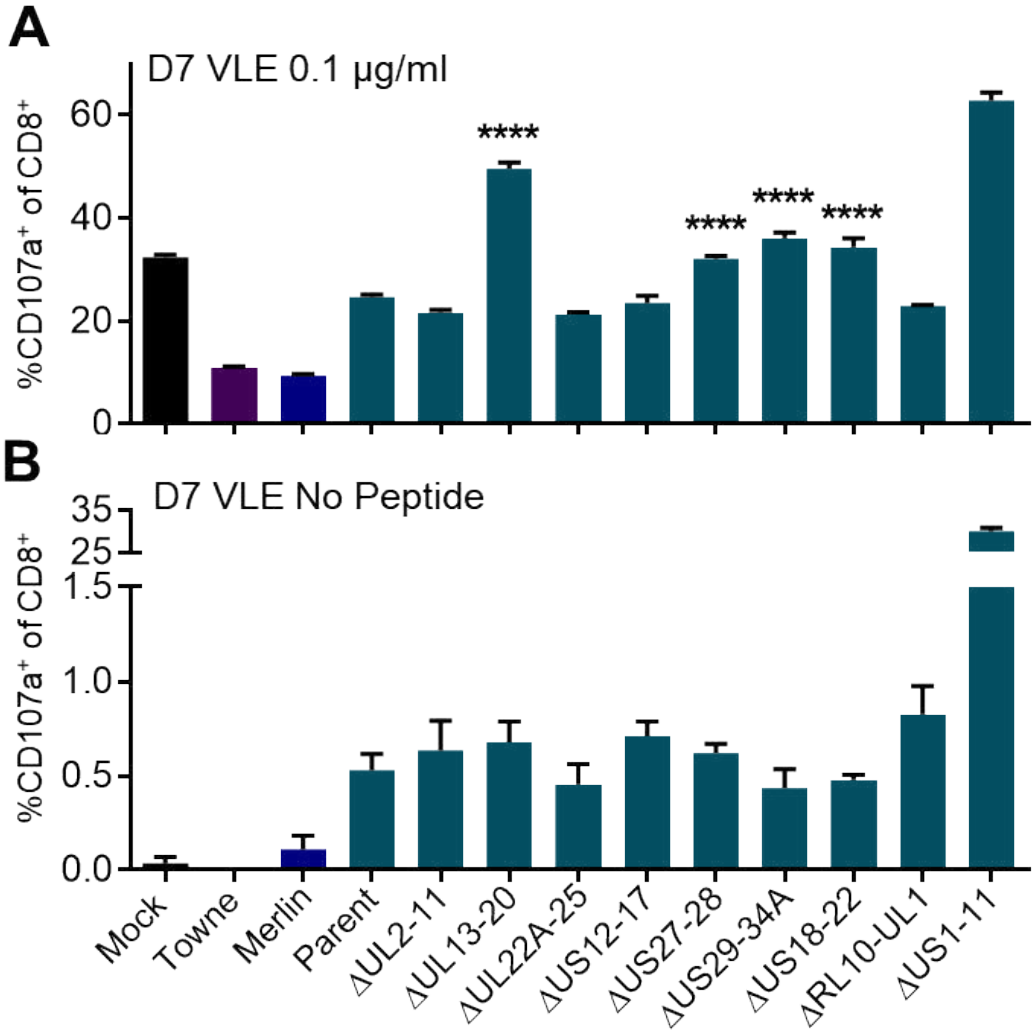

Figure 3.6 Effect of deleting regions of the HCMV genome on CD8+ T-cell activation. D7-SFi cells were infected with HCMV or mock infected. At 72hpi, cells were (A) pulsed with 0.1µg of VLE peptide or (B) left un-pulsed and used as targets in a CD107a degranulation assay. Data shows mean %CD107a+ of CD8+ T-cells ±SEM of quadruplicate samples. Statistical analysis was performed comparing HCMV 'parent' with all other block mutants, but not including ΔUS1-11, which served as a positive control. One-way ANOVA with Tukey multiple comparison post-hoc tests showed significant differences at ****p<0.0001.

3.3.3 Effect of block deleted HCMV variants on CD8+ T-cell response at multiple peptide concentrations

Following the experiment with the deletion variants at a single peptide concentration, the screen was extended by using a range of peptide concentrations from 0.008 to 1µg/ml using a second HCMV-specific CD8+ T-cell line, D7-NLV. This was performed to see if, firstly, a different CD8+ T-cell line flagged the same regions; secondly, if regions flagged at a single peptide dose could act over a wider range of T-cell receptor signalling, and thirdly, whether there were genes that acted over a narrow peptide range that may have been missed by the single peptide concentration screen, as has been described for UL148 (Wang et al., 2018).

The top 4 panels in Figure 3.7 (ΔRL10-UL1, ΔUL13-20, ΔUL22-25A, ΔUL2-11) were performed in parallel. Whilst there were statistically significant increases in CD107a induction by all four of these variants compared to the parent HCMV at a peptide concentration of 1µg/ml, the increase in CD8+ T-cell degranulation induced by ΔUL13-20 was much higher than the other deletion mutants (59% vs 38%). The difference between parent and ΔUL13-20 was significant at all lower peptide concentrations too. The result further strengthened the data suggesting that UL13-20 contains other T-cell evasins other than UL16 and UL18 (absent from the parent and all HCMV block mutants).

In a second screen performed separately but with the same effector T-cell line (lower 4 panels Figure 1.7), significant increases in CD8+ T-cell activation were observed over a limited range of peptide concentrations with ΔUS27-28 (0.2µg/ml) and ΔUS18-22 (0.2, 0.04µg/ml), with no significant differences at the highest and lowest peptide concentrations (0.008 and 1µg/ml respectively). No increase in CD107a+, CD8+ cells was detected at any peptide concentration with ΔUS29-34A.

Compared to the previous experiment described in section 3.3.2, which was performed with the D7-VLE at 1µg/ml, the same mutants that induced an increase in CD107a expression (ΔUL13-20, ΔUS27-28, ΔUS18-22) also resulted in increased degranulation with the D7-NLV line, though no difference was observed using ΔUS29-34A.

3.3.4 Summary of screening with HCMV deletion mutants

Screening of the HCMV genome showed that in the presence of peptide, deleting the genes UL13-20 induced the largest increase in CD8+ T-cell activation. Deleting RL10-UL1 also induced an increase in the CD8+ T-cell response against HCMV-infected cells though this was only observed without peptide with 2 different CD8+ T-cell lines. Increases in degranulation were also recorded with ΔUS18-22, both with and without

peptide pulsing. This region was not investigated in further detail as the aim of this screen was to identify novel regions of immune evasion, and ongoing work had already identified US18 and US20 as immune evasins (Fielding et al., 2014, Fielding et al., 2017). From these data, the two regions that were investigated further were UL13-20 and RL10-UL1 as the largest response with peptide was measured with ΔUL13-20 and the largest response without peptide was measured with ΔRL10-UL1. In both cases the levels of HLA-I were comparable to the parent HCMV, indicating that the genes within these two regions were not impacting on the level of expression of HLA-I and that any immune evasion mechanism was most likely occurring by other means.

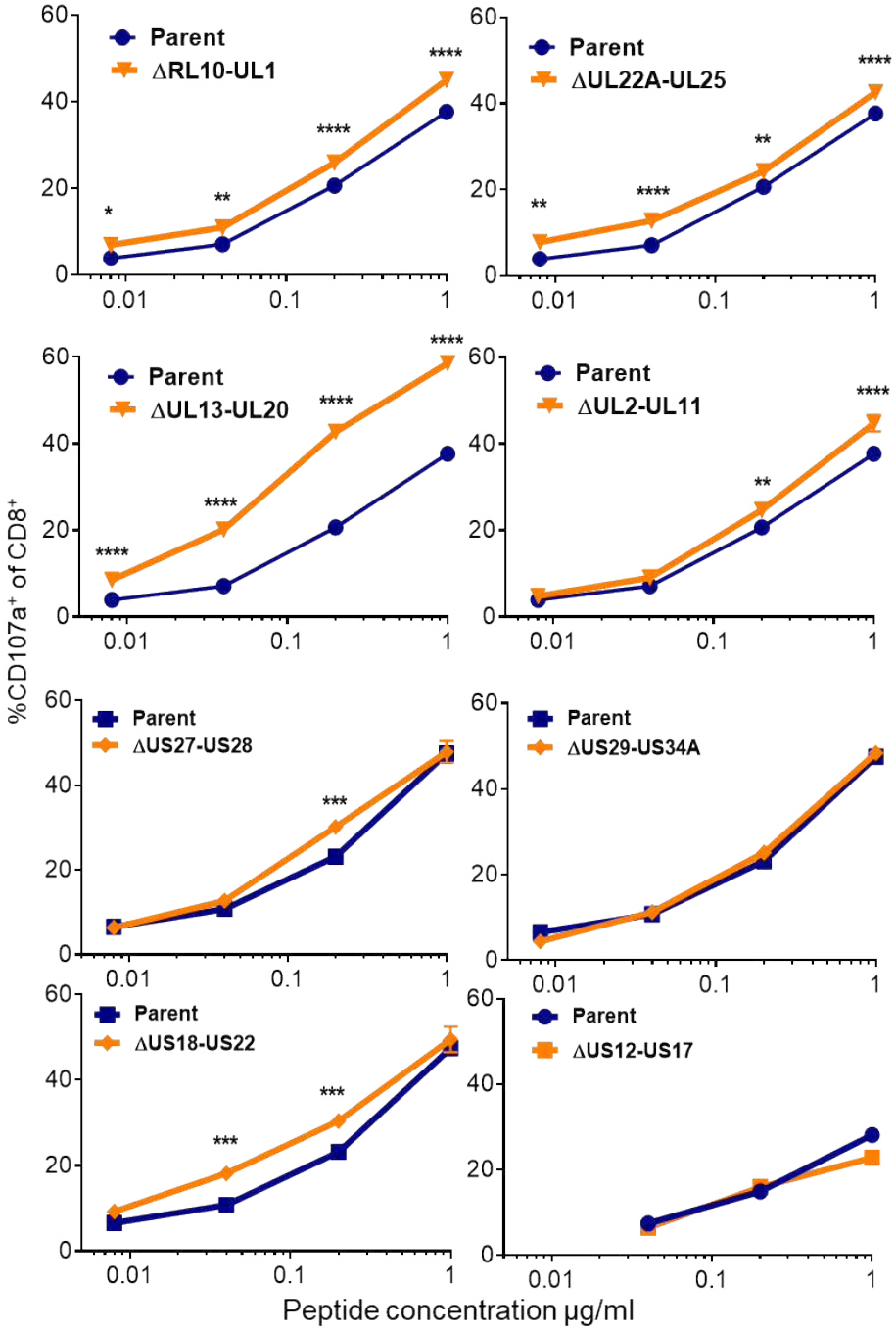

Figure 3.7 Assessing the effect of deleting regions of the HCMV genome on CD8+ T-cell activation at multiple peptide concentrations. D7-SFi cells were infected with parent HCMV (blue) or the indicated block-deletion mutants (orange). At 72hpi, cells were pulsed with the indicated concentration of NLV peptide and T-cell assays were performed using D7-NLV as effector T-cells. Following the assay, cells were analysed by flow cytometry. Infections with ΔRL10-UL1, ΔUL22A-25, ΔUL13-20 and ΔUL2-11 deletion mutants was performed in one experiment and ΔUS27-28, ΔUS29-34A and ΔUS18-22 deletions was performed in another separate experiment. Data shows mean %CD107a+ of CD8+ T-cells and SEM of quadruplicate values. Two-way ANOVA with Bonferroni multiple comparison post-hoc tests showed significant differences at **** $p<0.0001$, ***$p<0.001$, **$p<0.01$, *$p<0.05$.

3.4 Impact of RL11 family on CD8+ T-cell responses

The data from Figure 3.4 indicated that in the absence of exogenous peptide and in the context of a HCMV infection, genes within the RL10-UL1 region can reduce degranulation of T-cells as measured by CD107a surface recycling. These genes encode a series of cell surface glycoproteins and are part of the larger RL11 family (Davison et al., 2003a). The RL11 family consists of RL5A, RL6, RL11, RL12, RL13, UL1 and UL4-UL11 (Fig 1.3). Whilst many genes within HCMV are necessary for replication and are well conserve amongst Herpes viruses, RL11 family genes are dispensable for replication *in vitro* (Dolan et al., 2004). Furthermore, members of the RL11 family are amongst the most genetically divergent HCMV genes (Sijmons et al., 2015). Experiments using block deletions showed cells infected with ΔRL10-UL1 consistently increased NK cell degranulation compared to parent HCMV (personal communication, Dr Ceri Fielding) using PBMC from several donors. This, combined with the data in the previous section encouraged further experiments designed to identify the specific genes within the RL11 family region responsible for reducing CD8+ T-cell activation.

3.4.1 Use of block deletion viruses to assess the role of the RL11 family genes CD8+ T-cell activation

To assess the overall impact of the RL11 family on activation of degranulation of T-cells, an experiment was performed utilising three block deletions (MerlinΔRL11-UL11, ΔRL10-UL1 and ΔUL2-11). The aim was to map potential immune modulators to one of two regions within the gene family. The summary data from Figure 3.8B showed that the addition of peptide had no consistent effect on the activation of ΔRL10-UL1 infected cells. Given that all the block mutants were on a genetic background of ΔUL16/UL18, I hypothesised that the removal of these genes may have been masking other smaller effects induced by the deletion of other regions in the HCMV genome. By testing ΔRL11-UL11, the intention was to assess the effect of removing a larger proportion of the RL11 family on CD8+ T-cell activation. The ΔUL2-11 block deletion was included alongside the ΔRL10-UL1 mutant as previous data showed that cells infected with ΔUL2-UL11 induced a small, but significant increase in CD8+ T-cell degranulation (section 3.3.3). Deleting ΔRL11-UL11 resulted in decreased degranulation of CD8+ T-cells (Figure 3.8A and B). This result was the same for both D7-NLV and D7-VLE T-cell lines. Compared to the parent HCMV, deleting RL10-UL1 did not increase degranulation, and with both T-cell lines, deleting UL2-UL11 significantly decreased degranulation. This decrease was of a similar magnitude to that recorded between Merlin and MerlinΔRL11-UL11 (black bars).

Additional experiments were performed using the ΔRL10-UL1 block deletion, with and without peptide pulsing. This was so that I could generate enough data to statistically assess if the average CD107a values were consistently different when using two T-cells lines. The summary data includes all experiments with both D7-VLE and D7-NLV T-cell lines. Figure 3.8C showed that in the absence of peptide, deleting RL10-UL1 caused a significant increase in CD107a expression compared to the parent HCMV, when the means were compared by a Wilcoxon matched-pairs signed rank test (1.66±0.46 vs 2.78±0.88%, p=0.023, data was not normally distributed). The same analysis was performed with data from experiments with peptide pulsing (Figure 3.8D). This graph included data points where HCMV targets were coated with ≥0.1μg/ml of peptide (NLV or VLE). A small but significant difference in activation induced by the ΔRL10-UL1 infected cells (37.5±4.7 vs 40.5±4.4%, p=0.018). In summary, this data suggests that genes within the RL10-UL1 regions may have a role in reducing T-cell degranulation, but this was more consistent in the absence of exogenous peptide.

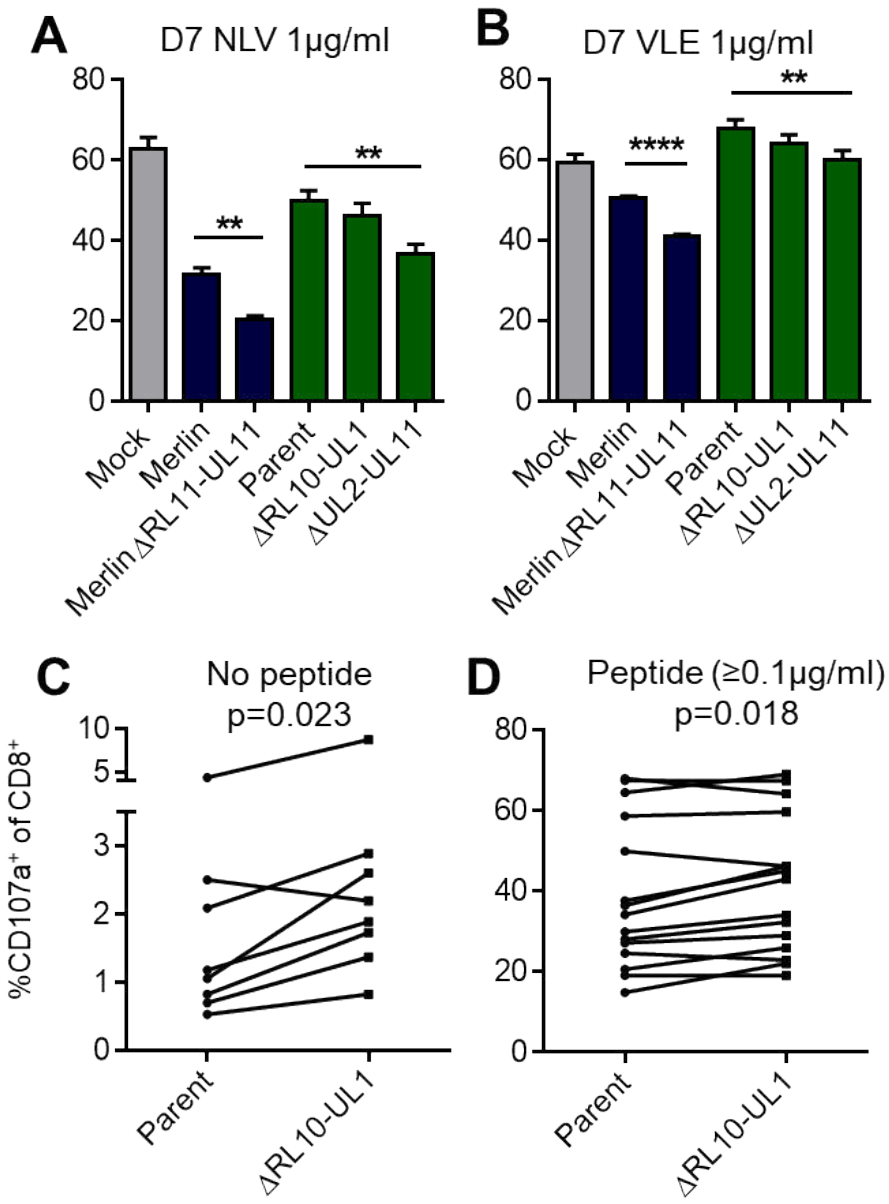

Figure 3.8 Assessing the effect of deleting HCMV genes within the RL11 family on CD8 T-cell activation. D7-SFI cells were infected with HCMV variants and used as targets in CD107a degranulation assays at 72hpi. Experiments from an assay performed comparing Merlin, MerlinΔRL11-UL11, parent and ΔRL10-UL1 using (A) D7-NLV and (B) D7-VLE. Data was analysed with one-way ANOVA with Tukey multiple comparison post-hoc tests. Summary data for all experiments comparing parent HCMV with ΔRL10-UL1 showing mean degranulation from experiments when (C) no exogenous peptide was used (analysed using Wilcoxon matched-pairs signed rank test was used as the data was non-parametric as assessed by) and where HCMV infected cells were (D) pulsed with ≥ 0.1µg/ml of NLV or VLE peptide (a paired two tailed t-test as the data was parametric). Each point shows mean %CD107a+ of CD8+ T-cells. Significant differences are shown at **** p<0.0001, ***p<0.001, **p<0.01.

3.4.2 Effect of individually expressing HCMV genes RL10-UL1 on CD8+ T-cell activation

The data from section 3.4.1 indicated that the genes within the RL10-UL1 region could reduce degranulation of CD8+ T-cells in the absence of peptide. Activation by ΔRL10-UL1 was not consistently observed in assays with peptide. One explanation could be that this region encodes genes with multiple competing effects including those that increase activation of some CD8+ T-cells, which could mask the effects of possible immune evasins. To test if these genes could affect T-cell activation in a positive expression system, HCMV genes were expressed with RAds, which allowed me to assess the genes in the RL10-UL1 region individually. In this system, expression of the transgenes is driven by the strong constitutive HCMV major IE promoter essentially in the absence of replication of the Ad vector (Materials and Methods). D7-SFi cells were infected with RAds and used as targets for a CD107a degranulation assay at 48hpi. T-cell activation was significantly lower against cells expressing RL11 and UL1 (Figure 3.9A). Other differences were not significant. These results indicate that UL1 and RL11 genes may be T-cell evasion functions.

With these experiments, one consideration was that the decrease in degranulation could be due to altered effector cell responsiveness due to toxicity in the target cells resulting from high MOI RAd infections. To address this, an experiment was performed using D7-SFi cells and MRC-5 fibroblasts in parallel (Figure 3.9B and C respectively), both of which are positive for the HLA-A2, the HLA-I that presents the cognate peptide to the effector D7-VLE T-cell line. Whilst an MOI of 500 is required for complete infection of D7-SFi cells, efficient infection of MRC-5 cells with RAds was achievable at MOI of 20, as shown in Material and Methods (section 2.5.5). With both cells lines the result was similar, with a significant reduction in degranulation observed with RAd-UL1 and RAd-RL11 infected cells compared to RAd-CTRL infected cell. There was also a significant increase in degranulation with RAd-RL10 infected cells. The data from these two experiments showed that both RL11 and UL1 could independently reduce activation of CD8+ T-cells in a positive expression system.

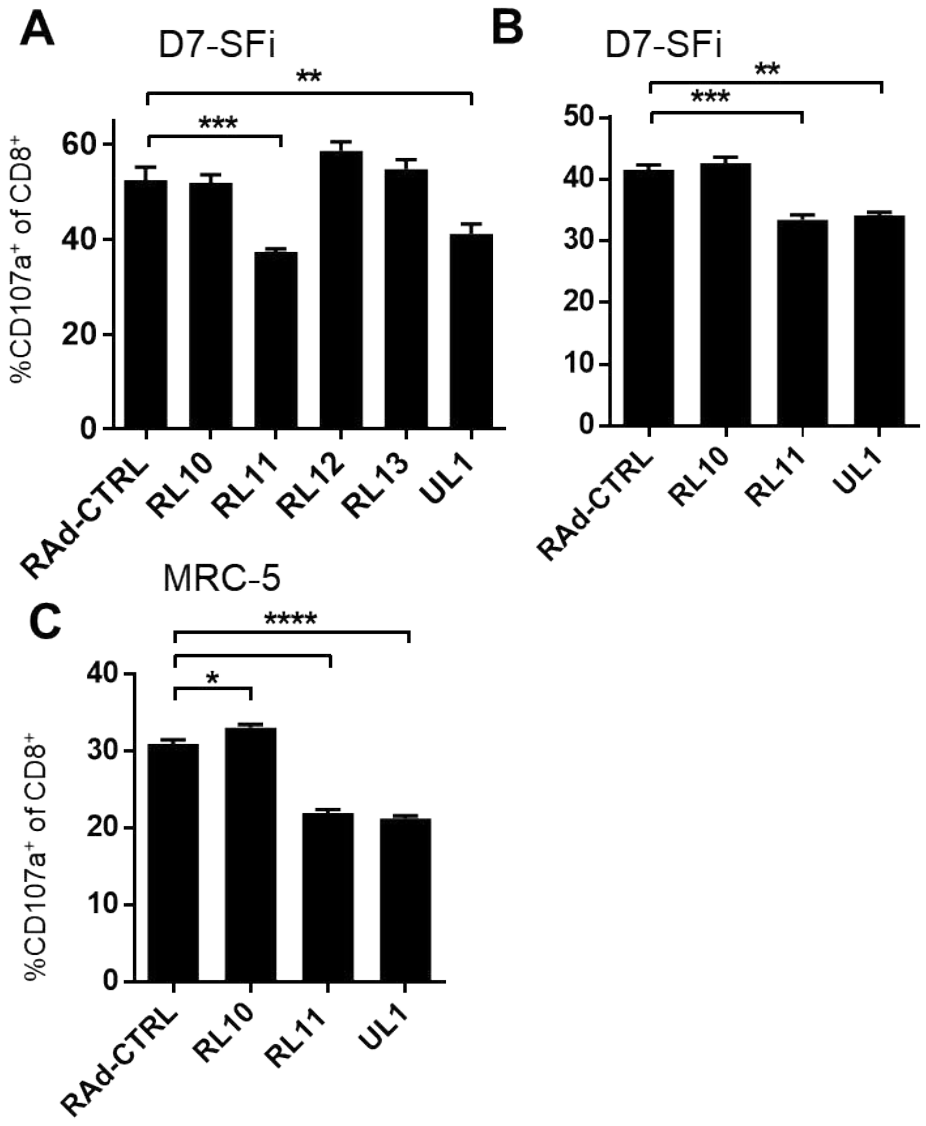

Figure 3.9 Assessing effect of genes RL10-UL1 on CD8+ T-cell activation. (A) and (B) were infected with adenoviruses expressing genes from the RL10-UL1 region. At 48hpi, cells were pulsed with 1µg/ml of peptide and used as targets in a CD107a degranulation assay. Experiment (C) was performed with MRC-5 fibroblasts. Bars show mean %CD107a+ of CD8+ cells ±SEM of quadruplicate values. Compared to RAd-CTRL, one-way ANOVA with Tukey multiple comparison post-hoc tests showed significance compared at ****p<0.0001, ***p<0.001, **p<0.01, *p<0.05.

3.4.3 Assessing impact of deleting HCMV RL11 on CD8+ T-cell function

Whilst performing screens with the RAds (section 3.4.2) ongoing work in the laboratory resulted in the generation of a MerlinΔRL11 virus. The RL11 gene was deleted from the virus to test its role as an immunevasin in the context of a productive HCMV infection. Results from NK assays using primary NK cell cultures from ≥3 donors had shown a consistent decrease in NK cell degranulation when RL11 was expressed in HF-CAR cells using RAd-RL11 as compared with an Ad vector control (personal communication, Dr Rebecca Aicheler). By assessing MerlinΔRL11, I could assess the effect of RL11 on T-cell activation in the context of an HCMV infection.

In two experiments, D7-SFi cells were infected with Merlin, MerlinΔRL11, parent (MerlinΔUL16/UL18) and parentΔRL10-UL1. These cells were used as targets for a CD107a degranulation assay at 72hpi. Both D7-VLE and D7-NLV were used as effector cells. Whilst there was a significant increase in degranulation between parent and ΔRL10-UL1 with both T-cell lines there was no increase in degranulation between Merlin and MerlinΔRL11 (Figure 3.10A and B). This experiment was repeated, though the converse was seen. There was a significant increase in degranulation between Merlin and MerlinΔRL11, but there was no increase in degranulation induced by ΔRL10-UL1 compared to the parent HCMV (Figure 3.10C and D). One consideration was that the level of infection for MerlinΔRL11 was 92%, as measured by HLA-I downregulation, with the HLA-I on non-infected cells potentially influencing the result, by increasing the presentation of exogenous peptide.

To test if there were any effects of deleting RL11 over a wider range of T-cell receptor signalling, an assay was performed comparing Merlin and MerlinΔRL11, and a range of different peptide concentrations (0.5-0.0005μg/ml). D7-SFi cells were infected with Merlin or MerlinΔRL11 and were used in a standard degranulation assay at 72hpi. In this experiment, the infection was complete for both viruses. Both D7-NLV and D7-VLE were used as effectors. With both T-cell lines, there was a significant difference between Merlin and MerlinΔRL11 at 0.5μg/ml of peptide (Figure 3.10). The difference was greater with the NLV line (21.2 vs 27.0%). The degranulation of D7-VLE induced by Merlin versus ΔRL11 was significant, but small (15.7% vs 17.6%). At lower peptide concentrations, the absence of RL11 decreased degranulation. This data showed that RL11 may act as a T-cell evasin, increasing degranulation, however the magnitude of this, as measured by CD107a expression varied between the T-cell lines.

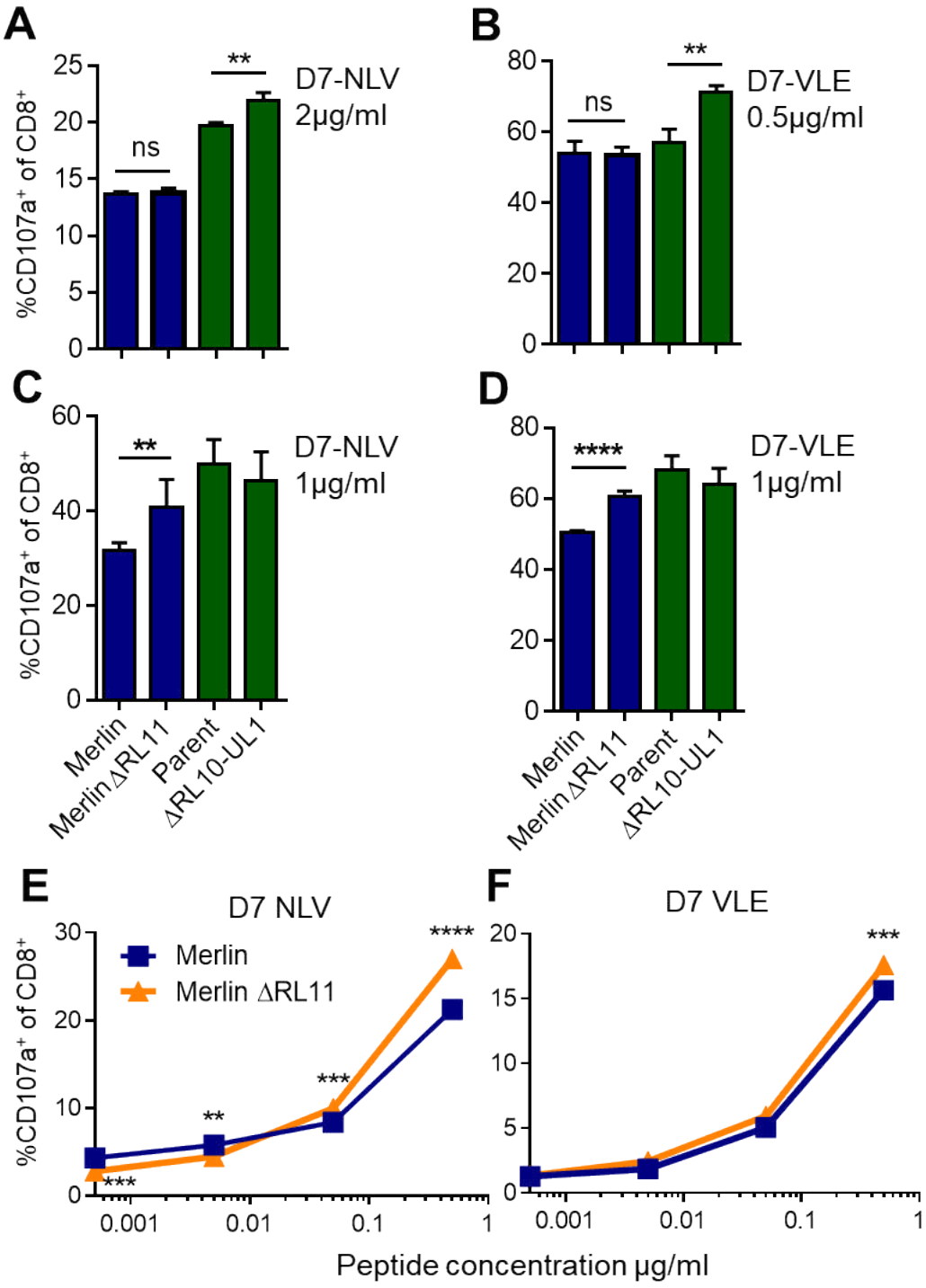

Figure 3.10 Assessing the effect of deleting RL11 from the HCMV genome on CD8+ T-cell activation. D7-SFi cells were infected with Merlin or MerlinΔRL11. At 72hpi, cells were pulsed with NLV or VLE peptide and used as targets in a CD107a degranulation assay. Experiments (A) and (B) were performed in parallel, as were (C) and (D). Data was analysed with a one-way ANOVA. (E and F) The experiment was repeated at multiple peptide concentrations. Data was analysed with a two-way ANOVA with a Bonferroni multiple comparison post-hoc test. In all experiments bars/points show mean %CD107a+ of CD8+ cells ± SEM of quadruplicate values with significance shown at ****p<0.0001, ***p<0.001, **p<0.01.

3.4.4 Summary of screens performed with RL11 family knockouts

Table 3.1 summarises the main findings from this section of work, showing data from experiments with knockout HCMV viruses. The table shows the number of assays where cells infected with the knockout virus resulted in 'activation' of the effector cells line compared to the parental HCMV. Activation was assigned as significant if the %CD107a+ of CD8+ cells induced by the knockout HCMV was ≥1.15x that induced by the control HCMV infected cells and showed significance by statistical testing. This criterion was used to take into consideration assays which produced a significant difference due to very tight data points in the quadruplicate, but where the difference was very small.

Considering all the data, cells infected with ΔRL10-UL1 resulted in activation of CD8+ T-cells in 75% of experiments performed without peptide. On average, degranulation increased 1.7-fold ($p=0.023$). The table shows that when peptide was added, the experiments were more variable. In 6/17 experiments there was significant activation of T-cells induced by ΔRL10-UL1 infected cells. When the mean CD107a+ of CD8+% from all experiments were compared using a paired t-test, there was also a significant difference, although on average there was only a 1.1-fold increase in the proportion of degranulating CD8+ T-cells. I also performed this analysis for ΔUL2-UL11. Whilst there was a small increase in degranulation in one experiment (Figure 3.7), relative to the parent, none of the other experiments revealed an increase in degranulation induced by ΔUL2-UL11 infected cells.

When the genes RL10-UL1 were overexpressed with adenoviruses, in two experiments RL11 and UL1 resulted in a reduction in degranulation. This suggested that both RL11 and UL1 may function as immune evasins. To assess the ability of RL11 to impair activation of T-cells against HCMV infected cells, experiments were conducted using MerlinΔRL11. Based on six experiments, MerlinΔRL11 induced a non-significant 1.15-fold increase in degranulation. Another consideration was that in two of these experiments the level of infection was incomplete, which could have adversely affected results.

Table 3.1 Summary of data from experiments showing potential immune evasion capability of RL11 genes. The table includes all data using both D7-VLE and D7-NLV.

	Knockout	Activation[a]	Mean degranulation %CD107a+ of CD8+ cells[b]			p-value[e]
			Parental HCMV[c]	Knockout	Mean fold change[d]	
No peptide	ΔRL10-UL1	6/8 (75%)	1.7 ± 0.5	2.8 ± 0.9	1.7	0.023
Peptide[f]	ΔRL10-UL1	6/17 (35%)	38.7 ± 4.5	42.3 ± 4.4	1.1	0.018
	ΔUL2-UL11	2/6 (33%)	38.5± 7.3	37.1± 5.7	1.0	0.84
	MerlinΔRL11	3/6 (50%)	31.2 ± 7.2	35.6± 7.9	1.1	0.09

[a] Activation was assigned if the difference was statistically significant, and was greater than a 1.15x the mean %CD107a of CD8+ cells induced by the comparator.
[b] Equivalent data from experiments were pooled and averaged. Values show mean %CD107a+ of CD8+ cells ±SEM.
[c] Parental HCMV was parent (ΔUL16/UL18) for assays with ΔRL10-UL1 and ΔUL2-UL11, or Merlin for MerlinΔRL11.
[d] For each individual experiment the mean CD107a+,CD8+ value from parent HCMV was set as 1 and the fold change in degranulation was calculated.
[e] The p-value was determined by a paired two-tailed t-test. Normality of data was determined by D'Agostino Pearson omnibus normality test. Where n≤6 or data was non-parametric, a two tailed a Wilcoxon signed rank test was performed.
[f] Peptide data included data from all experiments where ≥ 0.1µg/ml of peptide was used to pulse cells.

3.4.5 Impact of HCMV genes UL13-UL20 on CD8+ T-cell response

Screening of the HCMV genome showed that deleting genes UL13-UL20 increased activation of CD8+ T-cells far more than any other deletion mutant in assays using exogenous peptide. The assays in the previous sections (section 3.3, 3.4) showed an increase between Merlin and the parent HCMV. This indicated that deleting UL16 and/or UL18 was influencing T-cell activation and at least one other gene in the UL13-20 region was acting as a CD8+ T-cell evasin. The previous section (3.4.2) showed that even though a reduction in degranulation was observed with RAd-RL11, the role of RL11 as a T-cell evasin was not entirely supported with a complementary increase in T-cell activation when MerlinΔRL11 was used. This informed my decision to not use RAds as a primary screen, preferring knockout HCMV viruses, as: firstly, they provide a more physiological context to study the function of an HCMV gene during HCMV infection; secondly, one can easily control for levels of infection by measuring the proportion of cells downregulated for HLA-I, and; thirdly, they avoid toxicity in cell cultures due to over expression of certain HCMV genes, as has been observed with some RAds (Seirafian, 2012).

3.4.6 Effect of UL16 and UL18 on the CD8+ T-cell response

Firstly, I wanted to assess the difference in degranulation between Merlin and parent (referred to as ΔUL16/UL18 in this section). A dose response experiment was performed comparing the activation of T-cells induced by uninfected (Mock), Merlin and ΔUL16/UL18 infected targets. This was to assess whether there were differences depending on the strength of signal received by the T-cell receptor. D7-SFi cells were infected with Merlin, ΔUL16/UL18 and at 72hpi, cells were pulsed with different peptide concentrations and used as targets in a CD107a degranulation assay. Removing these genes resulted in an increase in CD8+ T-cell activation at concentrations of 1 and 0.1μg/ml (Figure 3.11A). At 10μg/ml of peptide there was no difference between Merlin and ΔUL16/UL18, indicating that the inhibitory effects of UL16/UL18 observed at the lower concentrations could be overcome by an excess of exogenous peptide. Multiple experiments were performed using Merlin and ΔUL16/UL18 and I analysed the differences in the responses of CD8+ T-cells as a whole to assess if these two genes were consistently affecting degranulation. In 10/11 experiments ΔUL16/UL18 infected cells significantly increased degranulation compared to Merlin. When the mean degranulation values from each experiment were pooled and analysed there was a

significant and consistent increase in activation of CD8+ T-cells against cells infected with ΔUL16/UL18 (2.0±0.8% vs 3.8±1.0%, p=0.0002, Figure 3.11B).

A similar approach was taken with data from 18 assays performed with exogenous peptide (≥0.1μg/ml) to coat HCMV-infected cells (Figure 3.11C). In 12/18 experiments there was a significant increase in degranulation against ΔUL16/UL18 infected cells. When considering all data points, degranulation between Merlin and ΔUL16/UL18 infected cells was significantly higher (34.1±3.6 vs 42.7±3.8% p=0.0025, Figure 3.11C). In summary, these experiments show that UL16/UL18 reduced activation of CD8+ T-cells as the deletion of genes from HCMV increased the ability of T-cell to degranulate against HCMV infected cells in the presence and absence of exogenous peptide.

I wanted to assess how each of these genes were contributing to this effect. To assess this, I performed a T-cell assay using individual ΔUL16 and ΔUL18 knockout viruses. MFI was assessed as well as the proportion of cells expressing each marker. Assessing the MFI shows how much of each cytokine is being produced by the activated population. Of the cytokines analysed, T-cells activated by ΔUL16 produced significantly more TNF, compared to Merlin. The differences in the level of IFNγ, IL-2 and MIP-1β production by D9-VTE was the same against Merlin, ΔUL16 and ΔUL18 infected cells.

The proportion of activated T-cells was also assessed. The data presented in Figure 3.12B showed that UL16 significantly increased the activation of CD8+ T-cells as assessed by degranulation (CD107a) and cytokine production (TNF, IFNγ, and MIP-1β). No significant increase in IL-2 production was recorded. In contrast, deleting UL18 did not result in an increase in any T-cell activation markers, and there was a significant decrease in MIP-1β production. This showed that infecting cells with ΔUL16 resulted in more activation D9-VTE T-cells, and that the responding cells produced more TNF. This showed that UL16 is likely involved with downregulation of T-cell activity.

This experiment was not repeated with the other T-cell lines, but flow cytometry for NKG2D and LIR1 was performed, which are the ligands for UL16 and UL18 respectively. This was carried out to provide potential mechanism as to how UL16 may affect T-cells. Figure 3.12C showed that D9-VTE lacked LIR1, but uniformly expressed NKG2D. In summary this suggests that UL16 impairs T-cells, and that sequestering of NKG2D ligands, a known function of UL16, may contribute to reduced CD8+ T-cell activation.

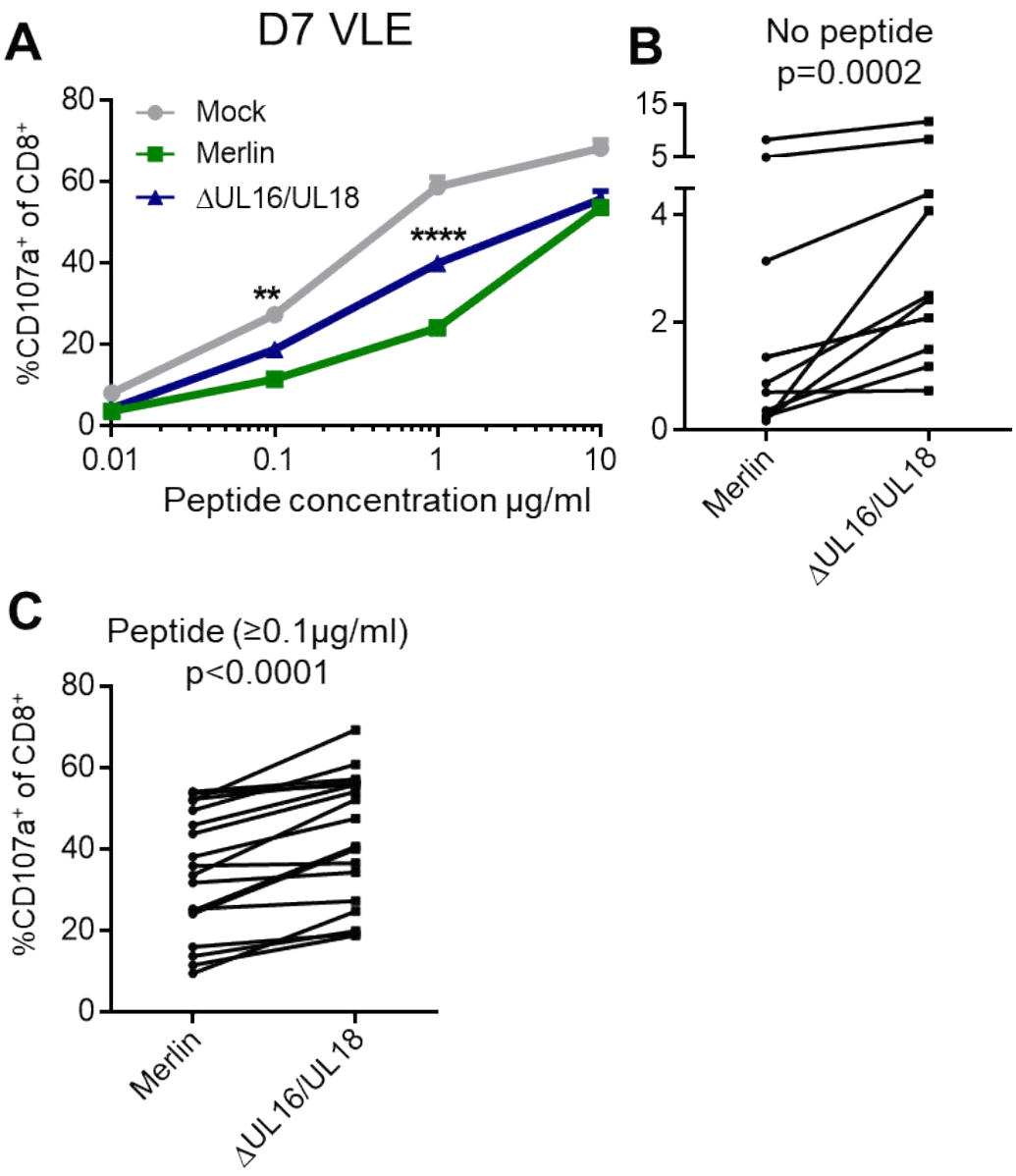

Figure 3.11 Effect of deleting HCMV genes UL16 /UL18 on degranulation of HCMV specific T-cells. (A) D7-Sfi cells were infected with Merlin or ΔUL16/UL18 and used as targets in a CD107a degranulation assay at 72hpi. Dose response showing changes in degranulation induced by mock, Merlin or ΔUL16/UL18 infected fibroblasts. Data points show mean %CD107a+ of CD8+ cells ±SEM of quadruplicate values and were analysed with a two-way ANOVA with Bonferroni multiple comparison post-hoc tests. Significant differences are shown at ****p<0.0001, **p<0.01. Summary data is shown for all experiments comparing Merlin and ΔUL16/UL18 comparing mean %CD107a+ of CD8+ cells from experiments when (B) no exogenous peptide was used (analysed using Wilcoxon matched-pairs signed rank test, data was non-parametric, as assessed by a D'agostino Pearson omnibus normality test) and where HCMV infected cells were (C) pulsed with ≥ 0.1µg/ml of NLV or VLE peptide (paired two tailed t-test was used as the data was parametric).

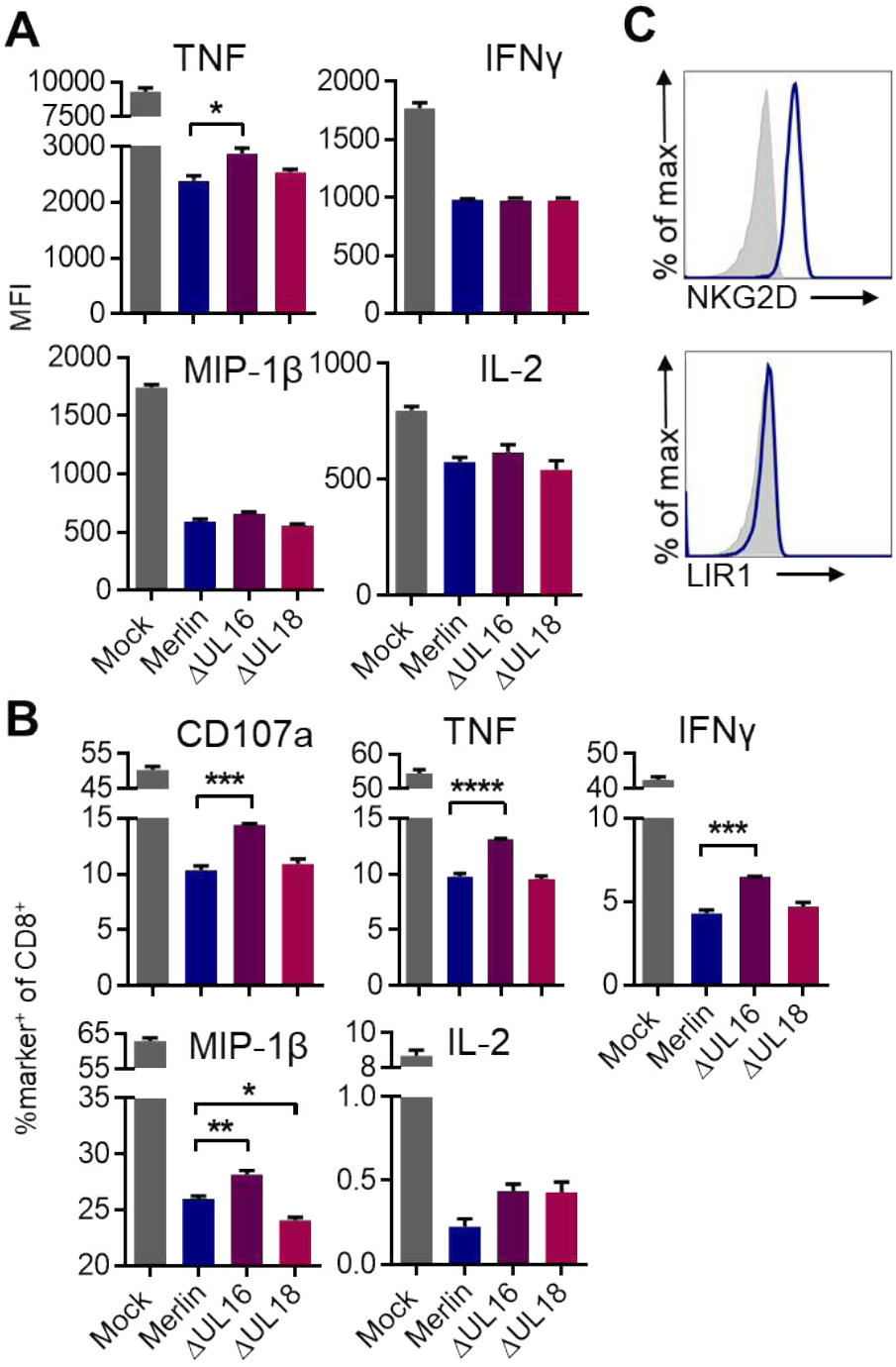

Figure 3.12 T-cell activation assay assessing the effect of deleting genes UL16 and UL18 on CD8+ T-cell activation. D9-SFi cells were mock infected or infected with the indicated HCMV viruses. At 72h cells were pulsed with 1µg/ml of VTE peptide. Intracellular staining for IL-2, IFNγ, MIP-1β and TNF was performed after the 5-hour incubation period. Data shows mean (A) MFI of cytokine by activated CD8+ T-cells and (B) % positive for each readout, +SEM of quadruplicate values. One-way ANOVA with Tukey post-test showed significance at **** p<0.0001, ***p<0.001, **p<0.01, *p<0.05. (C) Flow cytometry histograms showing NKG2D and LIR1 expression on D9-VTE T-cell line (isotype control shown in grey).

3.4.7 Screening of deletion mutants within the UL13-UL20 region on the CD8+ T-cell response

Screening with the block deletions showed that deleting the UL13-20 region increased CD8+ T-cell activation compared to parent HCMV. A summary graph is shown displaying the mean data from all experiments with peptide (≥ 0.1µg/ml) (Figure 3.13A). This showed that cells infected with ΔUL13-20 induced significantly large increases in T-cell degranulation, compared to the parent HCMV (38.4±6.7% vs 51.7±5.2% p=0.0026). This data indicated other genes in the UL13-20 regions (UL13, UL14, UL15A, UL17, UL19 and UL20) function as T-cell evasins. Additional deletions available for testing in this region included ΔUL14 and ΔUL19.

D9-SFi cells were infected with Merlin, ΔUL14 and ΔUL19, as these were the only deletion mutants available within the UL13-20 region, other than ΔUL16 and UL18. At 72hpi, cells were coated with 1µg/ml of peptide and were used as targets in a standard T-cell activation assay. Along with CD107a, cytokine production was assessed (TNF, IFNγ, MIP-1β and IL-2). Amongst the activated T-cells, the MFI from each cytokine was not altered by UL19 or UL14 (Figure 3.13B). When the proportions of activated cells were assessed, the experiment showed that ΔUL19 induced a significant increase in degranulation of CD8+ T-cells (10.4±0.4 vs 12.6±0.4% CD107a+CD8+, p=0.05), whilst ΔUL14 did not alter the proportion of degranulating cells compared to Merlin. ΔUL19 did induce a significant increase in the proportion of MIP-1β producing CD8+ T-cells, but only by 2% (26.0±0.2 vs 28.0±0.5% p=0.04). TNF and IFNγ were not significantly increased. This data indicated that UL19 may be an additional immune evasion gene, reducing the activation and degranulation of CD8+ T-cells, and impairing production of some cytokines (MIP-1β), but not others.

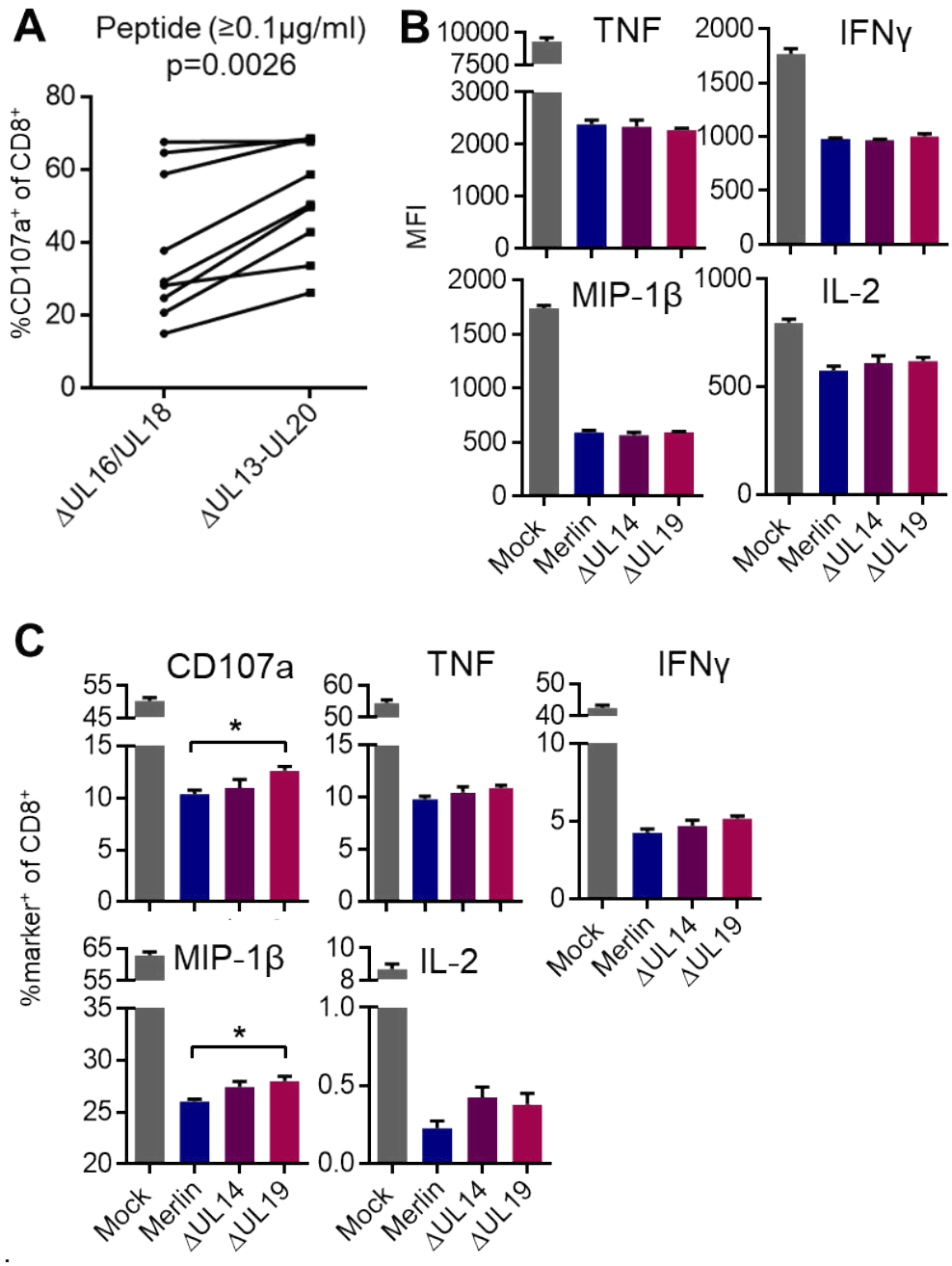

Figure 3.13. Affect of other genes in the UL13-20 region, distinct from UL16 and UL18, on CD8+ T-cell activation. (A) Summary data is shown for all experiments including ΔUL16/UL18 vs ΔUL13-20 with peptide at ≥0.1µg/ml showing mean %CD107a+ of CD8+ cells. Data was analysed with a paired, two-tailed t-test. (B and C) T-cell activation assay assessing the effect of deleting genes UL14 and UL19 on activation of D9 VTE T-cell line. D9-SFi cells were mock infected or infected with the indicated HCMV viruses. At 72h cells were pulsed with 1µg/ml of VTE peptide. Intracellular staining for IL-2, IFNγ, MIP-1β and TNF was performed after the 5-hour incubation period. Data shows (A) mean MFI of cytokine by activated CD8+ T-cells and (B) mean %positive for each readout, +SEM of quadruplicate values. One-way ANOVA with Tukey post-test comparing showed significance at *p<0.05.

3.4.8 Effect of UL19 on CD8+ T-cell response

The next set of experiments focussed on UL19, as the previous screen suggested it was acting as a T-cell evasin, with no previous descriptions of function in the literature. Additionally, preliminary data using RAd-UL19 suggested that UL19 could inhibit NK-cells (personal communication Dr Rebecca Aicheler). To further describe the role of UL19 as an immune evasin, experiments were performed with three T-cell lines (D7-NLV, D7-VLE and D9-VTE). In each experiment, skin fibroblasts (D7, D9) were infected and pulsed at different peptide concentrations covering from 0.008 to 10μg/ml. Across a range of peptide concentrations, deleting UL19 induced an increase in T-cell activation compared to Merlin infected cells (Figure 3.14). Each experiment was performed independently. With both D7 derived T-cell lines, ΔUL19 induced a significant increase in degranulation at all peptide concentrations (Figure 3.14A and B). CD107a expression was recovered to mock levels at 3/4 peptide concentrations (5.0,1.0 and 0.2 μg/ml). The magnitude of the difference between Merlin and ΔUL19 was less with D9-VTE compared to the other two T-cell lines though still significant (Figure 3.14C). At 0.04μg/ml, the difference in degranulation was non-significant, unlike the experiments with D7-NLV and VLE T-cells which were inhibited by UL19 at all concentrations. At all higher peptide concentrations there was significantly higher degranulation induced by ΔUL19 compared to Merlin. HLA-I expression of ΔUL19 infected cells was comparable to Merlin infected cell at 72hpi indicating that UL19 did not affect the surface expression of HLA-I (Figure 3.14D), in line with the result which showed that deleting the UL13-20 block did not affect HLA-I expression (Figure 3.5A). This data provided strong evidence that UL19 is a CD8+ T-cell evasion molecule.

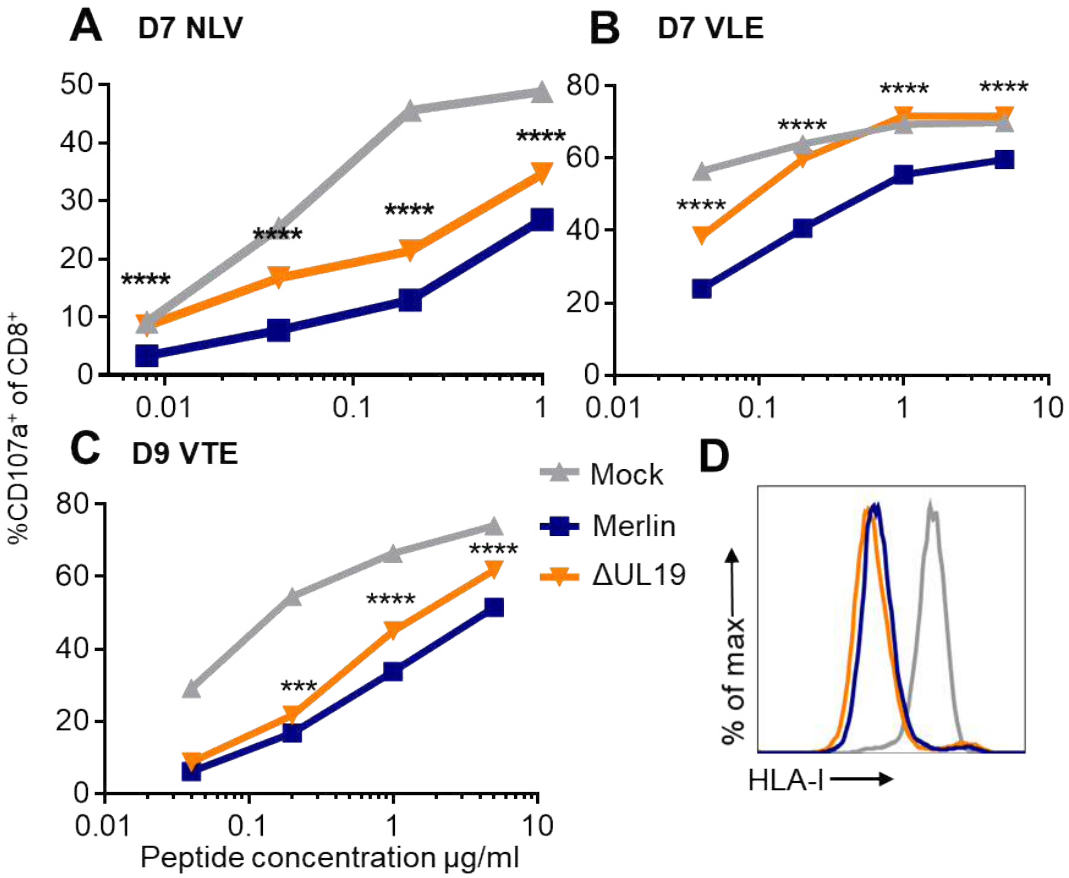

Figure 3.14 Dose response curves showing effect of deleting UL19 on CD8+T-cell activation at different peptide concentrations. Skin fibroblast-cells (D7, D9) were mock infected or infected with Merlin, or ΔUL19. At 72hpi, cells were pulsed with (A) NLV, (B) VLE, or (C) VTE peptide at different concentrations and used as target in a CD107a degranulation assay. Experiments were performed independently. Experiments B and C were performed by Dr Simone Forbes. Points show mean %CD107a+ of CD8+ cells and ±SEM of quadruplicate values. A two-way ANOVA with Bonferroni multiple comparison post-hoc tests showed significance at **** p<0.0001, ***p<0.001. (D) Flow cytometric histograms showing HLA-I expression of infected cells.

3.4.9 Summary of screens performed with UL13-20 knockouts

Data from this section is summarised in Table 3.2. Deleting UL16 and UL18 significantly increased activation by CD8+T-cells in assays performed with and without peptide pulsing. This was observed in almost all experiments without peptide (10/11). In 12/18 experiments performed with peptide, significant activation was recorded, as determined by a significant increase in CD107a+ CD8+ T-cells ≥1.15x induced by Merlin infected target cells. On average deleting UL16 and UL18 increased degranulation 1.4-fold with peptide. Further screening with single deletion mutants showed that this effect could be attributable to UL16, which when deleted from Merlin resulted in a significant increase in 4/5 activation markers (CD107a, TNF, IFNγ and MIP-1β). This experiment was performed once, and therefore the individual effect of UL18 on D7-NLV and D7-VLE T-cells lines was not determined. The largest increase was observed when UL13-20 was deleted, which increased degranulation 1.5-fold above ΔUL16/UL18. Six of the nine assays resulted in activation, and in those that did not, the level of degranulation of the parent HCMV was at or above 60%, which was close to the saturation point of the assay, where addition of more peptide often did not increase the proportion of CD107a expressing T-cells (e.g. Figure 3.14B).

Deleting UL19 resulted in significantly increased degranulation across a range of peptide concentration. In all experiments performed with >0.1µg/ml of peptide, with all T-cell lines (D7-NLV, D7-VLE and D9-VTE), there was activation of CD8+ T-cells compared to Merlin. Cells infected with ΔUL19 increased degranulation by 1.3-fold. This data indicated UL19 can function as CD8+ T-cell evasins across multiple T-cells lines derived from different donors.

Table 3.2 Summary data from experiments showing potential immune evasion genes in UL13-20 region. The table included all data using both D7-VLE, D7-NLV and D9-VTE.

	Knockout	Activation[a]	Mean degranulation %CD107a+ CD8+ cells [b]			p-value [e]
			Parental HCMV[c]	Knockout	Mean fold change [d]	
No Peptide	Merlin ΔUL16/UL18	10/11 (91%)	2.0 ± 0.8	3.75 ± 1.0	2.2	0.0002
Peptide[f]	ΔUL13-UL20	6/9 (67%)	38.4 ± 6.7	51.7 ± 5.2	1.5	0.0026
	Merlin ΔUL19	9/9 (100%)	34.2 ± 3.0	44.5 ± 3.7	1.3	0.0004
	Merlin ΔUL16/UL18	12/18 (67%)	34.1 ± 3.6	42.7 ± 3.8	1.4	<0.0001

[a] Activation was assigned if the difference was statistically significant, and was greater than 1.15x the mean %CD107a of CD8+ cells induced by the parent HCMV.
[b] Equivalent data from experiments were averaged. Values show mean %CD107a+ CD8+ cells ±SEM.
[c] Parental HCMV is parent (ΔUL16/UL18) for assays with ΔUL13-UL20, or Merlin for other assays.
[d] For each individual experiment the mean %CD107a+, CD8+ value from parent HCMV was set as 1 and the fold change in degranulation was calculated for the knockout.
[e] The p-value was determined by a paired two-tailed t-test. Normality of the data was determined by D'Agostino Pearson omnibus normality test. If the data was non-parametric, a two tailed a Wilcoxon signed rank test was performed.
[f] Peptide data included data from all valid experiments where ≥ 0.1µg/ml of peptide was used to pulse cells.

3.5 Summary of findings

The main aim of this chapter was to identify candidate HCMV CD8+ T-cell evasion genes. The majority of experiments utilised two HLA-A2 restricted T-cell lines; D7-VLE and D7-NLV. When used as effector cells against fibroblasts infected with a series of HCMV block deletions in the absence of peptide, a significantly higher proportion of these cells degranulated against ΔRL10-UL1 infected fibroblasts compared to the parent HCMV. This result was shown in 6/8 of all experiments with both T-cell lines but experiments with peptide were less conclusive. Whilst the average degranulation of T-cells against ΔRL10-UL1 was significantly increased, this only equated to a 1.1-fold increase in CD107a expression. Significant activation was recorded in 6/17 experiments. Gain of function experiments using RAd expressing HCMV genes showed that RL11 and UL1 could reduce T-cell activation. Despite this, loss of function experiments using MerlinΔRL11 were variable, with activation of T-cells induced in 3/6 experiments when compared to Merlin. The 1.15-fold increase was not considered significant.

I found that ΔUL16/UL18 infected cells increased the proportion of degranulating CD8+ effectors, compared to Merlin infected cells. The mean degranulation of CD8+ T-cells increased 2.2-fold and 1.4-fold in experiments without and with peptide respectively. To explore this further an experiment performed with single knockout viruses showed that UL16 was able to downregulate D9-VTE T-cells, as ΔUL16 infected cells significantly increased degranulation (CD107a) and cytokine (TNF, IFNγ and MIP-1β) expression by CD8+ T-cells. Surface staining of T-cells showed that line D9-VTE expressed NKG2D, but not LIR1, suggesting UL16 could be affecting T-cells in a similar way to how it affects NK-cells.

Experiments using D7-VLE and D7-NLV T-cell lines showed that ΔUL13/UL20 infected cells caused a further significant increase in CD107a expressing T-cells compared to ΔUL16/UL18 infected cells. The mean increase in the proportion of activating cells was 1.5-fold. Screening with further knockout viruses showed that this effect is likely attributable in part to UL19. Experiments with three different T-cell lines at multiple peptide concentrations showed that deleting UL19 significantly increased the mean proportion of CD107a expressing T-cells by 1.3-fold, showing that UL19 had a strong effect on inhibiting CD8+T-cell activation against HCMV infected cells.

4 Identification of HCMV genes regulating TNF receptor expression

4.1 Introduction

The aim of this chapter was to identify genes further regulating TNFR1/2, as this would influence how HCMV infected cells respond to TNF. This was inspired by proteomic data which showed that TNFR2 is increased on the cell surface during lytic HCMV infection (Weekes et al., 2014). Receptor expression should influence how HCMV infected cells respond to TNF, and the remaining two chapters of work were devoted to identifying how TNFR1/2 are regulated by HCMV. HCMV infected cells would be influenced by TNF, an inflammatory cytokine released by lymphoid cells including HCMV specific T-cells and NK cells (Lachmann et al., 2012). Whilst HCMV UL138 is known to maintain TNFR1 on the surface of HCMV infected cells (Montag et al., 2011), there are no published studies investigating TNFR2 on HCMV infected cells, which is why this warranted investigation.

4.2 Identifying genes involved in TNFR2 upregulation

4.2.1 Comparison of TNF receptor expression between high and low passage HCMV strains

Initial work investigating the effect of HCMV on TNFR1 reported an unpublished observation which stated that TNFR2 surface expression did not change upon infection with HCMV strain AD169 (Baillie et al., 2003). Our laboratory, in partnership with collaborators at Cambridge University used mass spectrometry to assess the temporal expression of host and viral proteins over the course of a HCMV infection in fibroblasts (Weekes et al., 2014). BAC derived Merlin was used in this study had intact copies of as all the HCMV canonical genes excepting for natural in RL13 and UL128L selected by in vitro propagation (Stanton et al., 2010). Following infection with strain Merlin, TNFR1 surface expression increased and peaked at 18-24hpi, and then returned to mock levels at 48hpi. The increase at 24hpi correlated with UL138 expression (Figure 4.1A). TNFR2 though was present in relatively small amounts on the surface of fibroblasts (0hpi) with expression increasing and peaking at 72hpi (Figure 4.1B). This information, led to the hypothesis that TNFR2 is upregulated by genes encoded by Merlin, but not by AD169.

To test the reported differences in TNFR2 expression by different HCMV strains, HF-TERT cells were infected with high passage HCMV strains lacking the U_L/*b'* region

(AD169 and Towne) and low passage HCMV strains (Merlin and Toledo). At 72hpi, cells were stained with anti-TNFR2 mAbs and flow cytometry was used to assess TNFR2 expression. At 72hpi, cells infected with Merlin and Toledo expressed more TNFR2, though there was a minimal increase in cells infected with Towne and AD169 (

Figure 4.1C). To assess the temporal profile of TNFR2 expression, a time course experiment was performed by infecting HF-TERT cells at the same time and performing flow cytometry at different points along the 72h time course. The largest increase in surface TNFR2 occurred between 48 and 72hpi which correlated with proteomic data (Figure 4.1B). In summary, this data showed that infection with low passage HCMV strains Merlin and Toledo resulted in an increase in surface TNFR2, which did not occur following infection with AD169 or Towne.

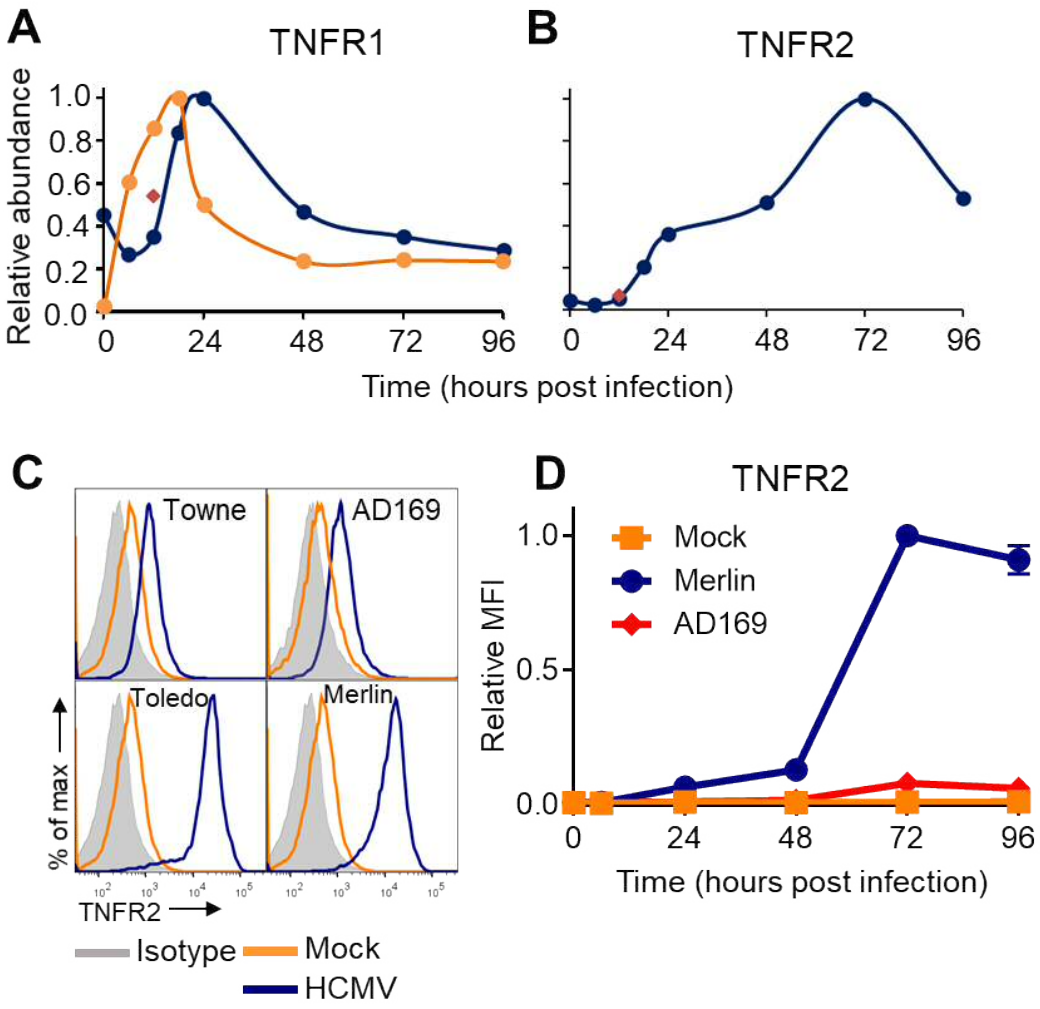

Figure 4.1 Effect of infection with high and low passage HCMV strains on TNFR2 expression. (A) Proteomic data showing the temporal plasma membrane profiles of TNFR1 (blue) and whole cell levels of UL138 (orange). Surface levels of TNFR2 are shown in (B). Red rhombus shows data following infection with gamma-irradiated virus at 12hpi. Data were derived from the resource paper (Weekes et al., 2014). (C) HF-TERT cells were infected with Towne, AD169, Toledo and Merlin and flow cytometry for TNFR2 was performed at 72hpi. (D) HF-TERTs were infected with the indicated HCMV strains and flow cytometry was performed at the indicated timepoints. Maximum MFI was set as 1, with other values plotted as a relative value. Data points show mean ± SEM of triplicate infections.

4.2.2 Analysing the U_L/*b'* region for genes regulating TNFR2 expression

HCMV strains Towne and AD169 have accumulated mutations during in vitro passage, the most prominent being a 13-15kb deletion of the UL/*b*' gene region (UL132-UL150A) (Bradley et al., 2009). I hypothesised that the gene or genes responsible for TNFR2 upregulation were likely to be within this region of the HCMV genome. To test this, I used a series of HCMV strain Merlin mutants, each deleted for one gene of the U_L/*b*' region. Flow cytometry for TNFR2 and HLA-I was performed at 72hpi, which is when surface TNFR2 was shown to peak. Only infected cells demonstrating HLA-I downregulation were gated on for assessing TNFR2 expression. The data showed that whilst there was some variation amongst the mutants, the UL148 and UL148D deletion mutants clearly did not upregulate TNFR2 as much compared to the parental Merlin control (

Figure 4.2A). ΔUL138 did not differentially regulate TNFR2 upregulation, thus the UL138 mechanism of TNFR1 upregulation appears not to impact TNFR2. ΔUL150A may also have had a minor effect on TNFR2 expression. To assess this further, the experiment was repeated with several of the knockout viruses (ΔUL138, ΔUL148, ΔUL148D and ΔUL150A) in triplicate. The data in Figure 4.2C showed that the absence of TNFR2 upregulation seen in Figure 4.2B were consistent, with ΔUL150A causing a small downregulation in TNFR2 expression (this will be discussed in 4.2.3).

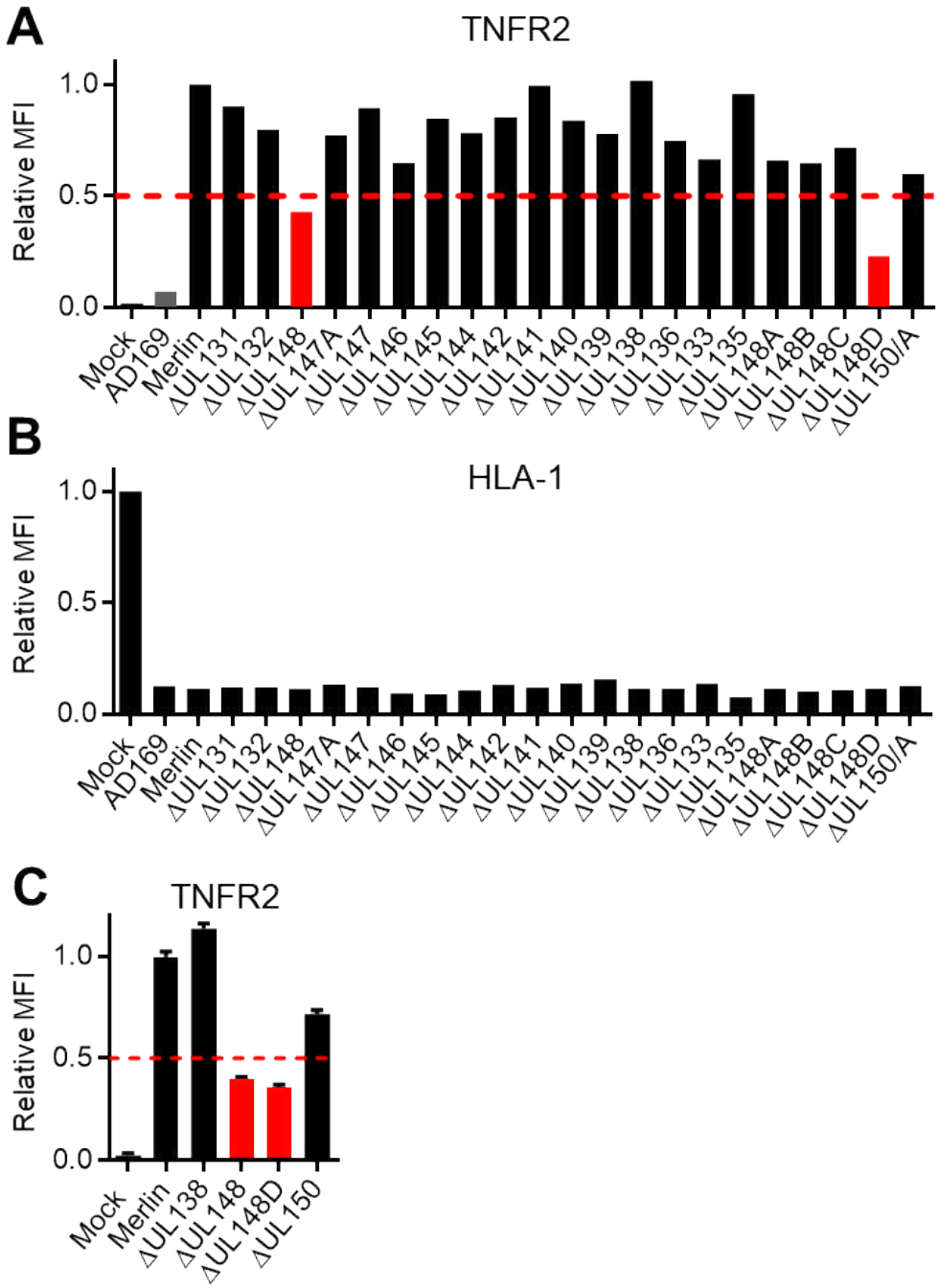

Figure 4.2 Screening of the U_L/b' region for regulators of TNFR2 expression.(A) HF-TERT were infected with HCMV strains missing the indicated U_L/b' genes. Flow cytometry for (A)TNFR2 was performed at 72hpi. TNFR2 MFI for Merlin was set at 1 with other values plotted as a relative value. (B) HLA-I staining on cells from the same experiment was used to measure the level of infection. HLA-I low cells were gated on to identify those infected with HCMV. MFI of mock HLA-I was set as 1, with other values plotted as a relative value. (C) The experiment was repeated with selected knockouts. Bars show mean relative MFI of TNFR2 +SEM of triplicate infections.

4.2.3 Proteomic analysis of UL148 and UL148D deficient HCMV

A comprehensive proteomic analysis was performed on the series of individual HCMV gene knockout viruses across the U_L/*b*' region in a project headed by Dr Peter Tomasec and Dr Michael Weekes. Infections with HCMV ΔUL148 and ΔUL148D revealed a reduction in surface TNFR2 compared to Merlin infected cells consistent with the flow cytometric screen (section 4.2). When the data from the proteomic analysis is presented as dot plots, multiple changes in cell surfaces proteins are evident on HCMV ΔUL148 and ΔUL148D infected cells (Figure 4.3). Proteins with a negative Log_2 change meant there was less of the protein on the surface of infected cells compared to Merlin infected cells. The Log_2 change in TNFR2 expression from ΔUL148 and ΔUL148D infected cells was -0.81 and -1.40 respectively. These were the only two knockout viruses which altered relative TNFR2 expression more than -$Log_2$0.5. Infection with ΔUL150/A resulted in a Log_2 change of TNFR2 of -0.47 ($p<0.0005$), which suggested that this gene may have a small effect on TNFR2 expression, as suggested by the small decrease in TNFR2 expression observed with the flow cytometric screen (Figure 4.2). Deletion of UL150 also significantly affected UL148D expression by decreasing the expression of UL148D, causing a -$Log_2$1.33 reduction in UL148D expression (Appendix). Therefore, the change in TNFR2 following deletion of UL150/A was likely caused by a knock-on effect of reduced UL148D expression. Other proteins which were significantly downregulated with both ΔUL148 and ΔUL148D included NRG1, MEGF10 and GFRA2. This indicated that UL148 and UL148D can both independently regulate TNFR2 levels on the surface of HCMV infected cells, and that these genes may also regulate other cellular proteins too.

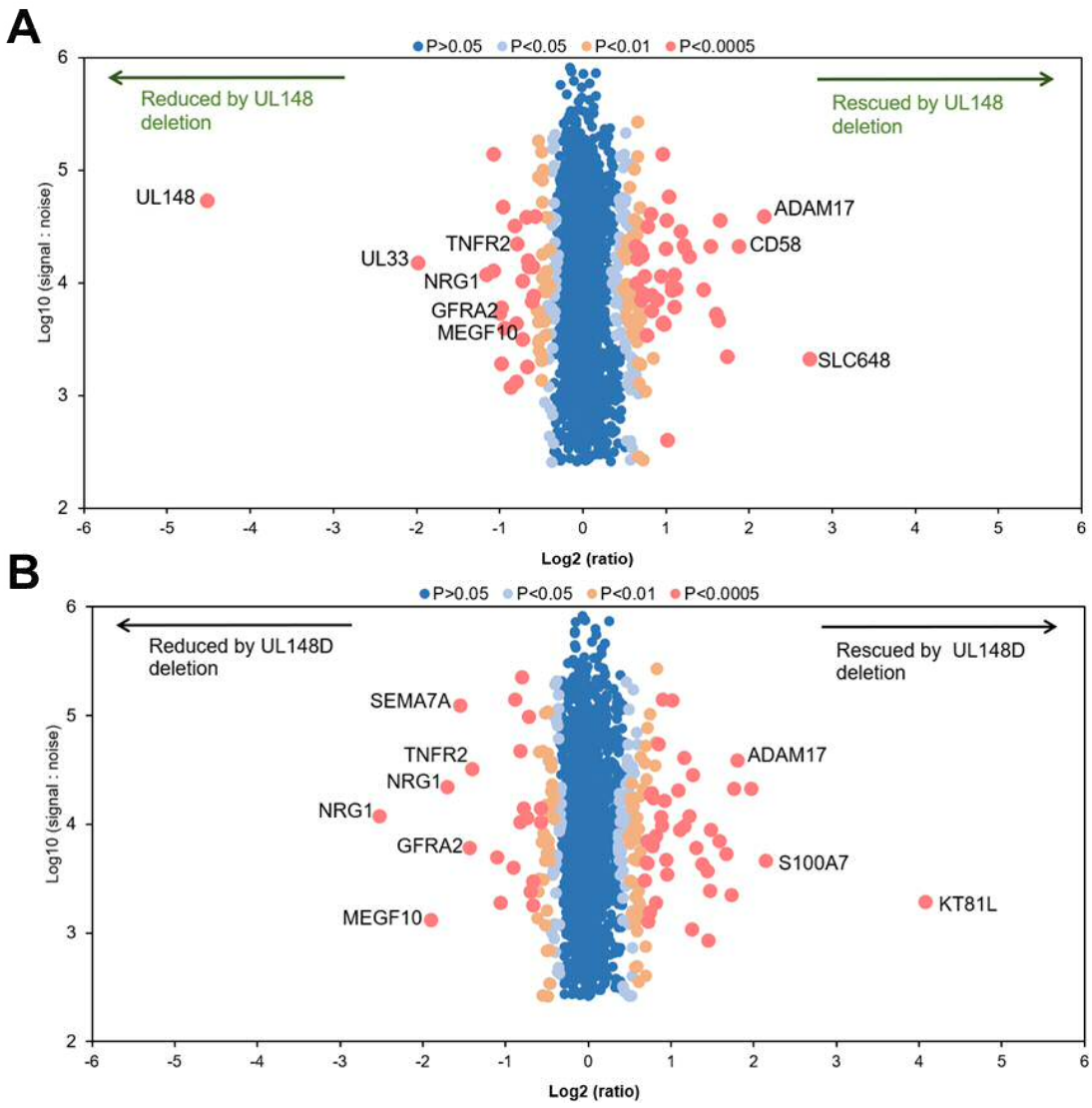

Figure 4.3 Plasma membrane profiling of ΔUL148 and ΔUL148D infected cells.HF-TERT cells infected with Merlin or U_L/*b*' knockout virus were processed to give plasma membrane or whole cell fractions and analyzed by TMT mass spectrometry. Scatter plot of proteins is shown for (A) ΔUL148 and (B) ΔUL148D. Fold change (ΔUL148 or ΔUL148D/ Merlin infected cells) is shown as the $\log_2$ ratio on the x-axis and the signal:noise on the y-axis as $\log_{10}$. Proteins unaltered by the deletion are at the center of the plots (0 $\log_2$), whereas proteins to the left or right of center represent proteins down regulated or upregulated respectively by the deletion of UL148 or UL148D. P values are for for the ratios of expression from each mutant compared to HCMV Merlin using Benjamini-Hochberg corrected Significance B values. Experiment and data analysis were performed by Dr Peter Tomasec and Dr Michael Weekes.

4.3 Effects of deleting both UL148 and UL148D on TNF receptor expression

4.3.1 Recombineering of ΔUL148/UL148D virus

The screen of the U_L/*b*' region showed that UL148 and UL148D were responsible for upregulating TNFR2. This suggested that the two genes may be acting synergistically as the impairment of upregulation was not to the level observed with strains AD169 or Towne (section 4.2.1). To test this hypothesis, a double knockout virus (ΔUL148/UL148D) was recombineered to see whether the TNFR2 phenotype of strains Towne or AD169 could be replicated. The recombineering process is described in the Materials and Methods section 1.7 (Stanton et al., 2010). UL148D was deleted from the ΔUL148 BAC (Wang et al., 2018). The rpsL cassette was amplified by PCR with arms of homology to UL148D (Figure 4.4A and B, red base pairs) and to the rpsL cassette (green base pairs). The insertion of the cassette into ΔUL148 BAC conferred resistance to kanamycin and caused bacteria to grow in blue colonies due to the presence of X-Gal. Blue colonies were chosen, and DNA was extracted from minipreps. The DNA was digested by *Hin*dIII to check that recombination had not altered other areas of the HCMV BAC (Figure 2.3). A PCR was performed to amplify the UL148D region, and the size was assessed by separation on an agarose gel. If the cassette had been incorporated, then this region would be larger than the equivalent region from the Merlin BAC. Removal of the cassette was performed by utilising the remove primer (Figure 4.4D), with 50bps having homology upstream of the UL148D start codon and the other 50 having homology to a region of UL148D and part of UL150A. If the remove primer had replaced the rpsL cassette than bacteria would grow in white colonies on streptomycin containing plates as the cassette confers streptomycin susceptibility. The BAC was digested with *Hin*dIII and compared to the digest pattern of the Merlin HCMV BAC. If the pattern of digested DNA from the manipulated BAC was the same as Merlin, then the UL148D region was amplified by PCR. If the cassette had been removed, then the fragment was smaller than that of the Merlin BAC. The fragment was then gel purified and sent for sequencing. After showing that the purified sequence was the same as the predicted sequence (Figure 4.4E), the ΔUL148/UL148D BAC amplified and transfected into HF-TERT cells.

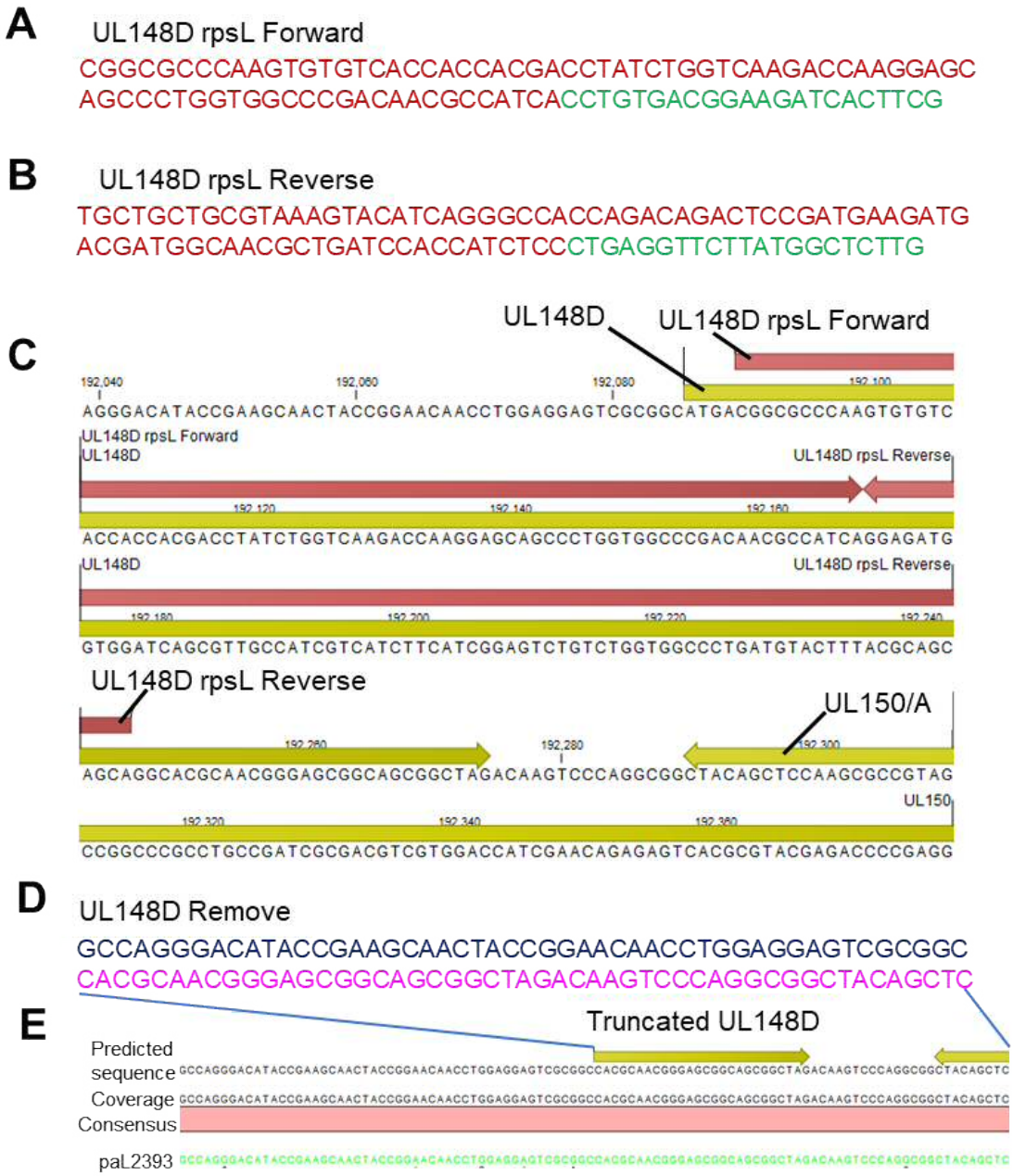

Figure 4.4 Recombineering of ΔUL148/UL148D. (A) Forward and (B) reverse primers for amplification of rpsL cassette. Homology to UL148 is shown in red and homology to the rpsL cassette is in green. (C) UL148D region from Merlin (GenBank GU179001) showing the homology of primers to UL148D. (D) UL148D remove primer. The blue sequence shows 50bp with homology to the sequence upstream of UL148D. The pink sequence corresponds to a truncated region of UL148D and a region of UL150. (E) Consensus sequence of UL148D region from pAL2393 (ΔUL148/UL148D) compared to the predicted sequence.

4.3.2 Effect of deleting UL148 and UL148D on TNFR2 expression

After generation of ΔUL148/UL148D, flow cytometry was used to assess if deleting both genes would further impair TNFR2 upregulation compare to the single deletion mutants. HF-TERT cells were infected in triplicate with HCMV strains Merlin, ΔUL138, ΔUL148, ΔUL148D, ΔUL148/UL148D, AD169 or mock infected. At 24h intervals, flow cytometry for surface TNFR2 was performed (Figure 4.5). The increase in surface TNFR2 by Merlin was similar to that shown in Figure 4.1A. At 48hpi, TNFR2 levels were comparable for ΔUL148 and ΔUL148D. At 72hpi, levels of TNFR2 were half that of Merlin, as assessed by MFI. There was no difference in the expression pattern of TNFR2 between Merlin and ΔUL138. As with AD169, there was no increase in TNFR2 surface expression following infection with ΔUL148/UL148D, indicating that both UL148 and UL148D are required for the upregulation of TNFR2 observed with Merlin infected fibroblasts.

4.3.3 Effect of deleting UL148 and UL148D on TNFR1 expression

To assess the effect of deleting UL148 and UL148D on TNFR1 expression, the experiment performed in 4.3.1 was repeated. HF-TERT infected with HCMV strains Merlin, ΔUL138, ΔUL148, ΔUL148D, ΔUL148/UL148D, AD169. At 24h intervals, flow cytometry for surface TNFR1 was performed. Unlike TNFR2, TNFR1 is constitutively expressed on fibroblasts. From cell surface proteomics (Figure 4.1A), it was shown that TNFR1 was upregulated at 24hpi. This experiment also showed this, with TNFR1 upregulated at 24hpi compared to mock infected cells, but then reducing to levels observed on uninfected cells by 48hpi. UL138 has previously been reported as maintaining TNFR1 expression on the surface of HCMV infected cells (Montag et al., 2011). Here, its deletion reduced TNFR1 surface expression to levels observed on uninfected cells at 24hpi. TNFR1 remained consistently lower than uninfected cells at 48 and 72hpi (Figure 4.6). The deletion of UL148 had no effect on TNFR1 expression compared to Merlin. The absence of UL148D did however affect TNFR1 expression. TNFR1 was reduced on the surface of ΔUL148D infected cells, compared to Merlin. Between 48 and 72hpi, there was an increase in surface TNFR1, though levels were still lower than mock and Merlin infected cells. Deleting ΔUL148/UL148D caused a reduction in TNFR1 expression. Surface levels of TNFR1 were reduced by 24hpi and remained low at 48 and 72hpi. This showed that despite the presence of UL138, the genes UL148 and UL148D had a dominant effect and the removal of both impaired TNFR1 expression altogether. This shows that UL148 and UL148D are required for TNFR1 maintenance.

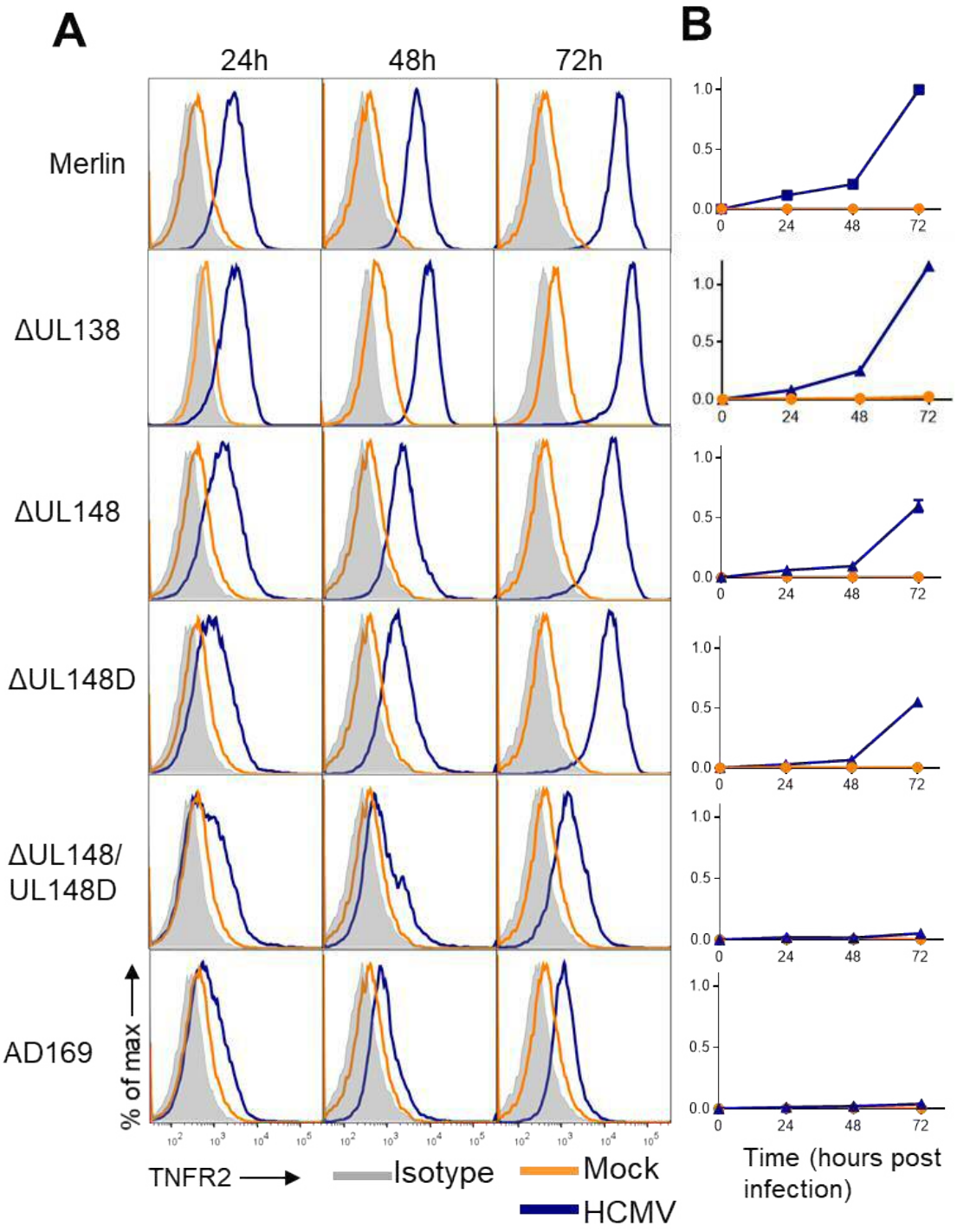

Figure 4.5 Effect of deleting UL148 and UL148D on TNFR2 expression.(A) Representative flow cytometric histograms of TNFR2 surface expression following infection with the indicated HCMV variants. Cells were infected at the same time with flow cytometry being performed at each time point. (B) Relative surface TNFR2 expression over the 72h infection. In each case the maximum TNFR2 MFI of Merlin at 72hpi was set at 1.0 with other values plotted relative to this. Data points show mean relative TNFR2 and SEM of triplicate infections.

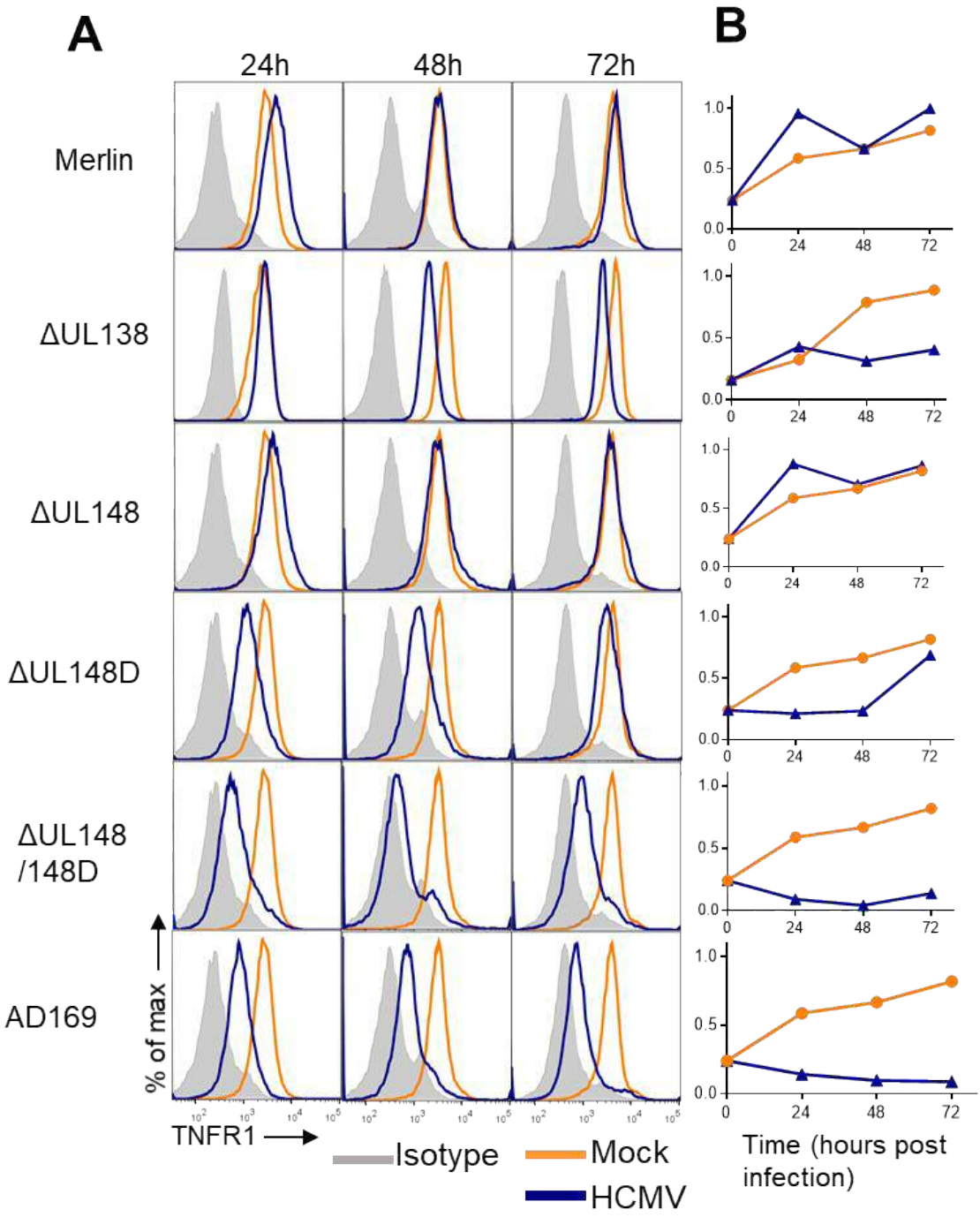

Figure 4.6 Effect of deleting UL148 and UL148D on TNFR1 expression.(A) Representative flow cytometric histograms of TNFR1 surface expression following infection with indicated HCMV variants. Cells were infected at the same time with flow cytometry being performed at each time point. (B) Relative surface TNFR1 expression over the 72h infection. In each case the maximum TNFR1 MFI (Merlin, 24hpi) was set at 1.0 with other values plotted relative to this. Data points show mean relative TNFR1 ± SEM of triplicate infections.

4.4 Effect of RAd-UL148/UL148D on TNFR2 expression

Having identified UL148 and UL148D as genes involved with TNFR2 upregulation, I sought to further explore this effect in a positive expression system by expressing these two genes from adenovirus vectors. This would provide information as to whether the proteins UL148 and UL148D can function in isolation, or whether other HCMV induced changes are required in addition to the expression of these genes. HF-CAR cells were used as the CAR receptor allows for less virus to be used to achieve efficient infection of adenovirus. There was no increase in TNFR2 expression at 48hpi (data not shown). One possibility was that higher levels of protein were needed to elicit an effect. As expression from RAd vectors tend to increase substantially ('ramp') over time, cells were left for 72h to increase the level of expression driven by the IE1 promoter in the constructs. Figure 4.7A shows the expression of TNFR2 following infection with RAd into HF-CAR cells. This data showed that isolated expression of UL148 increased TNFR2 expression, though the effect was small (Figure 4.7A). UL148D stimulated TNFR2 surface expression marginally more than did RAd-UL148 (Figure 4.7A). When both RAd-UL148 and RAd-UL148D were expressed in the same cell culture, there was no additional increase in TNFR2 expression above that of RAd-UL148D. Merlin + RAd-CTRL is shown in grown in this panel as a comparator. This indicated that UL148 and UL148D, individually or together, did not induce TNFR2 expression to the same degree as Merlin infection.

One theory was that UL148 and UL148D may function more efficiently in the context of an HCMV infection. To test this possibility, a reconstitution experiment was performed in which cells were infected with knockout HCMV variants and RAds in the same inoculum. Staining for TNFR2 was performed at 72hpi. Figure 4.7B showed that adding Rad-UL148 or UL148D had no effect on TNFR2 upregulation even in the context of a ΔUL148/UL148D HCMV infection. Furthermore, the addition of RAd-UL148 significantly decreased TNFR2 expression in a HCMVΔUL148 infection. This indicated that in the context of a HCMV infection, co-infection with an adenovirus impaired TNFR2 upregulation.

The partial upregulation of TNFR2 by RAd-UL148D could have been nonspecific, so all adenoviruses expressing genes in the U_L/*b*' region were tested, to assess if other HCMV genes expressed through RAds did the same. This indeed was the case and several RAd expressed HCMV genes did partially increase TNFR2, such as UL138, UL136 and UL148A (Figure 4.7C). These increases were unlikely to be due to the gene expression itself as knockout HCMV viruses lacking these genes did not result in reduced TNFR2

expression (Figure 4.2A). Therefore, the small increase in surface TNFR2 upon RAd-UL148D infection was considered a non-specific effect. In summary, when expressed from an adenovirus, UL148 and UL148D failed to substantially upregulate TNFR2 in mock and HCMV infected fibroblasts, as was observed with Merlin infection alone.

4.5 Effect of irradiated HCMV on TNF receptor expression

To determine if the regulation of TNF receptors was linked to virion proteins or if this required an active HCMV infection, an experiment was performed with irradiated virus. HCMV was gamma irradiated, which denatures viral DNA, but allows for virus entry. An early time point of 24h was chosen to assess if changes in TNFR expression were a result of an innate immune response, which would be induced soon after entry of the virion. HF-TERT cells were infected with either Merlin, or irradiated Merlin and flow cytometry for TNFR1 and TNFR2 was performed at 24hpi. HLA-I was again used to assess infection as an active HCMV infected would reduce surface HLA-I, whereas activation of intrinsic immune defences irradiated HCMV could potentially increase HLA-I expression. As with previous experiments there was an increase in surface TNFR1 and TNFR2 on Merlin infected cells at 24hpi (Figure 4.8). At the same timepoint, there was no difference in surface TNFR1/2 expression between uninfected cells and irradiated Merlin treated cells. This result indicated that active HCMV infection, rather than virion components delivered on entry, were required to upregulate TNFR2.

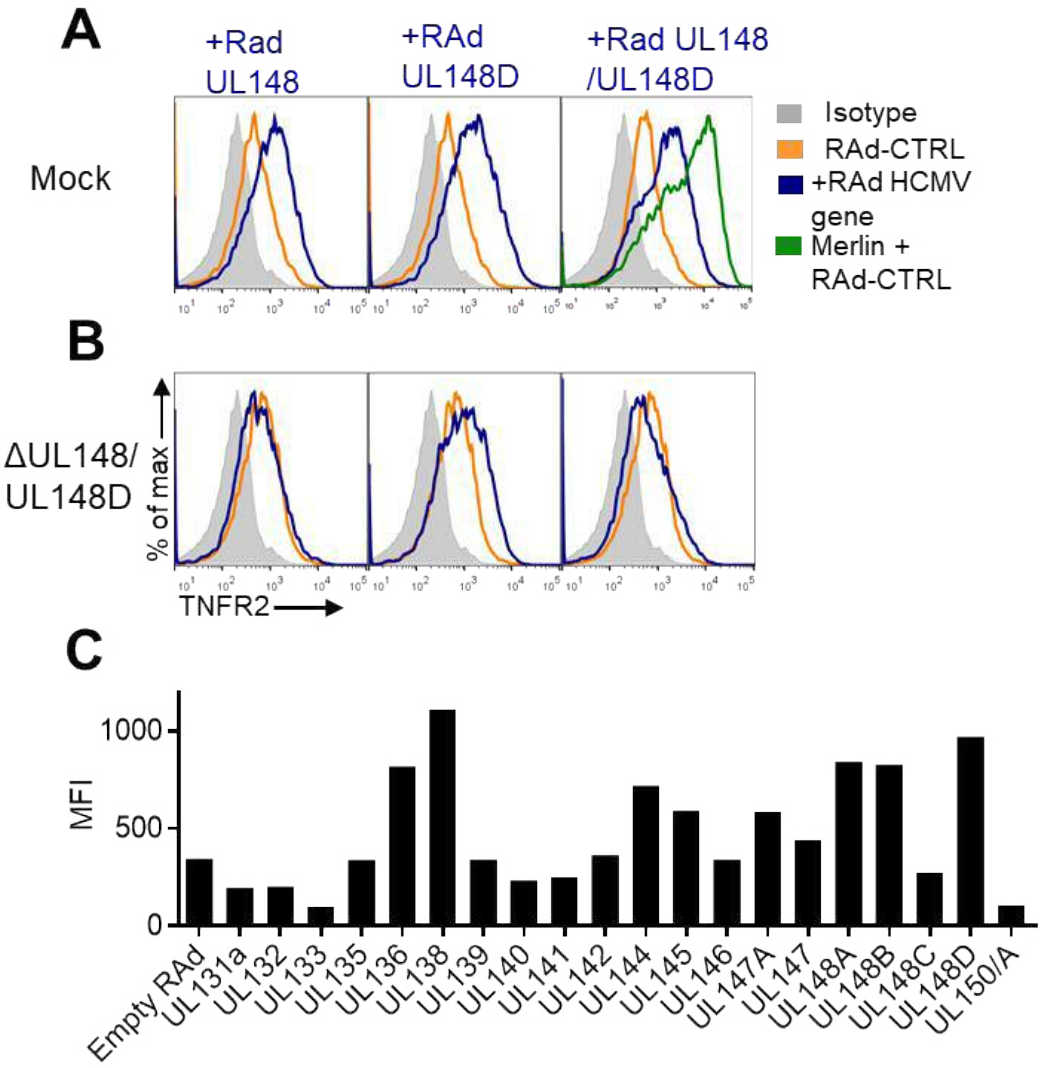

Figure 4.7 Effect of ectopically expressing UL148 and UL148D in isolation and in the context of a HCMV infection. HF-CAR cells were infected with single or combined RAd-UL148, RAd-UL148D or both RAds. The cells were then infected with Merlin, ΔUL148, ΔUL148D, or ΔUL148/UL148D. Each condition was performed in triplicate. At 72hpi, cells were stained for TNFR2. Representative flow cytometric histograms are shown for (A) mock and (B) ΔUL148/UL148D. (C) TNFR2 expression in RAd infected HF-CAR cells. Flow cytometry was performed at 48hpi.

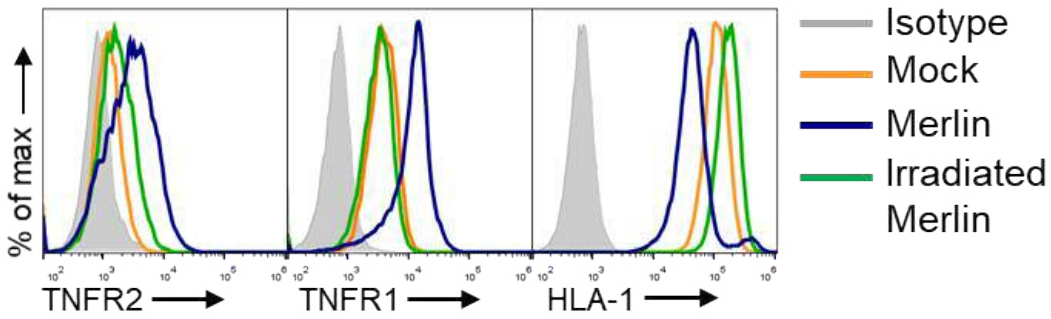

Figure 4.8 Effect of irradiated HCMV virions on TNFR1/2 expression. HF-TERT cells were infected with Merlin or treated with irradiated Merlin. (3500gy of gamma irradiation), or mock infected. Data shows flow cytometric histograms for TNFR1, TNFR2 and HLA-I performed at 24hpi.

4.6 Regulation of TNFR2 protein at a whole cell level

4.6.1 Analysis of whole cell TNFR2 by western blotting

To assess the impact of HCMV infection on the total level of TNFR2 protein in cells, a Western blot was performed. HF-TERT cells were left uninfected (mock) or infected with Merlin or ΔUL148/UL148D. At 72hpi, cells were harvested and lysed. Proteins were separated by SDS-PAGE under reduced denaturing conditions, before blotting for TNFR2 and actin (loading control). The low abundance 55kDa protein in uninfected cell lysates was due to TNFR2 and corresponds with data shown on the manufacturers website (Abcam (2018),Figure 4.9). This is indicated by a red arrow and correlated with the low surface expression shown by flow cytometry (Figure 4.1). From Merlin infected cells, more TNFR2 was detected as shown by a more intense band at the same molecular weight. Deleting UL148 and UL148D had no effect on total TNFR2 levels compared to Merlin. At 50kDa, a fainter band was observed, which was consistent in intensity across all three samples and was considered to be a non-specific signal. In summary, this indicated that the amount of TNFR2 was low in uninfected fibroblasts. Upon HCMV infection, the whole cell level of TNFR2 increased. Deletion of HCMV UL148/UL148D did not influence the whole cell increase in TNFR2.

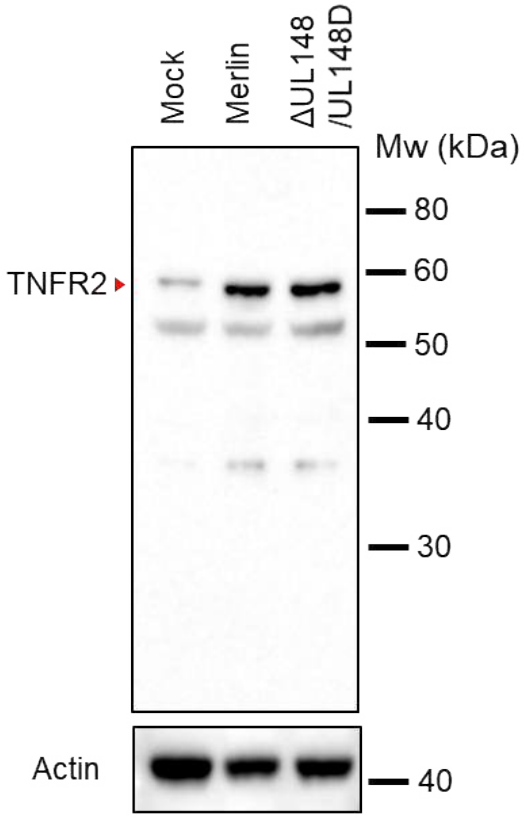

Figure 4.9 Effect of HCMV infection on total TNFR2 protein levels.HF-TERT cells were infected with Merlin, ΔUL148/UL148D or mock infected. Whole cell lysates were prepared at 72hpi. Proteins were separated by SDS-PAGE then transferred to a PVDF membrane and probed with α-TNFR2 primary antibody and HRP conjugated secondary antibody. Signal was visualised by chemiluminescence. Actin was used as a loading control.

4.6.2 Analysis of TNFR1/2 mRNA during HCMV infection

Having shown that HCMV infection increased TNFR2 within the cell, data was assessed to ascertain if HCMV was affecting levels of steady state TNFR2 mRNA. To investigate if HCMV was altering steady state TNFR2 mRNA, transcriptomic data from various sources was assessed. Table 4.1 (experiment performed by Dr Peter Tomasec, and Professor Andrew Davison) and Table 4.2 (data taken from Tirosh et al. (2015)) both show that the whole cell mRNA of TNFR2 increased following a HCMV infection with Merlin. There was no increase measured with UV inactivated virus or interferon treated cells. This indicated the increase in TNFR2 mRNA is not mediated by HCMV virions alone but requires a productive HCMV infection (Table 4.2). At 24hpi, there was twice the amount of TNFR1 mRNA, though this reduced back to mock levels at 72hpi. UV irradiated Merlin, and IFN alone, had no effect on TNFR1 mRNA, with levels within two-fold of untreated cells.

HF-TERT cells were infected in triplicate and harvested at 24 and 72hpi, and the RNA sequences for host and cellular proteins were analysed (experiment was performed by Dr Peter Tomasec and Dr Michael Weekes). As with the other two sets of data, which were from a single source, when performed in triplicate, mRNA of TNFR2 increased over the course of the lytic cycle (Figure 4.10B). This was not the case for TNFR1 RNA, which remained constant over the course of the infection (Figure 4.10A). These data indicate that an increase in steady state TNFR2 correlates with increased cells surface and whole cell TNFR2, though levels of TNFR1 mRNA were unaffected.

Table 4.1 Copy number of TNFR2 mRNA transcripts in HCMV infected cells.HF-TERT cells were mock infected or infected with Merlin. Values show reads per kilobase of transcript per million (RPKM) at 72hpi. Unpublished data kindly provided by Professor Andrew Davison (Centre for Virus Research, Glasgow).

	Mock	Merlin	ΔUL148
TNFR2	2.18	12.57	15.58

Table 4.2 Timecourse of TNFR2 mRNA transcripts in HCMV infected cells.HFFF cells were infected with Merlin or UV treated Merlin and harvested at the indicated timepoints. Cells were also treated with IFN and harvested after 5h. Values show reads per kilobase of transcript per million (RPKM). Data taken from source paper (Tirosh et al., 2015).

	Mock	Merlin (12h)	Merlin (24h)	Merlin (72h)	UV Merlin (5h)	IFN (5h)
TNFR1	73.021	58.06	112.16	63.11	49.99	76.80
TNFR2	0.55	1.48	7.77	14.05	0.53	1.03

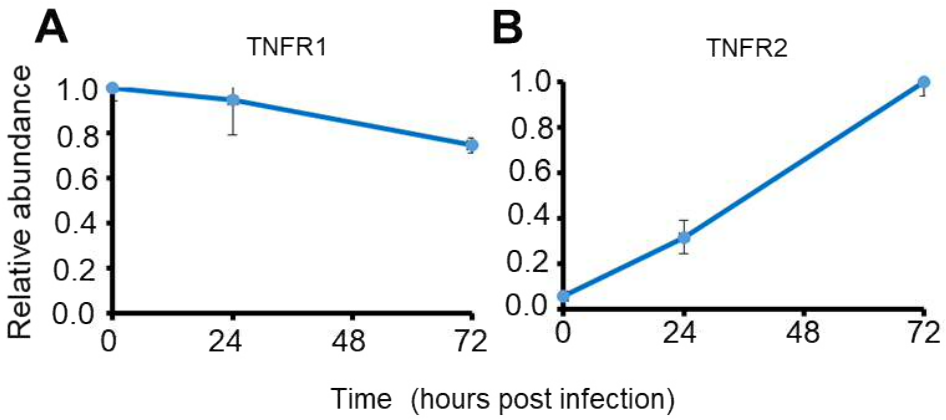

Figure 4.10. RNAseq data for TNF receptor transcripts in HCMV infected cells.HF-TERT cells were infected and harvested at 0, 24 and 72hpi. The data shows relative abundance of (A) TNFR1 and (B) TNFR2 mRNA ± SEM of triplicate infections. Experiment was performed by Dr Michael Weekes and Dr Peter Tomasec. Unpublished data kindly provided by Dr Michael Weekes.

4.7 Effect of block mutants on TNFR2 expression

The Western blot and flow cytometry data indicated that UL148 and UL148D had no effect on the whole cell levels of TNFR2 protein, but profoundly affected surface expression. Transcriptome data showed that HCMV infection induced an increase in TNFR2 mRNA. This could have been mediated by another gene within the HCMV genome. To assess this, screening for other modulators of TNFR2 surface expression was performed with the block deletions. HF-TERT cells were infected with block deletions and these were stained for TNFR2 at 72hpi. Whilst the expression levels varied slightly between the different mutants, ΔUL13-20 impaired upregulation of TNFR2. This was repeated, with both results showing a clear shift in TNFR2 expression (Figure 4.11). Given that the parent HCMV is deleted for UL16 and UL18, this result implies that one or more genes within UL13, UL14, UL15, UL17, UL19 or UL20 also contributes to TNFR2 upregulation.

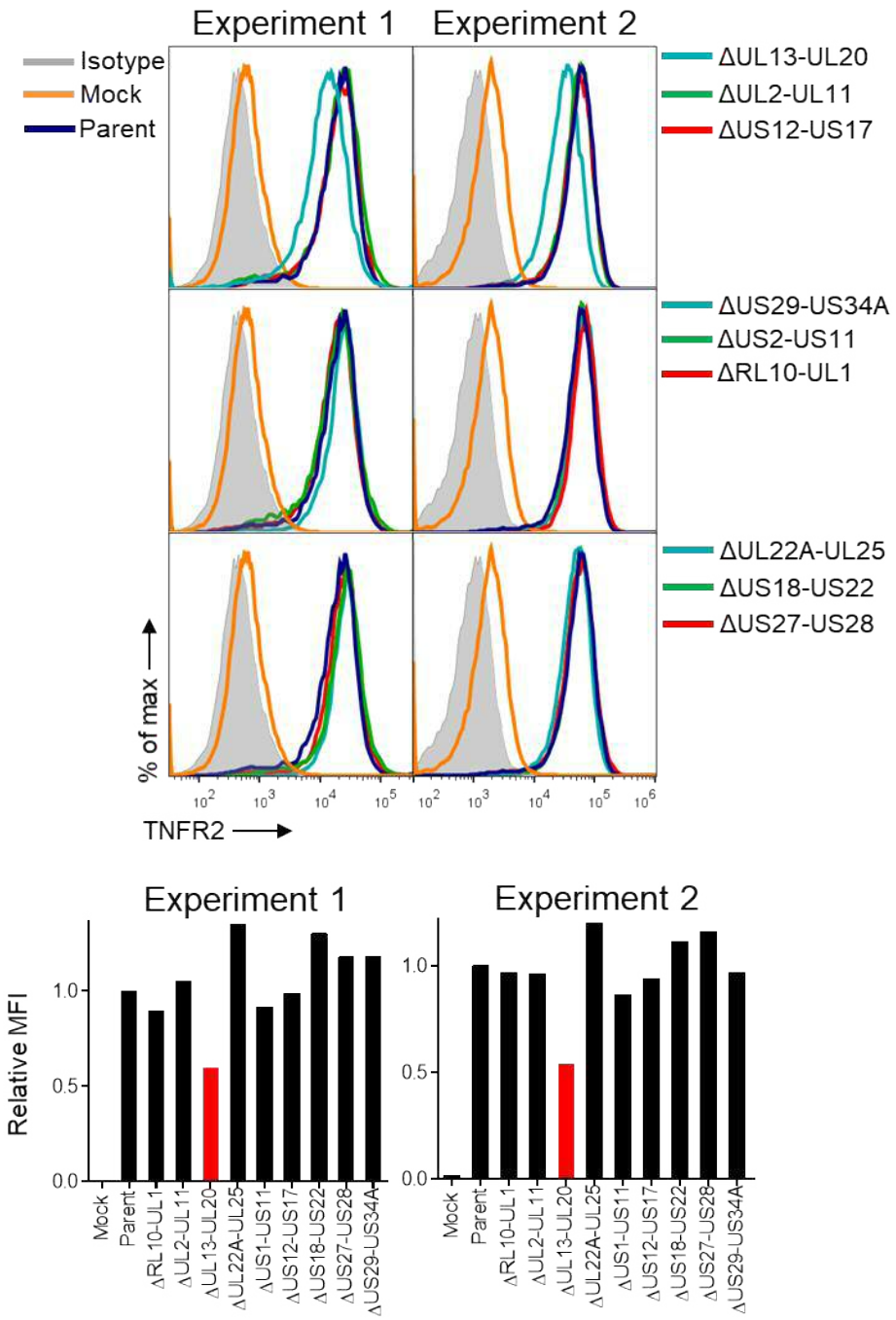

Figure 4.11 Effect of deleting blocks of HCMV genes on TNFR2 expression. HF-TERT cells were infected with block deletions or mock infected. At 72hpi, cells were stained for TNFR2. As block deletions and parent HCMV all encode GFP, gating was performed on GFP high, HLA-I low cells to identify those infected with HCMV. (A) Flow cytometry histograms and (B) Relative median fluorescence of TNFR2. MFI of parent HCMV was set at 1 with other values plotted relative to this.

4.8 Summary

The aim of this chapter was to identify the mechanism of TNFR2 upregulation during a HCMV infection. At the mRNA level, HCMV infection resulted in more steady state TNFR2 mRNA over the course of the lytic infection. Western blotting showed that HCMV induced an increase in whole cell TNFR2 protein too. At the cell surface, TNFR2 increased the most between 48-72hpi.

The most striking difference in TNFR2 surface expression amongst HCMV strains was with AD169 and Towne. These strains resulted in minimal change in surface TNFR2 expression compared to Merlin or Toledo. Screening with single U_L/*b'* gene knockout viruses revealed that UL148 and UL148D upregulate TNFR2. When both genes were knocked out (ΔUL148/UL148D), upregulation of cell surface TNFR2 did not occur, indicating that these two genes may act together to produce the large upregulation in TNFR2 observed with a Merlin infection. UL148 and UL148D did not impact on whole cell levels of TNFR2. This would suggest that UL148 and UL148D effect TNFR2 at the surface and likely encode a specific mechanism that allows for TNFR2 to accumulate or be stabilised at the cell surface. Additionally, adenoviruses expressing UL148/UL148D were not able to achieve the upregulation of TNFR2 observed on Merlin infected cells indicating that other cellular changes induced by HCMV may be required for TNFR2 upregulation.

Deleting both UL148 and UL148D had a similar effect on TNFR1, in that the presence of these two HCMV genes were required for sustained TNFR1 expression. Deletion of both genes decreased TNFR1 expression at 24hpi, with surface levels remaining low, despite UL138 expression, which has been shown to stabilise TNFR1 at the cell surface (Montag et al., 2011). This data indicated that UL148 and UL148D are essential for sustained expression of TNFR1/2 during a HCMV lytic infection.

5 Mechanism of TNFR2 upregulation and its functional impact

5.1 Introduction

The findings to date indicate that UL148 and UL148D have an additive effect, with both genes upregulating TNFR2 and allow for TNFR1 to be maintained on the surface of HCMV infected cells (Chapter 4). However, the precise mechanism by which these genes regulate cell surface expression of TNFR1/2, and the functional significance of TNFR1/2 during HCMV infection had yet to be addressed. Ectopic expression of UL148 and UL148D failed to upregulate TNFR2, indicating an indirect mechanism which was deemed worthy of further investigation.

TNFR1 was shown to be constitutively expressed on fibroblasts, but TNFR2 was present in very low amounts on the surface and within the cell (section 4.3). Therefore, it would seem that TNFR2 may have a specific function which could be utilised by HCMV in order to prevent cell death or influence the inflammatory response to TNF. The working hypothesis was that HCMV upregulates TNFR2 in order to re-route the apoptotic signal delivered to the cell upon treatment with TNF. This would therefore confer a survival advantage to the cell when challenged with TNF from leukocytes, or other TNF producing cells.

5.2 Identifying ADAM17 as a target for UL148 and UL148D

5.2.1 Proteomic analysis of ADAM17 during HCMV infection

The increase in TNFR2 on HCMV infected cells was accompanied by a transcriptional increase in mRNA of TNFR2 and an increase in the whole cell levels of TNFR2. However, Western blotting showed that knocking out UL148/UL148D had no effect on the whole cell levels of TNFR2 during HCMV infection (Figure 4.9), even though surface TNFR2 levels changed substantially (Figure 4.5). Surface TNFR2 was also not affected by ectopic expression of UL148 and UL148D (Figure 4.7), suggesting the mechanism of action of these genes was indirect and post-translational. Thus, the data from chapter 4 would suggests that UL148 and UL148D act at the cell surface. In this context, it is interesting that TNFR2 can be cleaved from the cell surface by a disintegrin and metalloproteinase 17 (ADAM17), generating a soluble receptor lacking the transmembrane domain (Solomon et al., 1999). It was therefore hypothesized that

UL148 and UL148D may act by causing dysregulation of TNFR2 cleavage from the cell surface.

To provide initial information, the expression of ADAM17 over the course of a HCMV infection was assessed using multiple available proteomics datasets. A comparison between mock and Merlin infected cells showed that ADAM17 was downregulated, with most of the surface downregulation occurring by 24hpi (Figure 5.1A). The downregulation was rapid, with less than half of the initial abundance recorded at 12hpi. The proteomic data comparing knockout viruses with Merlin was assessed to see if UL148 or UL148D could affect surface ADAM17 on HCMV infected cells. Compared to Merlin infected cells, ΔUL148 and ΔUL148D infected cells had significantly more ADAM17 on the surface ($Log_2$2.18 and $Log_2$1.81 respectively, Figure 4.3), indicating that the removal of these two genes rescued ADAM17 expression.

Data obtained from whole cell lysates showed ADAM17 protein levels increasing over the first 16 hours of infection before rapidly falling, correlating with its surface downregulation (Figure 5.1). This data would fit the hypothesis that a reduction of ADAM17 allows for increased stabilisation of TNFR2 on the cell surface. It also suggested that a reduction in surface ADAM17 may in part be due to reduced overall levels of ADAM17 protein.

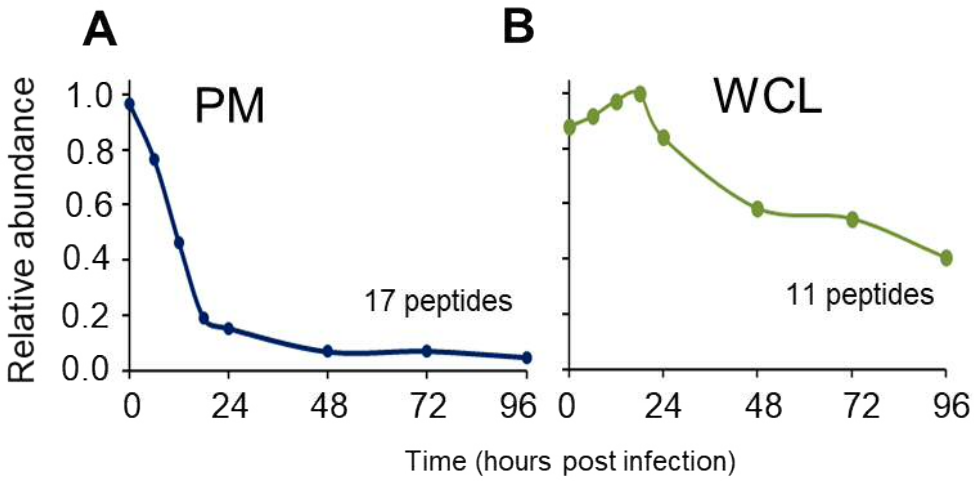

Figure 5.1 Proteomic analysis of ADAM17 following infection with HCMV.Data generated from the resource paper Weekes et al. (2014). HF-TERT cells were infected with Merlin. Cells were harvested and (A) plasma membrane (PM) or (B) whole cell lysates (WCL) were prepared prior to sample preparation and mass spectrometry. Data shows relative expression of ADAM17 over a 96h timecourse. The number of ADAM17 specific peptides quantified is shown within the graph.

5.2.2 Effect of HCMV on ADAM17 expression

A limitation of proteomic data is that it compares relative protein levels between different sets of preparations and therefore, combined with its high sensitivity, can lead to false positives if starting levels of a target protein are low. Consequently, it was important to be able to validate the plasma membrane profiling data for ADAM17 by an independent method.

Flow cytometry was used to assess to what extent HCMV affected ADAM17 expression, and the potential influence of UL148 and UL148D. HF-TERT cells were infected with Merlin, ΔUL148, ΔUL148D, and ΔUL148/UL148D, and flow cytometry for ADAM17 was performed at 24-hour intervals. HCMV infection resulted in a rapid downregulation of ADAM17, with anti-ADAM17 staining being identical to isotype staining levels by 48hpi (Figure 5.2A). At 24hpi there was little difference in ADAM17 expression between Merlin and ΔUL148 infected cells however a recovery of ADAM17 was discernible by 48hpi. This was more apparent at 72hpi, with a clear distinction between isotype and anti-ADAM17 staining. Compared to Merlin infected cells, ADAM17 was not downregulated to the same degree on ΔUL148D infected cells at 24hpi. A decrease in surface ADAM17 did occur at 48 and 72hpi and the expression profile of ADAM17 was reduced on ΔUL148D infected cells, though still above isotype levels. On ΔUL148/UL148D infected cells, surface ADAM17 expression remained stable throughout the 72h timecourse, albeit lower than on mock infected cells. At 24hpi, ADAM17 expression was similar between ΔUL148D and ΔUL148/UL148D infected cells, indicating that of the two genes, UL148D is responsible for ADAM17 downregulation at an earlier stage in the lytic cycle. In summary, the deletion of UL148 and UL148D act synergistically to suppress surface ADAM17 expression following Merlin infection.

At 72hpi, ΔUL148/UL148D infected cells showed comparable levels of surface ADAM17 to AD169 infected cells, suggesting these 2 genes are primarily responsible for the differences in ADAM17 expression observed between AD169 and Merlin (Figure 5.2C). Interestingly, surface ADAM17 was not recovered to mock levels at any timepoint and was reduced compared to uninfected cells at 24hpi. This indicates other factors are affecting ADAM17 at an early timepoint, independent of UL148 and UL148D.

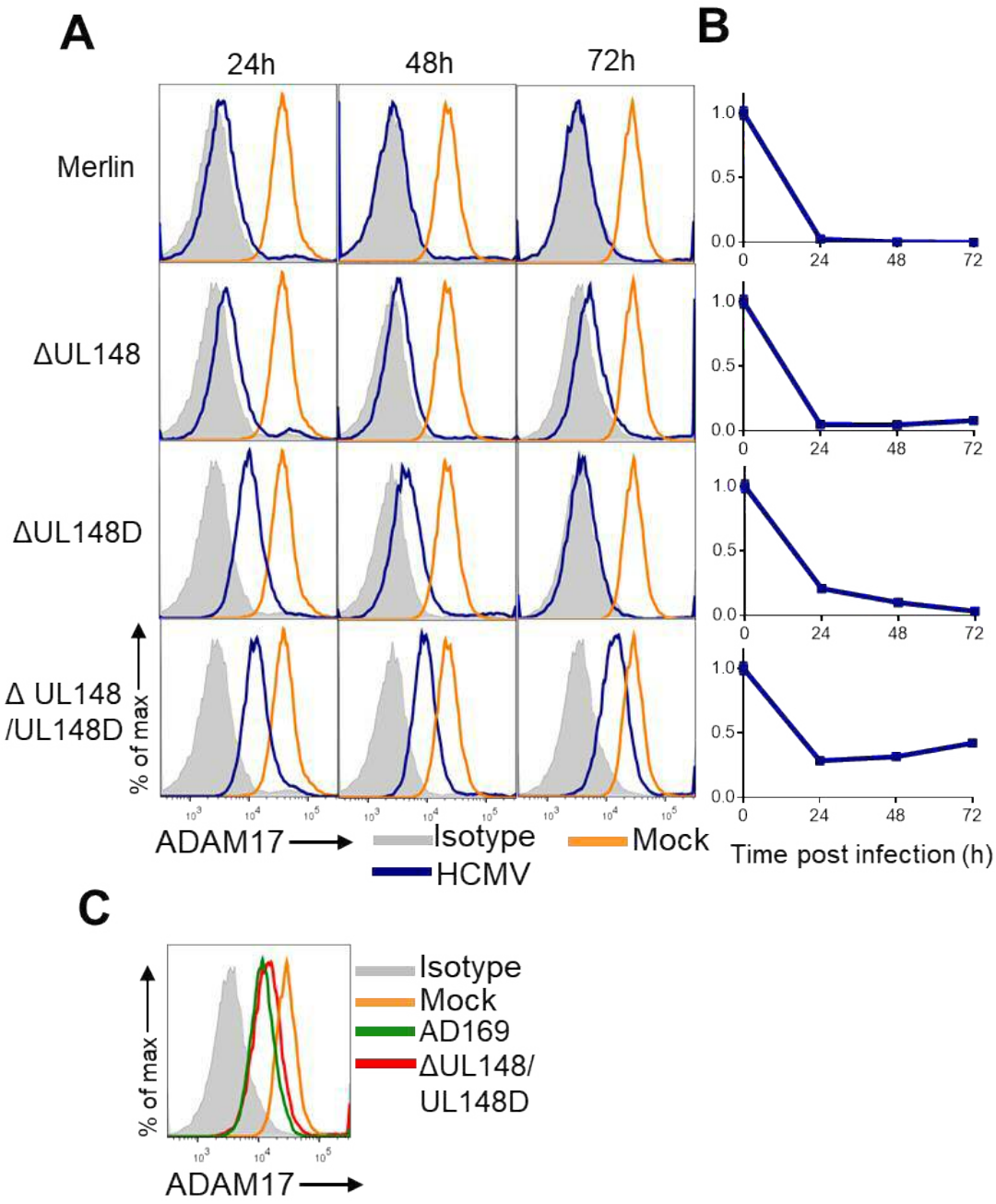

Figure 5.2 Timecourse of ADAM17 expression during HCMV infection.HF-TERT cells were infected with HCMV variants or mock infected. At 24h intervals cells were stained for ADAM17. (A) Representative flow cytometry histograms comparing HCMV to mock infected cells. (B) Relative fluorescence of ADAM17 for HCMV mutants. Each point shows mean relative ADAM17 ±SEM of triplicate infections. ADAM17 MFI of mock infected cells was set at 1.0 with other values plotted as a relative value (C) Comparison between AD169 and ΔUL148/UL148D infected cells at 72hpi.

5.2.3 Effects of ectopic expression of UL148 and UL148D on surface ADAM17

Timecourse experiments showed that UL148 and UL148D affect ADAM17 at different points during a lytic HCMV infection, with UL148D impacting on ADAM17 expression prior to 24h post infection. This suggested that both these genes were capable of affecting ADAM17 independently. To test if UL148 and UL148D could downregulate surface ADAM17 in isolation, these genes were expressed in HF-CAR cells with RAd-UL148 and RAd-UL148D. HF-CAR cells were used to allow for lower PFU infections that reduce potential toxicity from high amounts of input virus. Flow cytometry for ADAM17 was performed at 72hpi. The experiment showed that UL148 and UL148D both reduced ADAM17 in isolation (Figure 5.3A). Overexpression of either gene alone partially reduced surface ADAM17 expression, while both RAds together resulted in a further decrease in surface ADAM17, indicating an additive effect (Figure 5.3A, right panel). The MFI data is quantified in Figure 5.3D.

To assess whether the effect of UL148 and UL148D could be reconstituted in the context of a HCMV infection, a co-infection with RAds and knockout HCMV viruses was performed. This experiment showed that addition of RAd-UL148 and RAd-UL148D to ΔUL148 and ΔUL148D infected cells respectively, reduced ADAM17 expression close to isotype levels, and recapitulated the ADAM17 phenotype observed with Merlin infected HF-CAR cells (Figure 5.3B).

When both RAd UL148 and RAd-UL148D were used in the context of the double knockout virus (ΔUL148/UL148D), individually the RAds caused a partial downregulation of ADAM17, but when both RAd-UL148/UL148D were used, there was a significantly greater downregulation of ADAM17(Figure 5.3D, right). In summary, ectopically expressed UL148 and UL148D can downregulate ADAM17. It was further shown that UL148 and UL148D act together, resulting in greater downregulation of surface ADAM17.

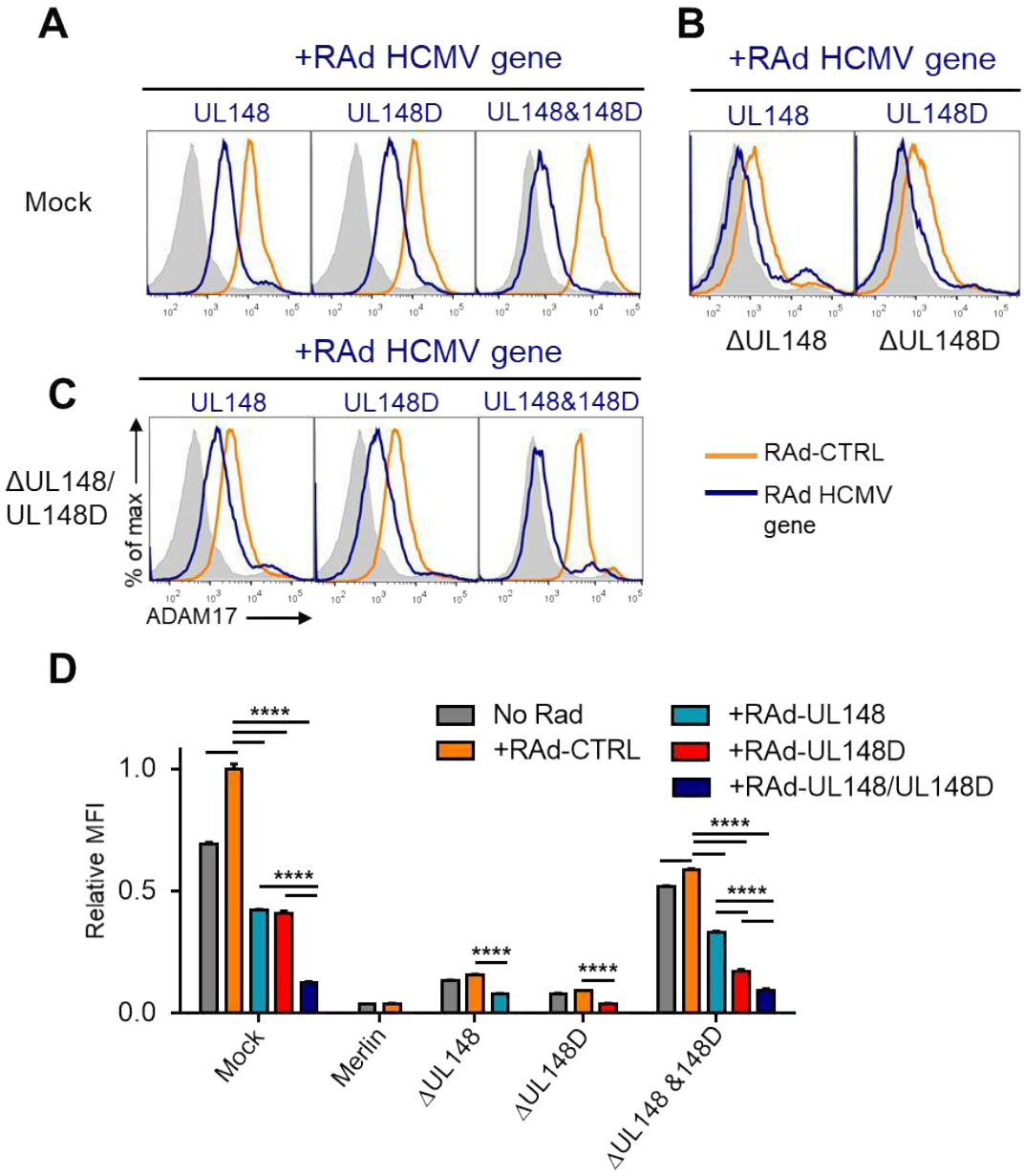

Figure 5.3 Effect on surface ADAM17 of expressing UL148 and UL148 in isolation, and in the context of a HCMV infection.HF-CAR cells were infected with single or combined RAd-UL148, RAd-UL148D. The cells were then infected with Merlin, ΔUL148, ΔUL148D, ΔUL148/UL148D. Each condition was performed in triplicate. At 72hpi, cells were stained for ADAM17. Representative flow cytometric histograms are shown for (A) mock and (B) ΔUL148 and ΔUL148D and (C) ΔUL148/UL148D. (D) The maximum ADAM17 MFI (Mock, RAd-CTRL) was set at 1, with other values plotted as a relative value. Bars show mean relative ADAM17 MFI +SEM of triplicate infections. One-way ANOVA with Sidak multiple comparison post-hoc tests showed significant differences at **** $p<0.0001$.

5.2.4 Assessing the effect of HCMV virions on ADAM17

Downregulation of ADAM17 occurred by 24hpi and part of this effect was attributable to UL148/UL148D (Figure 5.2). Given how early the downregulation was post-infection, this suggested that part of the effect could be mediated by an innate response to HCMV virions. To test this HCMV variants were gamma irradiated to denature viral DNA. This leaves virions intact, and able to enter cells, though unable to replicate and inhibit the interferon, or other host innate immune responses. All deletion variants were tested as UL148 is found in the virion (Murrell, 2014) and therefore it was possible that virion derived UL148 could have been affecting ADAM17 surface levels at early timepoints.

HF-TERT cells were infected with HCMV or irradiated HCMV deletion variants and flow cytometry for ADAM17 was performed at 6,12 and 24hpi. Within the first 6hpi the expression of ADAM17 on Merlin and ΔUL148 infected cells was similar, with rapid downregulation occurring. As irradiated Merlin did not affect surface ADAM17, this suggested that virion derived UL148 was not affecting surface ADAM17. At 6hpi, the expression of ADAM17 was similar between ΔUL148D and ΔUL148/UL148D infected cells (Figure 5.4A and B). Even at 6hpi, in the absence of both UL148/UL148D, ADAM17 was still downregulated compared to uninfected cells (Figure 5.4C). At 24hpi, surface ADAM17 expression on ΔUL148D began to decrease compared to ΔUL148/UL148D infected cells. This showed that whilst UL148D is responsible for most of the downregulation of ADAM17 prior to 24hpi, there are other factors involved, independent of UL148 and UL148D. The block mutants (Figure 3.3) were screened for the ability of other genes to affect ADAM17 at two time points (24 and 72hpi), but there was no difference between any of the mutants and the parent HCMV (Appendix).

In summary virion binding and virion proteins do not affect ADAM17 expression. This affirms that *de novo* UL148 and UL148D expression are required for ADAM17 downregulation.

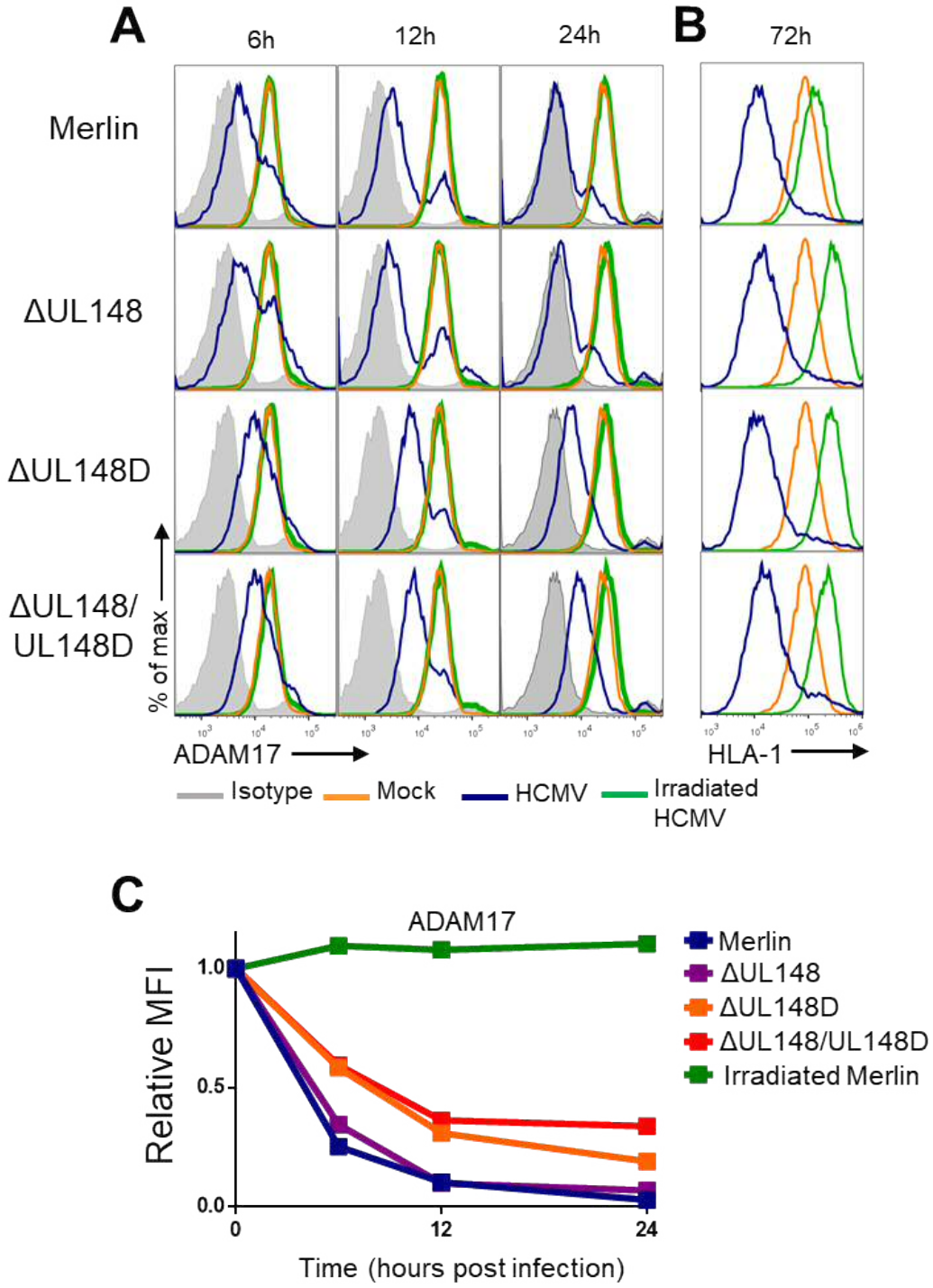

Figure 5.4 Effect of HCMV on ADAM17 expression at early timepoints. (A) Merlin, ΔUL148, ΔUL148D and ΔUL148/UL148D were left unirradiated or irradiated (3500Gy). HF-TERT cells were infected with these viruses and surface ADAM17 was assessed by flow cytometry at the indicated timepoints. (B) Cells were stained for HLA-I at 72hpi to assess infection efficiency. (C) Relative expression of ADAM17 across 24h time course. ADAM17 MFI from mock infected cells was set as 1 with other values plotted relative to this.

5.3 Assessing the effect of ADAM17 on TNFR2 expression

5.3.1 Measuring soluble TNFR2 in response to HCMV

Section 5.2 showed that the downregulation of ADAM17 was in large part due to UL148 and U148D. My working hypothesis was that a reduction in ADAM17 prevented cleavage of surface TNFR2, therefore allowing it to accumulate on the cell surface. A concomitant effect of this would be alterations in the product of this cleavage, soluble TNFR2 (sTNFR2). To pursue this hypothesis, the supernatants of cell cultures were tested for sTNFR2.

HF-TERT cells were mock infected or infected with Merlin, ΔUL148, ΔUL148D and ΔUL148/UL148D. The supernatant was taken at 72hpi and an ELISA was performed. There was a significant increase in sTNFR2 production between mock and Merlin (11.3±0.5 vs 96±1.6pg/ml $p<0.05$) infected cultures, showing that a HCMV infection increased both surface and soluble TNFR2. This showed that some TNFR2 is shed from the surface of HCMV infected cells, even in the presence of very low levels of surface ADAM17 (Figure 5.5). Deleting UL148D resulted in significantly more TNFR2 being shed compared to deleting UL148 (504.7±8.6 vs 313.9±8.5pg/ml, $p<0.0001$). This occurred despite there being less ADAM17 on the surface of the ΔUL148D, compared to ΔUL148 infected cells at 72hpi, as shown in the previous section (Figure 5.2). Deleting both genes resulted in significantly more sTNFR2 being released into the medium (574.5±5.5pg/ml), compared to either single knockout virus. Interestingly, there was only a small increase in sTNFR2 between ΔUL148D and ΔUL148/UL148D, even though there was far more surface ADAM17 on ΔUL148/UL148D infected cells (Figure 5.2). This data further supported the idea that the increase in surface TNFR2 mediated by UL148 and UL148D is due to reduced shedding of the TNFR2 from the surface of the cell.

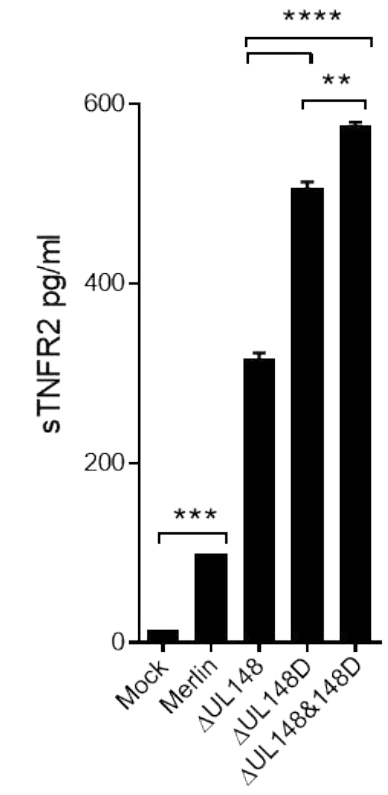

Figure 5.5 Levels of soluble TNFR2 in tissue culture medium following infection with HCMV. HF-TERT cells were mock infected or infected with Merlin, ΔUL148, ΔUL148D or ΔUL148/UL148D. At 72hpi the supernatant was analysed for sTNFR2 by ELISA. Bars shows mean sTNFR2 +SEM of duplicate supernatants. A one-way ANOVA with Tukey multiple comparison post-hoc tests showed significance at **** $p<0.0001$, ***$p<0.001$, **$p<0.01$.

5.3.2 Effect of blocking ADAM17 on soluble and surface TNFR2

Section 5.3.1 showed that TNFR2 could be accumulating on the surface of HCMV infected cells due to decreased cleavage. To test whether the shedding of sTNFR2 by ΔUL148, ΔUL148D and ΔUL148/UL148D infected cells was due to ADAM17, a blocking experiment was performed. The antibody used, D1(A12), only blocks ADAM17 without affecting other members of the ADAM family of metalloproteinases (Tape et al., 2011). D1(A12) is a human antibody, therefore human IgG was used as an isotype control. Chapter 4 showed the main increase in surface TNFR2 occurred between 48 and 72h, and therefore it was reasoned that blocking ADAM17 at 48hpi should provide enough time for levels of TNFR2 to re-accumulate on ΔUL148/UL148D infected cells and be measurable by flow cytometry. Additionally, the antagonism of ADAM17 needed to occur early enough in the lytic cycle to prevent release of sTNFR2 into the supernatant. HF-TERT cells were mock infected or infected with HCMV. At 48hpi the media was replaced with fresh media containing D1(A12) or hIgG (both at 100nM). At 72hpi, the supernatant was collected and analysed by ELISA and flow cytometry was performed for TNFR1 and TNFR2 on cells. TNFR1 was included in the analysis as it is also an ADAM17 substrate.

Supernatant collected at 48hpi was tested for sTNFR2, to assess the temporal profile of HCMV TNFR2 shedding. By 48hpi, there was a significant difference in sTNFR2 production between Mock and Merlin infected cells (5.6±0.3pg/ml vs 26±3pg/ml $p=0.01$, Figure 5.5A). Deleting UL148/UL148D increased TNFR2 shedding though there was no significant difference between ΔUL148D (159±4pg/ml) and ΔUL148/UL148D (155±6pg/ml) at this timepoint. Supernatant from ΔUL148 infected cells had levels of sTNFR2 lower than ΔUL148/UL148D, or ΔUL148D, though still significantly higher than from Merlin infected cells (61±2 vs 26±3pg/ml $p<0.001$).

An experiment was performed comparing cells treated with DMEM10 or hIgG at 48hpi, but no difference was observed in the levels of sTNFR2 indicating that the hIgG was not affecting sTNFR2 production (Appendix). Without blocking ADAM17, the production of sTNFR2 between 48 and 72hpi followed a similar pattern to that shown in Figure 5.5. Merlin infected cells produced sTNFR2, while deleting UL148 increased its production, with further significant increases measured within ΔUL148D and ΔUL148/UL148D supernatants. Deleting both UL148 and UL148D resulted in the most soluble TNFR2 production. Comparing sTNFR2 released by ΔUL148/UL148D infected cells in Figure 5.5 and Figure 5.6B (454 vs 579pg/ml) revealed that most (78%) of sTNFR2 was produced between 48 and 72hpi.

Blocking of ADAM17 at 48hpi resulted in no difference in soluble TNFR2 in mock infected cells. Blocking of ADAM17 on Merlin infected cells partially reduced sTNFR2 (70.3±4.5 vs 38.7±1.3pg/ml), which suggested some active ADAM17 present on the HCMV infected cells, even though the flow cytometry data was unable to detect any ADAM17 on Merlin infected cells at 48hpi (Figure 5.2). Blocking of ADAM17 on ΔUL148, ΔUL148D, and ΔUL148/UL148D infected cells resulted in reduction of sTNFR2 production to levels detected in Merlin supernatant. This result was consistent with sTNFR2 from knockout viruses being produced by ADAM17 mediated shedding of TNFR2 from the surface of ΔUL148/UL148D infected cells.

Flow cytometry for surface TNFR1/2 was also performed on cells with or without ADAM17 blocking, to assess if blocking was resulting in recovery of TNFR1/2 at the cell surface (Figure 5.6C and D). Following treatment with D1(A12), both TNFR1 and TNFR2 were recovered on the surface of ΔUL148/UL148D infected cells. Expression of both these receptors increased to levels comparable to those found on Merlin infected cells. This showed that downregulation of ADAM17 is necessary for maintaining TNFR1 expression throughout the course of a HCMV infection, and for the increase in TNFR2 expression. In summary, these data show that TNFR2 upregulation is dependent on UL148/UL148D mediated ADAM17 downregulation.

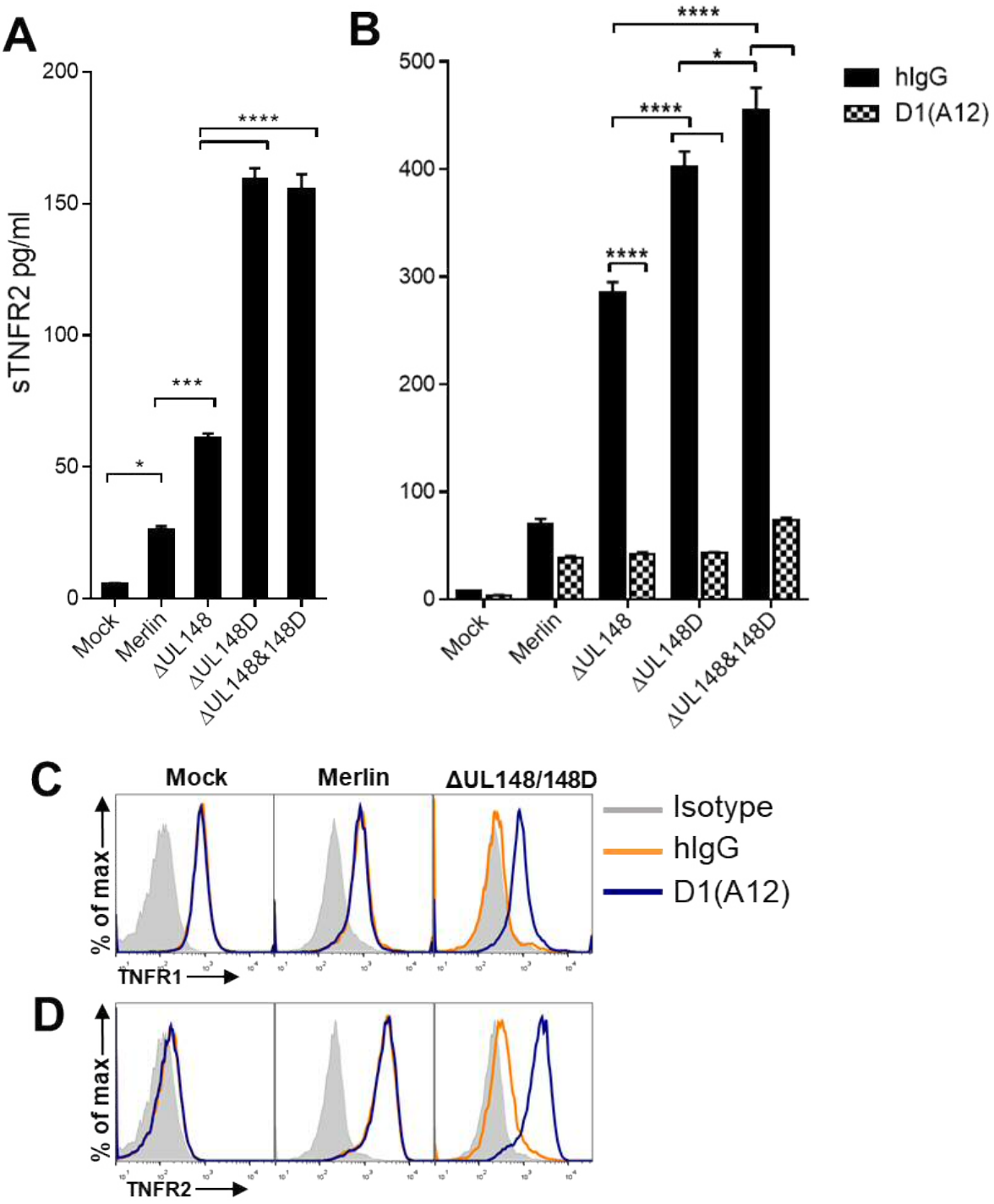

Figure 5.6 Effect of blocking ADAM17 function on soluble and surface TNFR2. HF-TERT cells were infected with HCMV variants. At 48hpi, the supernatant was replaced with fresh medium containing 100nM hIgG or D1(A12). Supernatant was collected at 72hpi. Supernatant collected at (A) 48hpi and (B) 72hpi was quantified in the same ELISA. Bars shown mean sTNFR2 and SEM of triplicate samples. A two-way ANOVA with a Bonferroni post test showed significance at **** $p<0.0001$, ***$p<0.001$, *$p<0.05$. The cells from the experiment were analysed for (C) surface TNFR1 and (D) surface TNFR2 by flow cytometry. Grey shows isotype staining. ADAM17 signal from cells treated with hIgG or D1(A12) is shown in orange and blue respectively.

5.4 Cellular regulation of ADAM17

The efficiency with which ADAM17 was downregulated by HCMV was quite remarkable and it was felt that this warranted further investigation as to how UL148 and UL148D achieve this. Proteomics had already suggested that whole cell levels of ADAM17 are reduced following HCMV infection (Figure 5.1A). One hypothesis was that HCMV could be inducing the degradation of ADAM17 inside the cell. ADAM17 is synthesised as an enzymatically inactive, immature form in the endoplasmic reticulum. Removal of the N-terminal pro-domain by furin protease is required to produce enzymatically active mature ADAM17 (Schlondorff et al., 2000). I wanted to assess the effect of HCMV infection on the mature and immature forms of ADAM17, as this would provide information about whether the processing pathway is being targeted by HCMV.

5.4.1 Analysis of whole cell ADAM17 by western blotting

HF-TERT cells were infected with Merlin, ΔUL148/UL148D or mock infected. At 72hpi cells were harvested, samples prepared, and proteins were separated under reduced denaturing conditions. Following transfer to a PVDF membrane, the membrane was probed for ADAM17 and the lysate was tested for actin. The strongest signal was at 90kDa, which is likely to be the mature form of ADAM17 (Figure 5.7; Grieve et al. (2017)). A band of higher molecular weight was seen at 120kDa, which most likely corresponded to the immature form of ADAM17. In mock infected cells, there was more mature ADAM17 present compared to the immature form. When cells were infected with Merlin, the band corresponding to mature ADAM17 was not present indicating the absence of mature ADAM17 in HCMV infected cells. The band corresponding to immature ADAM17 was more intense compared to uninfected cells. Lysates from ΔUL148/UL148D infected cells showed a partial recovery in mature ADAM17, though not to the level observed from uninfected cells. There was also a reduction in immature ADAM17, comparable to levels observed from mock infected cell lysates. This showed that UL148 and UL148 were influencing the conversion of immature ADAM17 to mature ADAM17.

One possibility was that HCMV was inducing degradation of ADAM17 by cellular proteases. Recent work by Grieve et al. (2017), showed that the N-terminus of iRhom2, an ADAM17 chaperone, is required for the interaction with ADAM17. Data in the paper showed that the N-terminus of iRhom2 is required for binding of iRhom2 to mature ADAM17. In the absence of this iRhom2-ADAM17 interaction, mature ADAM17 is degraded by lysosomes (Grieve et al., 2017).

I analysed proteomic data (Fielding et al., 2017) which compared Merlin infected cells treated with leupeptin, a protease inhibitor. As with previous proteomic (Figure 5.1) and flow cytometry data (Figure 5.2), there was a large reduction in surface ADAM17, though addition of leupeptin to cultures did not rescue surface ADAM17 (Figure 5.7B). Leupeptin did not influence whole cell ADAM17 at any timepoint. There was still an increase at 24hpi, relative to mock infected cells, with a gradual decrease over the next 48h, with levels comparable to uninfected cells at 72hpi (Figure 5.7C).

In summary, this data suggests that HCMV induces a decrease in total ADAM17, though the key finding was that the mature form of ADAM17 was absent in HCMV infected cells and there was more immature ADAM17. Deleting UL148 and UL148D partially recovered the whole cell levels of mature ADAM17, suggesting that these genes alter the maturation of ADAM17, rather than affecting total levels of cellular ADAM17.

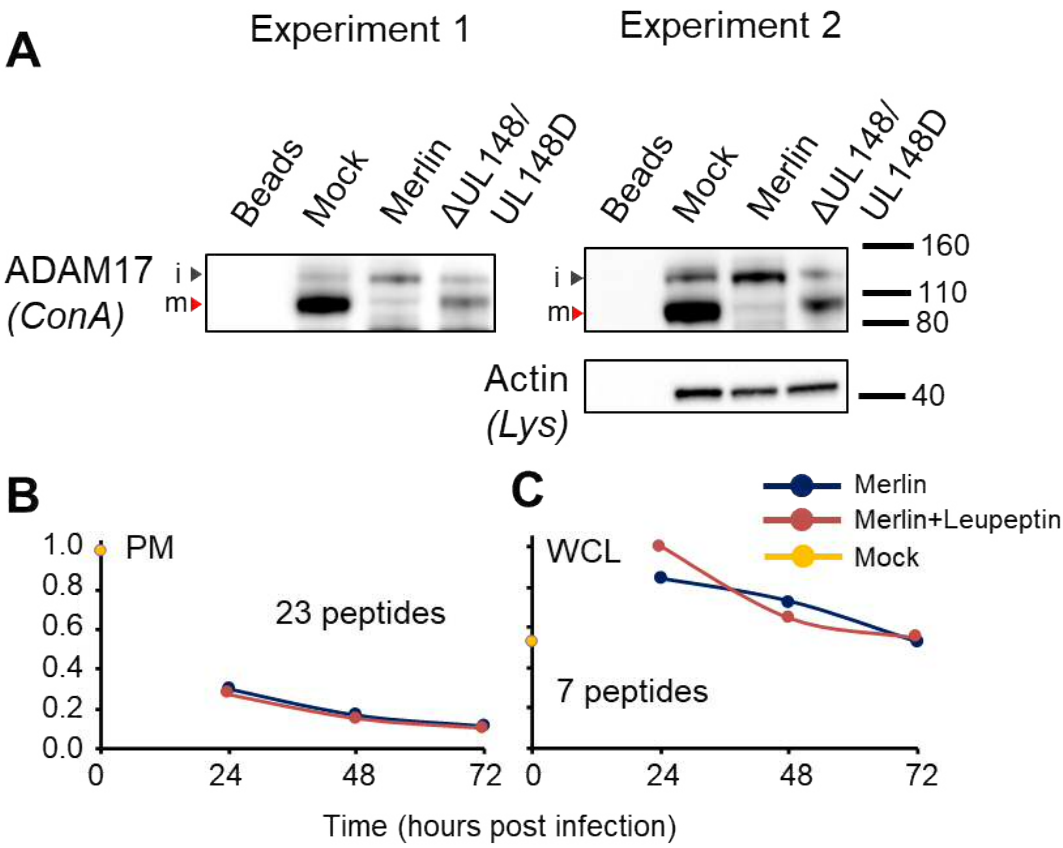

Figure 5.7 Effect of HCMV on whole cell ADAM17. HF-TERT cells were mock infected or infected with Merlin, or ΔUL148/UL148D. At 72hpi cells were washed and lysed. ADAM17 was captured overnight with concanavalin A (ConA) beads and eluted the following day. Proteins were separated under reduced denatured conditions by SDS-PAGE and transferred to a PVDF membrane and probed form ADAM17. Signal was visualized by chemiluminescence. Black arrow corresponds to immature ADAM17 (i), and the red arrow (m) indicates the mature form. Experiment 1 and 2 were performed independently, with 20% of ConA eluted sample being loaded (10µl) and 2% (20µl) of lysate being loaded for actin staining. (B, C) Effect of proteasomal inhibition on whole and surface ADAM17 expression. Data generated from the resource paper (Fielding et al., 2017). HF-TERT cells were infected with Merlin. For lysosome inhibitor studies, cells were treated with leupeptin 12h prior to harvesting. (A) Plasma membrane or (B) whole cell lysates were prepared. The number of peptides quantified are shown in each plot.

5.4.2 Regulation of iRhom1 and iRhom2 by HCMV

Figure 5.7 provided evidence that UL148 and UL148D may impair the maturation of ADAM17. One possibility was that UL14/UL148D could affect levels of the chaperone proteins iRhom1/2. Recent work has highlighted the role of iRhom1 and iRhom2 in ADAM17 regulation (Adrain et al., 2012, Li et al., 2015b, Grieve et al., 2017). These proteins have been identified as essential regulators of ADAM17 maturation, controlling ER to Golgi transport. Recently Grieve et al. (2017), showed that iRhom2 remains binds to ADAM17 throughout the secretory pathway and stabilises ADAM17 on the cellular surface. A possible mechanism by which UL148 and UL148D could affect ADAM17 maturation by reducing iRhom1/2 within infected cells, thereby preventing maturation of ADAM17.

I referred to the proteomic data to assess WCL levels of iRhoms. The results suggested a gradual decrease in relative amounts of both iRhom1 and iRhom2 over the course of lytic infection (Figure 5.8A). To validate this using western blotting, HF-TERT cells were mock infected or infected with Merlin or ΔUL148/UL148D. At 72hpi, cells were lysed, and SDS-PAGE was used to separate proteins, followed by transfer to a PVDF membrane. The membrane was probed for iRhom1 and iRhom2. The expected Mw of iRhom1 is 97401Da and 96686Da for iRhom2, based on amino acid sequences. Bands corresponding to these proteins are denoted by the red arrow (Figure 5.8B). Unlike the proteomic data, Western blotting did not reveal large changes in iRhom1/2 expression upon infection with Merlin (lanes 1 and 2). There was no difference in iRhom1/2 expression between Merlin or ΔUL148/UL148D infected cells. Overall these results show that HCMV does not impact on whole cell levels of iRhom1/2 proteins, with Western blots suggesting there was no substantial change in iRhom1/2 levels upon HCMV infection.

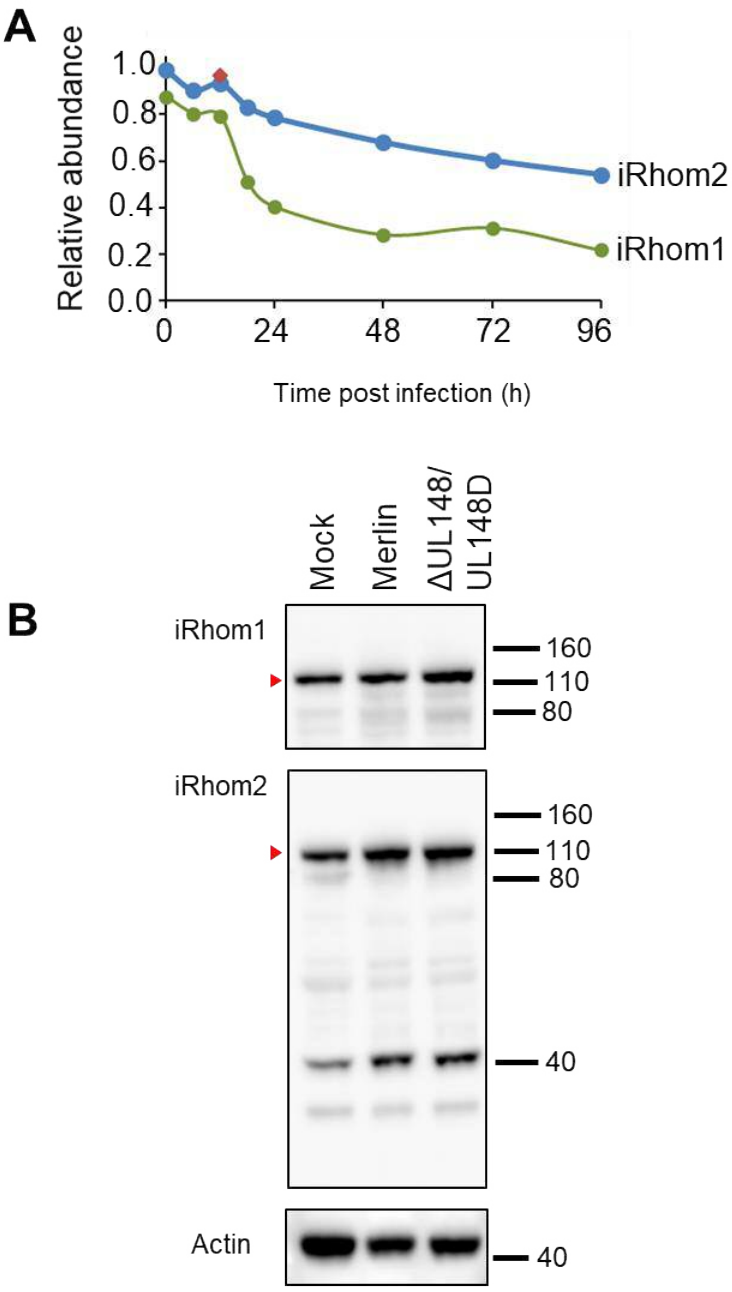

Figure 5.8 Regulation of iRhom1 and iRhom2 by HCMV. (A) Whole cell lysate proteomics was performed over the course of the lytic infection. The green line shows iRhom1 (4 peptides) and the blue line shows iRhom2 (3 peptides). Data was taken from Weekes et al. (2014). (B) Western blot for iRhom1 and 2. HF-TERT cells were mock infected or infected with Merlin or ΔUL148/UL148D. At 72hpi, lysates were prepared and separated under reducing denatured conditions by SDS-PAGE. Proteins were transferred to a PVDF membrane and probed for iRhom1/2. Red arrows indicate bands corresponding to iRhom proteins. Actin was used as a loading control.

5.4.3 Analysis of ADAM17 mRNA during HCMV infection

Having found that the mature form of ADAM17 was reduced in cell lysates in HCMV infected cells, it was possible that HCMV infection induced changes in ADAM17 mRNA. HF-TERT cells were infected with Merlin or ΔUL148, RNA extracted for transcriptional analysis (performed by Dr Peter Tomasec and Professor Andrew Davison). At 72hpi, there was a reduction in ADAM17 mRNA by 72hpi in Merlin infected cells, compared to mock infected cells (11.49 vs 3.49 RPKM, Table 5.1). This showed that within HCMV, a potential reduction in steady state mRNA of ADAM17 could contribute to the overall reduction in ADAM17.

Published transcriptome data from Tirosh et al. (2015), (Table 5.2) suggested a smaller reduction in ADAM17 mRNA at 72hpi (12.48 vs 9.08 RPKM). The data also suggested that by 24hpi, ADAM17 transcription was increased. When cells were treated with IFN or UV irradiated Merlin, there was also an increase in ADAM17 mRNA at 5 hours post treatment (14.05 and 17.48 RPKM respectively), suggesting that the initial increase ins ADAM17 transcription may be an innate immune response. RNAseq data was analysed from Merlin infected HF-TERT cells in triplicate (Dr Pete Tomasec and Dr Mike Weekes). As with the data in Table 5.2, there was an increase at 24hpi, but at 72hpi, ADAM17 mRNA was similar to levels in uninfected cells (Figure 5.9).

In summary, these datasets show that HCMV causes a modest increase in ADAM17 transcription at 24hpi, which correlated with an increase in whole cell ADAM17 at 24hpi (Figure 5.1, Figure 5.7). Regardless, this had no effect on surface ADAM17, which was downregulated at 6hpi (Figure 5.4), and by 72hpi, the level of ADAM17 mRNA level was comparable to uninfected cells.

Table 5.1 Copy number of ADAM17 mRNA transcripts in HCMV infected cells.HF-TERT cells were mock infected or infected with Merlin. Values show reads per kilobase of transcript per million (RPKM) at 72hpi. Unpublished data kindly provided by Professor Andrew Davison (Centre for Virus Research, Glasgow).

	Mock	Merlin	ΔUL148
ADAM17 (RPKM)	11.19	3.49	3.51

Table 5.2 Timecourse of ADAM17 mRNA transcripts in HCMV infected cells.HFF cells were infected with Merlin or UV treated Merlin and harvested at the indicated timepoints. Cells were also treated with IFN and harvested after 5h. Values show reads per kilobase of transcript per million (RPKM). Data taken from source paper Tirosh et al. (2015).

	Mock	**Merlin (24h)**	**Merlin (72h)**	**UV Merlin (5h)**	**IFN (5h)**
ADAM17 (RPKM)	12.18	20.23	9.08	14.05	17.48

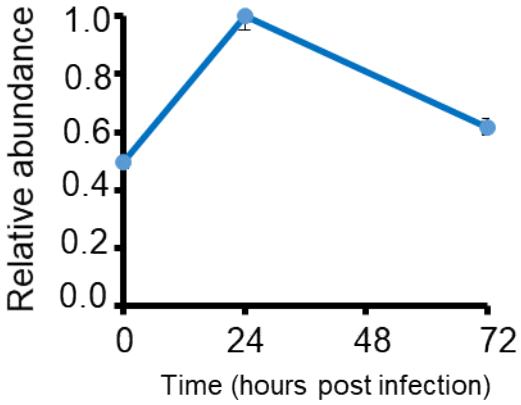

Figure 5.9 RNAseq data for TNF receptor transcripts in HCMV infected.HF-TERT cells were infected and harvested at 0,24 and 72hpi. The data shows relative abundance of ADAM17 mRNA ± SEM of triplicate infections. Experiment was performed by Dr Mike Weekes and Dr Pete Tomasec.

5.5 Effect of UL148/UL148D on CD8+ T-cell activation

To assess functional effects of UL148/UL148D, a T-cell assay was performed with ΔUL148, ΔUL148D and ΔUL148/UL148D. We have recently demonstrated that UL148 impairs T-cell activation by downregulating CD58, a co-stimulatory molecule which binds CD2 on T-cells (Wang et al., 2018). An increase in degranulation and cytokine expression with ΔUL148 was expected, but it was possible that the synergistic activity between UL148 and UL148D could further affect the ability of T-cells to recognise HCMV infected cells. Many co-stimulatory, co-inhibitory and adhesion molecules are also ADAM17 substrates (Scheller et al., 2011, Moss and Minond, 2017). When both genes are present, it was predicted that a reduction of ADAM17 would allow certain co-inhibitory molecules to increase on the surface of the HCMV infected cell. These molecules may then be cleaved off when ADAM17 is recovered on ΔUL148/UL148D infected cells. Whilst proteomic data from ΔUL148 and ΔUL148D was available, other than CD58, no other obvious T-cell co-signalling molecules appeared to be affected (Figure 4.3). However, it could be that the combined deletion had a larger effect on molecules, which was not detectable when assessing the individual mutants.

D9-SFi cells were mock infected or infected with Merlin, ΔUL148, ΔUL148D and ΔUL148/UL148D. The cells were used as targets for a T-cell activation assay at 72hpi. Using ICS, cytokine production (TNF, IFNγ, IL-2 and MIP-1β) was assessed alongside CD107a surface exposure. UL148 acted to suppress TNF, MIP-1β and IFNγ production against HCMV infected targets by CD8+ T-cells, as assessed by MFI (Figure 5.10A). UL148D did not significantly affect cytokine induction by T-cells: there was no significant difference in TNF, IFNγ and MIP-1β levels between ΔUL148D and Merlin nor between ΔUL148 and ΔUL148/UL148D. IL-2 induction was suppressed by HCMV infection, but not impacted by either UL148 or UL148D.

The proportion of cells activated was analysed and showed that compared to Merlin infected cells, ΔUL148 infected cells increased the number of activated T-cells as measured by a significant increase in the proportion of cells expressing each marker (CD107a, TNF, IFNγ, IL-2 and MIP-1β, Figure 5.10B). Compared to Merlin, deleting UL148D alone had no significant effect on T-cell activation other than significantly increasing the MIP-1β producing cells, though the difference was small (26.0±0.2 vs 28.5±0.5% MIP-1β+CD8+, p=0.02). Cells infected with ΔUL148/UL148D induced a significant increase in all activation markers compared to Merlin (Figure 5.10B). To assess what effect the absence of UL148/UL148D was having compared to UL148, the data from these two infections were also compared. ΔUL148/UL148D induced a

marginal increase in the proportion of degranulating (CD107a+) and TNF producing cells compared to ΔUL148 (17.4±0.5 vs 19.9±0.7% CD107a+CD8+ p=0.02, 16.2±0.6 vs 18.5±0.6% TNF+CD8+ p=0.01). The proportion of cells producing IFNγ, MIP-1β and IL-2 was not significantly different between ΔUL148 vs ΔUL148/UL148D.

In summary, UL148D had no appreciable effect on T-cell activation compared with UL148, which is established as a T-cell evasin. ΔUL148/UL148D induced higher T-cell activation and cytokine degranulation compared to Merlin, though this was comparable to ΔUL148. Therefore, the deletion of UL148D did not affect T-cell activation and effect function.

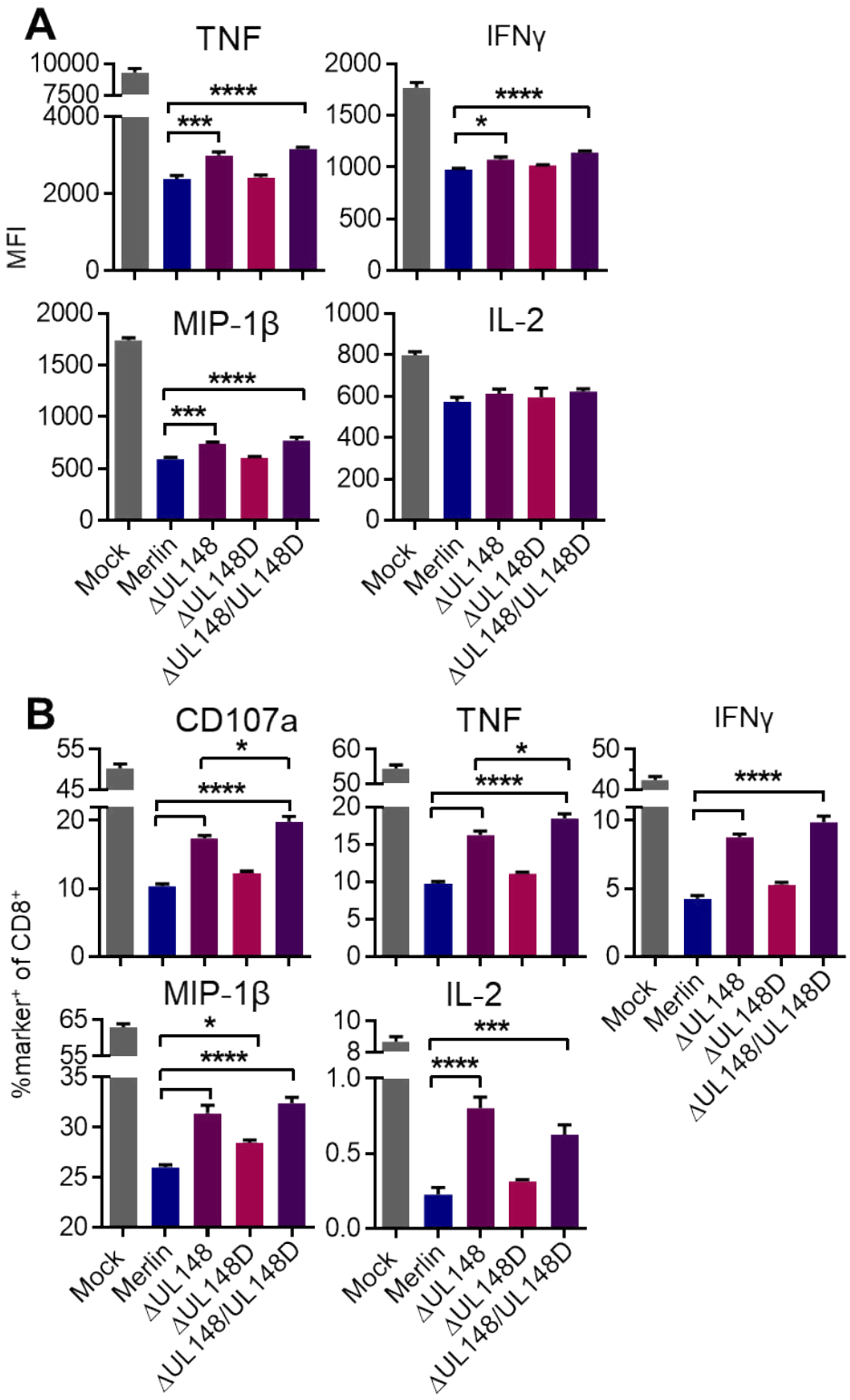

Figure 5.10 T-cell activation assay assessing the effect of deleting UL148 and UL148D on activation of D9 VTE T-cell line.At 72hpi, cells were pulsed with 1µg/ml of VTE peptide and used as targets in a T-cell activation assay. Intracellular staining for IL-2, IFNγ, MIP-1β and TNF was performed after the 5-hour incubation period. Data shows (A) MFI of each cytokine amongst activated cells and (B) % positive CD8+ T-cells, +SEM of quadruplicate values. A one-way ANOVA with Tukey multiple comparison post-hoc tests showed significance at **** p<0.0001, ***p<0.001, *p<0.05.

5.6 Effect of UL148 and UL148D on TNF mediated cell death

As UL148 and UL148D affected the surface levels of TNF receptors, the response of HCMV infected cells to their ligand TNF was investigated. Activation of TNFR1/2 initiates intracellular pathways including the I-kB kinase (IKK), c-Jun N-terminal kinase (JNK) and p38 mitogen activated protein kinase (p38 MAPK) pathways which control proinflammatory gene expression via the transcription factors NF-kB and AP-1 (Varfolomeev and Ashkenazi, 2004). Whilst TNF is a mediator of apoptosis by triggering of caspase pathways, NF-kB drives the production of anti-apoptotic proteins such as cIAP1, cIAP2 and c-FLIP (Wang et al., 2008). This balance between apoptosis and cell survival suggested that TNF receptors may influence HCMV cell viability upon challenge with TNF.

The hypothesis was that the presence of TNF receptors would result in TNF mediated cell death, and that TNF signalling through TNFR2 could act to prevent apoptosis (Naude et al., 2011). Annexin-V binds to phosphatidylserine, which is normally maintained inside live cells through the action of a flippase, but it becomes exposed during cell death due to the action of a scramblase (Nagata et al., 2016); Live/Dead EF660 is an amine binding dye that is excluded from live cells. Cells positive for both were considered dead. HF-TERT cells were mock infected or infected with Merlin, ΔUL148/UL148D and ΔUL138. TNF was added at 72hpi, as this is when there is maximum TNFR2 expression on Merlin infected cells. a multimeric form of TNF (mTNF) was assessed in parallel as this was reported by the manufacturer to signal through both TNFR1 and TNFR2, compared to sTNF which primarily signals through TNFR1 (Grell et al., 1995, Grell et al., 1998). Following 48h of TNF treatment (120hpi), cells were stained with annexin-V and Live/Dead EF660.

Without TNF treatment, all HCMV infected cells showed the same proportion of dead cells (black bars, Figure 5.11A). This suggested that during lytic cycle, UL138 and UL148/UL148D were not influencing intrinsic cell death in the absence of TNF. Low cell death (<2%) was observed with mock infected cells, even following TNF treatment. The proportion of Merlin infected that were dead following sTNF treatment was significantly increased (9.2±0.1 to 18.0±0.5% $p<0.0001$). Whilst there was a significant increase in cell death of ΔUL138 infected cells upon TNF treatment (8.4±0.8 vs 14.3±0.75%, $p<0.0001$), the proportion of dead cells was significantly lower than with Merlin infected cells treated with sTNF (14.3±0.75 vs 18.0±0.5% $p<0.01$). There was minimal increase

in cell death of ΔUL148/UL148D infected cells when sTNF was added. Across the conditions tested, significantly less cell death was achieved with ΔUL148/UL148D, compared to ΔUL138 and Merlin. In an attempt to increase TNFR2 signalling, 80M2, a TNFR2 receptor trimerizing antibody was used in conjunction with mTNF. The combination of TNF and 80M2 has been shown to activate TNFR2 signalling (Krippner-Heidenreich et al., 2002). This combination had no effect on the cell death compared to sTNF or mTNF treated cells (purple bars).

To confirm that the cells were dying due to TNF induced apoptosis, a second readout was used that included a dye that fluoresced upon cleavage by activated caspase-3. As with the previous experiment, a very similar pattern was observed, and caspase activation was significantly higher in Merlin infected cells treated with sTNF compared to untreated control cells (8.2±0.5 vs 19.6±0.9% $p<0.0001$). Whilst there was a significant increase in apoptosing cells infected with ΔUL138 following sTNF treatment (7.4±0.5 vs 14.3±1.6% $p<0.01$), the proportion was significantly lower than with Merlin infected cells (19.6±0.9 vs 14.3±1.6, $p<0.05$). This showed that UL138 increased the susceptibility to TNF mediated apoptosis. There was no significant change in apoptosing cell when ΔUL148/UL148D were treated with sTNF. Use of mTNF or mTNF+80M2 did not alter the proportion of apoptosing cells.

In summary, upon HCMV infection, cells became sensitive to TNF induced apoptosis. Attempts to rescue cells from apoptosis by using mTNF and 80M2, which should increase TNFR2 signalling, were not successful. Apoptosis was the highest amongst Merlin infected cells, then ΔUL138 infected cells, with ΔUL148/UL148D almost unaffected by TNF. These cells were shown to have high, intermediate and low levels of TNFR1 respectively (Figure 4.6). This suggests that the protection against TNF induced cell death primarily relates to TNFR1 expression, with minimal impact of altered TNFR2 expression in HCMV infected cells (Figure 4.6).

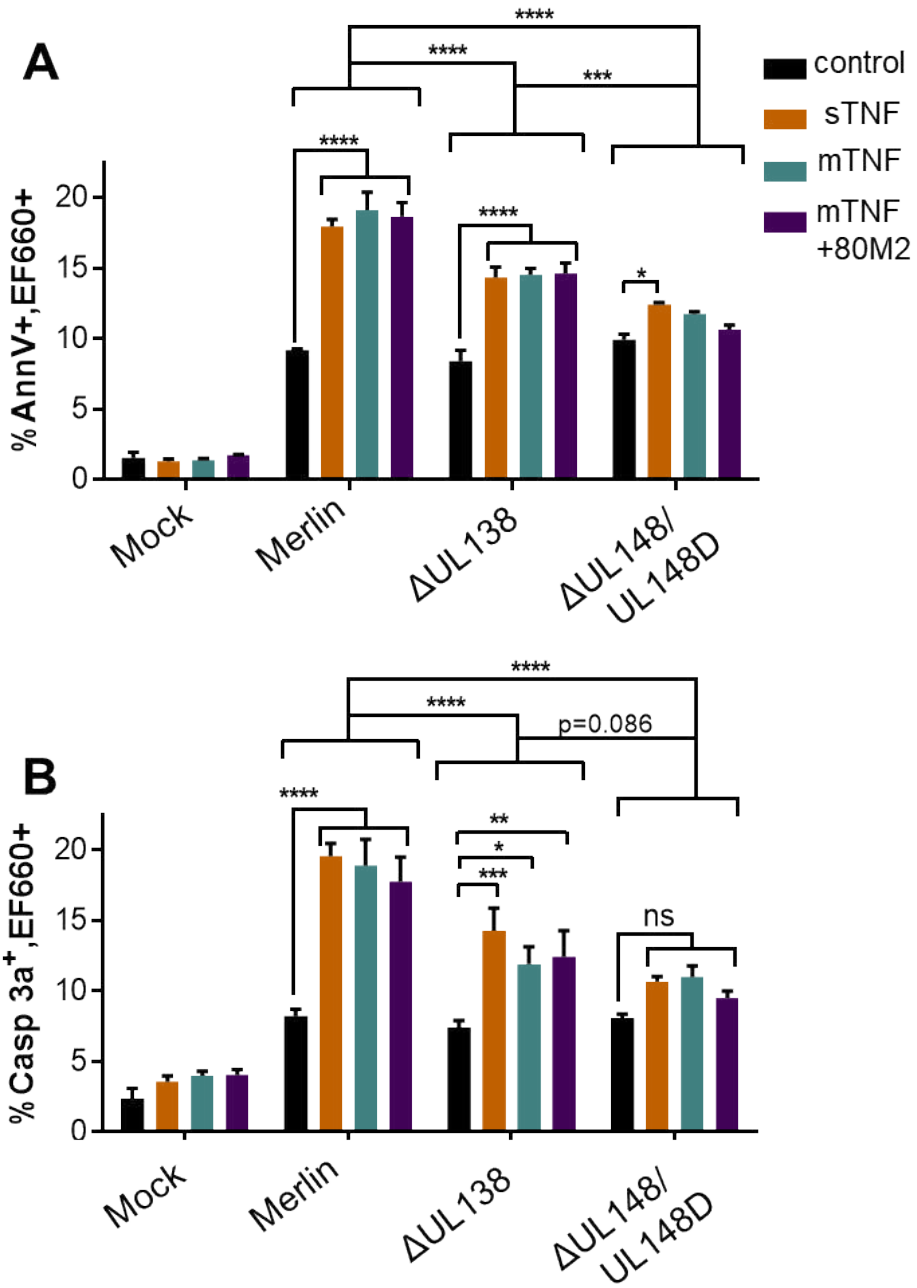

Figure 5.11Effect of HCMV infection on TNF induced cell death. HF-TERT cells were mock infected or infected with HCMV mutants. At 72hpi, the media was removed, and cells were treated with 30ng/ml of sTNF, mTNF or mTNF+80M2. At 120hpi cells were detached and stained for (A) annexin-V and live/dead EF660 or (B) activated caspase 3 and Live/dead EF660 before analysis by flow cytometry. Bars show mean +SEM of triplicate infections. A two-way ANOVA with Tukey multiple comparison post-hoc tests showed significance at **** p<0.0001, ***p<0.001, **p<0.01, *p<0.05.

5.7 Effect of UL148 and UL148 on TNF mediated cytokine production

The previous section showed that TNF receptor expression correlated with increased TNF mediated apoptosis (section 5.6). This result did not fit the hypothesis that increased TNFR2 signalling could prevent TNF induced apoptosis. This suggested that the receptor may induce another function. TNF induced cytokine production by HCMV infected cells was assessed. It was hypothesised that knocking out UL148/UL148D would reduce TNF mediated signalling due to reduced TNFR1/2, as a result of receptor shedding by ADAM17 and therefore result in lower cytokine induction. The list of cytokines downstream of TNF receptor signalling selected for investigation included CXCL10, CCL2, IL-6, IL-8, GM-CSF, CXCL1 and RANTES (Pang et al., 1994).

5.7.1 Effect of HCMV infection on cytokine production

To assess cytokines produced from fibroblasts infected with HCMV, HF-TERTS cells were mock infected or infected with Merlin or ΔUL148/UL148D. Cells were left for 72hpi and a cytometric bead array was used to assess cytokine levels (experiment 1, Figure 5.12A). From uninfected cells, RANTES levels were low and were close to the lowest calibration standard (2.5pg/ml) whereas IL-8 and CCL2 were above the limit of calibration (>10000pg/ml). Mock levels of CXCL10, IL-6, GM-CSF, CXCL1 were within 2-fold of that produced by Merlin infected cells, indicating that HCMV infection was not markedly affecting the production of these cytokines. In contrast, the level of IL-8 recorded was 2633±427pg/ml. The level of CCL2 from Merlin infected cells was 50±2pg/ml. Given that IL-8 and CCL2 were too high to be quantified from uninfected fibroblasts, this suggests that HCMV lytic function impairs IL-8 and CCL2 secretion in fibroblasts. Following the deletion of UL148/UL148D, the levels of CXCL10, IL-6, GM-CSF, CXCL1 and IL-8 in the supernatant were within 2-fold of the levels produced by Merlin, indicating that these genes were not having a large effect on the general production of these cytokines. CCL2 production increased from 51±2 to 278±24pg/ml as a result of deleting UL148/UL148D, though this recovery was not large when considering that the mock level was >10000pg/ml.

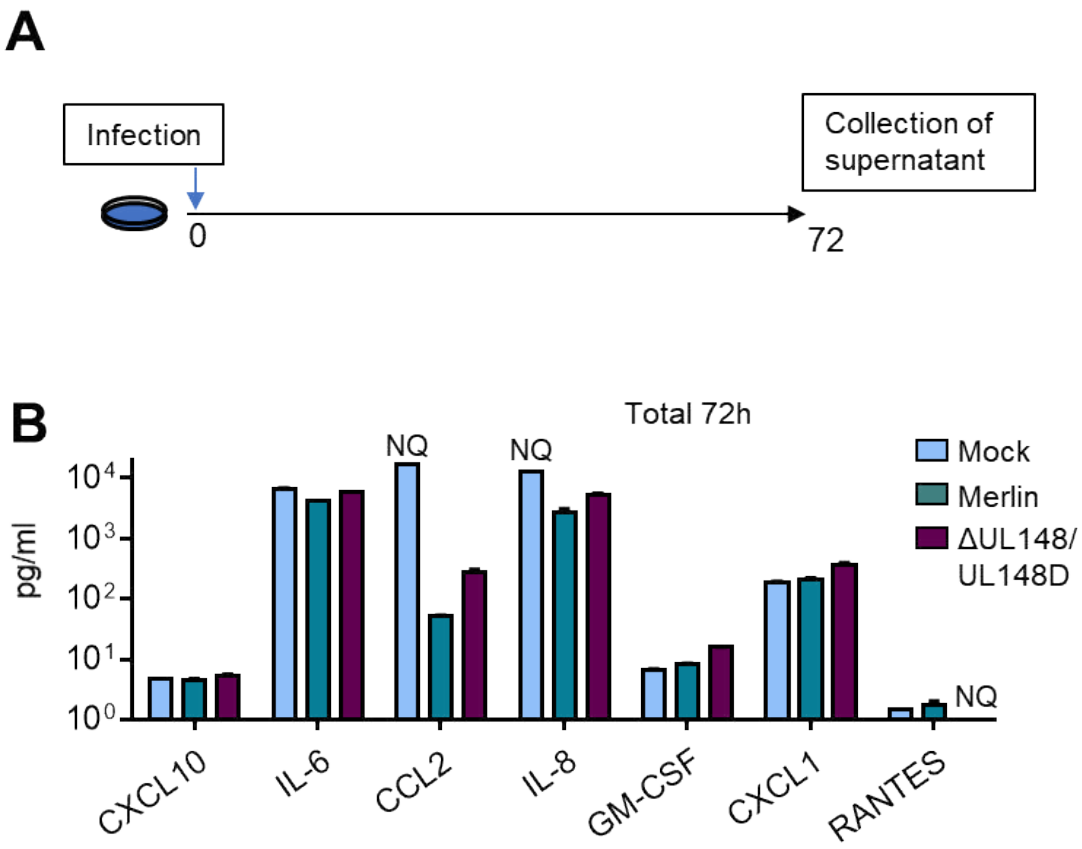

Figure 5.12 Effect of HCMV infection on cytokine production. (A) HF-TERTS were infected and supernatant was collected 72hpi (experiment 1). (B) Cytokine production from cells infected with Merlin, ΔUL148/UL148D or mock infected cells (experiment 1, duplicate infections) NQ- Not quantified. This denotes values which were above or below the limit of quantification. All other values were in the linear range.

5.7.2 Impact of HCMV on TNF induced cytokine production

A further experiment was performed to assess the effect of sTNF, mTNF and the additional effect of blocking ADAM17. Cells were infected with Merlin or with ΔUL148/UL148D and at 48hpi the supernatant was removed and was replaced with DMEM10 containing 100nM D1(A12) or hIgG. Blocking of ADAM17 was performed for 6h to recover surface TNFR1/2; studies had shown complete inhibition of shedding of ADAM17 ligands after only one hour of treatment (Tape et al., 2011). At 54hpi sTNF, mTNF (both at 30ng/ml) or an equivalent volume of media was added (Figure 5.12A). At 72hpi, the supernatant was kept and frozen. This provided six conditions; hIgG + no TNF (referred to as control), +sTNF, +mTNF, D1(A12), D1(A12)+sTNF, and D1(A12)+mTNF. All conditions for experiment 2 were performed in triplicate. All cytokine levels produced from HCMV infected cells were within the linear limit of detection.

The levels of cytokines from TNF treated cells is presented as a fold change over non-treated cells. Upon addition of mTNF IL-8 was increased 2.6-fold, but none of the other cytokines were increase by more than 2-fold. In contrast, treatment of ΔUL148/UL148D resulted induced an 18-fold increase in IL-8 production. There was also a significant 5.5-fold increase in CCL2 production. There was a 5-fold increase in GM-CSF, but due to the variability across all GM-CSF data meant this was not statistically significant ($p=0.051$). IL-6 was increased 2.5-fold, though this was non-significant.

This data showed that fibroblasts infected with HCMV Merlin are not able to respond to TNF, when using cytokine release as a readout, but cells infected with ΔUL148/UL148D were able to increase production of IL-8, CCL2 and GM-CSF. This result was not expected as the expression of TNFR1/2 is lower on ΔUL148/UL148D compared to Merlin infected cells. Therefore, this this data suggests that UL148 and UL148D are involved in modulating the response to TNF or influencing IL-8 release independent of their effect on surface TNFR1/2 expression.

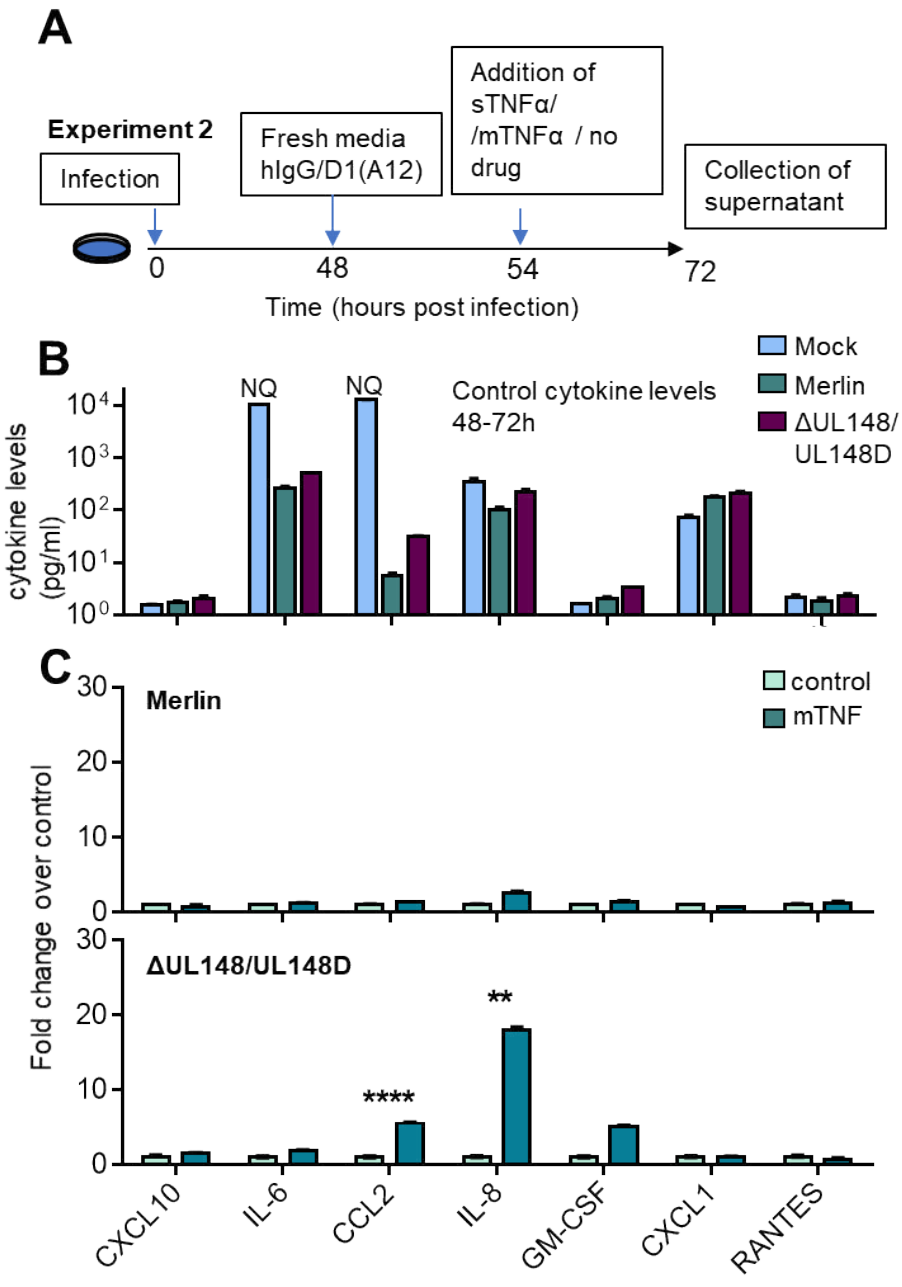

Figure 5.13 Effect of TNF on production of cytokines within HCMV infected cells.(A) HF-TERT cells were infected with Merlin or ΔUL148/UL148D. At 48hpi the media was replaced with fresh media. At 54hpi sTNF, mTNF or media were added. At 72hpi, the supernatant was collected, and cytokines levels were quantified using a cytometric bead array. (B) Cytokine levels between 48-72h without TNF treatment were set as control levels. (C) Effect of mTNF on cytokine production by HCMV infected cells. Data is displayed as fold change compared to control supernatant shown in (B). Bars show mean +SEM of triplicates. Data from the Merlin and ΔUL148/UL148D infected cells from the whole experiment was pooled. A 2-way ANOVA with Tukey multiple comparison post-hoc tests showed significance at **** $p<0.0001$, ** $p<0.01$.

5.7.3 Effect of blocking ADAM17 on TNF responsiveness of HCMV

To assess if recovering TNF receptors on the surface of ΔUL148/UL148D could have an effect on TNF induced cytokine production, ADAM17 was blocked at 48hpi, which would recover TNFR1/2 on the cell surface. At 54hpi, sTNF or mTNF was added to cultures (Figure 5.14B). Blocking of ADAM17 was performed for 6h to recover surface TNFR1/2; studies had shown complete inhibition of shedding of ADAM17 ligands after only one hour of treatment (Tape et al., 2011). It was predicted that the recovery in TNF receptors due to ADAM17 blocking (Figure 5.6) would increase TNF induced cytokine production on ΔUL148/UL148D due to increased TNF signalling. Cytokine levels were compared to the supernatant was were not treated with D1(A12) or TNF (Figure 5.13B) and represented as fold changes.

Blocking of ADAM17 by D1(A12) had no effect on cytokine production from Merlin or ΔUL148/UL148D infected cells (Figure 5.14B). This result showed that any differences following the addition of TNF following blocking of ADAM17 would be due to a difference in TNF mediated signalling, and not due to an off-target effect of D1(A12) or blocking ADAM17 function.

A statistical comparison was made between cells treated with mTNF with and without D1(A12) pre-treatment (Figure 5.14C). This shows that upon adding mTNF there were no significant increases in cytokine production from D1(A12) pre-treated Merlin infected cells compare to cells treated with mTNF alone. Apart from IL-8 (4-fold increase), none of the other cytokines measured were increased more than 2-fold compared to control cytokine levels. D1(A12) pre-treatment had a significant effect on cytokine production from ΔUL148/UL148D infected cells treated with mTNF. There were significant increases in CXCL10, CCL2, CXCL1, IL-6, IL-8 and GM-CSF compared to cells treated with mTNF. Most striking was the 45-fold increase in IL-8 by D1(A12)+mTNF treated cells, which was increase 18-fold by mTNF alone. There was a 10 and 12-fold increase in GM-CSF and CCL2 production respectively. IL-6, CXCL1, GM-CSF were also significantly increased but less than 5-fold. RANTES levels were unaffected by D1(A12) and mTNF treatment. This showed that D1(A12) pre-treatment did not affect cytokine production by Merlin infected cells but increased multiple cytokines produced in response to mTNF by ΔUL148/UL148D infected cells.

As mTNF was reported by the manufacturer to have a greater signalling capacity through TNFR2 and act through TNFR1, it was not possible to assign the cytokine output shown by Figure 5.14 to either receptor. However, sTNF predominantly binds to and activates

TNFR1. Therefore, any difference in cytokine production between sTNF and mTNF could theoretically be attributed to the greater activity of mTNF on TNFR2. To assess this, a statistical comparison of cytokine release was made between D1(A12)+sTNF and D1(A12)+mTNF treated cells. The TNF response of Merlin infected cells was comparable between sTNF and mTNF treated cells (Figure 5.14D), with no significant differences in cytokine production. In contrast the production of CXCL10, CCL2, CXCL1, IL-6, IL-8 and GM-CSF was significantly higher from D1(A12)+mTNF treated cells compared to D1(A12)+sTNF treated cells. This suggests functional signalling of TNFR2, but only in the context of a ΔUL148/UL148D infected cell.

In summary the data in section 5.7 shows HCMV alters the profile of cytokine production by fibroblasts. Baseline CCL2 production by fibroblasts was impaired upon HCMV infection. Treatment of Merlin infected cells did not significantly increase cytokine production, however cells infected with ΔUL148/UL148D significantly increased IL-8 production upon TNF challenge. Recovery of TNFR1/2, by blocking ADAM17 function on ΔUL148/UL148D infected cells resulted in a further increase in CXCL10, IL-6, CCL, GM-CSF, IL-8 and GM-CSF production, with a 45-fold increase in IL-8, compared to control supernatant. This data shows functional response of TNF receptors in HCMV infected cells in response to TNF treatment, but only when UL148 and UL148D were deleted.

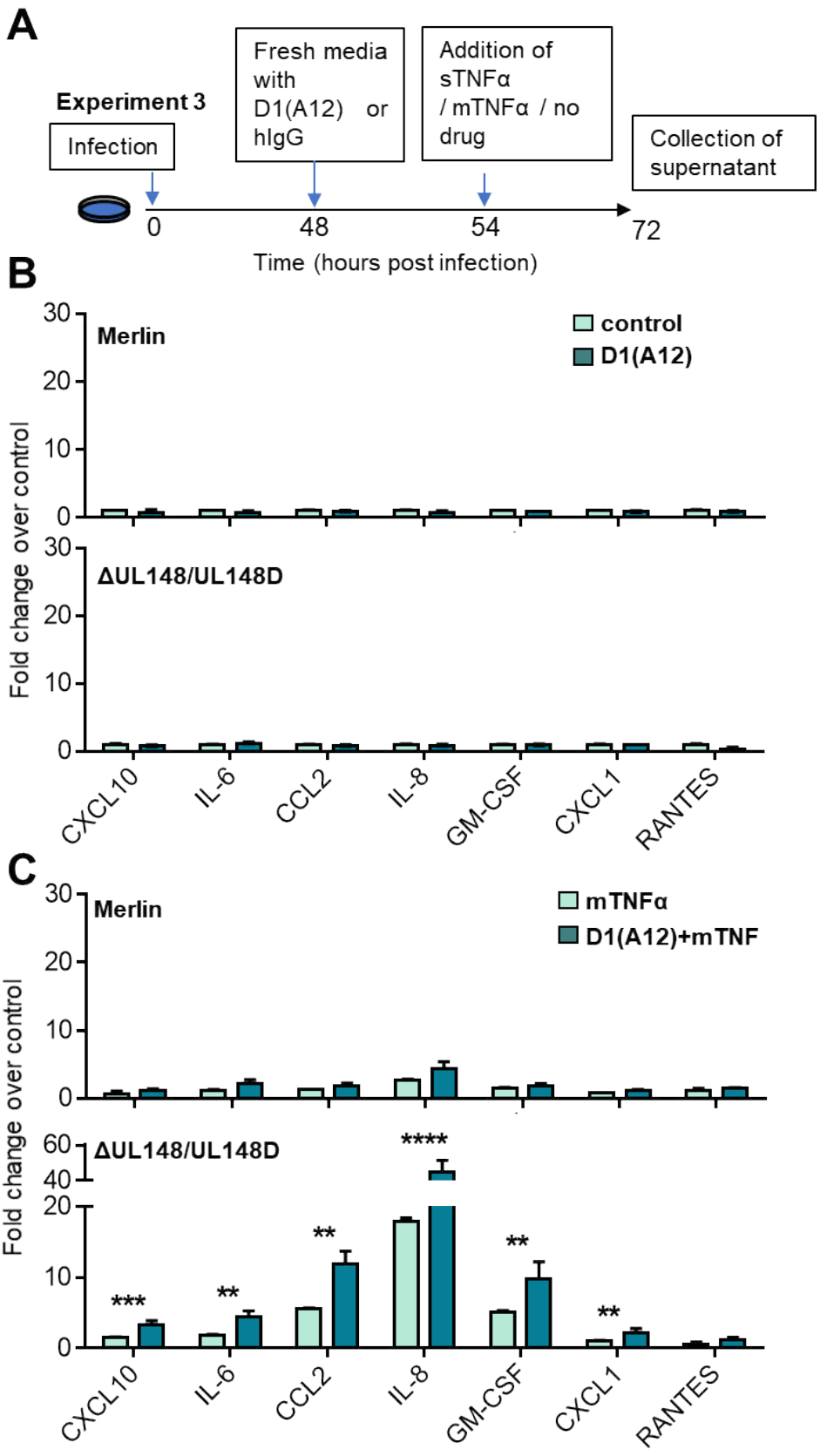
A
Experiment 3
Infection
Fresh media with D1(A12) or hIgG
Addition of sTNFα / mTNFα / no drug
Collection of supernatant
0
48
54
72
Time (hours post infection)
B
Merlin
control
D1(A12)
ΔUL148/UL148D
Fold change over control
30
20
10
0
CXCL10
IL-6
CCL2
IL-8
GM-CSF
CXCL1
RANTES
C
Merlin
mTNFα
D1(A12)+mTNF
ΔUL148/UL148D
Fold change over control
60
40
20
10
0
***
**
**
****
**
**

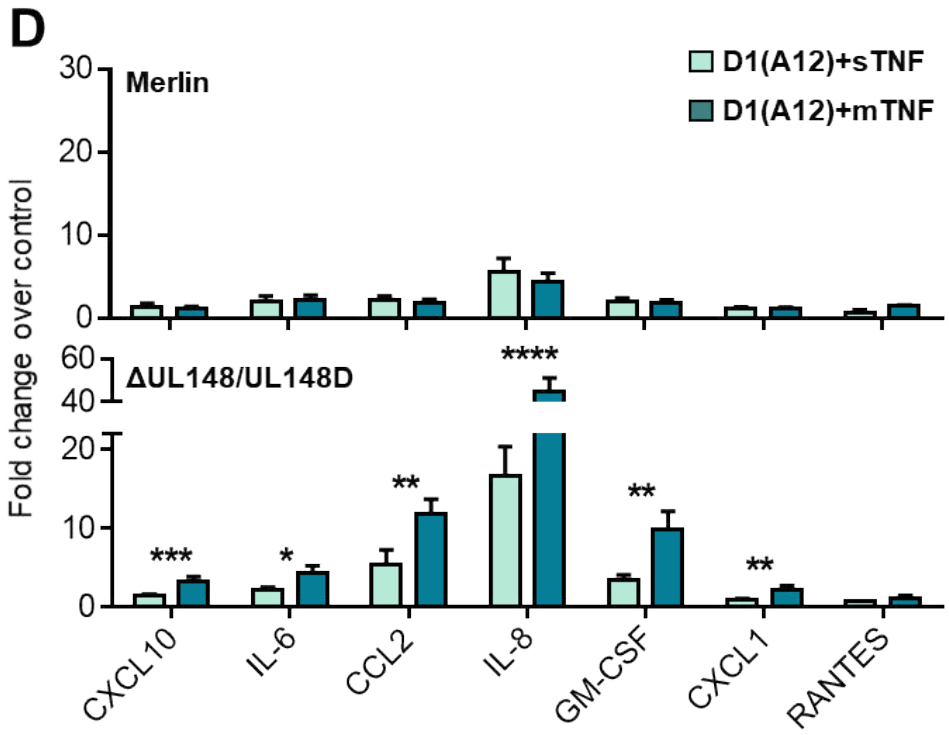

Figure 5.14 Assessing the effect of blocking ADAM17 on TNF induced cytokine production.(A)HF-TERT cells were infected with Merlin or ΔUL148/UL148D. At 48hpi the media was replaced with fresh media containing 100ng/ml of D1(A12). At 54hpi sTNF and mTNF (30ng/ml) were added. At 72hpi, the supernatant was collected, and cytokines levels were quantified using a cytometric bead array. Data is displayed as fold change compared to control supernatant (levels from Figure 5.13B). (B) Effect of D1(A12) on cytokine release (C) Effect of D1(A12) pre-treatment on mTNF induced cytokine production (D) Comparison between sTNF and mTNF, on cells treated with D1(A12). Bars show mean and SEM of triplicates. Data from the Merlin and ΔUL148/UL148D infected cells from the whole experiment was pooled. A 2-way ANOVA with Tukey multiple comparison post test showed significance at **** $p<0.0001$, ***$p<0.001$, **$p<0.01$, *$p<0.05$.

5.8 Summary

The aim of this chapter was to understand how UL148/UL148D act to upregulate TNFR2 over the course of a HCMV infection and the functional significance of increased TNF receptor expression on infected cells. Proteomics predicted that ADAM17, the sheddase of TNFR2, is downregulated during HCMV infection and this is in part by UL148 and UL148D. HCMV efficiently downregulated surface ADAM17, which was rescued by deleting UL148 and UL148D. This was a synergistic effect as whilst deleting each gene in isolation had a small effect, deleting both led to a large recovery in surface ADAM17. Increased ADAM17 was accompanied by a large increase in soluble TNFR2 detected in the supernatant from ΔUL148/UL148D compared to Merlin infected cells. Blocking ADAM17 on ΔUL148/UL148D infected cells, led to a recovery of surface TNFR2 expression and a reduction of sTNFR2 production, showing that surface TNFR2 expression was dependent on ADAM17 downregulation.

Western blots showed that the mature form of ADAM17 was not detectable in cell lysates from Merlin infected cells, and the immature form was increased compared to mock infected cells. Mature ADAM17 was partially recovered in ΔUL148/UL148D infected cell lysates indicating that UL148 and UL148D likely affect the maturation of ADAM17. Western blots for the ADAM17 chaperone proteins iRhom1 and iRhom2 showed no difference between Mock, Merlin and ΔUL148/UL148D cell lysates. Proteomic analysis of HCMV infected cells showed that degradation by proteases was unlikely to be contributing to the reduction in ADAM17. Thus, the precise mechanism by which UL148 and UL148D affect ADAM17 within the cell remains unclear, though a preliminary hypothesis would be that these genes interfere with ADAM17 maturation.

When assessing the functional significance of TNFR on cells, it was shown that Merlin infected cells became susceptible to TNF induced apoptosis though attempts to rescue cell death by increasing TNFR2 signalling were unsuccessful. Deletion of UL148/UL148D prevented TNF induced cell death, which correlated with reduced surface TNFR1 expression. When cytokine production was assessed, HCMV was found to have a suppressive effect on the ability of fibroblasts to produce cytokines following TNF treatment. Even though fewer TNF receptors were present on the surface of ΔUL148/UL148D infected cells, TNF induced significant increases in cytokine production, particularly IL-8. This was further increased when ADAM17 was blocked. Collectively this data showed that HCMV genes UL148 and UL148D affects TNF signalling, impacting on cell death and cytokine release by cells.

6 Discussion

This thesis describes a number of novel findings. In a screen of HCMV genes non-essential for replication, UL19 was identified as a novel T-cell inhibitor with further demonstration of the RL10-UL1 region as encoding novel T-cell inhibitors. The last two chapters demonstrated that UL148 and UL148D were shown to increase TNFR2 on the surface of HCMV infected cells. This was achieved through impairment of ADAM17 maturation and downregulated surface expression, thereby allowing TNFR2 to accumulate, and TNFR1 to be maintained, at the cell surface. This impacted on cell death, and cytokine production, induced by TNF.

6.1 Screening for genes regulating T-cell activation

6.1.1 Growth of HCMV specific T-cells

In section 3.1, the growth and degranulation potential of HCMV specific T-cell lines was studied. Of the three T-cells lines used in this thesis (D7-VLE, D7-NLV and D9-VTE), two were from an HLA-A2 positive donor (D7) and the third was from a HLA-A1 individual (D9). As the majority of published HCMV research has been performed in Europe and America this has led to an abundance of information concerning HLA-A2 restricted T-cell responses, as this is very common in Caucasian individuals. This may does not reflect the immune response to HCMV across the world given the vast heterogeneity in HLA haplotype among different ethnic groups. Whilst HLA-A2 is present in half of all Welsh people, in Vietnam HLA-A11 is the most common HLA-A gene (Gonzalez-Galarza et al., 2015). The use of multiple T-cell lines with different HLA specificities would provide more information about the response to HCMV around the world and could provide a causal link as to why certain populations or patients deal with HCMV infection better than others. Certain individuals have been shown to be resistant to HCMV-encoded immune regulating genes. For example, US9 was shown to specifically target MICA*008, which escapes UL142 targeting (Seidel et al., 2015). Additionally, the heavy chain of HLA*B07 was found to escape US2 mediated degradation, so presentation of antigenic peptides should be theoretically increased (Llano et al., 2003, Barel et al., 2003).

Future work would utilise T-cell line lines from donors with different HLA haplotypes and from a range of ethnicities, to ensure broader coverage of polymorphic immune genes such as HLA-I molecules, but also KIR (killer-cell immunoglobulin-like receptors) which are also on the surface of CD8+ T-cells and are subject to allelic variation (Wills et al.,

2013, Sylwester et al., 2005). Experiments could also be performed ex-vivo, allowing for assessment of T-cell responses in a more physiological setting.

6.1.2 Role of HCMV UL16 and UL18 in T-cell evasion

In experiments performed with and without exogenous peptide, fibroblasts infected with ΔUL16/UL18 induced increased degranulation of CD8+ T-cells. Since its discovery, the role of NKG2D in CD8+ T-cell activation is well established, with blocking of NKG2D able to reduce lysis of target cells (Bauer et al., 1999, Verneris et al., 2004). On T-cells, the receptor acts in a co-stimulatory manner and was unable to activate the cell with a cross linking antibody, in the absence of T-cell receptor signalling (Jamieson et al., 2002). In this thesis, one T-cell line (D9) was activated by ΔUL16 with peptide suggesting that UL16 may be involved in T-cell evasion. Whilst only one T-cell assay was performed the presence of NKG2D on the T-cells and the increased activation upon deletion of UL16 would imply that UL16 can reduce the activation of NKG2D positive T-cells as it does with NKG2D+ NK cells, although another mechanism has not been ruled out. NKG2D blocking experiments with antagonising antibodies would validate function directly.

Whilst D9-VTE was negative for LIR1, a conclusion cannot be made about the effect of UL18 on T-cells from this one experiment. Using a range of tetramers, LIR1 expression on CD8+ T-cells was shown to be higher in HCMV seropositive individuals (Antrobus et al., 2005). Ex vivo assays from HCMV positive donors showed that antagonising LIR1 on HCMV specific T-cells increased proliferation, which is in line with the role of LIR1 as an inhibitory receptor (Gustafson et al., 2017). However, blocking LIR1 did not cause an increase in cytokine production, suggesting that the role of UL18 could be restricted to limiting the proliferation of cells responding to HCMV infection. A soluble form of UL18 decreased IFNγ production by LIR1+ T-cells (Wagner et al., 2007). This contrasted with data which showed that HCMVΔUL18 virus resulted in impaired IFN production (Antrobus et al., 2005). Thus, as with NK cells, UL18 may have activating and inhibitory functions on different T-cell subsets. Complications arise when considering the potential role of UL18 in T-cell evasion. In HCMV isolates, the amino acid sequence of UL18 was found to vary by up to 20 amino acids (Valés-Gómez et al., 2005). Unlike classical HLA molecules, where allelic polymorphism is observed within the peptide binding groove, variability in UL18 was mapped to areas outside this region (Yang and Bjorkman, 2008). Thus, a lack of interactions between Merlin UL18 and a donor T/NK cell may not replicate what occurs in vivo as the strength of UL18-LIR1 interaction may be different due to sequence variation of UL18 within clinical strains. Furthermore, there is diversity in the LIR1 gene itself which can affect the strength of UL18 binding (Kuroki et al., 2005). This was shown to be clinically relevant when Yu and colleagues (Yu et al., 2018)

demonstrated that different LIR1 genotypes can control HCMV disease in renal transplant patients and alter NK cell killing. Both UL18 and LIR-1 variation could therefore affect the response of LIR1 expressing T-cells to HCMV infected cells in vivo.

The role of co-stimulatory molecules in T-cell evasion was highlighted in recent work from our group which showed UL148 sequestered CD58 (LFA-3) inside the cell (Wang et al., 2018). CD58 binds to CD2, which is found on all T and NK cells. Functionally, HCMV infected cells lacking UL148, and therefore expressing more CD58, induced greater degranulation of NK and CD8+ T-cells. This was blocked upon antagonism of CD58. Interestingly, blocking of CD58 did not influence degranulation against uninfected target cells. This suggests that co-stimulatory pathways may become of greater relevance when general activation signals are reduced, as is the case following HCMV infection (Wang et al., 2018). In turn, HCMV has developed multiple strategies to target these mechanisms of activation. The ability of the immune system to exploit non-HLA-I mediated activation of CD8+ T-cells was demonstrated with CMV vaccines, which have been reported to drive unconventional HLA-II and HLA-E restricted CD8+ T-cell responses and produce SIV clearance in rhesus macaques (Hansen et al., 2013, Hansen et al., 2016).

Our laboratory has also shown that the US12 family target other co-signalling immune ligands for degradation, including those involved with formation of the immune synapse and activation of T-cells such as ALCAM, CXADR, B7-H2 (ICOSL) and B7-H3 (Fielding et al., 2014, Fielding et al., 2017). Intriguingly, B7-H2 is co-stimulatory whist B7-H3 is co-inhibitory. It is possible that the targeting of different immune ligands could have evolved as counter mechanisms against different immune subsets, or as a way of driving other responses. An example is the UL40 mediated upregulation of HLA-E (Tomasec et al., 2000). The second transcriptional start sites of UL40 was shown to be responsible for the upregulation of UL18 (Prod'homme et al., 2012). Additionally, UL18 can impair LIR1+ NK cells, but activates LIR1- NK cells (Prod'homme et al., 2007). It is possible that there are additional genes which drive immunosuppressive T-cell subsets, as with UL11 which was shown to drive immunosuppressive IL-10 production by CD4+ T-cells (Zischke et al., 2017). This has been observed with other herpes viruses such as with HHV-6 which was shown to induce CD4 and CD8 T-reg expansions, which could impair the overall T-cell response due to production of immunosuppressive cytokines (Wang et al., 2014). This has also been demonstrated between NK and T-cells in HCMV. HLA-I downregulation largely affects HLA-A and HLA-B, though HLA-C is relatively resistant. As a result, HLA-A/B restricted T-cell clones were shown to be less effective than HLA-C specific restricted clones which recognized and killed virally infected cells (Ameres et al.,

2013). This allowed HLA-C expressing cells to escape killing from NK cells expressing KIR2DL3, an inhibitory receptor which binds HLA-C. These findings suggest that the ability of HCMV to regulate immune ligands may reflect the need of the virus to impair multiple immune activation pathways used by anti-viral T and NK cells, resulting in a compromise that impairs the overall immune response to HCMV.

6.1.3 Identification of HCMV UL19 as a T-cell evasion gene

UL19 was shown to be a potent T-cell evasin across a range of peptide concentrations. Data from our lab showed that UL19 can also impair NK cell activation (personal communication; Rebecca Aicheler). It is possible that the same mechanism of inhibition affects both T and NK cells, although distinct mechanisms for immune evasion cannot be discounted at this stage. Proteomic analysis of HCMVΔUL19 infected cells showed that UL19 did not alter the expression of cell surface proteins significantly compared to the parental strain (unpublished data; Dr Pete Tomasec, Dr Mike Weekes). However, PMP only detects glycoproteins, therefore an effect on a cell surface protein cannot be ruled out. UL19 may act by binding to and preventing the function of another protein, rather than causing a change in the whole cell level of the target protein. Currently, there is no published information on UL19 and proteomics was not able to determine if it is on the cell surface (Weekes et al., 2014). A BLAST search revealed no obvious homologues with any human proteins, though UL19 orthologues are found in chimp and macaque CMVs. This suggests that UL19 may target a conserved activation pathway.

UL19 had no effect on surface HLA-I downregulation though it could be possible that it augments the ability of HLA to bind to the TCR. An important observation was that UL19 was able to induce an inhibitory effect when the strength of the T-cell receptor signal was varied. Whilst US2-11 genes downregulated HLA-I, this effect is not complete, and residual HLA-I molecules are present on HCMV infected cells. It is possible that UL19 could bind to HLA-I molecules that have escaped degradation and impair the ability of the TCR on CD8+ T-cells and activating KIRs or LIRs on NK cells to bind to HLA-I. This would be analogous to the murine CMV protein m4/gp34, which forms a complex with MHC-I molecules in the Golgi, which is then exported to the cell surface (Kavanagh et al., 2001). This is seen with EBV gp42, which impairs the reaction between HLA-II and TCR, which impaired the activation of CD4+ T-cells (Ressing et al., 2003). This principle of impairing function rather than the presentation of a molecule could also apply to co-signalling molecule too. Imaging of UL19, whether by ectopic expression (Seirafian, 2012), or in tagged HCMV constructs (Yang, 2011) were consistent in their observation that UL19 is diffusely localised within the cytosol. Therefore, UL19 could bind to a protein to the cytosolic domain of HLA-I or a costimulatory molecule that is being trafficked

between the Golgi and the plasma membrane. In this regard, it is interesting to note that UL19 is similar to UL135, which is largely expressed in the cytosol (Stanton et al., 2014). Whilst UL135 was found to alter the actin cytoskeleton and impair synapse formation between infected cells and T/NK cells, other HCMV proteins were not ruled out and it is possible that UL19 could affect structural proteins involved with synapse formation.

6.1.4 Role of RL11 family in T-cell activation

The RL11 family is an example of a genomic accordion, which is proposed as a series of related genes that have arisen due to gene duplication and mutation in order to deal with a constantly evolving host defence system (Elde et al., 2012). As with the US12 family, this would suggest that this family includes multiple immune modulatory functions.

Degranulation by CD8+ T-cells against HCMVΔUL2-11 infected cells was not increased compared to the parent HCMV in chapter 3. Immune evasion genes have been reported in the UL2-UL11 region of the RL11 family. UL10 is a secreted protein and binds to immune cells, reducing inflammatory cytokine production from CD4+ T-cells (Bruno et al., 2016). UL11 binds to and activates CD45 on IL-10 producing CD4+ cells, which increased the production of immunosuppressive IL-10, and therefore reduced IFNy production (Zischke et al., 2017). UL7, and more recently UL8 were found to be soluble glycoproteins and impaired cytokine production by myeloid cells (Engel et al., 2011, Perez-Carmona et al., 2018). Our lab also showed that UL4, another soluble glycoprotein, has NK inhibitory effects (Seirafian, 2012). This growing body of work on the RL11 family of proteins indicates that the T-cell modulatory activity of genes in the UL2-UL11 region may be dependent on the proteins being present in the supernatant, which can impair immune cell recognition prior to immune synapse formation. In the assays presented in chapter 3, HCMV infected cells were washed multiple times in fresh media prior to co-culture with effector cells. Therefore, determining the effect of UL2-11 genes from my data could be considered a moot point as soluble UL4, UL7, UL8 and UL10 were removed from the experimental setup. In the above cited studies soluble forms of UL11, UL10 and UL8 were all found to bind to CD8+ T-cells. Our assays would need to be modified to assess how these genes affect CD8+ T-cells.

In the absence of peptide, deleting the RL10-UL1 region reduced degranulation by HCMV specific CD8+ T-cells, occurring more frequently than in assays when HCMV infected cells were pulsed with peptide, which gave quite variable results. This suggests that the activation signal provided by exogenous peptide concealed a subtler effect that may not be dependent on pHLA-TCR. It is possible that RL10-UL1 genes activate inhibitory KIR or inhibit activating KIRs. Whilst the role of KIRs was not investigated in

this work, flow cytometry showed that the D7-VLE T-cell line is positive for inhibitory KIR2DL3, 3DL1 and 3DL2 (personal communication Dr Simon Kollnberger). It is possible that *in vivo*, in the absence of strong pHLA-TCR signal, co-stimulatory molecules and NK receptors on CD8+ T-cells become more important for activation by providing additional avidity for their HCMV infected targets.

Using RL11 and UL1 expressing vectors, these genes were flagged as possible immune evasins as they reduced T-cell degranulation. RL11 was shown to be toxic and therefore its ability to suppress T-cell activation when expressed ectopically could be questioned. In assays performed with peptide, the deletion of RL11 had limited effect on T-cell activation. Even when significant increases in degranulation was observed with ΔRL11 infected cells, these were modest compared to those observed with ΔUL19 and ΔUL148 (Wang et al., 2018). RL11 has been shown to bind to FcYIII on NK cells and inhibit ADCC (Corrales-Aguilar et al., 2014). It is possible that if RL11 is involved in impairing T-cell activation, then it is binding to an immune receptor on the surface of T-cells. High levels of UL1 can only be expressed when it is codon optimised (personal communication, Dr Ceri Fielding), therefore the increased degranulation that was measured from RAd-UL1 infected cells was unlikely to be due to toxicity from transgene expression, and more likely due to an effect of UL1 itself. UL1 has significant homology with members of the human carcinoembryonic antigen (CEA) family, which primarily mediate cell adhesion and act as receptors for bacteria and viruses (Kuespert et al., 2006). UL1 could act as a decoy receptor for effector cells and prevent cell adhesion. It has been shown that blocking of homotypic CEACAM1/CEACAM1 interactions result in increased CD8+ T-cell activation, suggesting an inhibitory receptor function. If UL1 can bind to the CEACAM1, this could potentiate the inhibition of CEACAM1 on T-cells. UL1 is thought to have arisen out of RL11-RL13 gene duplication but is also mutated in up to 10% of clinical strains (Sijmons et al., 2015). It is possible that the variability in the RL11 gene family members, such as UL1, reflects the interplay between host and virus and the selection pressures exerted on these genes to mutate.

6.1.5 Future directions

The main limitation of this work was the inability to find mechanism by which UL19 or RL10-UL1 genes may function, therefore this would be focussed to uncover how these genes impair CD8+T-cell activation. To assess how UL19 functions mechanistically, SILAC-IP could be performed with a tagged UL19 variant to identify the proteins to which UL19 binds. Detailed phenotyping of the T and NK cell lines sensitive to UL19 mediated inhibition could provide clues as to how UL19 functions as an immune evasin. To assess the immune evasion capacity of HCMV genes within the RL11 family, functional readouts

should also be expanded to include inflammatory cytokine production and T-cell proliferation. A range of proteomic approaches could be used including SILAC-IP and mass spectrometry to identify binding partners for these proteins, although this approach may be limited if they are acting as ligands for inhibitory receptors on effector cells. Ectopically expressing HCMV genes and assessing binding using a range of reporter lines would inform if members of the RL11 family can bind KIRs or other inhibitory/activating receptors. Previous studies have used Fc fusion proteins to elucidate the binding capacity and mechanism of other RL11 family proteins, therefore this would be an attractive approach for studying the whole family of RL11 family proteins as thus could allow for isolation of ligands on CD8+ T-cells. Demonstration of an interaction could be shown using the yeast-2 hybrid assay which was utilised for identifying UL135 binding proteins (Stanton et al., 2014).

6.2 Function and Mechanism of TNFR2 upregulation

6.2.1 HCMV UL148 and UL148D upregulation of TNFR2

Chapter 4 showed that TNFR2 upregulation on HCMV infected cells was due to UL148 and UL148D mediated downregulation of ADAM17. The impairment of ectodomain shedding allowed TNFR2 to accumulate on the surface of infected cells. Genes UL148 and UL148D were also necessary for surface expression of TNFR1 and deletion of both genes caused a reduction in TNFR1 expression. TNFR2 joins the growing list of receptors regulated by genes of the U_L/*b'* region. Whilst UL138 co-precipitates with TNFR1 (Le et al., 2011), UL138 deletion did not affect TNFR2 surface. Although my results are consistent with UL138 increasing TNFR1 expression during lytic infection, UL148 and UL148D are necessary for UL138 to function; otherwise TNFR1/2 would be cleaved by ADAM17 and released from the surface.

The upregulation in TNFR2 protein occurred at the cell surface and whole cell level. This was preceded by an increase in TNFR2 mRNA. The whole cell increase was independent of UL148/UL148D, and could be a host response to HCMV infection, or mediated by other HCMV genes. Whilst this was not the focus of the project it is interesting to note that TNFR1 was not transcriptionally upregulated upon HCMV infection. Cells treated with irradiated virus did not upregulate TNFR2 or TNFR1 showing that virus binding, virion proteins or innate interferon signalling do not affect TNFR2. This is in keeping with published data (Tirosh et al., 2015). Given that TNFR2 was upregulated as early as 24hpi, this would suggest that the initial transcriptional increase may be regulated by an early HCMV gene. It is possible that the whole cell increase in TNFR2

protein could be induced by IE1/IE2, which were shown to induce upregulation of immune ligands such as ULBPs and MICA (Fielding et al., 2014).

Western blotting showed that whole cell TNFR2 was increased independently of UL148 and UL148D, thus these genes regulate TNFR2 at the cell surface only. When knockout viruses were assessed, comparable effects on surface TNFR2 were observed between UL148/UL148D using flow cytometry. Interestingly, when ADAM17 blocking experiments were performed, soluble TNFR2 was not completely removed from the supernatant. A spliced variant of TNFR2 that encodes a soluble form of TNFR2 has been reported which could explain this observation (Lainez et al., 2004).

6.2.2 HCMV downregulates ADAM17

This work reports the first function for UL148D and a novel function for UL148. These two proteins act synergistically to downregulate ADAM17 over the course of a lytic infection. It was shown that infection with Merlin prevented the formation of the mature form of ADAM17. An increase in pro-ADAM17 was detected, indicating that HCMV may interfere with the maturation of the enzyme. In macrophages, maturation of ADAM17 is regulated by iRhom2, which binds ADAM17 and promotes its exit from the ER (Adrain et al., 2012). Western blotting showed no discernible change in the expression of iRhom1/2 proteins upon HCMV infection. It is possible that UL148/UL148D could influence the activity of these molecules without influencing their overall levels within the cell. Regulation of ADAM17 was also shown to be influenced by PACS-2, which sustains ADAM17 expression by diverting it away from degradative pathways (Dombernowsky et al., 2015). This is a less likely function for UL148/UL148D as Western blotting and multiple proteomic datasets showed that ADAM17 was not being degraded.

Even in the absence of UL148 and UL148D (ΔUL148/UL148D), ADAM17 was still partially downregulated and enzymatically active. This was not due to the virion itself as irradiated HCMV did not affect surface ADAM17. When blocking of ADAM17 was performed there was no increase in the cell or soluble TNFR1 on uninfected cells. This suggested that HCMV infection induces a physiological switch from inactive to active ADAM17. Early studies showed that infections with HCMV strains lacking U_L/*b'* resulted in a suppression of TNFR1 expression (Baillie et al., 2003, Montag et al., 2006). In the absence of the U_L/*b'* region, not only would UL138 not be there to stimulate TNFR1 expression, but enzymatically active ADAM17 would remain on the surface in the absence of UL148/UL148D.

The activation of ADAM17 to the enzymatically form at the cell surface was shown to occur upon LPS treatment of cells which induced iRhom2 phosphorylation and the

recruitment of 14-3-3 proteins to relieve the inhibitory interaction between iRhom2 and mature ADAM17 (Grieve et al., 2017, Cavadas et al., 2017). As a consequence, ADAM17 becomes phosphorylated (Adrian, 2012). Moreover, the activation of STING can lead to ADAM17 activation and subsequent substrate shedding (Motani and Kosako, 2018). It is possible that upon HCMV entry into the cell, DNA sensing mechanisms could induce phosphorylation of iRhom2, releasing it from ADAM17, resulting in cleavage of cell surface substrates. One model for the mode of action UL148 and/or UL148D is that they could be acting on iRhom2 by impairing its regulatory role in ADAM17 expression, rather than effecting whole cell levels.

Understanding how UL148 and UL148D affect ADAM17 would be of interest as it could uncover key regulatory steps involved with ADAM17 biology. This is of importance as ADAM17 is a master regulator of inflammatory and developmental pathways such as TNFR1/2, EGFR and IL-6 signalling (Scheller et al., 2011).

6.2.3 Regulation of other ADAM17 substrates by HCMV

The downregulation of ADAM17 rationally leads to a prediction UL148/UL148D will impact the expression of additional cellular receptors, specifically those known to be modulated by the metallopeptidase. Over 80 substrates have been shown to be cleaved by ADAM17 (Moss and Minond, 2017). Indeed, proteomics comparing Merlin infected cells with ΔUL148 and ΔUL148D, showed that in addition to TNFR2, NRG1, MEGF10, and GFRA2 were downregulated. NRG1 is a known ADAM17 substrate, and therefore its upregulation may be dependent on ADAM17 downregulation. Although ICAM1 is upregulated on the surface of HCMV infected cells, this was independent of UL148/UL148D (Appendix) (Bentz et al., 2006).

The accumulation of certain ADAM17 substrates on the cell surface may not necessarily be compatible with virus persistence in vivo. The HCMV US12 family plays a major role in modulating the expression of immune ligands on the cell surface, those known to be ADAM17 substrates include B7-H6, MICA, MICB, TWEAK receptor, JAM3, ALCAM, SDC4 and ICOSL (Fielding et al., 2017). Thus, a complex scenario emerges in a HCMV infected cell where certain ADAM17 substrates are permitted to the surface (such as TNFR2, TNFR1 and NRG1), whereas other molecules with distinct immune functions are prevented from accumulation by the US12 genes family and potentially other HCMV immunevasins. Even further complexity is introduced by the upregulation of ADAM10 on HCMV infected cells (Fielding et al., 2014, Weekes et al., 2014), which can cleave a number of the same targets as ADAM17. HCMV infects an exceptionally wide range of cell types in vivo and ADAM17 expression is ubiquitous. HCMV UL148/UL148D can be

expected to impact on additional cell-specific immune and inflammatory pathways regulated by ADAM17 in endothelial cells, dendritic cells, macrophages and other cell types.

6.2.4 Effect of HCMV on TNF induced cell death

TNF was shown to induce apoptosis in HCMV infected cells. This in itself is an important finding as uninfected fibroblasts treated with TNF did not undergo apoptosis. This suggests that the cellular mechanisms that prevent TNF induced apoptosis in a healthy cell may be impaired during HCMV infection. Indeed, proteomics shows that cIAP is reduced during a lytic infection (Weekes et al., 2014), which could reflect a host response of increased sensitivity to apoptosis inducing molecules during infection.

Whilst TNF was able to kill Merlin infected cells, when UL148 and UL148D were deleted from the virus, infected cells were less susceptible to TNF induced apoptosis. This result could be predicted as ΔUL148/UL148D cells have less surface TNFR1, consistent with an inverse correlation between the amount of TNFR1 and susceptibility to TNF induced apoptosis. Another contributory factor could be that sTNFR2 from UL148/UL148D infected cells can bind to TNF and prevent binding to membrane bound TNFR1/2. As the presence of TNFR1 was increasing the sensitivity of cells to TNF induced apoptosis, this is counterintuitive. Why does the virus maintain TNFR1 in a lytic infection if it increases apoptosis? It is possible that the host induces the increase in TNFR2 at the mRNA level, and that this is beneficial for the host in clearance of virally infected cells. On macrophages, cellular upregulation of TNFR2 sensitizes cells to TNF induced necroptosis (Siegmund et al., 2016). This could act as an alternative death pathway that bypasses the inhibition of caspase pathways by UL36 (McCormick et al., 2010). This seems unlikely as HCMV has evolved many mechanisms to downregulate receptors that induce apoptosis such as FAS and TRAIL-R1/R2 (Seirafian et al., 2014, Smith et al., 2013), and if TNFR2 was a threat to infected cells then the virus may have evolved mechanisms to subvert this. The relevance of TNFR1/2 in HCMV infection may be uncovered in cells of the myeloid lineage. Further work is needed to assess the functional significance of these receptors including the study of HCMV infected DCs, where TNFR1/2 signalling differentially regulate DC maturation and survival (Maney et al., 2014).

Another possibility is that the dose of TNF used was too high, therefore any activity of mTNF of TNFR2, could have been masked by an overwhelming apoptotic signal through TNFR1. A dose response incorporating lower doses of TNF would be important for future studies. An important consideration is that TNF can bind to both receptors, but it is

generally considered that signalling is more efficient through TNFR1, due to an increased binding affinity (Grell et al., 1998). To identify the role of TNFR2 here, specific TNF mutants that only activate TNFR2 or agonistic antibodies could be used to rescue TNF induced apoptosis. These have been shown to increase activation of TNFR2 without affecting TNFR1 and would allow any affects to be attributed to one or other receptor (Fischer et al., 2017, Nguyen and Ehrenstein, 2016).

6.2.5 Effect of HCMV on cytokine production

HCMV infection results in a reduction in constitutive cytokine production. CCL2 production by fibroblasts was substantially impaired. A previous study showed that HCMV infection increased CCL2 mRNA and protein within the supernatant, though different cells (MRC-5), virus (low MOI AD169) and cell culture media were used (Hamilton et al., 2013). CCL2 is a chemoattractant and whilst it was suggested that increased CCL2 may allow for monocyte attraction and viral dissemination, the data in Chapter 5 would suggest that during replication, CCL2 production is prevented. IL-8 levels were similar to those in mock infected cells. This contrasts with other studies that have assessed the HCMV secretome. In these studies IL-8 was one of many cytokines increased compared to uninfected cells (Dumortier et al., 2008, Botto et al., 2011, Mason et al., 2012). These studies all showed a different cytokine profile which can be attributed to differences in cell type (endothelial cells), HCMV strain (VR1814) and culture methods. I showed that in fibroblasts, in a productive infection, cytokine levels did not increase. In HF-TERT cells infected with Merlin, IL-6 and IL-8 mRNA has been reported by others to increase after HCMV infection compared to uninfected cells (Tirosh et al., 2015). This also occurred upon treatment of cells with UV inactivated virus indicating that the host cell probably releases these cytokines as an intrinsic response to infection. It has been suggested that IL-8 production by HCMV infected cells may aid in viral dissemination by infection of neutrophils, which are chemotactically attracted to cells releasing IL-8 (Costa et al., 2013).

Merlin infected cells did not increase cytokine production upon TNF treatment and it was expected that ΔUL148/UL148D infected cells would result in reduced cytokine production upon TNF challenge due to the reduced expression of TNFR1/2, but the opposite was observed. IL-8 and CCL-2 production were increased in ΔUL148/UL148D infected cells. This would indicate that UL148 and UL148D have a role in preventing TNF signalling or cytokine release independent of their effect on TNFR1/2. Whilst there is less TNFR1/2 on the surface of ΔUL148/UL148D infected cells as assessed by flow cytometry, enough receptors could still be present on the surface of the cells before cleavage by ADAM17. Only a few seconds of TNF exposure can activate the NF-kB pathway in HeLa cells (Lee

et al., 2016). In a similar experimental setup to the one I performed, in which TNF treated HCMV infected fibroblasts were assessed, TNF induced IL-8, IL-6, CCL-2 and CXCL1 mRNA were reduced compared to uninfected cells (Jarvis et al., 2006). Immunofluorescence showed that impairment of IL-8 production by HCMV infected cells occurred with the low passage strain TR and high passage AD169-ATCC, which lacks UL148 and UL148D, though this study did not assess the release of IL-8. This suggests that the impairment of HCMV infected cells to produce IL-8 could be dependent on a conserved viral gene present in all HCMV strains or reflect the diversion of cellular resources that occurs in a lytic infection to accommodate virus replication. However, the release of IL-8 from the cell could still be influenced by other genes such as UL148 and UL148D as demonstrated here.

Of all the cytokines assessed, RANTES was the only one which was not detectable in HCMV supernatant, across all conditions. This could be explained by other HCMV genes which have been shown to target RANTES such as miRNA-UL148D (encoded by the UL150 ORF) and US28 (Kim et al., 2012, Billstrom et al., 1999). This in theory would result in reduced homing of lymphocytes to virally infected cells. Prevention of RANTES release, even following TNF treatment suggests that RANTES is an important chemokine for inhibition by HCMV. Clinically this could be important as defects in RANTES have been reported to result in impaired responses to chronic viral infections (Crawford et al., 2011). The cytokine multiplex presented in chapter 5 would suggest that IL-8 and other TNF induced cytokines are subject to suppression in HCMV infected fibroblasts, and that UL148/UL148D may be responsible for this.

One explanation for the inability of Merlin infected fibroblasts to increase cytokine production upon TNF challenge is that elements of NF-κB signalling are impaired and that deleting UL148/UL148D could have released this suppression. Data concerning NF-κB and HCMV infections is mixed. Some studies have shown that HCMV increased NF-κB activation. Other proteins have been shown to impair NF-κB signalling such as pp65, UL26 and IE1 (Hancock and Nelson, 2017). Proteomic analysis and Western blotting suggests reduced NF-κB in HCMV infected cells (Weekes et al., 2014). Pathway analysis suggested that other TNF induced pathways were also affected such as MAPK signalling. HCMV impairs interferon signalling by a number of mechanisms, such as downregulating IRFs, and regulating interferon receptors (Marshall and Geballe, 2009). This implies that HCMV employs multiple strategies to inhibit the response to inflammatory cytokines such as TNF and IFN.

When Toledo infected cells were treated with TNF, there was an increase in NF-κB expression as with uninfected cells (Montag et al., 2011). This suggests that the impairment of cytokine production from TNF treated HCMV infected cells may be due to an overall impairment in cytokine release, rather than an impairment in TNF signalling. TNF treatment normally results in degradation of IκBα, which allows NF-κB to enter the nucleus. TNF caused IκBα degradation in HCMV infected cells, further suggesting that if UL148/UL148D are affecting TNF signalling, then this is not occurring via the NF-κB pathway (Le et al., 2011). This contrasted with previous data which showed that HCMV was impairing TNF induced IκBα degradation (Jarvis et al., 2006). Regardless of what occurs at the signalling level, functionally this thesis showed that TNF induced cytokine production is certainly impaired during a HCMV lytic infection.

6.3 Future directions

To assess functionally how TNFR1/2 could affect HCMV infected dendritic cells, a co-culture assay could be utilised to infect DCs (Murrell et al., 2017). This could be followed by treatment with TNF and subsequent phenotyping for maturation markers and assessment of cell death. The mechanisms by which ADAM17 molecules are trafficked and regulated are complex. Further work assessing how it is downregulated by HCMV would require the use of tagged UL148 and UL148D. SILAC-IP coupled with mass spectrometry would show the proteins to which UL148 and UL148D binding within the cell. Co-IP experiments with iRhom1 and iRhom2 would show if UL148 and UL148D interfere with the trafficking of ADAM17. To assess what other substrates are regulated by HCMV, plasma membrane profiling could be performed on ΔUL148/UL148D infected cells and compared to ΔUL148/UL148D infected cells treated with D1(A12). Flow cytometry showed that TNFR1/2 were recovered on the latter, and therefore it would be expected that other ADAM17 substrates would be recovered as well. This could also identify novel ADAM17 substrates. Finally, a comprehensive secretomics study could be performed to uncover how HCMV infection alters the level of soluble molecules and the cytokine mileau during a lytic infection, but also in response to cytokine treatment.

6.4 Conclusions

This thesis firstly aimed to identify novel HCMV-encoded genes that could impair T-cell degranulation. My research achieved this by identifying UL19 and genes within the RL10-UL1 region in controlling activation of CD8+ T-cells against HCMV infected cells.

Whilst our lab has historically investigated HCMV encoded NK evasion genes, this work adds to a growing body of evidence that suggests that immune evasion mechanisms may be applicable to both T and NK cells. UL135 and UL148 both influence T and NK cells. US12-21 has been shown to degrade both T and NK cell activating ligands. UL16 and UL18 likely impact T-cells that express their respective receptors; NKG2D and LIR1. Flow cytometry also showed D9-VTE uniformly expressed DNAM-1 (Appendix), therefore UL141 could target activation of this T-cell lines. This work showed that UL19 and RL10-UL1 can regulate T-cell activation and we have data showing that these genes suppress NK cell degranulation too (Dr Ceri Fielding and Dr Rebecca Aicheler). Therefore, evidence is mounting suggesting that immune evasion genes have converged on receptors and mechanisms that impair both NK cells and CD8+ T cells. Genome-wide DNA methylation analyses revealed a strikingly similar pattern of DNA methylation between expanded NK and CD8+T cells from HCMV+ donors (Schlums et al., 2015). This showed CD8+ T cells and adaptive NK cells share pathogen driven differentiation pathways, that help these cells to control HCMV infection.

The second aim was also achieved as the genes responsible for TNFR2 upregulation were identified. UL148 and UL148D were shown to upregulate TNFR2 by synergistically downregulating surface ADAM17 and preventing the cleavage of TNFR2 (and TNFR1) by ADAM17. UL148/UL148D were shown to impair the maturation of ADAM17. The efficiency with which ADAM17 is downregulated suggests there is a clear benefit to the virus to not having this protein on the cell surface over the course of the lytic cycle.

Thirdly the response of HCMV infected cells to TNF was assessed. The presence of UL148/UL148D made cells more sensitive to TNF induced apoptosis, which was attributed to TNFR1. Cytokine production showed that these genes have an anti-inflammatory effect by inhibiting IL-8 production upon TNF challenge. This suggests that UL148/UL148D may be involved with regulating elements of TNF signalling or cytokine release independent of their effect on ADAM17. The control of ADAM17 surface expression is likely to affect how HCMV infected cells respond to immune cells and inflammatory cytokines given that ADAM17 is responsible for controlling multiple cytokines, cytokine receptors, adhesion molecules and immune cell receptors.

References

ABCAM. 2018. *Anti-TNF Receptor II antibody [EPR1653] (HRP) (ab200006)* [Online]. Available: http://www.abcam.com/tnf-receptor-ii-antibody-epr1653-hrp-ab200006.html [Accessed 09.05.2018].

ADRAIN, C., ZETTL, M., CHRISTOVA, Y., TAYLOR, N. & FREEMAN, M. 2012. Tumor necrosis factor signaling requires iRhom2 to promote trafficking and activation of TACE. *Science,* 335**,** 225-8.

AHLQVIST, J. & MOCARSKI, E. 2011. Cytomegalovirus UL103 controls virion and dense body egress. *J Virol,* 85**,** 5125-35.

AHN, K., GRUHLER, A., GALOCHA, B., JONES, T. R., WIERTZ, E. J., PLOEGH, H. L., PETERSON, P. A., YANG, Y. & FRUH, K. 1997. The ER-luminal domain of the HCMV glycoprotein US6 inhibits peptide translocation by TAP. *Immunity,* 6**,** 613-21.

AICHELER, R. 2005. *Immunomodulation of the cellular immune response by human cytomegalovirus.* Ph.D, Cardiff University.

AKTER, P., CUNNINGHAM, C., MCSHARRY, B. P., DOLAN, A., ADDISON, C., DARGAN, D. J., HASSAN-WALKER, A. F., EMERY, V. C., GRIFFITHS, P. D., WILKINSON, G. W. & DAVISON, A. J. 2003. Two novel spliced genes in human cytomegalovirus. *J Gen Virol,* 84**,** 1117-22.

ALI, T., KAITHA, S., MAHMOOD, S., FTESI, A., STONE, J. & BRONZE, M. S. 2013. Clinical use of anti-TNF therapy and increased risk of infections. *Drug Healthc Patient Saf,* 5**,** 79-99.

ALWINE, J. C. 2012. The human cytomegalovirus assembly compartment: a masterpiece of viral manipulation of cellular processes that facilitates assembly and egress. *PLoS Pathog,* 8**,** e1002878.

AMERES, S., MAUTNER, J., SCHLOTT, F., NEUENHAHN, M., BUSCH, D. H., PLACHTER, B. & MOOSMANN, A. 2013. Presentation of an immunodominant immediate-early CD8+ T cell epitope resists human cytomegalovirus immunoevasion. *PLoS Pathog,* 9**,** e1003383.

ANTONIOU, A. N., POWIS, S. J. & ELLIOTT, T. 2003. Assembly and export of MHC class I peptide ligands. *Curr Opin Immunol,* 15**,** 75-81.

ANTROBUS, R. D., KHAN, N., HISLOP, A. D., MONTAMAT-SICOTTE, D., GARNER, L. I., RICKINSON, A. B., MOSS, P. A. & WILLCOX, B. E. 2005. Virus-specific cytotoxic T lymphocytes differentially express cell-surface leukocyte immunoglobulin-like receptor-1, an inhibitory receptor for class I major histocompatibility complex molecules. *J Infect Dis,* 191**,** 1842-53.

ASHIRU, O., BENNETT, N. J., BOYLE, L. H., THOMAS, M., TROWSDALE, J. & WILLS, M. R. 2009. NKG2D ligand MICA is retained in the cis-Golgi apparatus by human cytomegalovirus protein UL142. *J Virol,* 83**,** 12345-54.

ASHKENAZI, A. & DIXIT, V. M. 1998. Death receptors: signaling and modulation. *Science,* 281**,** 1305-8.

BAILLIE, J., SAHLENDER, D. A. & SINCLAIR, J. H. 2003. Human cytomegalovirus infection inhibits tumor necrosis factor alpha (TNF-alpha)

signaling by targeting the 55-kilodalton TNF-alpha receptor. *J Virol,* 77**,** 7007-16.
BANCHEREAU, J., BRIERE, F., CAUX, C., DAVOUST, J., LEBECQUE, S., LIU, Y. J., PULENDRAN, B. & PALUCKA, K. 2000. Immunobiology of dendritic cells. *Annu Rev Immunol,* 18**,** 767-811.
BANNER, D. W., D'ARCY, A., JANES, W., GENTZ, R., SCHOENFELD, H. J., BROGER, C., LOETSCHER, H. & LESSLAUER, W. 1993. Crystal structure of the soluble human 55 kd TNF receptor-human TNF beta complex: implications for TNF receptor activation. *Cell,* 73**,** 431-45.
BAREL, M. T., RESSING, M., PIZZATO, N., VAN LEEUWEN, D., LE BOUTEILLER, P., LENFANT, F. & WIERTZ, E. J. 2003. Human cytomegalovirus-encoded US2 differentially affects surface expression of MHC class I locus products and targets membrane-bound, but not soluble HLA-G1 for degradation. *J Immunol,* 171**,** 6757-65.
BARNES, P. D. & GRUNDY, J. E. 1992. Down-regulation of the class I HLA heterodimer and beta 2-microglobulin on the surface of cells infected with cytomegalovirus. *J Gen Virol,* 73 (Pt 9)**,** 2395-403.
BAUER, S., GROH, V., WU, J., STEINLE, A., PHILLIPS, J. H., LANIER, L. L. & SPIES, T. 1999. Activation of NK cells and T cells by NKG2D, a receptor for stress-inducible MICA. *Science,* 285**,** 727-9.
BECK, K., MEYER-KONIG, U., WEIDMANN, M., NERN, C. & HUFERT, F. T. 2003. Human cytomegalovirus impairs dendritic cell function: a novel mechanism of human cytomegalovirus immune escape. *Eur J Immunol,* 33**,** 1528-38.
BECK, S. & BARRELL, B. G. 1988. Human cytomegalovirus encodes a glycoprotein homologous to MHC class-I antigens. *Nature,* 331**,** 269-72.
BEERSMA, M. F., BIJLMAKERS, M. J. & PLOEGH, H. L. 1993. Human cytomegalovirus down-regulates HLA class I expression by reducing the stability of class I H chains. *J Immunol,* 151**,** 4455-64.
BENEDICT, C. A., BANKS, T. A., SENDEROWICZ, L., KO, M., BRITT, W. J., ANGULO, A., GHAZAL, P. & WARE, C. F. 2001. Lymphotoxins and cytomegalovirus cooperatively induce interferon-beta, establishing host-virus détente. *Immunity,* 15**,** 617-26.
BENEDICT, C. A., BUTROVICH, K. D., LURAIN, N. S., CORBEIL, J., ROONEY, I., SCHNEIDER, P., TSCHOPP, J. & WARE, C. F. 1999. Cutting edge: a novel viral TNF receptor superfamily member in virulent strains of human cytomegalovirus. *J Immunol,* 162**,** 6967-70.
BENTZ, G. L., JARQUIN-PARDO, M., CHAN, G., SMITH, M. S., SINZGER, C. & YUROCHKO, A. D. 2006. Human cytomegalovirus (HCMV) infection of endothelial cells promotes naive monocyte extravasation and transfer of productive virus to enhance hematogenous dissemination of HCMV. *J Virol,* 80**,** 11539-55.
BEZIAT, V., DALGARD, O., ASSELAH, T., HALFON, P., BEDOSSA, P., BOUDIFA, A., HERVIER, B., THEODOROU, I., MARTINOT, M., DEBRE, P., BJORKSTROM, N. K., MALMBERG, K. J., MARCELLIN, P. & VIEILLARD, V. 2012. CMV drives clonal expansion of NKG2C+ NK cells expressing self-specific KIRs in chronic hepatitis patients. *Eur J Immunol,* 42**,** 447-57.
BIGDA, J., BELETSKY, I., BRAKEBUSCH, C., VARFOLOMEEV, Y., ENGELMANN, H., BIGDA, J., HOLTMANN, H. & WALLACH, D. 1994.

Dual role of the p75 tumor necrosis factor (TNF) receptor in TNF cytotoxicity. *J Exp Med,* 180**,** 445-60.

BILLSTROM, M. A., LEHMAN, L. A. & SCOTT WORTHEN, G. 1999. Depletion of extracellular RANTES during human cytomegalovirus infection of endothelial cells. *Am J Respir Cell Mol Biol,* 21**,** 163-7.

BIRON, C. A., BYRON, K. S. & SULLIVAN, J. L. 1989. Severe herpesvirus infections in an adolescent without natural killer cells. *N Engl J Med,* 320**,** 1731-5.

BLACK, R. A., RAUCH, C. T., KOZLOSKY, C. J., PESCHON, J. J., SLACK, J. L., WOLFSON, M. F., CASTNER, B. J., STOCKING, K. L., REDDY, P., SRINIVASAN, S., NELSON, N., BOIANI, N., SCHOOLEY, K. A., GERHART, M., DAVIS, R., FITZNER, J. N., JOHNSON, R. S., PAXTON, R. J., MARCH, C. J. & CERRETTI, D. P. 1997. A metalloproteinase disintegrin that releases tumour-necrosis factor-alpha from cells. *Nature,* 385**,** 729-33.

BORCHERS, S., BREMM, M., LEHRNBECHER, T., DAMMANN, E., PABST, B., WOLK, B., ESSER, R., YILDIZ, M., EDER, M., STADLER, M., BADER, P., MARTIN, H., JARISCH, A., SCHNEIDER, G., KLINGEBIEL, T., GANSER, A., WEISSINGER, E. M. & KOEHL, U. 2012. Sequential anti-cytomegalovirus response monitoring may allow prediction of cytomegalovirus reactivation after allogeneic stem cell transplantation. *PLoS One,* 7**,** e50248.

BORYSIEWICZ, L. K., MORRIS, S., PAGE, J. D. & SISSONS, J. G. 1983. Human cytomegalovirus-specific cytotoxic T lymphocytes: requirements for in vitro generation and specificity. *Eur J Immunol,* 13**,** 804-9.

BOTTO, S., STREBLOW, D. N., DEFILIPPIS, V., WHITE, L., KREKLYWICH, C. N., SMITH, P. P. & CAPOSIO, P. 2011. IL-6 in human cytomegalovirus secretome promotes angiogenesis and survival of endothelial cells through the stimulation of survivin. *Blood,* 117**,** 352-61.

BOURGEOIS, C., ROCHA, B. & TANCHOT, C. 2002. A role for CD40 expression on CD8+ T cells in the generation of CD8+ T cell memory. *Science,* 297**,** 2060-3.

BOYCE, B. F. & XING, L. 2007. Biology of RANK, RANKL, and osteoprotegerin. *Arthritis Res Ther,* 9 Suppl 1**,** S1.

BRADLEY, A. J., LURAIN, N. S., GHAZAL, P., TRIVEDI, U., CUNNINGHAM, C., BALUCHOVA, K., GATHERER, D., WILKINSON, G. W., DARGAN, D. J. & DAVISON, A. J. 2009. High-throughput sequence analysis of variants of human cytomegalovirus strains Towne and AD169. *J Gen Virol,* 90**,** 2375-80.

BRANDT, C. S., BARATIN, M., YI, E. C., KENNEDY, J., GAO, Z., FOX, B., HALDEMAN, B., OSTRANDER, C. D., KAIFU, T., CHABANNON, C., MORETTA, A., WEST, R., XU, W., VIVIER, E. & LEVIN, S. D. 2009. The B7 family member B7-H6 is a tumor cell ligand for the activating natural killer cell receptor NKp30 in humans. *J Exp Med,* 206**,** 1495-503.

BRAUD, V., JONES, E. Y. & MCMICHAEL, A. 1997. The human major histocompatibility complex class Ib molecule HLA-E binds signal sequence-derived peptides with primary anchor residues at positions 2 and 9. *Eur J Immunol,* 27**,** 1164-9.

BRAUD, V. M., ALLAN, D. S., O'CALLAGHAN, C. A., SÖDERSTRÖM, K., D'ANDREA, A., OGG, G. S., LAZETIC, S., YOUNG, N. T., BELL, J. I.,

PHILLIPS, J. H., LANIER, L. L. & MCMICHAEL, A. J. 1998a. HLA-E binds to natural killer cell receptors CD94/NKG2A, B and C. *Nature,* 391**,** 795-9.
BRAUD, V. M., ALLAN, D. S., WILSON, D. & MCMICHAEL, A. J. 1998b. TAP- and tapasin-dependent HLA-E surface expression correlates with the binding of an MHC class I leader peptide. *Curr Biol,* 8**,** 1-10.
BROWNE, H., SMITH, G., BECK, S. & MINSON, T. 1990. A complex between the MHC class I homologue encoded by human cytomegalovirus and beta 2 microglobulin. *Nature,* 347**,** 770-2.
BRUNO, L., CORTESE, M., MONDA, G., GENTILE, M., CALO, S., SCHIAVETTI, F., ZEDDA, L., CATTANEO, E., PICCIOLI, D., SCHAEFER, M., NOTOMISTA, E., MAIONE, D., CARFI, A., MEROLA, M. & UEMATSU, Y. 2016. Human cytomegalovirus pUL10 interacts with leukocytes and impairs TCR-mediated T-cell activation. *Immunol Cell Biol,* 94**,** 849-860.
CABAL-HIERRO, L. & LAZO, P. S. 2012. Signal transduction by tumor necrosis factor receptors. *Cell Signal,* 24**,** 1297-305.
CANNON, M. J., HYDE, T. B. & SCHMID, D. S. 2011. Review of cytomegalovirus shedding in bodily fluids and relevance to congenital cytomegalovirus infection. *Rev Med Virol,* 21**,** 240-55.
CARPENTIER, I., COORNAERT, B. & BEYAERT, R. 2004. Function and regulation of tumor necrosis factor receptor type 2. *Curr Med Chem,* 11**,** 2205-12.
CARROLL, M. C., KATZMAN, P., ALICOT, E. M., KOLLER, B. H., GERAGHTY, D. E., ORR, H. T., STROMINGER, J. L. & SPIES, T. 1987. Linkage map of the human major histocompatibility complex including the tumor necrosis factor genes. *Proc Natl Acad Sci U S A,* 84**,** 8535-9.
CARSWELL, E. A., OLD, L. J., KASSEL, R. L., GREEN, S., FIORE, N. & WILLIAMSON, B. 1975. An endotoxin-induced serum factor that causes necrosis of tumors. *Proc Natl Acad Sci U S A,* 72**,** 3666-70.
CAVADAS, M., OIKONOMIDI, I., GASPAR, C. J., BURBRIDGE, E., BADENES, M., FELIX, I., BOLADO, A., HU, T., BILECK, A., GERNER, C., DOMINGOS, P. M., VON KRIEGSHEIM, A. & ADRAIN, C. 2017. Phosphorylation of iRhom2 Controls Stimulated Proteolytic Shedding by the Metalloprotease ADAM17/TACE. *Cell Rep,* 21**,** 745-757.
CHA, S. S., SUNG, B. J., KIM, Y. A., SONG, Y. L., KIM, H. J., KIM, S., LEE, M. S. & OH, B. H. 2000. Crystal structure of TRAIL-DR5 complex identifies a critical role of the unique frame insertion in conferring recognition specificity. *J Biol Chem,* 275**,** 31171-7.
CHA, T. A., TOM, E., KEMBLE, G. W., DUKE, G. M., MOCARSKI, E. S. & SPAETE, R. R. 1996. Human cytomegalovirus clinical isolates carry at least 19 genes not found in laboratory strains. *J Virol,* 70**,** 78-83.
CHALUPNY, N. J., REIN-WESTON, A., DOSCH, S. & COSMAN, D. 2006. Down-regulation of the NKG2D ligand MICA by the human cytomegalovirus glycoprotein UL142. *Biochem Biophys Res Commun,* 346**,** 175-81.
CHAN, C. J., SMYTH, M. J. & MARTINET, L. 2014. Molecular mechanisms of natural killer cell activation in response to cellular stress. *Cell Death Differ,* 21**,** 5-14.
CHAN, G., NOGALSKI, M. T. & YUROCHKO, A. D. 2009. Activation of EGFR on monocytes is required for human cytomegalovirus entry and mediates cellular motility. *Proc Natl Acad Sci U S A,* 106**,** 22369-74.

CHAPLIN, D. D. 2010. Overview of the immune response. *J Allergy Clin Immunol,* 125**,** S3-23.

CHAPMAN, T. L., HEIKEMAN, A. P. & BJORKMAN, P. J. 1999. The inhibitory receptor LIR-1 uses a common binding interaction to recognize class I MHC molecules and the viral homolog UL18. *Immunity,* 11**,** 603-13.

CHARPAK-AMIKAM, Y., KUBSCH, T., SEIDEL, E., OIKNINE-DJIAN, E., CAVALETTO, N., YAMIN, R., SCHMIEDEL, D., WOLF, D., GRIBAUDO, G., MESSERLE, M., CICIN-SAIN, L. & MANDELBOIM, O. 2017. Human cytomegalovirus escapes immune recognition by NK cells through the downregulation of B7-H6 by the viral genes US18 and US20. *Sci Rep,* 7**,** 8661.

CHEE, M. S., BANKIER, A. T., BECK, S., BOHNI, R., BROWN, C. M., CERNY, R., HORSNELL, T., HUTCHISON, C. A., 3RD, KOUZARIDES, T., MARTIGNETTI, J. A. & ET AL. 1990. Analysis of the protein-coding content of the sequence of human cytomegalovirus strain AD169. *Curr Top Microbiol Immunol,* 154**,** 125-69.

CHEN, D. H., JIANG, H., LEE, M., LIU, F. & ZHOU, Z. H. 1999. Three-dimensional visualization of tegument/capsid interactions in the intact human cytomegalovirus. *Virology,* 260**,** 10-6.

CHEN, L. & FLIES, D. B. 2013. Molecular mechanisms of T cell co-stimulation and co-inhibition. *Nat Rev Immunol,* 13**,** 227-42.

CHEUNG, T. C., HUMPHREYS, I. R., POTTER, K. G., NORRIS, P. S., SHUMWAY, H. M., TRAN, B. R., PATTERSON, G., JEAN-JACQUES, R., YOON, M., SPEAR, P. G., MURPHY, K. M., LURAIN, N. S., BENEDICT, C. A. & WARE, C. F. 2005. Evolutionarily divergent herpesviruses modulate T cell activation by targeting the herpesvirus entry mediator cosignaling pathway. *Proc Natl Acad Sci U S A,* 102**,** 13218-23.

CHIOU, S. H., LIU, J. H., HSU, W. M., CHEN, S. S., CHANG, S. Y., JUAN, L. J., LIN, J. C., YANG, Y. T., WONG, W. W., LIU, C. Y., LIN, Y. S., LIU, W. T. & WU, C. W. 2001. Up-regulation of Fas ligand expression by human cytomegalovirus immediate-early gene product 2: a novel mechanism in cytomegalovirus-induced apoptosis in human retina. *J Immunol,* 167**,** 4098-103.

CHIOU, S. H., YANG, Y. P., LIN, J. C., HSU, C. H., JHANG, H. C., YANG, Y. T., LEE, C. H., HO, L. L., HSU, W. M., KU, H. H., CHEN, S. J., CHEN, S. S., CHANG, M. D., WU, C. W. & JUAN, L. J. 2006. The immediate early 2 protein of human cytomegalovirus (HCMV) mediates the apoptotic control in HCMV retinitis through up-regulation of the cellular FLICE-inhibitory protein expression. *J Immunol,* 177**,** 6199-206.

CHOU, S. 2008. Cytomegalovirus UL97 mutations in the era of ganciclovir and maribavir. *Rev Med Virol,* 18**,** 233-46.

COLBERG-POLEY, A. M., SANTOMENNA, L. D., HARLOW, P. P., BENFIELD, P. A. & TENNEY, D. J. 1992. Human cytomegalovirus US3 and UL36-38 immediate-early proteins regulate gene expression. *J Virol,* 66**,** 95-105.

COMPTON, T., NOWLIN, D. M. & COOPER, N. R. 1993. Initiation of human cytomegalovirus infection requires initial interaction with cell surface heparan sulfate. *Virology,* 193**,** 834-41.

CORRALES-AGUILAR, E., TRILLING, M., HUNOLD, K., FIEDLER, M., LE, V. T., REINHARD, H., EHRHARDT, K., MERCE-MALDONADO, E., ALIYEV, E., ZIMMERMANN, A., JOHNSON, D. C. & HENGEL, H. 2014. Human

cytomegalovirus Fcgamma binding proteins gp34 and gp68 antagonize Fcgamma receptors I, II and III. *PLoS Pathog,* 10**,** e1004131.
COSMAN, D., FANGER, N., BORGES, L., KUBIN, M., CHIN, W., PETERSON, L. & HSU, M. L. 1997. A novel immunoglobulin superfamily receptor for cellular and viral MHC class I molecules. *Immunity,* 7**,** 273-82.
COSMAN, D., MÜLLBERG, J., SUTHERLAND, C. L., CHIN, W., ARMITAGE, R., FANSLOW, W., KUBIN, M. & CHALUPNY, N. J. 2001. ULBPs, novel MHC class I-related molecules, bind to CMV glycoprotein UL16 and stimulate NK cytotoxicity through the NKG2D receptor. *Immunity,* 14**,** 123-33.
COSTA, H., NASCIMENTO, R., SINCLAIR, J. & PARKHOUSE, R. M. 2013. Human cytomegalovirus gene UL76 induces IL-8 expression through activation of the DNA damage response. *PLoS Pathog,* 9**,** e1003609.
CRAIG, J. M., MACAULEY, J. C., WELLER, T. H. & WIRTH, P. 1957. Isolation of intranuclear inclusion producing agents from infants with illnesses resembling cytomegalic inclusion disease. *Proc Soc Exp Biol Med,* 94**,** 4-12.
CRAWFORD, A., ANGELOSANTO, J. M., NADWODNY, K. L., BLACKBURN, S. D. & WHERRY, E. J. 2011. A role for the chemokine RANTES in regulating CD8 T cell responses during chronic viral infection. *PLoS Pathog,* 7**,** e1002098.
CRISA, L., MCMASTER, M. T., ISHII, J. K., FISHER, S. J. & SALOMON, D. R. 1997. Identification of a thymic epithelial cell subset sharing expression of the class Ib HLA-G molecule with fetal trophoblasts. *J Exp Med,* 186**,** 289-98.
CURTSINGER, J. M. & MESCHER, M. F. 2010. Inflammatory cytokines as a third signal for T cell activation. *Curr Opin Immunol,* 22**,** 333-40.
DARGAN, D. J., DOUGLAS, E., CUNNINGHAM, C., JAMIESON, F., STANTON, R. J., BALUCHOVA, K., MCSHARRY, B. P., TOMASEC, P., EMERY, V. C., PERCIVALLE, E., SARASINI, A., GERNA, G., WILKINSON, G. W. & DAVISON, A. J. 2010. Sequential mutations associated with adaptation of human cytomegalovirus to growth in cell culture. *J Gen Virol,* 91**,** 1535-46.
DAS, S., VASANJI, A. & PELLETT, P. E. 2007. Three-dimensional structure of the human cytomegalovirus cytoplasmic virion assembly complex includes a reoriented secretory apparatus. *J Virol,* 81**,** 11861-9.
DAVISON, A. J., AKTER, P., CUNNINGHAM, C., DOLAN, A., ADDISON, C., DARGAN, D. J., HASSAN-WALKER, A. F., EMERY, V. C., GRIFFITHS, P. D. & WILKINSON, G. W. 2003a. Homology between the human cytomegalovirus RL11 gene family and human adenovirus E3 genes. *J Gen Virol,* 84**,** 657-63.
DAVISON, A. J., DOLAN, A., AKTER, P., ADDISON, C., DARGAN, D. J., ALCENDOR, D. J., MCGEOCH, D. J. & HAYWARD, G. S. 2003b. The human cytomegalovirus genome revisited: comparison with the chimpanzee cytomegalovirus genome. *J Gen Virol,* 84**,** 17-28.
DE LA CÁMARA, R. 2016. CMV in Hematopoietic Stem Cell Transplantation. *Mediterranean Journal of Hematology and Infectious Diseases,* 8**,** e2016031.
DE TOGNI, P., GOELLNER, J., RUDDLE, N. H., STREETER, P. R., FICK, A., MARIATHASAN, S., SMITH, S. C., CARLSON, R., SHORNICK, L. P., STRAUSS-SCHOENBERGER, J. & ET AL. 1994. Abnormal development

of peripheral lymphoid organs in mice deficient in lymphotoxin. *Science,* 264**,** 703-7.
DOLAN, A., CUNNINGHAM, C., HECTOR, R. D., HASSAN-WALKER, A. F., LEE, L., ADDISON, C., DARGAN, D. J., MCGEOCH, D. J., GATHERER, D., EMERY, V. C., GRIFFITHS, P. D., SINZGER, C., MCSHARRY, B. P., WILKINSON, G. W. & DAVISON, A. J. 2004. Genetic content of wild-type human cytomegalovirus. *J Gen Virol,* 85**,** 1301-12.
DOLLARD, S. C., GROSSE, S. D. & ROSS, D. S. 2007. New estimates of the prevalence of neurological and sensory sequelae and mortality associated with congenital cytomegalovirus infection. *Rev Med Virol,* 17**,** 355-63.
DOMBERNOWSKY, S. L., SAMSOE-PETERSEN, J., PETERSEN, C. H., INSTRELL, R., HEDEGAARD, A. M., THOMAS, L., ATKINS, K. M., AUCLAIR, S., ALBRECHTSEN, R., MYGIND, K. J., FROHLICH, C., HOWELL, M., PARKER, P., THOMAS, G. & KVEIBORG, M. 2015. The sorting protein PACS-2 promotes ErbB signalling by regulating recycling of the metalloproteinase ADAM17. *Nat Commun,* 6**,** 7518.
DUMORTIER, J., STREBLOW, D. N., MOSES, A. V., JACOBS, J. M., KREKLYWICH, C. N., CAMP, D., SMITH, R. D., ORLOFF, S. L. & NELSON, J. A. 2008. Human cytomegalovirus secretome contains factors that induce angiogenesis and wound healing. *J Virol,* 82**,** 6524-35.
DUNN, C., CHALUPNY, N. J., SUTHERLAND, C. L., DOSCH, S., SIVAKUMAR, P. V., JOHNSON, D. C. & COSMAN, D. 2003a. Human cytomegalovirus glycoprotein UL16 causes intracellular sequestration of NKG2D ligands, protecting against natural killer cell cytotoxicity. *J Exp Med,* 197**,** 1427-39.
DUNN, W., CHOU, C., LI, H., HAI, R., PATTERSON, D., STOLC, V., ZHU, H. & LIU, F. 2003b. Functional profiling of a human cytomegalovirus genome. *Proc Natl Acad Sci U S A,* 100**,** 14223-8.
DUSTIN, M. L. 2014. The immunological synapse. *Cancer Immunol Res,* 2**,** 1023-33.
ELDE, N. C., CHILD, S. J., EICKBUSH, M. T., KITZMAN, J. O., ROGERS, K. S., SHENDURE, J., GEBALLE, A. P. & MALIK, H. S. 2012. Poxviruses deploy genomic accordions to adapt rapidly against host antiviral defenses. *Cell,* 150**,** 831-41.
ELGUETA, R., BENSON, M. J., DE VRIES, V. C., WASIUK, A., GUO, Y. & NOELLE, R. J. 2009. Molecular mechanism and function of CD40/CD40L engagement in the immune system. *Immunol Rev,* 229**,** 152-72.
ENGEL, P., PEREZ-CARMONA, N., ALBA, M. M., ROBERTSON, K., GHAZAL, P. & ANGULO, A. 2011. Human cytomegalovirus UL7, a homologue of the SLAM-family receptor CD229, impairs cytokine production. *Immunol Cell Biol,* 89**,** 753-66.
ERICE, A. 1999. Resistance of human cytomegalovirus to antiviral drugs. *Clin Microbiol Rev,* 12**,** 286-97.
ESENSTEN, J. H., HELOU, Y. A., CHOPRA, G., WEISS, A. & BLUESTONE, J. A. 2016. CD28 Costimulation: From Mechanism to Therapy. *Immunity,* 44**,** 973-88.
FAHNESTOCK, M. L., JOHNSON, J. L., FELDMAN, R. M., NEVEU, J. M., LANE, W. S. & BJORKMAN, P. J. 1995. The MHC class I homolog encoded by human cytomegalovirus binds endogenous peptides. *Immunity,* 3**,** 583-90.

FARBER, D. L., YUDANIN, N. A. & RESTIFO, N. P. 2014. Human memory T cells: generation, compartmentalization and homeostasis. *Nat Rev Immunol,* 14**,** 24-35.

FAUSTMAN, D. & DAVIS, M. 2010. TNF receptor 2 pathway: drug target for autoimmune diseases. *Nat Rev Drug Discov,* 9**,** 482-93.

FEUCHTINGER, T., OPHERK, K., BETHGE, W. A., TOPP, M. S., SCHUSTER, F. R., WEISSINGER, E. M., MOHTY, M., OR, R., MASCHAN, M., SCHUMM, M., HAMPRECHT, K., HANDGRETINGER, R., LANG, P. & EINSELE, H. 2010. Adoptive transfer of pp65-specific T cells for the treatment of chemorefractory cytomegalovirus disease or reactivation after haploidentical and matched unrelated stem cell transplantation. *Blood,* 116**,** 4360-7.

FIELDING, C. A., AICHELER, R., STANTON, R. J., WANG, E. C., HAN, S., SEIRAFIAN, S., DAVIES, J., MCSHARRY, B. P., WEEKES, M. P., ANTROBUS, P. R., PROD'HOMME, V., BLANCHET, F. P., SUGRUE, D., CUFF, S., ROBERTS, D., DAVISON, A. J., LEHNER, P. J., WILKINSON, G. W. & TOMASEC, P. 2014. Two novel human cytomegalovirus NK cell evasion functions target MICA for lysosomal degradation. *PLoS Pathog,* 10**,** e1004058.

FIELDING, C. A., WEEKES, M. P., NOBRE, L. V., RUCKOVA, E., WILKIE, G. S., PAULO, J. A., CHANG, C., SUAREZ, N. M., DAVIES, J. A., ANTROBUS, R., STANTON, R. J., AICHELER, R. J., NICHOLS, H., VOJTESEK, B., TROWSDALE, J., DAVISON, A. J., GYGI, S. P., TOMASEC, P., LEHNER, P. J. & WILKINSON, G. W. 2017. Control of immune ligands by members of a cytomegalovirus gene expansion suppresses natural killer cell activation. *Elife,* 6.

FISCHER, R., MARSAL, J., GUTTA, C., EISLER, S. A., PETERS, N., BETHEA, J. R., PFIZENMAIER, K. & KONTERMANN, R. E. 2017. Novel strategies to mimic transmembrane tumor necrosis factor-dependent activation of tumor necrosis factor receptor 2. *Sci Rep,* 7**,** 6607.

FONTANA, S., MORATTO, D., MANGAL, S., DE FRANCESCO, M., VERMI, W., FERRARI, S., FACCHETTI, F., KUTUKCULER, N., FIORINI, C., DUSE, M., DAS, P. K., NOTARANGELO, L. D., PLEBANI, A. & BADOLATO, R. 2003. Functional defects of dendritic cells in patients with CD40 deficiency. *Blood,* 102**,** 4099-106.

FOULONGNE, V., TURRIERE, C., DIAFOUKA, F., ABRAHAM, B., LASTERE, S. & SEGONDY, M. 2004. Ganciclovir resistance mutations in UL97 and UL54 genes of Human cytomegalovirus isolates resistant to ganciclovir. *Acta Virol,* 48**,** 51-5.

FOWLER, K. B., STAGNO, S., PASS, R. F., BRITT, W. J., BOLL, T. J. & ALFORD, C. A. 1992. The outcome of congenital cytomegalovirus infection in relation to maternal antibody status. *N Engl J Med,* 326**,** 663-7.

FUTOHI, F., SABER, A., NEMATI, E., EINOLLAHI, B. & ROSTAMI, Z. 2015. Human Leukocyte Antigen Alleles and Cytomegalovirus Infection After Renal Transplantation. *Nephrourol Mon,* 7**,** e31635.

GABAEV, I., ELBASANI, E., AMERES, S., STEINBRUCK, L., STANTON, R., DORING, M., LENAC ROVIS, T., KALINKE, U., JONJIC, S., MOOSMANN, A. & MESSERLE, M. 2014. Expression of the human

cytomegalovirus UL11 glycoprotein in viral infection and evaluation of its effect on virus-specific CD8 T cells. *J Virol,* 88**,** 14326-39.

GABAEV, I., STEINBRUCK, L., POKOYSKI, C., PICH, A., STANTON, R. J., SCHWINZER, R., SCHULZ, T. F., JACOBS, R., MESSERLE, M. & KAY-FEDOROV, P. C. 2011. The human cytomegalovirus UL11 protein interacts with the receptor tyrosine phosphatase CD45, resulting in functional paralysis of T cells. *PLoS Pathog,* 7**,** e1002432.

GALLANT, J. E., MOORE, R. D., RICHMAN, D. D., KERULY, J. & CHAISSON, R. E. 1992. Incidence and natural history of cytomegalovirus disease in patients with advanced human immunodeficiency virus disease treated with zidovudine. The Zidovudine Epidemiology Study Group. *J Infect Dis,* 166**,** 1223-7.

GEARING, A. J., BECKETT, P., CHRISTODOULOU, M., CHURCHILL, M., CLEMENTS, J., DAVIDSON, A. H., DRUMMOND, A. H., GALLOWAY, W. A., GILBERT, R., GORDON, J. L. & ET AL. 1994. Processing of tumour necrosis factor-alpha precursor by metalloproteinases. *Nature,* 370**,** 555-7.

GEORGE, B., PATI, N., GILROY, N., RATNAMOHAN, M., HUANG, G., KERRIDGE, I., HERTZBERG, M., GOTTLIEB, D. & BRADSTOCK, K. 2010. Pre-transplant cytomegalovirus (CMV) serostatus remains the most important determinant of CMV reactivation after allogeneic hematopoietic stem cell transplantation in the era of surveillance and preemptive therapy. *Transpl Infect Dis,* 12**,** 322-9.

GERARD, L., LEPORT, C., FLANDRE, P., HOUHOU, N., SALMON-CERON, D., PEPIN, J. M., MANDET, C., BRUN-VEZINET, F. & VILDE, J. L. 1997. Cytomegalovirus (CMV) viremia and the CD4+ lymphocyte count as predictors of CMV disease in patients infected with human immunodeficiency virus. *Clin Infect Dis,* 24**,** 836-40.

GIANELLA, S., REDD, A. D., GRABOWSKI, M. K., TOBIAN, A. A., SERWADDA, D., NEWELL, K., PATEL, E. U., KALIBBALA, S., SSEBBOWA, P., GRAY, R. H., QUINN, T. C. & REYNOLDS, S. J. 2015a. Vaginal Cytomegalovirus Shedding Before and After Initiation of Antiretroviral Therapy in Rakai, Uganda. *J Infect Dis,* 212**,** 899-903.

GIANELLA, S., SCHEFFLER, K., MEHTA, S. R., LITTLE, S. J., FREITAS, L., MORRIS, S. R. & SMITH, D. M. 2015b. Seminal Shedding of CMV and HIV Transmission among Men Who Have Sex with Men. *Int J Environ Res Public Health,* 12**,** 7585-92.

GILBERT, M. J., RIDDELL, S. R., PLACHTER, B. & GREENBERG, P. D. 1996. Cytomegalovirus selectively blocks antigen processing and presentation of its immediate-early gene product. *Nature,* 383**,** 720-2.

GILLESPIE, G. M., WILLS, M. R., APPAY, V., O'CALLAGHAN, C., MURPHY, M., SMITH, N., SISSONS, P., ROWLAND-JONES, S., BELL, J. I. & MOSS, P. A. 2000. Functional heterogeneity and high frequencies of cytomegalovirus-specific CD8(+) T lymphocytes in healthy seropositive donors. *J Virol,* 74**,** 8140-50.

GOLDFELD, A. E., FLEMINGTON, E. K., BOUSSIOTIS, V. A., THEODOS, C. M., TITUS, R. G., STROMINGER, J. L. & SPECK, S. H. 1992. Transcription of the tumor necrosis factor alpha gene is rapidly induced by anti-immunoglobulin and blocked by cyclosporin A and FK506 in human B cells. *Proc Natl Acad Sci U S A,* 89**,** 12198-201.

GOLDMACHER, V. S., BARTLE, L. M., SKALETSKAYA, A., DIONNE, C. A., KEDERSHA, N. L., VATER, C. A., HAN, J. W., LUTZ, R. J., WATANABE, S., CAHIR MCFARLAND, E. D., KIEFF, E. D., MOCARSKI, E. S. & CHITTENDEN, T. 1999. A cytomegalovirus-encoded mitochondria-localized inhibitor of apoptosis structurally unrelated to Bcl-2. *Proc Natl Acad Sci U S A,* 96**,** 12536-41.

GOMPELS, U. A., LARKE, N., SANZ-RAMOS, M., BATES, M., MUSONDA, K., MANNO, D., SIAME, J., MONZE, M., FILTEAU, S. & GROUP, C. S. 2012. Human cytomegalovirus infant infection adversely affects growth and development in maternally HIV-exposed and unexposed infants in Zambia. *Clin Infect Dis,* 54**,** 434-42.

GONZALEZ-GALARZA, F. F., TAKESHITA, L. Y., SANTOS, E. J., KEMPSON, F., MAIA, M. H., DA SILVA, A. L., TELES E SILVA, A. L., GHATTAORAYA, G. S., ALFIREVIC, A., JONES, A. R. & MIDDLETON, D. 2015. Allele frequency net 2015 update: new features for HLA epitopes, KIR and disease and HLA adverse drug reaction associations. *Nucleic Acids Res,* 43**,** D784-8.

GRAHAM, F. L., SMILEY, J., RUSSELL, W. C. & NAIRN, R. 1977. Characteristics of a human cell line transformed by DNA from human adenovirus type 5. *J Gen Virol,* 36**,** 59-74.

GRELL, M., DOUNI, E., WAJANT, H., LOHDEN, M., CLAUSS, M., MAXEINER, B., GEORGOPOULOS, S., LESSLAUER, W., KOLLIAS, G., PFIZENMAIER, K. & SCHEURICH, P. 1995. The transmembrane form of tumor necrosis factor is the prime activating ligand of the 80 kDa tumor necrosis factor receptor. *Cell,* 83**,** 793-802.

GRELL, M., WAJANT, H., ZIMMERMANN, G. & SCHEURICH, P. 1998. The type 1 receptor (CD120a) is the high-affinity receptor for soluble tumor necrosis factor. *Proc Natl Acad Sci U S A,* 95**,** 570-5.

GRIEVE, A. G., XU, H., KUNZEL, U., BAMBROUGH, P., SIEBER, B. & FREEMAN, M. 2017. Phosphorylation of iRhom2 at the plasma membrane controls mammalian TACE-dependent inflammatory and growth factor signalling. *Elife,* 6.

GUBERINA, H., DA SILVA NARDI, F., TOMOYA MICHITA, R., DOLFF, S., BIENHOLZ, A., HEINEMANN, F. M., WILDE, B., TRILLING, M., HORN, P. A., KRIBBEN, A., WITZKE, O. & REBMANN, V. 2017a. Susceptibility of HLA-E*01:03 allele carriers to develop Cytomegalovirus replication after living-donor kidney transplantation. *J Infect Dis*.

GUBERINA, H., TOMOYA MICHITA, R., DOLFF, S., BIENHOLZ, A., TRILLING, M., HEINEMANN, F. M., HORN, P. A., KRIBBEN, A., WITZKE, O. & REBMANN, V. 2017b. Recipient HLA-G +3142 CC Genotype and Concentrations of Soluble HLA-G Impact on Occurrence of CMV Infection after Living-Donor Kidney Transplantation. *Int J Mol Sci,* 18.

GUMA, M., ANGULO, A., VILCHES, C., GOMEZ-LOZANO, N., MALATS, N. & LOPEZ-BOTET, M. 2004. Imprint of human cytomegalovirus infection on the NK cell receptor repertoire. *Blood,* 104**,** 3664-71.

GUSTAFSON, C. E., QI, Q., HUTTER-SAUNDERS, J., GUPTA, S., JADHAV, R., NEWELL, E., MAECKER, H., WEYAND, C. M. & GORONZY, J. J. 2017. Immune Checkpoint Function of CD85j in CD8 T Cell Differentiation and Aging. *Front Immunol,* 8**,** 692.

HAHN, G., REVELLO, M. G., PATRONE, M., PERCIVALLE, E., CAMPANINI, G., SARASINI, A., WAGNER, M., GALLINA, A., MILANESI, G., KOSZINOWSKI, U., BALDANTI, F. & GERNA, G. 2004. Human cytomegalovirus UL131-128 genes are indispensable for virus growth in endothelial cells and virus transfer to leukocytes. *J Virol,* 78**,** 10023-33.

HAMILTON, S. T., SCOTT, G. M., NAING, Z. & RAWLINSON, W. D. 2013. Human cytomegalovirus directly modulates expression of chemokine CCL2 (MCP-1) during viral replication. *J Gen Virol,* 94**,** 2495-503.

HAMMER, Q., RUCKERT, T., BORST, E. M., DUNST, J., HAUBNER, A., DUREK, P., HEINRICH, F., GASPARONI, G., BABIC, M., TOMIC, A., PIETRA, G., NIENEN, M., BLAU, I. W., HOFMANN, J., NA, I. K., PRINZ, I., KOENECKE, C., HEMMATI, P., BABEL, N., ARNOLD, R., WALTER, J., THURLEY, K., MASHREGHI, M. F., MESSERLE, M. & ROMAGNANI, C. 2018. Peptide-specific recognition of human cytomegalovirus strains controls adaptive natural killer cells. *Nat Immunol,* 19**,** 453-463.

HANCOCK, M. H. & NELSON, J. A. 2017. Modulation of the NFκb Signalling Pathway by Human Cytomegalovirus. *Virology (Hyderabad),* 1.

HANSEN, S. G., SACHA, J. B., HUGHES, C. M., FORD, J. C., BURWITZ, B. J., SCHOLZ, I., GILBRIDE, R. M., LEWIS, M. S., GILLIAM, A. N., VENTURA, A. B., MALOULI, D., XU, G., RICHARDS, R., WHIZIN, N., REED, J. S., HAMMOND, K. B., FISCHER, M., TURNER, J. M., LEGASSE, A. W., AXTHELM, M. K., EDLEFSEN, P. T., NELSON, J. A., LIFSON, J. D., FRÜH, K. & PICKER, L. J. 2013. Cytomegalovirus vectors violate CD8+ T cell epitope recognition paradigms. *Science,* 340**,** 1237874.

HANSEN, S. G., WU, H. L., BURWITZ, B. J., HUGHES, C. M., HAMMOND, K. B., VENTURA, A. B., REED, J. S., GILBRIDE, R. M., AINSLIE, E., MORROW, D. W., FORD, J. C., SELSETH, A. N., PATHAK, R., MALOULI, D., LEGASSE, A. W., AXTHELM, M. K., NELSON, J. A., GILLESPIE, G. M., WALTERS, L. C., BRACKENRIDGE, S., SHARPE, H. R., LÓPEZ, C. A., FRÜH, K., KORBER, B. T., MCMICHAEL, A. J., GNANAKARAN, S., SACHA, J. B. & PICKER, L. J. 2016. Broadly targeted CD8 T cell responses restricted by major histocompatibility complex E. *Science,* 351**,** 714-20.

HASSAN, J., O'NEILL, D., HONARI, B., DE GASCUN, C., CONNELL, J., KEOGAN, M. & HICKEY, D. 2016. Cytomegalovirus Infection in Ireland: Seroprevalence, HLA Class I Alleles, and Implications. *Medicine (Baltimore),* 95**,** e2735.

HATHCOCK, K. S., LASZLO, G., PUCILLO, C., LINSLEY, P. & HODES, R. J. 1994. Comparative analysis of B7-1 and B7-2 costimulatory ligands: expression and function. *J Exp Med,* 180**,** 631-40.

HENGEL, H., FLOHR, T., HAMMERLING, G. J., KOSZINOWSKI, U. H. & MOMBURG, F. 1996. Human cytomegalovirus inhibits peptide translocation into the endoplasmic reticulum for MHC class I assembly. *J Gen Virol,* 77 (Pt 9)**,** 2287-96.

HO, M. 2008. The history of cytomegalovirus and its diseases. *Med Microbiol Immunol,* 197**,** 65-73.

HSU, J. L., VAN DEN BOOMEN, D. J., TOMASEC, P., WEEKES, M. P., ANTROBUS, R., STANTON, R. J., RUCKOVA, E., SUGRUE, D., WILKIE, G. S., DAVISON, A. J., WILKINSON, G. W. & LEHNER, P. J. 2015. Plasma membrane profiling defines an expanded class of cell surface

proteins selectively targeted for degradation by HCMV US2 in cooperation with UL141. *PLoS Pathog,* 11**,** e1004811.

IRMIERE, A. & GIBSON, W. 1983. Isolation and characterization of a noninfectious virion-like particle released from cells infected with human strains of cytomegalovirus. *Virology,* 130**,** 118-33.

JACKSON, S. E., MASON, G. M. & WILLS, M. R. 2011. Human cytomegalovirus immunity and immune evasion. *Virus Res,* 157**,** 151-60.

JAMIESON, A. M., DIEFENBACH, A., MCMAHON, C. W., XIONG, N., CARLYLE, J. R. & RAULET, D. H. 2002. The role of the NKG2D immunoreceptor in immune cell activation and natural killing. *Immunity,* 17**,** 19-29.

JARVIS, M. A., BORTON, J. A., KEECH, A. M., WONG, J., BRITT, W. J., MAGUN, B. E. & NELSON, J. A. 2006. Human cytomegalovirus attenuates interleukin-1beta and tumor necrosis factor alpha proinflammatory signaling by inhibition of NF-kappaB activation. *J Virol,* 80**,** 5588-98.

JONES, T. R., HANSON, L. K., SUN, L., SLATER, J. S., STENBERG, R. M. & CAMPBELL, A. E. 1995. Multiple independent loci within the human cytomegalovirus unique short region down-regulate expression of major histocompatibility complex class I heavy chains. *J Virol,* 69**,** 4830-41.

JONES, T. R. & SUN, L. 1997. Human cytomegalovirus US2 destabilizes major histocompatibility complex class I heavy chains. *J Virol,* 71**,** 2970-9.

JONES, T. R., WIERTZ, E. J., SUN, L., FISH, K. N., NELSON, J. A. & PLOEGH, H. L. 1996. Human cytomegalovirus US3 impairs transport and maturation of major histocompatibility complex class I heavy chains. *Proc Natl Acad Sci U S A,* 93**,** 11327-33.

JOUAND, N., BRESSOLLETTE-BODIN, C., GERARD, N., GIRAL, M., GUERIF, P., RODALLEC, A., OGER, R., PARROT, T., ALLARD, M., CESBRON-GAUTIER, A., GERVOIS, N. & CHARREAU, B. 2018. HCMV triggers frequent and persistent UL40-specific unconventional HLA-E-restricted CD8 T-cell responses with potential autologous and allogeneic peptide recognition. *PLoS Pathog,* 14**,** e1007041.

KAECH, S. M. & AHMED, R. 2001. Memory CD8+ T cell differentiation: initial antigen encounter triggers a developmental program in naive cells. *Nat Immunol,* 2**,** 415-22.

KAVANAGH, D. G., KOSZINOWSKI, U. H. & HILL, A. B. 2001. The murine cytomegalovirus immune evasion protein m4/gp34 forms biochemically distinct complexes with class I MHC at the cell surface and in a pre-Golgi compartment. *J Immunol,* 167**,** 3894-902.

KELLY, C., VAN DRIEL, R. & WILKINSON, G. W. 1995. Disruption of PML-associated nuclear bodies during human cytomegalovirus infection. *J Gen Virol,* 76 (Pt 11)**,** 2887-93.

KEMPEN, J. H., JABS, D. A., WILSON, L. A., DUNN, J. P., WEST, S. K. & TONASCIA, J. 2003a. Mortality risk for patients with cytomegalovirus retinitis and acquired immune deficiency syndrome. *Clin Infect Dis,* 37**,** 1365-73.

KEMPEN, J. H., MARTIN, B. K., WU, A. W., BARRON, B., THORNE, J. E., JABS, D. A. & STUDIES OF OCULAR COMPLICATIONS OF, A. R. G. 2003b. The effect of cytomegalovirus retinitis on the quality of life of patients with AIDS in the era of highly active antiretroviral therapy. *Ophthalmology,* 110**,** 987-95.

KHAN, N., COBBOLD, M., KEENAN, R. & MOSS, P. A. 2002. Comparative analysis of CD8+ T cell responses against human cytomegalovirus proteins pp65 and immediate early 1 shows similarities in precursor frequency, oligoclonality, and phenotype. *J Infect Dis,* 185**,** 1025-34.

KIM, S., LEE, S., SHIN, J., KIM, Y., EVNOUCHIDOU, I., KIM, D., KIM, Y. K., KIM, Y. E., AHN, J. H., RIDDELL, S. R., STRATIKOS, E., KIM, V. N. & AHN, K. 2011. Human cytomegalovirus microRNA miR-US4-1 inhibits CD8(+) T cell responses by targeting the aminopeptidase ERAP1. *Nat Immunol,* 12**,** 984-91.

KIM, S., SNIDER, J. J. & GILL, M. J. 2006. Cytomegalovirus disease in HIV infection: twenty years of a regional population's experience. *Clin Infect Dis,* 42**,** 1808-9.

KIM, Y., LEE, S., KIM, S., KIM, D., AHN, J. H. & AHN, K. 2012. Human cytomegalovirus clinical strain-specific microRNA miR-UL148D targets the human chemokine RANTES during infection. *PLoS Pathog,* 8**,** e1002577.

KLEIN, J. & SATO, A. 2000a. The HLA system. First of two parts. *N Engl J Med,* 343**,** 702-9.

KLEIN, J. & SATO, A. 2000b. The HLA system. Second of two parts. *N Engl J Med,* 343**,** 782-6.

KOCH, U. & RADTKE, F. 2011. Mechanisms of T cell development and transformation. *Annu Rev Cell Dev Biol,* 27**,** 539-62.

KOVACS, A., SCHLUCHTER, M., EASLEY, K., DEMMLER, G., SHEARER, W., LA RUSSA, P., PITT, J., COOPER, E., GOLDFARB, J., HODES, D., KATTAN, M. & MCINTOSH, K. 1999. Cytomegalovirus infection and HIV-1 disease progression in infants born to HIV-1-infected women. Pediatric Pulmonary and Cardiovascular Complications of Vertically Transmitted HIV Infection Study Group. *N Engl J Med,* 341**,** 77-84.

KRAEMER, T., BLASCZYK, R. & BADE-DOEDING, C. 2014. HLA-E: a novel player for histocompatibility. *J Immunol Res,* 2014**,** 352160.

KREUZ, S., SIEGMUND, D., SCHEURICH, P. & WAJANT, H. 2001. NF-kappaB inducers upregulate cFLIP, a cycloheximide-sensitive inhibitor of death receptor signaling. *Mol Cell Biol,* 21**,** 3964-73.

KRIEGLER, M., PEREZ, C., DEFAY, K., ALBERT, I. & LU, S. D. 1988. A novel form of TNF/cachectin is a cell surface cytotoxic transmembrane protein: ramifications for the complex physiology of TNF. *Cell,* 53**,** 45-53.

KRIPPNER-HEIDENREICH, A., TUBING, F., BRYDE, S., WILLI, S., ZIMMERMANN, G. & SCHEURICH, P. 2002. Control of receptor-induced signaling complex formation by the kinetics of ligand/receptor interaction. *J Biol Chem,* 277**,** 44155-63.

KUBIN, M., CASSIANO, L., CHALUPNY, J., CHIN, W., COSMAN, D., FANSLOW, W., MÜLLBERG, J., ROUSSEAU, A. M., ULRICH, D. & ARMITAGE, R. 2001. ULBP1, 2, 3: novel MHC class I-related molecules that bind to human cytomegalovirus glycoprotein UL16, activate NK cells. *Eur J Immunol,* 31**,** 1428-37.

KUESPERT, K., PILS, S. & HAUCK, C. R. 2006. CEACAMs: their role in physiology and pathophysiology. *Curr Opin Cell Biol,* 18**,** 565-71.

KURATH, S., HALWACHS-BAUMANN, G., MULLER, W. & RESCH, B. 2010. Transmission of cytomegalovirus via breast milk to the prematurely born infant: a systematic review. *Clin Microbiol Infect,* 16**,** 1172-8.

KUROKI, K., TSUCHIYA, N., SHIROISHI, M., RASUBALA, L., YAMASHITA, Y., MATSUTA, K., FUKAZAWA, T., KUSAOI, M., MURAKAMI, Y., TAKIGUCHI, M., JUJI, T., HASHIMOTO, H., KOHDA, D., MAENAKA, K. & TOKUNAGA, K. 2005. Extensive polymorphisms of LILRB1 (ILT2, LIR1) and their association with HLA-DRB1 shared epitope negative rheumatoid arthritis. *Hum Mol Genet,* 14**,** 2469-80.

LACHMANN, R., BAJWA, M., VITA, S., SMITH, H., CHEEK, E., AKBAR, A. & KERN, F. 2012. Polyfunctional T cells accumulate in large human cytomegalovirus-specific T cell responses. *J Virol,* 86**,** 1001-9.

LAINEZ, B., FERNANDEZ-REAL, J. M., ROMERO, X., ESPLUGUES, E., CANETE, J. D., RICART, W. & ENGEL, P. 2004. Identification and characterization of a novel spliced variant that encodes human soluble tumor necrosis factor receptor 2. *Int Immunol,* 16**,** 169-77.

LANG, I., FULLSACK, S., WYZGOL, A., FICK, A., TREBING, J., ARANA, J. A., SCHAFER, V., WEISENBERGER, D. & WAJANT, H. 2016. Binding Studies of TNF Receptor Superfamily (TNFRSF) Receptors on Intact Cells. *J Biol Chem,* 291**,** 5022-37.

LANZIERI, T. M., KRUSZON-MORAN, D., GAMBHIR, M. & BIALEK, S. R. 2016. Influence of parity and sexual history on cytomegalovirus seroprevalence among women aged 20-49 years in the USA. *Int J Gynaecol Obstet,* 135**,** 82-5.

LARSSON, S., SODERBERG-NAUCLER, C., WANG, F. Z. & MOLLER, E. 1998. Cytomegalovirus DNA can be detected in peripheral blood mononuclear cells from all seropositive and most seronegative healthy blood donors over time. *Transfusion,* 38**,** 271-8.

LAU, L. L., JAMIESON, B. D., SOMASUNDARAM, T. & AHMED, R. 1994. Cytotoxic T-cell memory without antigen. *Nature,* 369**,** 648-52.

LAYDON, D. J., BANGHAM, C. R. & ASQUITH, B. 2015. Estimating T-cell repertoire diversity: limitations of classical estimators and a new approach. *Philos Trans R Soc Lond B Biol Sci,* 370.

LE, V. T., TRILLING, M. & HENGEL, H. 2011. The cytomegaloviral protein pUL138 acts as potentiator of tumor necrosis factor (TNF) receptor 1 surface density to enhance ULb'-encoded modulation of TNF-alpha signaling. *J Virol,* 85**,** 13260-70.

LEE, R. E., QASAIMEH, M. A., XIA, X., JUNCKER, D. & GAUDET, S. 2016. NF-κB signalling and cell fate decisions in response to a short pulse of tumour necrosis factor. *Sci Rep,* 6**,** 39519.

LEE, S. O., HWANG, S., PARK, J., PARK, B., JIN, B. S., LEE, S., KIM, E., CHO, S., KIM, Y., CHO, K., SHIN, J. & AHN, K. 2005. Functional dissection of HCMV US11 in mediating the degradation of MHC class I molecules. *Biochem Biophys Res Commun,* 330**,** 1262-7.

LEHNER, P. J., KARTTUNEN, J. T., WILKINSON, G. W. & CRESSWELL, P. 1997. The human cytomegalovirus US6 glycoprotein inhibits transporter associated with antigen processing-dependent peptide translocation. *Proc Natl Acad Sci U S A,* 94**,** 6904-9.

LI, G., NGUYEN, C. C., RYCKMAN, B. J., BRITT, W. J. & KAMIL, J. P. 2015a. A viral regulator of glycoprotein complexes contributes to human cytomegalovirus cell tropism. *Proc Natl Acad Sci U S A,* 112**,** 4471-6.

LI, X., MARETZKY, T., WESKAMP, G., MONETTE, S., QING, X., ISSUREE, P. D., CRAWFORD, H. C., MCILWAIN, D. R., MAK, T. W., SALMON, J. E. &

BLOBEL, C. P. 2015b. iRhoms 1 and 2 are essential upstream regulators of ADAM17-dependent EGFR signaling. *Proc Natl Acad Sci U S A,* 112**,** 6080-5.
LINARES, L., SANCLEMENTE, G., CERVERA, C., HOYO, I., COFAN, F., RICART, M. J., PEREZ-VILLA, F., NAVASA, M., MARCOS, M. A., ANTON, A., PUMAROLA, T. & MORENO, A. 2011. Influence of cytomegalovirus disease in outcome of solid organ transplant patients. *Transplant Proc,* 43**,** 2145-8.
LLANO, M., GUMÁ, M., ORTEGA, M., ANGULO, A. & LÓPEZ-BOTET, M. 2003. Differential effects of US2, US6 and US11 human cytomegalovirus proteins on HLA class Ia and HLA-E expression: impact on target susceptibility to NK cell subsets. *Eur J Immunol,* 33**,** 2744-54.
MAHALINGAM, D., SZEGEZDI, E., KEANE, M., DE JONG, S. & SAMALI, A. 2009. TRAIL receptor signalling and modulation: Are we on the right TRAIL? *Cancer Treat Rev,* 35**,** 280-8.
MAISCH, T., KROPFF, B., SINZGER, C. & MACH, M. 2002. Upregulation of CD40 expression on endothelial cells infected with human cytomegalovirus. *J Virol,* 76**,** 12803-12.
MANEY, N. J., REYNOLDS, G., KRIPPNER-HEIDENREICH, A. & HILKENS, C. M. U. 2014. Dendritic cell maturation and survival are differentially regulated by TNFR1 and TNFR2. *J Immunol,* 193**,** 4914-4923.
MANICKLAL, S., EMERY, V. C., LAZZAROTTO, T., BOPPANA, S. B. & GUPTA, R. K. 2013. The "silent" global burden of congenital cytomegalovirus. *Clin Microbiol Rev,* 26**,** 86-102.
MARCHANT, A., APPAY, V., VAN DER SANDE, M., DULPHY, N., LIESNARD, C., KIDD, M., KAYE, S., OJUOLA, O., GILLESPIE, G. M., VARGAS CUERO, A. L., CERUNDOLO, V., CALLAN, M., MCADAM, K. P., ROWLAND-JONES, S. L., DONNER, C., MCMICHAEL, A. J. & WHITTLE, H. 2003. Mature CD8(+) T lymphocyte response to viral infection during fetal life. *J Clin Invest,* 111**,** 1747-55.
MARSHALL, E. E. & GEBALLE, A. P. 2009. Multifaceted evasion of the interferon response by cytomegalovirus. *J Interferon Cytokine Res,* 29**,** 609-19.
MASON, G. M., POOLE, E., SISSONS, J. G., WILLS, M. R. & SINCLAIR, J. H. 2012. Human cytomegalovirus latency alters the cellular secretome, inducing cluster of differentiation (CD)4+ T-cell migration and suppression of effector function. *Proc Natl Acad Sci U S A,* 109**,** 14538-43.
MCCORMICK, A. L., ROBACK, L., LIVINGSTON-ROSANOFF, D. & ST CLAIR, C. 2010. The human cytomegalovirus UL36 gene controls caspase-dependent and -independent cell death programs activated by infection of monocytes differentiating to macrophages. *J Virol,* 84**,** 5108-23.
MCLAUGHLIN-TAYLOR, E., PANDE, H., FORMAN, S. J., TANAMACHI, B., LI, C. R., ZAIA, J. A., GREENBERG, P. D. & RIDDELL, S. R. 1994. Identification of the major late human cytomegalovirus matrix protein pp65 as a target antigen for CD8+ virus-specific cytotoxic T lymphocytes. *J Med Virol,* 43**,** 103-10.
MCSHARRY, B. P., BURGERT, H. G., OWEN, D. P., STANTON, R. J., PROD'HOMME, V., SESTER, M., KOEBERNICK, K., GROH, V., SPIES, T., COX, S., LITTLE, A. M., WANG, E. C., TOMASEC, P. & WILKINSON, G. W. 2008. Adenovirus E3/19K promotes evasion of NK cell recognition by intracellular sequestration of the NKG2D ligands major

histocompatibility complex class I chain-related proteins A and B. *J Virol,* 82**,** 4585-94.
MCSHARRY, B. P., JONES, C. J., SKINNER, J. W., KIPLING, D. & WILKINSON, G. W. 2001. Human telomerase reverse transcriptase-immortalized MRC-5 and HCA2 human fibroblasts are fully permissive for human cytomegalovirus. *J Gen Virol,* 82**,** 855-63.
MCSHARRY, B. P., TOMASEC, P., NEALE, M. L. & WILKINSON, G. W. 2003. The most abundantly transcribed human cytomegalovirus gene (beta 2.7) is non-essential for growth in vitro. *J Gen Virol,* 84**,** 2511-6.
MICHEAU, O. & TSCHOPP, J. 2003. Induction of TNF receptor I-mediated apoptosis via two sequential signaling complexes. *Cell,* 114**,** 181-90.
MILLER, D. M., RAHILL, B. M., BOSS, J. M., LAIRMORE, M. D., DURBIN, J. E., WALDMAN, J. W. & SEDMAK, D. D. 1998. Human cytomegalovirus inhibits major histocompatibility complex class II expression by disruption of the Jak/Stat pathway. *J Exp Med,* 187**,** 675-83.
MOCARSKI, E., SHENK, T., GRIFFITHS, P. D. & PASS, R. F. 2013. Cytomegaloviruses. *In:* KNIPE, D. M. & HOWLEY, P. M. (eds.) *Fields Virology.* 6th ed.: Lippincott Williams & Wilkins.
MOHLER, K. M., SLEATH, P. R., FITZNER, J. N., CERRETTI, D. P., ALDERSON, M., KERWAR, S. S., TORRANCE, D. S., OTTEN-EVANS, C., GREENSTREET, T., WEERAWARNA, K. & ET AL. 1994. Protection against a lethal dose of endotoxin by an inhibitor of tumour necrosis factor processing. *Nature,* 370**,** 218-20.
MONTAG, C., WAGNER, J., GRUSKA, I. & HAGEMEIER, C. 2006. Human cytomegalovirus blocks tumor necrosis factor alpha- and interleukin-1beta-mediated NF-kappaB signaling. *J Virol,* 80**,** 11686-98.
MONTAG, C., WAGNER, J. A., GRUSKA, I., VETTER, B., WIEBUSCH, L. & HAGEMEIER, C. 2011. The latency-associated UL138 gene product of human cytomegalovirus sensitizes cells to tumor necrosis factor alpha (TNF-alpha) signaling by upregulating TNF-alpha receptor 1 cell surface expression. *J Virol,* 85**,** 11409-21.
MOSS, M. L., JIN, S. L., MILLA, M. E., BICKETT, D. M., BURKHART, W., CARTER, H. L., CHEN, W. J., CLAY, W. C., DIDSBURY, J. R., HASSLER, D., HOFFMAN, C. R., KOST, T. A., LAMBERT, M. H., LEESNITZER, M. A., MCCAULEY, P., MCGEEHAN, G., MITCHELL, J., MOYER, M., PAHEL, G., ROCQUE, W., OVERTON, L. K., SCHOENEN, F., SEATON, T., SU, J. L., BECHERER, J. D. & ET AL. 1997. Cloning of a disintegrin metalloproteinase that processes precursor tumour-necrosis factor-alpha. *Nature,* 385**,** 733-6.
MOSS, M. L. & MINOND, D. 2017. Recent Advances in ADAM17 Research: A Promising Target for Cancer and Inflammation. *Mediators Inflamm,* 2017**,** 9673537.
MOTANI, K. & KOSAKO, H. 2018. Activation of stimulator of interferon genes (STING) induces ADAM17-mediated shedding of the immune semaphorin SEMA4D. *J Biol Chem*.
MOUTAFTSI, M., MEHL, A. M., BORYSIEWICZ, L. K. & TABI, Z. 2002. Human cytomegalovirus inhibits maturation and impairs function of monocyte-derived dendritic cells. *Blood,* 99**,** 2913-21.
MURPHY, E. L., COLLIER, A. C., KALISH, L. A., ASSMANN, S. F., PARA, M. F., FLANIGAN, T. P., KUMAR, P. N., MINTZ, L., WALLACH, F. R., NEMO, G.

J. & VIRAL ACTIVATION TRANSFUSION STUDY, I. 2001. Highly active antiretroviral therapy decreases mortality and morbidity in patients with advanced HIV disease. *Ann Intern Med,* 135**,** 17-26.

MURPHY, J. C., FISCHLE, W., VERDIN, E. & SINCLAIR, J. H. 2002. Control of cytomegalovirus lytic gene expression by histone acetylation. *EMBO J,* 21**,** 1112-20.

MURRELL, I. 2014. *Developing a Human Cytomegalovirus strain for better in vitro research.* Ph.D, University of Cardiff.

MURRELL, I., BEDFORD, C., LADELL, K., MINERS, K. L., PRICE, D. A., TOMASEC, P., WILKINSON, G. W. G. & STANTON, R. J. 2017. The pentameric complex drives immunologically covert cell-cell transmission of wild-type human cytomegalovirus. *Proc Natl Acad Sci U S A,* 114**,** 6104-6109.

NACHMANI, D., LANKRY, D., WOLF, D. G. & MANDELBOIM, O. 2010. The human cytomegalovirus microRNA miR-UL112 acts synergistically with a cellular microRNA to escape immune elimination. *Nat Immunol,* 11**,** 806-13.

NAEGER, D. M., MARTIN, J. N., SINCLAIR, E., HUNT, P. W., BANGSBERG, D. R., HECHT, F., HSUE, P., MCCUNE, J. M. & DEEKS, S. G. 2010. Cytomegalovirus-specific T cells persist at very high levels during long-term antiretroviral treatment of HIV disease. *PLoS One,* 5**,** e8886.

NAGATA, S., SUZUKI, J., SEGAWA, K. & FUJII, T. 2016. Exposure of phosphatidylserine on the cell surface. *Cell Death Differ,* 23**,** 952-61.

NAUDE, P. J., DEN BOER, J. A., LUITEN, P. G. & EISEL, U. L. 2011. Tumor necrosis factor receptor cross-talk. *FEBS J,* 278**,** 888-98.

NAUTS, H. C. & MCLAREN, J. R. 1990. Coley toxins--the first century. *Adv Exp Med Biol,* 267**,** 483-500.

NEDWIN, G. E., NAYLOR, S. L., SAKAGUCHI, A. Y., SMITH, D., JARRETT-NEDWIN, J., PENNICA, D., GOEDDEL, D. V. & GRAY, P. W. 1985. Human lymphotoxin and tumor necrosis factor genes: structure, homology and chromosomal localization. *Nucleic Acids Res,* 13**,** 6361-73.

NEERINCX, A., CASTRO, W., GUARDA, G. & KUFER, T. A. 2013. NLRC5, at the Heart of Antigen Presentation. *Front Immunol,* 4**,** 397.

NEMČOVIČOVÁ, I., BENEDICT, C. A. & ZAJONC, D. M. 2013. Structure of human cytomegalovirus UL141 binding to TRAIL-R2 reveals novel, non-canonical death receptor interactions. *PLoS Pathog,* 9**,** e1003224.

NGUYEN, D. X. & EHRENSTEIN, M. R. 2016. Anti-TNF drives regulatory T cell expansion by paradoxically promoting membrane TNF-TNF-RII binding in rheumatoid arthritis. *J Exp Med,* 213**,** 1241-53.

NORIEGA, V., REDMANN, V., GARDNER, T. & TORTORELLA, D. 2012. Diverse immune evasion strategies by human cytomegalovirus. *Immunol Res,* 54**,** 140-51.

NORIEGA, V. M. & TORTORELLA, D. 2009. Human cytomegalovirus-encoded immune modulators partner to downregulate major histocompatibility complex class I molecules. *J Virol,* 83**,** 1359-67.

ODEBERG, J., BROWNE, H., METKAR, S., FROELICH, C. J., BRANDÉN, L., COSMAN, D. & SÖDERBERG-NAUCLÉR, C. 2003. The human cytomegalovirus protein UL16 mediates increased resistance to natural killer cell cytotoxicity through resistance to cytolytic proteins. *J Virol,* 77**,** 4539-45.

OLSSON, J., WIKBY, A., JOHANSSON, B., LÖFGREN, S., NILSSON, B. O. & FERGUSON, F. G. 2000. Age-related change in peripheral blood T-lymphocyte subpopulations and cytomegalovirus infection in the very old: the Swedish longitudinal OCTO immune study. *Mech Ageing Dev,* 121**,** 187-201.

ORANGE, J. S. 2013. Natural killer cell deficiency. *J Allergy Clin Immunol,* 132**,** 515-525.

OUYANG, Q., WAGNER, W. M., WIKBY, A., WALTER, S., AUBERT, G., DODI, A. I., TRAVERS, P. & PAWELEC, G. 2003. Large numbers of dysfunctional CD8+ T lymphocytes bearing receptors for a single dominant CMV epitope in the very old. *J Clin Immunol,* 23**,** 247-57.

OUYANG, Q., WAGNER, W. M., ZHENG, W., WIKBY, A., REMARQUE, E. J. & PAWELEC, G. 2004. Dysfunctional CMV-specific CD8(+) T cells accumulate in the elderly. *Exp Gerontol,* 39**,** 607-13.

PANG, G., COUCH, L., BATEY, R., CLANCY, R. & CRIPPS, A. 1994. GM-CSF, IL-1 alpha, IL-1 beta, IL-6, IL-8, IL-10, ICAM-1 and VCAM-1 gene expression and cytokine production in human duodenal fibroblasts stimulated with lipopolysaccharide, IL-1 alpha and TNF-alpha. *Clin Exp Immunol,* 96**,** 437-43.

PARI, G. S. 2008. Nuts and bolts of human cytomegalovirus lytic DNA replication. *Curr Top Microbiol Immunol,* 325**,** 153-66.

PARK, B., OH, H., LEE, S., SONG, Y., SHIN, J., SUNG, Y. C., HWANG, S. Y. & AHN, K. 2002. The MHC class I homolog of human cytomegalovirus is resistant to down-regulation mediated by the unique short region protein (US)2, US3, US6, and US11 gene products. *J Immunol,* 168**,** 3464-9.

PARK, B., SPOONER, E., HOUSER, B. L., STROMINGER, J. L. & PLOEGH, H. L. 2010. The HCMV membrane glycoprotein US10 selectively targets HLA-G for degradation. *J Exp Med,* 207**,** 2033-41.

PARKIN, J. & COHEN, B. 2001. An overview of the immune system. *Lancet,* 357**,** 1777-89.

PEGGS, K. S. 2009. Adoptive T cell immunotherapy for cytomegalovirus. *Expert Opin Biol Ther,* 9**,** 725-36.

PENNICA, D., NEDWIN, G. E., HAYFLICK, J. S., SEEBURG, P. H., DERYNCK, R., PALLADINO, M. A., KOHR, W. J., AGGARWAL, B. B. & GOEDDEL, D. V. 1984. Human tumour necrosis factor: precursor structure, expression and homology to lymphotoxin. *Nature,* 312**,** 724-9.

PEREYRA, F. & RUBIN, R. H. 2004. Prevention and treatment of cytomegalovirus infection in solid organ transplant recipients. *Curr Opin Infect Dis,* 17**,** 357-61.

PEREZ-CARMONA, N., MARTINEZ-VICENTE, P., FARRE, D., GABAEV, I., MESSERLE, M., ENGEL, P. & ANGULO, A. 2018. A prominent role of the human cytomegalovirus UL8 glycoprotein restraining pro-inflammatory cytokine production by myeloid cells at late times during infection. *J Virol*.

PICONE, O., COSTA, J. M., CHAIX, M. L., VILLE, Y., ROUZIOUX, C. & LERUEZ-VILLE, M. 2005. Human cytomegalovirus UL144 gene polymorphisms in congenital infections. *J Clin Microbiol,* 43**,** 25-9.

PIETRA, G., ROMAGNANI, C., MAZZARINO, P., FALCO, M., MILLO, E., MORETTA, A., MORETTA, L. & MINGARI, M. C. 2003. HLA-E-restricted recognition of cytomegalovirus-derived peptides by human CD8+ cytolytic T lymphocytes. *Proc Natl Acad Sci U S A,* 100**,** 10896-901.

PLOTKIN, S. A., FURUKAWA, T., ZYGRAICH, N. & HUYGELEN, C. 1975. Candidate cytomegalovirus strain for human vaccination. *Infect Immun,* 12**,** 521-7.

POOLE, E., KING, C. A., SINCLAIR, J. H. & ALCAMI, A. 2006. The UL144 gene product of human cytomegalovirus activates NFkappaB via a TRAF6-dependent mechanism. *EMBO J,* 25**,** 4390-9.

POOLE, E., LAU, J. C. & SINCLAIR, J. 2015. Latent infection of myeloid progenitors by human cytomegalovirus protects cells from FAS-mediated apoptosis through the cellular IL-10/PEA-15 pathway. *J Gen Virol,* 96**,** 2355-9.

PROD'HOMME, V., GRIFFIN, C., AICHELER, R. J., WANG, E. C., MCSHARRY, B. P., RICKARDS, C. R., STANTON, R. J., BORYSIEWICZ, L. K., LOPEZ-BOTET, M., WILKINSON, G. W. & TOMASEC, P. 2007. The human cytomegalovirus MHC class I homolog UL18 inhibits LIR-1+ but activates LIR-1- NK cells. *J Immunol,* 178**,** 4473-81.

PROD'HOMME, V., SUGRUE, D. M., STANTON, R. J., NOMOTO, A., DAVIES, J., RICKARDS, C. R., COCHRANE, D., MOORE, M., WILKINSON, G. W. & TOMASEC, P. 2010. Human cytomegalovirus UL141 promotes efficient downregulation of the natural killer cell activating ligand CD112. *J Gen Virol,* 91**,** 2034-9.

PROD'HOMME, V., TOMASEC, P., CUNNINGHAM, C., LEMBERG, M. K., STANTON, R. J., MCSHARRY, B. P., WANG, E. C., CUFF, S., MARTOGLIO, B., DAVISON, A. J., BRAUD, V. M. & WILKINSON, G. W. 2012. Human cytomegalovirus UL40 signal peptide regulates cell surface expression of the NK cell ligands HLA-E and gpUL18. *J Immunol,* 188**,** 2794-804.

QUINNAN, G. V., JR., DELERY, M., ROOK, A. H., FREDERICK, W. R., EPSTEIN, J. S., MANISCHEWITZ, J. F., JACKSON, L., RAMSEY, K. M., MITTAL, K., PLOTKIN, S. A. & ET AL. 1984. Comparative virulence and immunogenicity of the Towne strain and a nonattenuated strain of cytomegalovirus. *Ann Intern Med,* 101**,** 478-83.

QUINNAN, G. V., JR., KIRMANI, N., ROOK, A. H., MANISCHEWITZ, J. F., JACKSON, L., MORESCHI, G., SANTOS, G. W., SARAL, R. & BURNS, W. H. 1982. Cytotoxic t cells in cytomegalovirus infection: HLA-restricted T-lymphocyte and non-T-lymphocyte cytotoxic responses correlate with recovery from cytomegalovirus infection in bone-marrow-transplant recipients. *N Engl J Med,* 307**,** 7-13.

REEVES, M. & SINCLAIR, J. 2013. Regulation of human cytomegalovirus transcription in latency: beyond the major immediate-early promoter. *Viruses,* 5**,** 1395-413.

REEVES, M. B., DAVIES, A. A., MCSHARRY, B. P., WILKINSON, G. W. & SINCLAIR, J. H. 2007. Complex I binding by a virally encoded RNA regulates mitochondria-induced cell death. *Science,* 316**,** 1345-8.

REEVES, M. B., MACARY, P. A., LEHNER, P. J., SISSONS, J. G. & SINCLAIR, J. H. 2005. Latency, chromatin remodeling, and reactivation of human cytomegalovirus in the dendritic cells of healthy carriers. *Proc Natl Acad Sci U S A,* 102**,** 4140-5.

REITH, W., LEIBUNDGUT-LANDMANN, S. & WALDBURGER, J. M. 2005. Regulation of MHC class II gene expression by the class II transactivator. *Nat Rev Immunol,* 5**,** 793-806.

RESSING, M. E., VAN LEEUWEN, D., VERRECK, F. A., GOMEZ, R., HEEMSKERK, B., TOEBES, M., MULLEN, M. M., JARDETZKY, T. S., LONGNECKER, R., SCHILHAM, M. W., OTTENHOFF, T. H., NEEFJES, J., SCHUMACHER, T. N., HUTT-FLETCHER, L. M. & WIERTZ, E. J. 2003. Interference with T cell receptor-HLA-DR interactions by Epstein-Barr virus gp42 results in reduced T helper cell recognition. *Proc Natl Acad Sci U S A,* 100**,** 11583-8.

REYBURN, H. T., MANDELBOIM, O., VALES-GOMEZ, M., DAVIS, D. M., PAZMANY, L. & STROMINGER, J. L. 1997. The class I MHC homologue of human cytomegalovirus inhibits attack by natural killer cells. *Nature,* 386**,** 514-7.

RIBBERT, H. 1904. Uber protozoenartige Zellen in der Niere eines syphilitischen Neugeborenen und in der Parotis von Kindern. *Zbl Allg Pathol.,* 15**,** 945-948.

RÖLLE, A., MOUSAVI-JAZI, M., ERIKSSON, M., ODEBERG, J., SÖDERBERG-NAUCLÉR, C., COSMAN, D., KÄRRE, K. & CERBONI, C. 2003. Effects of human cytomegalovirus infection on ligands for the activating NKG2D receptor of NK cells: up-regulation of UL16-binding protein (ULBP)1 and ULBP2 is counteracted by the viral UL16 protein. *J Immunol,* 171**,** 902-8.

ROWE, W. P., HARTLEY, J. W., WATERMAN, S., TURNER, H. C. & HUEBNER, R. J. 1956. Cytopathogenic agent resembling human salivary gland virus recovered from tissue cultures of human adenoids. *Proc Soc Exp Biol Med,* 92**,** 418-24.

RYCKMAN, B. J., CHASE, M. C. & JOHNSON, D. C. 2008. HCMV gH/gL/UL128-131 interferes with virus entry into epithelial cells: evidence for cell type-specific receptors. *Proc Natl Acad Sci U S A,* 105**,** 14118-23.

SAFA, A. R. 2012. c-FLIP, a master anti-apoptotic regulator. *Exp Oncol,* 34**,** 176-84.

SAMPAIO, K. L., CAVIGNAC, Y., STIERHOF, Y. D. & SINZGER, C. 2005. Human cytomegalovirus labeled with green fluorescent protein for live analysis of intracellular particle movements. *J Virol,* 79**,** 2754-67.

SAVERINO, D., GHIOTTO, F., MERLO, A., BRUNO, S., BATTINI, L., OCCHINO, M., MAFFEI, M., TENCA, C., PILERI, S., BALDI, L., FABBI, M., BACHI, A., DE SANTANNA, A., GROSSI, C. E. & CICCONE, E. 2004. Specific recognition of the viral protein UL18 by CD85j/LIR-1/ILT2 on CD8+ T cells mediates the non-MHC-restricted lysis of human cytomegalovirus-infected cells. *J Immunol,* 172**,** 5629-37.

SCHELLER, J., CHALARIS, A., GARBERS, C. & ROSE-JOHN, S. 2011. ADAM17: a molecular switch to control inflammation and tissue regeneration. *Trends Immunol,* 32**,** 380-7.

SCHLONDORFF, J., BECHERER, J. D. & BLOBEL, C. P. 2000. Intracellular maturation and localization of the tumour necrosis factor alpha convertase (TACE). *Biochem J,* 347 Pt 1**,** 131-8.

SCHLUMS, H., CICHOCKI, F., TESI, B., THEORELL, J., BEZIAT, V., HOLMES, T. D., HAN, H., CHIANG, S. C., FOLEY, B., MATTSSON, K., LARSSON, S., SCHAFFER, M., MALMBERG, K. J., LJUNGGREN, H. G., MILLER, J. S. & BRYCESON, Y. T. 2015. Cytomegalovirus infection drives adaptive epigenetic diversification of NK cells with altered signaling and effector function. *Immunity,* 42**,** 443-56.

SCHNEIDER, K., MEYER-KOENIG, U. & HUFERT, F. T. 2008. Human cytomegalovirus impairs the function of plasmacytoid dendritic cells in lymphoid organs. *PLoS One,* 3**,** e3482.
SEIDEL, E., LE, V. T., BAR-ON, Y., TSUKERMAN, P., ENK, J., YAMIN, R., STEIN, N., SCHMIEDEL, D., OIKNINE DJIAN, E., WEISBLUM, Y., TIROSH, B., STASTNY, P., WOLF, D. G., HENGEL, H. & MANDELBOIM, O. 2015. Dynamic Co-evolution of Host and Pathogen: HCMV Downregulates the Prevalent Allele MICA 008 to Escape Elimination by NK Cells. *Cell Rep*.
SEIRAFIAN, S. 2012. *An analysis of human cytomegalovirus gene usage A. PhD Thesis, Cardiff University.* Ph.D, Cardiff University.
SEIRAFIAN, S., PROD'HOMME, V., SUGRUE, D., DAVIES, J., FIELDING, C., TOMASEC, P. & WILKINSON, G. W. 2014. Human cytomegalovirus suppresses Fas expression and function. *J Gen Virol,* 95**,** 933-9.
SHEDLOCK, D. J. & SHEN, H. 2003. Requirement for CD4 T cell help in generating functional CD8 T cell memory. *Science,* 300**,** 337-9.
SHIFRIN, N., RAULET, D. H. & ARDOLINO, M. 2014. NK cell self tolerance, responsiveness and missing self recognition. *Semin Immunol,* 26**,** 138-44.
SHIRAI, T., YAMAGUCHI, H., ITO, H., TODD, C. W. & WALLACE, R. B. 1985. Cloning and expression in Escherichia coli of the gene for human tumour necrosis factor. *Nature,* 313**,** 803-6.
SHNAYDER, M., NACHSHON, A., KRISHNA, B., POOLE, E., BOSHKOV, A., BINYAMIN, A., MAZA, I., SINCLAIR, J., SCHWARTZ, M. & STERN-GINOSSAR, N. 2018. Defining the Transcriptional Landscape during Cytomegalovirus Latency with Single-Cell RNA Sequencing. *MBio,* 9.
SIEGMUND, D., KUMS, J., EHRENSCHWENDER, M. & WAJANT, H. 2016. Activation of TNFR2 sensitizes macrophages for TNFR1-mediated necroptosis. *Cell Death Dis,* 7**,** e2375.
SIJMONS, S., THYS, K., MBONG NGWESE, M., VAN DAMME, E., DVORAK, J., VAN LOOCK, M., LI, G., TACHEZY, R., BUSSON, L., AERSSENS, J., VAN RANST, M. & MAES, P. 2015. High-throughput analysis of human cytomegalovirus genome diversity highlights the widespread occurrence of gene-disrupting mutations and pervasive recombination. *J Virol*.
SINCLAIR, J. 2008. Human cytomegalovirus: Latency and reactivation in the myeloid lineage. *J Clin Virol,* 41**,** 180-5.
SINCLAIR, J. & SISSONS, P. 2006. Latency and reactivation of human cytomegalovirus. *J Gen Virol,* 87**,** 1763-79.
SINZGER, C., GREFTE, A., PLACHTER, B., GOUW, A. S., THE, T. H. & JAHN, G. 1995. Fibroblasts, epithelial cells, endothelial cells and smooth muscle cells are major targets of human cytomegalovirus infection in lung and gastrointestinal tissues. *J Gen Virol,* 76 (Pt 4)**,** 741-50.
SISSONS, J. G. & CARMICHAEL, A. J. 2002. Clinical aspects and management of cytomegalovirus infection. *J Infect,* 44**,** 78-83.
SKALETSKAYA, A., BARTLE, L. M., CHITTENDEN, T., MCCORMICK, A. L., MOCARSKI, E. S. & GOLDMACHER, V. S. 2001. A cytomegalovirus-encoded inhibitor of apoptosis that suppresses caspase-8 activation. *Proc Natl Acad Sci U S A,* 98**,** 7829-34.
SLOBEDMAN, B. & MOCARSKI, E. S. 1999. Quantitative analysis of latent human cytomegalovirus. *J Virol,* 73**,** 4806-12.

SMITH, M. G. 1956. Propagation in tissue cultures of a cytopathogenic virus from human salivary gland virus (SGV) disease. *Proc Soc Exp Biol Med,* 92**,** 424-30.

SMITH, W., TOMASEC, P., AICHELER, R., LOEWENDORF, A., NEMCOVICOVA, I., WANG, E. C., STANTON, R. J., MACAULEY, M., NORRIS, P., WILLEN, L., RUCKOVA, E., NOMOTO, A., SCHNEIDER, P., HAHN, G., ZAJONC, D. M., WARE, C. F., WILKINSON, G. W. & BENEDICT, C. A. 2013. Human cytomegalovirus glycoprotein UL141 targets the TRAIL death receptors to thwart host innate antiviral defenses. *Cell Host Microbe,* 13**,** 324-35.

SODERBERG-NAUCLER, C., FISH, K. N. & NELSON, J. A. 1997. Reactivation of latent human cytomegalovirus by allogeneic stimulation of blood cells from healthy donors. *Cell,* 91**,** 119-26.

SOLOMON, K. A., PESTI, N., WU, G. & NEWTON, R. C. 1999. Cutting edge: a dominant negative form of TNF-alpha converting enzyme inhibits proTNF and TNFRII secretion. *J Immunol,* 163**,** 4105-8.

SONAR, S. & LAL, G. 2015. Role of Tumor Necrosis Factor Superfamily in Neuroinflammation and Autoimmunity. *Front Immunol,* 6**,** 364.

SOROCEANU, L., AKHAVAN, A. & COBBS, C. S. 2008. Platelet-derived growth factor-alpha receptor activation is required for human cytomegalovirus infection. *Nature,* 455**,** 391-5.

SPRINGER, K. L. & WEINBERG, A. 2004. Cytomegalovirus infection in the era of HAART: fewer reactivations and more immunity. *J Antimicrob Chemother,* 54**,** 582-6.

STAGG, H. R., THOMAS, M., VAN DEN BOOMEN, D., WIERTZ, E. J., DRABKIN, H. A., GEMMILL, R. M. & LEHNER, P. J. 2009. The TRC8 E3 ligase ubiquitinates MHC class I molecules before dislocation from the ER. *J Cell Biol,* 186**,** 685-92.

STANTON, R. J., BALUCHOVA, K., DARGAN, D. J., CUNNINGHAM, C., SHEEHY, O., SEIRAFIAN, S., MCSHARRY, B. P., NEALE, M. L., DAVIES, J. A., TOMASEC, P., DAVISON, A. J. & WILKINSON, G. W. 2010. Reconstruction of the complete human cytomegalovirus genome in a BAC reveals RL13 to be a potent inhibitor of replication. *J Clin Invest,* 120**,** 3191-208.

STANTON, R. J., PROD'HOMME, V., PURBHOO, M. A., MOORE, M., AICHELER, R. J., HEINZMANN, M., BAILER, S. M., HAAS, J., ANTROBUS, R., WEEKES, M. P., LEHNER, P. J., VOJTESEK, B., MINERS, K. L., MAN, S., WILKIE, G. S., DAVISON, A. J., WANG, E. C. Y., TOMASEC, P. & WILKINSON, G. W. G. 2014. HCMV pUL135 remodels the actin cytoskeleton to impair immune recognition of infected cells. *Cell Host Microbe,* 16**,** 201-214.

STARAS, S. A., DOLLARD, S. C., RADFORD, K. W., FLANDERS, W. D., PASS, R. F. & CANNON, M. J. 2006. Seroprevalence of cytomegalovirus infection in the United States, 1988-1994. *Clin Infect Dis,* 43**,** 1143-51.

STEINBERG, M. W., CHEUNG, T. C. & WARE, C. F. 2011. The signaling networks of the herpesvirus entry mediator (TNFRSF14) in immune regulation. *Immunol Rev,* 244**,** 169-87.

STERN-GINOSSAR, N., ELEFANT, N., ZIMMERMANN, A., WOLF, D. G., SALEH, N., BITON, M., HORWITZ, E., PROKOCIMER, Z., PRICHARD, M., HAHN, G., GOLDMAN-WOHL, D., GREENFIELD, C., YAGEL, S.,

HENGEL, H., ALTUVIA, Y., MARGALIT, H. & MANDELBOIM, O. 2007. Host immune system gene targeting by a viral miRNA. *Science,* 317**,** 376-81.

STERN-GINOSSAR, N., WEISBURD, B., MICHALSKI, A., LE, V. T., HEIN, M. Y., HUANG, S. X., MA, M., SHEN, B., QIAN, S. B., HENGEL, H., MANN, M., INGOLIA, N. T. & WEISSMAN, J. S. 2012. Decoding human cytomegalovirus. *Science,* 338**,** 1088-93.

SUN, J. C., BEILKE, J. N. & LANIER, L. L. 2009. Adaptive immune features of natural killer cells. *Nature,* 457**,** 557-61.

SYLWESTER, A. W., MITCHELL, B. L., EDGAR, J. B., TAORMINA, C., PELTE, C., RUCHTI, F., SLEATH, P. R., GRABSTEIN, K. H., HOSKEN, N. A., KERN, F., NELSON, J. A. & PICKER, L. J. 2005. Broadly targeted human cytomegalovirus-specific CD4+ and CD8+ T cells dominate the memory compartments of exposed subjects. *J Exp Med,* 202**,** 673-85.

TAKENAWA, T. & SUETSUGU, S. 2007. The WASP-WAVE protein network: connecting the membrane to the cytoskeleton. *Nat Rev Mol Cell Biol,* 8**,** 37-48.

TAPE, C. J., WILLEMS, S. H., DOMBERNOWSKY, S. L., STANLEY, P. L., FOGARASI, M., OUWEHAND, W., MCCAFFERTY, J. & MURPHY, G. 2011. Cross-domain inhibition of TACE ectodomain. *Proc Natl Acad Sci U S A,* 108**,** 5578-83.

TAYLOR-WIEDEMAN, J., SISSONS, J. G., BORYSIEWICZ, L. K. & SINCLAIR, J. H. 1991. Monocytes are a major site of persistence of human cytomegalovirus in peripheral blood mononuclear cells. *J Gen Virol,* 72 (Pt 9)**,** 2059-64.

TAYLOR-WIEDEMAN, J., SISSONS, P. & SINCLAIR, J. 1994. Induction of endogenous human cytomegalovirus gene expression after differentiation of monocytes from healthy carriers. *J Virol,* 68**,** 1597-604.

THOMAS, M. L. 1989. The leukocyte common antigen family. *Annu Rev Immunol,* 7**,** 339-69.

TIROSH, O., COHEN, Y., SHITRIT, A., SHANI, O., LE-TRILLING, V. T., TRILLING, M., FRIEDLANDER, G., TANENBAUM, M. & STERN-GINOSSAR, N. 2015. The Transcription and Translation Landscapes during Human Cytomegalovirus Infection Reveal Novel Host-Pathogen Interactions. *PLoS Pathog,* 11**,** e1005288.

TOMASEC, P., BRAUD, V. M., RICKARDS, C., POWELL, M. B., MCSHARRY, B. P., GADOLA, S., CERUNDOLO, V., BORYSIEWICZ, L. K., MCMICHAEL, A. J. & WILKINSON, G. W. 2000. Surface expression of HLA-E, an inhibitor of natural killer cells, enhanced by human cytomegalovirus gpUL40. *Science,* 287**,** 1031.

TOMASEC, P., WANG, E. C., DAVISON, A. J., VOJTESEK, B., ARMSTRONG, M., GRIFFIN, C., MCSHARRY, B. P., MORRIS, R. J., LLEWELLYN-LACEY, S., RICKARDS, C., NOMOTO, A., SINZGER, C. & WILKINSON, G. W. 2005. Downregulation of natural killer cell-activating ligand CD155 by human cytomegalovirus UL141. *Nat Immunol,* 6**,** 181-8.

TOMAZIN, R., BONAME, J., HEGDE, N. R., LEWINSOHN, D. M., ALTSCHULER, Y., JONES, T. R., CRESSWELL, P., NELSON, J. A., RIDDELL, S. R. & JOHNSON, D. C. 1999. Cytomegalovirus US2 destroys two components of the MHC class II pathway, preventing recognition by CD4+ T cells. *Nat Med,* 5**,** 1039-43.

TRGOVCICH, J., CEBULLA, C., ZIMMERMAN, P. & SEDMAK, D. D. 2006. Human cytomegalovirus protein pp71 disrupts major histocompatibility complex class I cell surface expression. *J Virol,* 80**,** 951-63.

ULBRECHT, M., MARTINOZZI, S., GRZESCHIK, M., HENGEL, H., ELLWART, J. W., PLA, M. & WEISS, E. H. 2000. Cutting edge: the human cytomegalovirus UL40 gene product contains a ligand for HLA-E and prevents NK cell-mediated lysis. *J Immunol,* 164**,** 5019-22.

VALÉS-GÓMEZ, M., SHIROISHI, M., MAENAKA, K. & REYBURN, H. T. 2005. Genetic variability of the major histocompatibility complex class I homologue encoded by human cytomegalovirus leads to differential binding to the inhibitory receptor ILT2. *J Virol,* 79**,** 2251-60.

VAN DEN BOOMEN, D. J., TIMMS, R. T., GRICE, G. L., STAGG, H. R., SKODT, K., DOUGAN, G., NATHAN, J. A. & LEHNER, P. J. 2014. TMEM129 is a Derlin-1 associated ERAD E3 ligase essential for virus-induced degradation of MHC-I. *Proc Natl Acad Sci U S A,* 111**,** 11425-30.

VARFOLOMEEV, E. E. & ASHKENAZI, A. 2004. Tumor necrosis factor: an apoptosis JuNKie? *Cell,* 116**,** 491-7.

VERMIJLEN, D. & PRINZ, I. 2014. Ontogeny of Innate T Lymphocytes - Some Innate Lymphocytes are More Innate than Others. *Front Immunol,* 5**,** 486.

VERNERIS, M. R., KARIMI, M., KARAMI, M., BAKER, J., JAYASWAL, A. & NEGRIN, R. S. 2004. Role of NKG2D signaling in the cytotoxicity of activated and expanded CD8+ T cells. *Blood,* 103**,** 3065-72.

VERWEIJ, M. C., HORST, D., GRIFFIN, B. D., LUTEIJN, R. D., DAVISON, A. J., RESSING, M. E. & WIERTZ, E. J. 2015. Viral inhibition of the transporter associated with antigen processing (TAP): a striking example of functional convergent evolution. *PLoS Pathog,* 11**,** e1004743.

VIOLA, A. & LANZAVECCHIA, A. 1996. T cell activation determined by T cell receptor number and tunable thresholds. *Science,* 273**,** 104-6.

WAGNER, C. S., RIISE, G. C., BERGSTRÖM, T., KÄRRE, K., CARBONE, E. & BERG, L. 2007. Increased expression of leukocyte Ig-like receptor-1 and activating role of UL18 in the response to cytomegalovirus infection. *J Immunol,* 178**,** 3536-43.

WAJANT, H. 2015. Principles of antibody-mediated TNF receptor activation. *Cell Death Differ,* 22**,** 1727-41.

WANG, D. & SHENK, T. 2005. Human cytomegalovirus UL131 open reading frame is required for epithelial cell tropism. *J Virol,* 79**,** 10330-8.

WANG, E. C., MCSHARRY, B., RETIERE, C., TOMASEC, P., WILLIAMS, S., BORYSIEWICZ, L. K., BRAUD, V. M. & WILKINSON, G. W. 2002. UL40-mediated NK evasion during productive infection with human cytomegalovirus. *Proc Natl Acad Sci U S A,* 99**,** 7570-5.

WANG, E. C. Y., PJECHOVA, M., NIGHTINGALE, K., VLAHAVA, V. M., PATEL, M., RUCKOVA, E., FORBES, S. K., NOBRE, L., ANTROBUS, R., ROBERTS, D., FIELDING, C. A., SEIRAFIAN, S., DAVIES, J., MURRELL, I., LAU, B., WILKIE, G. S., SUAREZ, N. M., STANTON, R. J., VOJTESEK, B., DAVISON, A., LEHNER, P. J., WEEKES, M. P., WILKINSON, G. W. G. & TOMASEC, P. 2018. Suppression of costimulation by human cytomegalovirus promotes evasion of cellular immune defenses. *Proc Natl Acad Sci U S A*.

WANG, F., CHI, J., PENG, G., ZHOU, F., WANG, J., LI, L., FENG, D., XIE, F., GU, B., QIN, J., CHEN, Y. & YAO, K. 2014. Development of virus-specific

CD4+ and CD8+ regulatory T cells induced by human herpesvirus 6 infection. *J Virol,* 88**,** 1011-24.
WANG, L., DU, F. & WANG, X. 2008. TNF-alpha induces two distinct caspase-8 activation pathways. *Cell,* 133**,** 693-703.
WANG, S. & EL-DEIRY, W. S. 2003. TRAIL and apoptosis induction by TNF-family death receptors. *Oncogene,* 22**,** 8628-33.
WARD-KAVANAGH, L. K., LIN, W. W., SEDY, J. R. & WARE, C. F. 2016. The TNF Receptor Superfamily in Co-stimulating and Co-inhibitory Responses. *Immunity,* 44**,** 1005-19.
WARREN, A. P., DUCROQ, D. H., LEHNER, P. J. & BORYSIEWICZ, L. K. 1994. Human cytomegalovirus-infected cells have unstable assembly of major histocompatibility complex class I complexes and are resistant to lysis by cytotoxic T lymphocytes. *J Virol,* 68**,** 2822-9.
WATERS, J. P., POBER, J. S. & BRADLEY, J. R. 2013. Tumour necrosis factor in infectious disease. *J Pathol,* 230**,** 132-47.
WEEKES, M. P., TAN, S. Y., POOLE, E., TALBOT, S., ANTROBUS, R., SMITH, D. L., MONTAG, C., GYGI, S. P., SINCLAIR, J. H. & LEHNER, P. J. 2013. Latency-associated degradation of the MRP1 drug transporter during latent human cytomegalovirus infection. *Science,* 340**,** 199-202.
WEEKES, MICHAEL P., TOMASEC, P., HUTTLIN, EDWARD L., FIELDING, CERI A., NUSINOW, D., STANTON, RICHARD J., WANG, EDDIE C. Y., AICHELER, R., MURRELL, I., WILKINSON, GAVIN W. G., LEHNER, PAUL J. & GYGI, STEVEN P. 2014. Quantitative Temporal Viromics: An Approach to Investigate Host-Pathogen Interaction. *Cell,* 157**,** 1460-1472.
WELLER, T. H. 1970. Review. Cytomegaloviruses: the difficult years. *J Infect Dis,* 122**,** 532-9.
WEN, T., BUKCZYNSKI, J. & WATTS, T. H. 2002. 4-1BB ligand-mediated costimulation of human T cells induces CD4 and CD8 T cell expansion, cytokine production, and the development of cytolytic effector function. *J Immunol,* 168**,** 4897-906.
WERTZ, I. E. & DIXIT, V. M. 2010. Regulation of death receptor signaling by the ubiquitin system. *Cell Death Differ,* 17**,** 14-24.
WHERRY, E. J. & AHMED, R. 2004. Memory CD8 T-cell differentiation during viral infection. *J Virol,* 78**,** 5535-45.
WHITE, A. E. & SPECTOR, D. H. 2007. Early viral gene expression and function. *Human Herpesviruses: Biology, Therapy and Immunoprophylaxis.* Cambridge: Cambridge University Press.
WIERTZ, E. J., JONES, T. R., SUN, L., BOGYO, M., GEUZE, H. J. & PLOEGH, H. L. 1996. The human cytomegalovirus US11 gene product dislocates MHC class I heavy chains from the endoplasmic reticulum to the cytosol. *Cell,* 84**,** 769-79.
WILKINSON, G. W., AKRIGG, A. & GREENAWAY, P. J. 1984. Transcription of the immediate early genes of human cytomegalovirus strain AD169. *Virus Res,* 1**,** 101-6.
WILKINSON, G. W., KELLY, C., SINCLAIR, J. H. & RICKARDS, C. 1998. Disruption of PML-associated nuclear bodies mediated by the human cytomegalovirus major immediate early gene product. *J Gen Virol,* 79 (Pt 5)**,** 1233-45.
WILKINSON, G. W., TOMASEC, P., STANTON, R. J., ARMSTRONG, M., PROD'HOMME, V., AICHELER, R., MCSHARRY, B. P., RICKARDS, C.

R., COCHRANE, D., LLEWELLYN-LACEY, S., WANG, E. C., GRIFFIN, C. A. & DAVISON, A. J. 2008. Modulation of natural killer cells by human cytomegalovirus. *J Clin Virol,* 41**,** 206-12.

WILLS, M. R., ASHIRU, O., REEVES, M. B., OKECHA, G., TROWSDALE, J., TOMASEC, P., WILKINSON, G. W. G., SINCLAIR, J. & SISSONS, J. G. P. 2005. Human Cytomegalovirus Encodes an MHC Class I-Like Molecule (UL142) That Functions to Inhibit NK Cell Lysis. *The Journal of Immunology,* 175**,** 7457-7465.

WILLS, M. R., CARMICHAEL, A. J., MYNARD, K., JIN, X., WEEKES, M. P., PLACHTER, B. & SISSONS, J. G. 1996. The human cytotoxic T-lymphocyte (CTL) response to cytomegalovirus is dominated by structural protein pp65: frequency, specificity, and T-cell receptor usage of pp65-specific CTL. *J Virol,* 70**,** 7569-79.

WILLS, M. R., CARMICHAEL, A. J., WEEKES, M. P., MYNARD, K., OKECHA, G., HICKS, R. & SISSONS, J. G. 1999. Human virus-specific CD8+ CTL clones revert from CD45ROhigh to CD45RAhigh in vivo: CD45RAhighCD8+ T cells comprise both naive and memory cells. *J Immunol,* 162**,** 7080-7.

WILLS, M. R., MASON, G. M. & PATRICK SISSONS, J. G. 2013. Adaptive Cellular Immunity to Human Cytomegalovirus. *In:* REDDEHASE, M. J. & LEMMERMANN, N. A. W. (eds.) *Cytomegaloviruses. From Molecular Pathogenesis to Intervention.* Norfolk Caister Academic Press.

WOODHALL, D. L., GROVES, I. J., REEVES, M. B., WILKINSON, G. & SINCLAIR, J. H. 2006. Human Daxx-mediated repression of human cytomegalovirus gene expression correlates with a repressive chromatin structure around the major immediate early promoter. *J Biol Chem,* 281**,** 37652-60.

WYZGOL, A., MULLER, N., FICK, A., MUNKEL, S., GRIGOLEIT, G. U., PFIZENMAIER, K. & WAJANT, H. 2009. Trimer stabilization, oligomerization, and antibody-mediated cell surface immobilization improve the activity of soluble trimers of CD27L, CD40L, 41BBL, and glucocorticoid-induced TNF receptor ligand. *J Immunol,* 183**,** 1851-61.

YAMASHITA, Y., SHIMOKATA, K., MIZUNO, S., YAMAGUCHI, H. & NISHIYAMA, Y. 1993. Down-regulation of the surface expression of class I MHC antigens by human cytomegalovirus. *Virology,* 193**,** 727-36.

YAMASHITA, Y., SHIMOKATA, K., SAGA, S., MIZUNO, S., TSURUMI, T. & NISHIYAMA, Y. 1994. Rapid degradation of the heavy chain of class I major histocompatibility complex antigens in the endoplasmic reticulum of human cytomegalovirus-infected cells. *J Virol,* 68**,** 7933-43.

YANG, E. 2011. *Proteomic Study of Human Cytomegalovirus Using an Epitope Tag System.* Ph.D, University of California.

YANG, Z. & BJORKMAN, P. J. 2008. Structure of UL18, a peptide-binding viral MHC mimic, bound to a host inhibitory receptor. *Proc Natl Acad Sci U S A,* 105**,** 10095-100.

YU, K., DAVIDSON, C. L., WÓJTOWICZ, A., LISBOA, L., WANG, T., AIRO, A. M., VILLARD, J., BURATTO, J., SANDALOVA, T., ACHOUR, A., HUMAR, A., BOGGIAN, K., CUSINI, A., VAN DELDEN, C., EGLI, A., MANUEL, O., MUELLER, N., BOCHUD, P. Y., BURSHTYN, D. N. & STUDY, S. T. C. 2018. LILRB1 polymorphisms influence posttransplant HCMV susceptibility and ligand interactions. *J Clin Invest,* 128**,** 1523-1537.

ZHAO, H., JAFFER, T., EGUCHI, S., WANG, Z., LINKERMANN, A. & MA, D. 2015. Role of necroptosis in the pathogenesis of solid organ injury. *Cell Death Dis,* 6**,** e1975.

ZISCHKE, J., MAMARELI, P., POKOYSKI, C., GABAEV, I., BUYNY, S., JACOBS, R., FALK, C. S., LOCHNER, M., SPARWASSER, T., SCHULZ, T. F. & KAY-FEDOROV, P. C. 2017. The human cytomegalovirus glycoprotein pUL11 acts via CD45 to induce T cell IL-10 secretion. *PLoS Pathog,* 13**,** e1006454.

Appendix

Appendix I Results

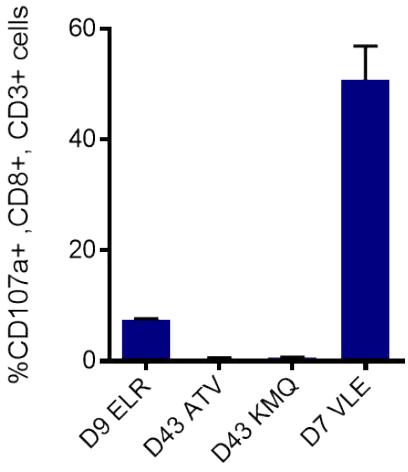

Degranulation potential of T-cell lines as assessed by degranulation of CD8+T-cells against peptide pulsed autologous fibroblasts. SFi cells were pulsed with the indicated peptide concentrations. These cells were then used as targets in a CD107a degranulation assay. Data shows mean %CD107a+ of CD8+ cells ±SEM of quadruplicate values.

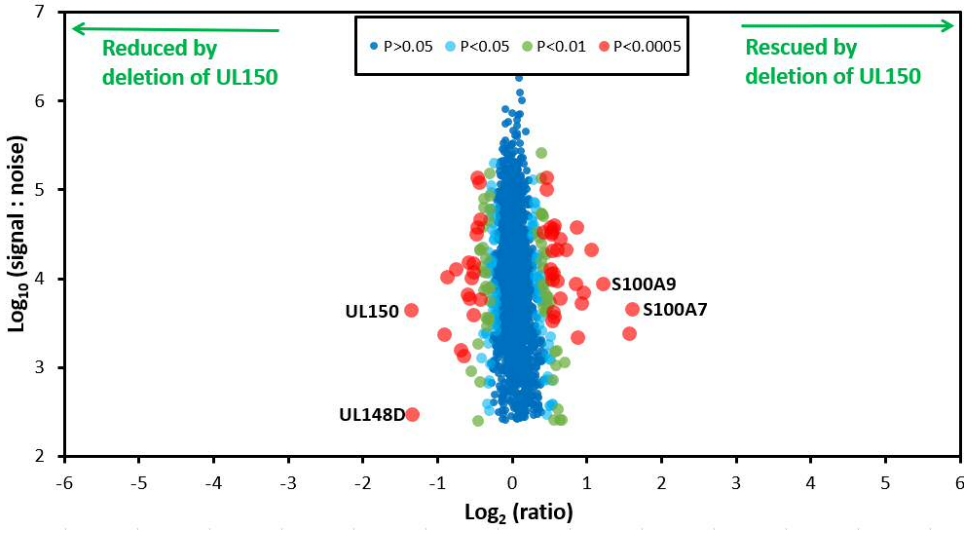

Proteomic analysis of ΔUL150/A infected HF-TERT cells. Data from Dr Pete Tomasec and Dr Michael Weekes. Proteins unaltered by the deletion are at the center of the plots (0 $\log_2$), whereas proteins to the left or right of center represent proteins down regulated or upregulated respectively by the deletion of UL150/A. P values are for for the ratios of expression from each mutant compared to HCMV Merlin using Benjamini-Hochberg corrected Significance B values.

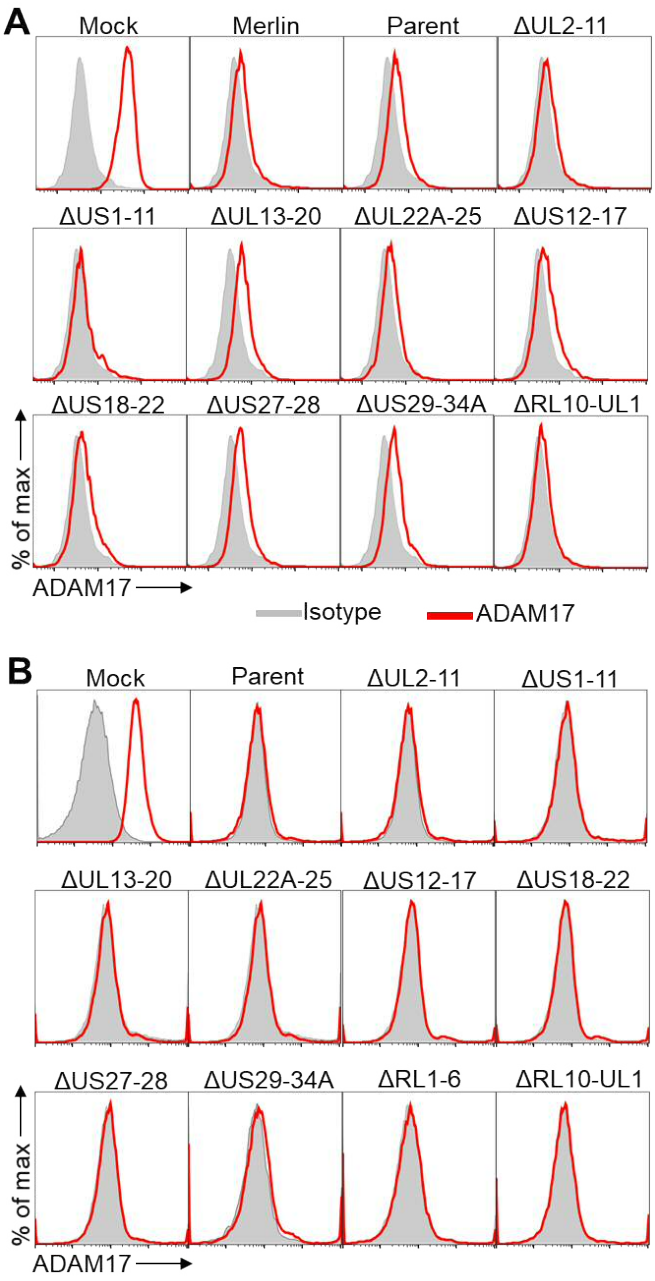

Effect of HCMV block mutants on ADAM17 expression. HF-TERTS were infected with indicated viruses. Flow cytometry was performed at (A) 24hpi and (B) 72hpi.

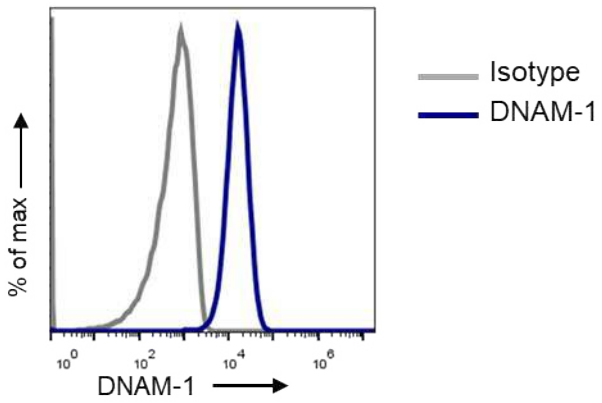

Flow cytometry for DNAM-1 on D9-VTE T-cell line.

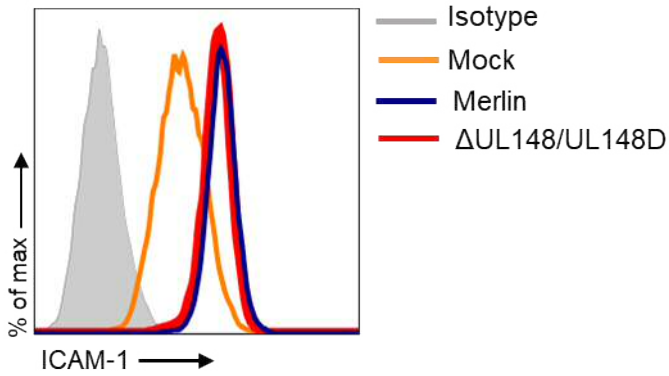

Assessing the effect of UL148/UL148D on ICAM1 expression. HF-TERT cells were infected Merlin or ΔUL148/UL148D. Flow cytometry for ICAM-1 was performed at 72hpi.

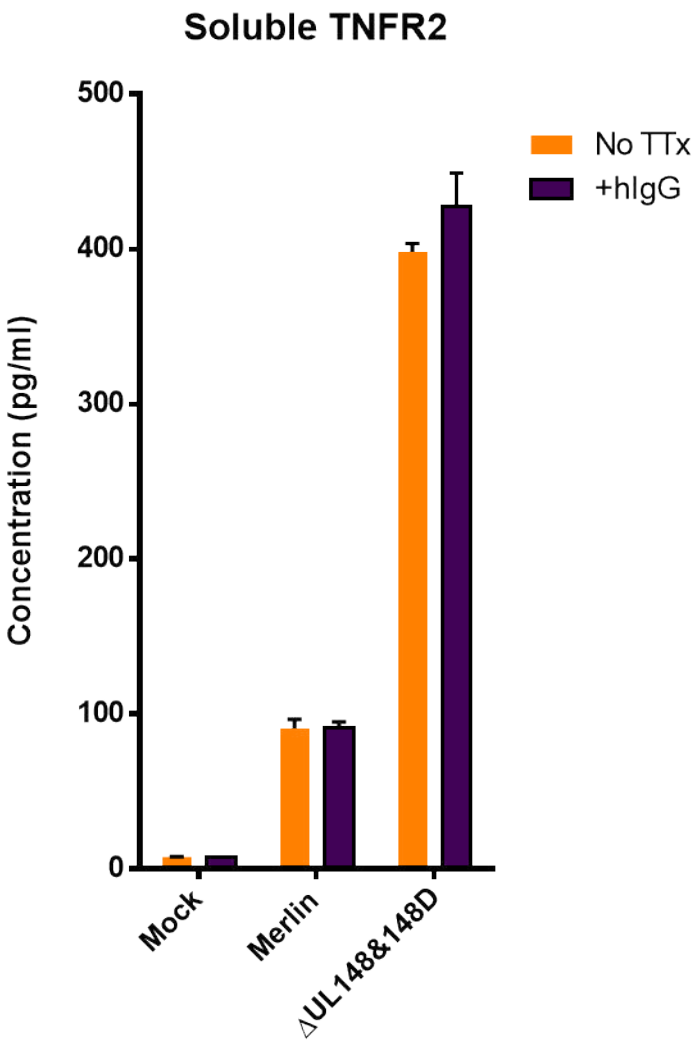

Assessing the effect of hIgG on sTNFR2 release. HF-TERT cells were infected Merlin or ΔUL148/UL148D. At 48hpi, the media was changed for fresh media (No TTx) or hIgG (100nM). An ELISA was for sTNFR2 was performed with supernatant at 72hpi.

Appendix II Publications